An Investigation of the Effectiveness of Skyhook Suspensions for Controlling Roll Dynamics of Sport Utility Vehicles Using Magneto-Rheological Dampers

by

David E. Simon

Dissertation submitted to the Faculty of the

Virginia Polytechnic Institute and State University

in partial fulfillment of the requirements for the degree of

Doctor of Philosophy

in

Mechanical Engineering

Approved:

____

Dr. Mehdi Ahmadian, Chairman

________________ ________________

Dr. Harry R. Robertshaw Dr. Pushkin Kachroo

________________ ________________

Dr. Mary E. F. Kasarda Dr. Donald Leo

November 28, 2001

Blacksburg, Virginia

Keywords: Damper, Magneto-Rheological, Semiactive, Controllable

An Investigation of the Effectiveness of Skyhook Suspensions for Controlling Roll Dynamics of Sport Utility Vehicles Using Magneto-Rheological Dampers

by
David E. Simon

Abstract

In recent years, many investigators have predicted that with a semiactive suspension it is possible to attain performance gains comparable to those possible with a fully active suspension. In achieving this, the method by which the damper is controlled is one of the crucial factors that ultimately determines the success or failure of a particular semiactive suspension. This study is an investigation into the effectiveness of a number of basic control strategies at controlling vehicle dynamics, particularly vehicle roll. The test vehicle is a Sport Utility Vehicle (SUV), a class of vehicle that regularly sees widely varying vehicle weight (as a result of passengers and load) and can exhibit undesirable levels of vehicle roll. This study includes a suspension system comprised of four controllable magneto-rheological dampers, associated sensors, and controller. There are three distinct phases in this investigation, the first of which is a numerical investigation performed on a four-degree-of-freedom vehicle roll-plane model. The model is subjected to a variety of road and driver induced inputs, and the vehicle response is characterized, with each semiactive control policy. The second phase of this study consists of laboratory testing performed on a Ford Expedition, with the front axle of the vehicle placed on a two-post dynamic rig (tire coupled), and a variety of road inputs applied. The third phase of this testing involves road testing the test vehicle to further evaluate the effectiveness of each of the semiactive control policies at controlling both vehicle comfort (vibration) and stability (roll). In each phase, the semiactive control policies that are investigated are tuned and modified such that the best possible performance is attained. The performance of each of these optimal semiactive systems is then compared.

In the first phase of this investigation, two basic skyhook control strategies are investigated and two modified strategies are proposed. Upon numerically investigating the effectiveness of the four control strategies, it is found that the performance achievable with each of the control strategies is heavily dependent on the properties of the controllable damper. The properties of the controllable damper that were particularly important were the upper and lower levels of force that the controllable damper was able to apply. Based on numerical results, the controllable dampers were tuned for each control system. The results indicate that a velocity-based skyhook control policy, in conjunction with force control, is most effective at controlling both road-induced vibration and driver-induced roll. In the second phase of this investigation, the effects of the two skyhook control strategies were again examined. Multiple system inputs including step inputs, chirp inputs, and multi-sine inputs were used, and the results indicate that significant performance gains using the basic skyhook policies are unlikely. The third phase involved road testing the vehicle through specific maneuvers modeling a wide variety of common driving situations. In addition to the two basic skyhook policies, two additional policies augmented with steering wheel position feedback were also examined. It was found that the velocity based skyhook control policy augmented with steering wheel position feedback achieved performance superior to both the stock passive dampers and other control policies tested here.

Acknowledgements

I would like to thank my advisor, Dr. Mehdi Ahmadian, for his help and support as I pursued my degrees at Virginia Tech. This project would not have been possible without his backing. In addition, I would like to thank Drs. Harry Robertshwaw, Pushkin Kachroo, Mary Kasarda, and Don Leo for being a part of my doctoral committee. I would also like to acknowledge the contributions of our corporate sponsors which include Visteon Corporation, Lord Corporation, PCB Piezotronics, dSpace, Unimeasure, and both the Mechanical Engineering Department and the Virginia Tech Transportation Institute at Virginia Tech. Special thanks are due to Visteon Corporation for providing the 2000 model Ford Expedition that was used during this study.

Last, but not least, I would express my appreciation to my family, and in particular my parents William and Marilyn Simon for their support and patience for the duration of my time at Virginia Tech.

CONTENTS

List of Tables

List of Figures

CHAPTER 1

INTRODUCTION

In recent years, the automobile industry has seen a market shift towards sport-utility vehicles (SUVs). Customers enjoy the size, adaptability, solid feel, and commanding view of the road that are hallmarks of vehicles in this class. In part due to exactly these characteristics, it is more difficult for a suspension designer to create a vehicle that will both be comfortable to the operator and occupants, and perform well during vehicle maneuvers. In particular, the relatively high center of gravity of vehicles in this class, combined with a large weight has led to a greater roll-over propensity than is common in an automobile. In order to maintain the level of comfort that customers expect from vehicles in this class, and still maintain the high safety standards of automobiles, suspension designers have been forced to look beyond conventional suspension systems.

1.1 Background

The perceived comfort level and ride stability of a vehicle are two of the most important factors in a subjective evaluation of a vehicle. There are many aspects of a vehicle that influence these two properties, the most important of which are the primary suspension components, which isolate the frame of the vehicle from the axle and wheel assemblies. In the design of a conventional primary suspension system there is a trade off between the two quantities of ride comfort and vehicle handling (safety), as is shown in Figure 1.1.

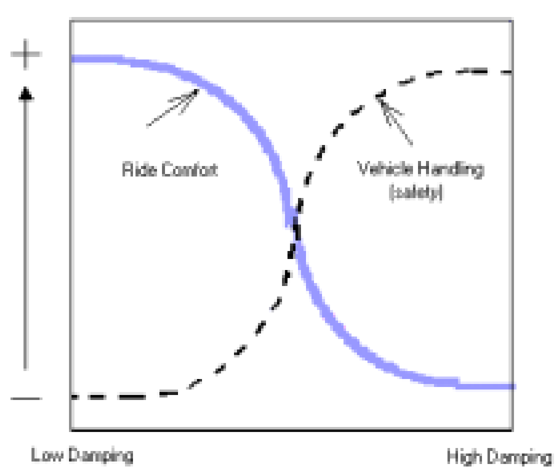

Figure 1.1. Passive Suspension Design Compromise

If a primary suspension is designed to optimize the handling and stability of the vehicle, the operator often perceives the ride to be rough and uncomfortable. On the other hand, if the suspension is designed for ride comfort alone, the vehicle may not be stable during maneuvers. As such, the performance of primary suspensions is always defined by the compromise between ride and handling. A primary suspension can only be optimized to a limited extent. To achieve a better performance, it is necessary to investigate different, non-conventional types of suspension systems. Though passive suspensions remain the most common class of suspension found on today's passenger cars and light trucks, there are other alternatives available to suspension designers. Examples of the other types of primary suspension systems that can be implemented in a passenger vehicle are adjustable, semiactive, active, and adaptive suspensions.

1.1.1 Primary Suspension

Primary suspension is the term used to designate those suspension components connecting the axle and wheel assemblies of a vehicle to the frame of the vehicle. This is in contrast to secondary suspensions, which are the elements connecting other components to the frame or body of a vehicle: such as engine mounts, seat suspensions, and cab mounts. There are two basic types of elements in conventional suspension systems. These elements are springs and dampers. The role of the spring in a vehicle's suspension system is to support the static weight of the vehicle. The role of the damper is to dissipate vibrational energy and control the input from the road that is transmitted to the vehicle. The basic function and form of a suspension is the same regardless of the type of vehicle or specific system. Primary suspensions can be generally divided into four categories:

- Passive suspensions,
- Active suspensions,
- Adjustable suspensions, and
- semiactive suspensions.

Each of these categories will be discussed further, within the context of this study.

1.1.2 Passive Suspension

A passive suspension system is one in which the characteristics of the suspension components (the springs and dampers) are fixed in time. The suspension designer, according to the intended application and the design goals, determines these characteristics. A heavily damped suspension will generally cause good vehicle handling and therefore yield a safer vehicle, but also transfers much of the road input to the vehicle body. When the vehicle is traveling at low speed on a rough road or at high speed in a straight line, the operator may perceive this as a harsh ride. The vehicle operators may find the harsh ride objectionable, or the transmitted vibration may damage cargo. A lightly damped suspension may provide a more comfortable ride, but can significantly reduce the stability of the vehicle during turns, lane change maneuvers, or in negotiating an exit ramp. A well-designed passive suspension can, to some extent optimize ride and handling, but it cannot eliminate this compromise.

1.1.3 Active Suspension

In an active suspension, the passive damper or both the passive damper and spring are replaced with a force actuator, as illustrated in Figure 1.2.

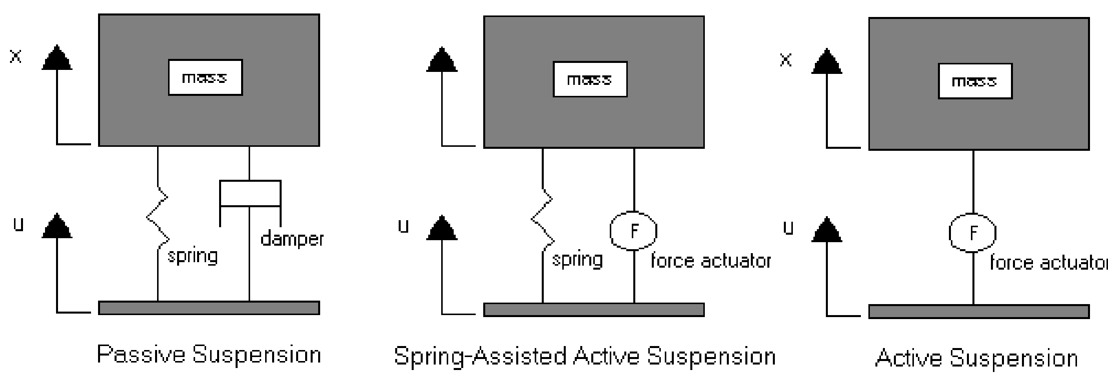

Figure 1.2. Passive and Active Suspensions

The force actuator is able to both add and dissipate energy from the system, unlike a passive damper, which can only dissipate energy. This is due to the ability of the force actuator to apply force independent of the relative displacement or velocity across the suspension. Given the correct control strategy, this results in a better compromise between ride comfort and vehicle stability as compared to a passive system, as shown in Figure 1.3 for a quarter-car model.

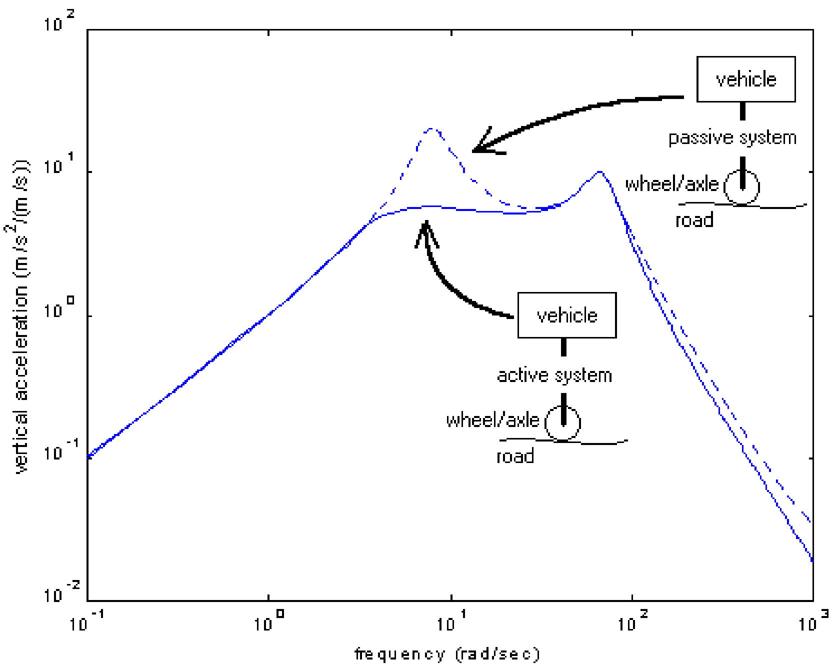

Figure 1.3. Passive and Active Suspension Comparison (adapted from [1], p.201)

A quarter-car model, shown in Figure 1.4, is a two-degree-of-freedom model that emulates the vehicle body and axle dynamics with a single tire (i.e., one-quarter of a car).

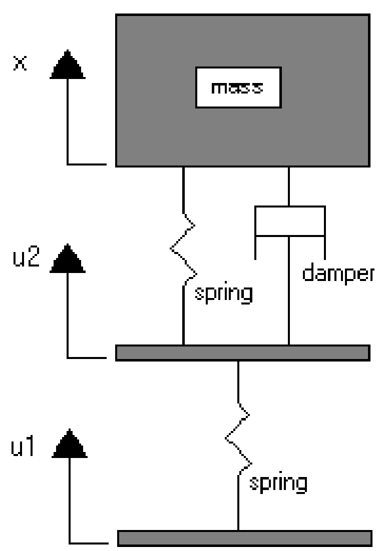

Figure 1.4. A Quarter Car Model.

In a study by Chalasani [1], a quarter car model was used to investigate the performance gains possible with an active suspension system. In that study, the road input was modeled as a white-noise velocity input. The study found that, within practical design limitations, an active suspension can reduce the RMS (Root Mean Square) acceleration of the sprung mass by 20%. This suspension configuration exhibited approximately the same level of suspension travel and wheel-hop damping ratio as a lightly damped, soft passive suspension. In a further study [2], similar simulations and analyses were performed for half car model. That study estimated that active suspensions could reduce the RMS value of the sprung mass acceleration by 15%.

Active suspension systems have the added advantage of controlling the attitude of a vehicle. They can reduce the effects of braking, which causes a vehicle to nose-dive, or acceleration, which causes a vehicle to squat. They also reduce the vehicle roll during cornering maneuvers.

Active suspension systems, though shown to be capable of improving both ride and stability, do have disadvantages. The force actuators necessary in an active suspension system typically have large power requirements (typically 4-5 hp). The power requirements decrease the overall performance of the vehicle, and are often unacceptable. Another disadvantage of active suspension systems is that they can have unacceptable failure modes. In the case of actuator failure, the vehicle would be left undamped, and possibly unsprung. This is a potentially dangerous situation for both the vehicle and operator.

1.1.4 Adjustable Suspension

An adjustable suspension system combines the passive spring element found in a passive suspension, with a damper element whose characteristics can be adjusted by the operator. As shown in Figure 1.5, the vehicle operator can use a selector device to set the desired level of damping based on their subjective feel.

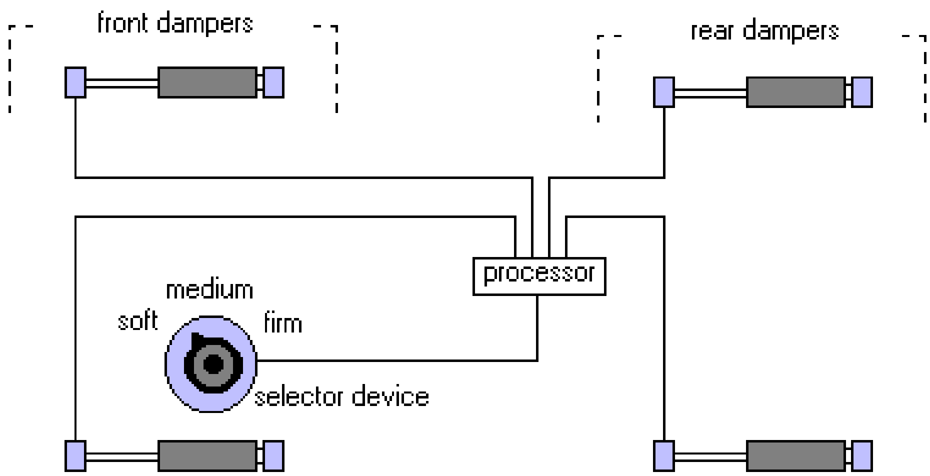

Figure 1.5. Adjustable Suspension (adapted from reference [3], p. 107)

This system has the advantage of allowing to operator to adjust the dampers according to the road characteristics. It is, however, unrealistic to expect the operator to adjust the suspension system in time to respond to potholes, turns, or other common road inputs.

1.1.5 Semiactive Suspension

Semiactive suspension systems were first proposed in the early 1970's. In this type of system, the conventional spring element is retained, but the damper is replaced with a controllable damper as shown in Figure 1.6.

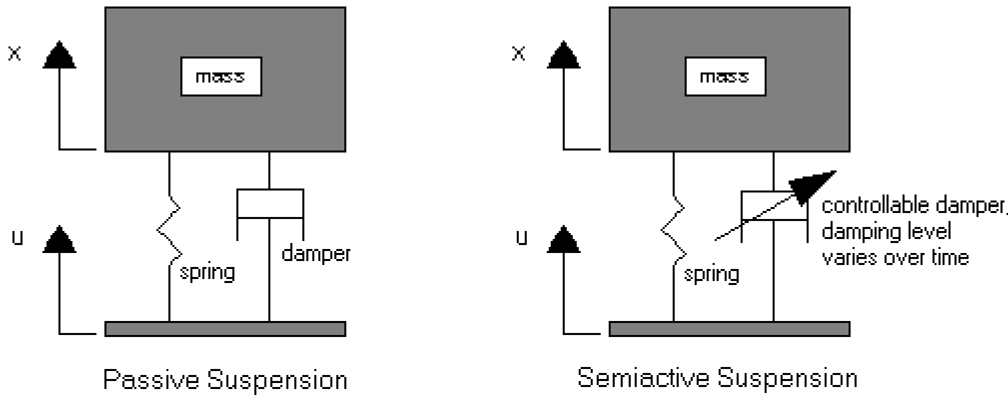

Figure 1.6. Passive and Semiactive Suspensions

Whereas an active suspension system requires an external energy source to power an actuator that controls the vehicle, a semiactive system uses external power only to adjust the damping levels, and operate an embedded controller and a set of sensors. The controller determines the level of damping based on a control strategy, and automatically adjusts the damper to achieve that damping. One of the most common semiactive control policies is skyhook control, which adjusts the damping level to emulate the effect of a damper connected from the vehicle to a stationary ground, as shown in Figure 1.7.

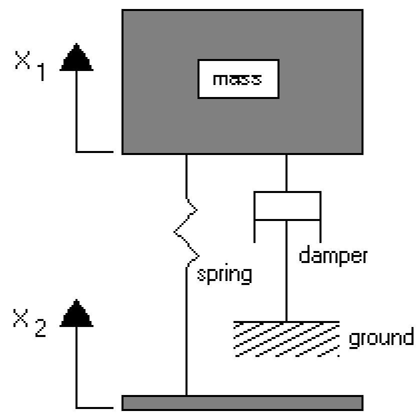

Figure 1.7. Quarter Car Model with Skyhook Damper

In its simplest form, skyhook control can be looked at as an on-off control. With this simplification, skyhook control can be described mathematically as:

$$\begin{aligned} &\dot{X}_1(\dot{X}_1 - \dot{X}_2) \geq 0 && C = high \quad damping \\ &\dot{X}_1(\dot{X}_1 - \dot{X}_2) < 0 && C = low \quad damping \end{aligned} \tag{2.1}$$

In this equation $\dot{X}_1$ is the velocity of the upper mass and $\dot{X}_2$ is the velocity of the lower mass. This is called on-off, or bang-bang skyhook control since the damper switches back and forth between two possible damping states. When the upper mass is moving up, and the two masses are getting closer, the damping constant should ideally be zero. Due to the physical limitations of a practical damper, a damping constant of zero is not practical and a low damping constant is used. When the upper mass is moving down and the two masses are getting closer, the skyhook control policy ideally calls for an infinite damping constant. An infinite damping constant is not physically attainable, so in practice, the adjustable damping constant is set to a maximum. The effect of the skyhook control scheme is to minimize the absolute velocity of the upper mass. This is shown in Figure 1.8.

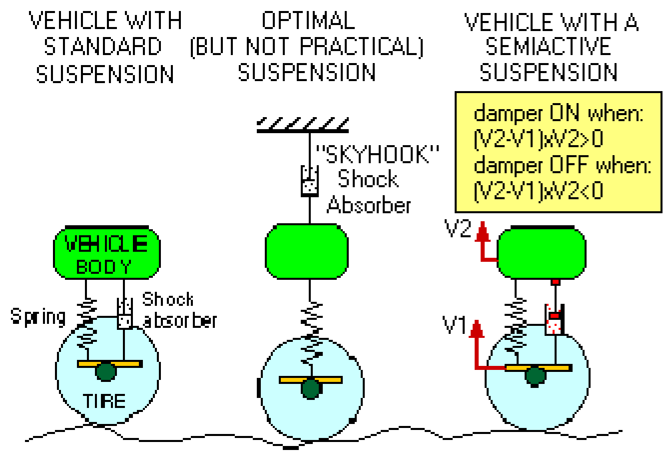

Figure 1.8. Skyhook Control Policy [4]

It has been shown that a continuously variable semiactive suspension system is able to achieve performance comparable to that of a fully active system [5]. It is also possible to develop a control policy in which the damper is not just switched between a high and low state, but has an infinite number of positions in-between. This type of system is called a continuously variable semiactive system. The ranges of damping values used in these two systems are illustrated in Figure 1.9.

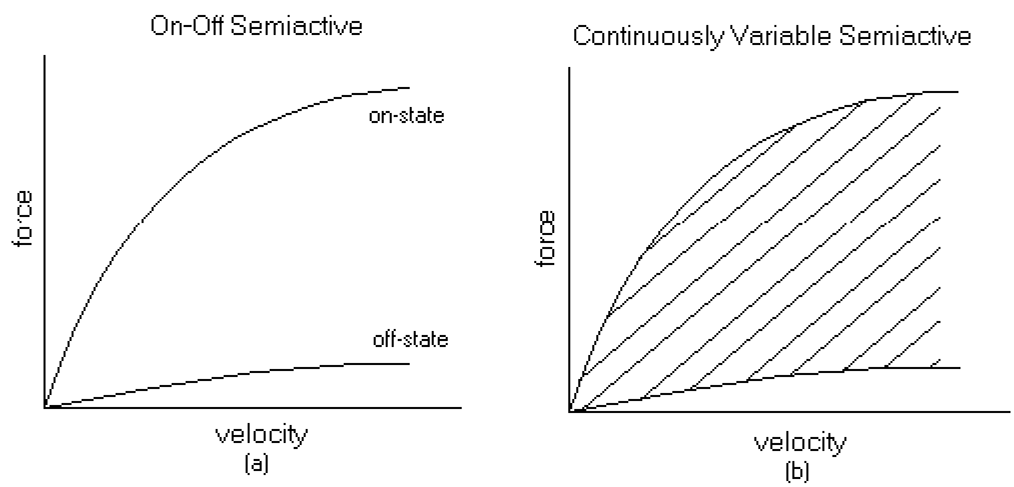

Figure 1.9. Range of Damping Force; (a) On-Off Semiactive Damping; (b) Continuously Variable Semiactive Damping

Further research indicated that performance of an on-off semiactive suspension system would be very close to the performance of a continuously variable semiactive system [6].

In the case that the controllable damper necessary in a semiactive suspension fails, the controllable damper will simply revert to a conventional damper. Semiactive systems not only have a less dangerous failure mode, but also are less complex, less prone to mechanical failure, and have much lower power requirements compared to active systems.

1.2 Literature Search

A review of the available literature in this area of research was performed to ensure that the work performed does not duplicate what has already been done. The areas of interest that were focused on within this literature search are controllable dampers, and semiactive suspensions.

1.2.1 Keyword: Controllable Damper

A search for the keyword controllable damper performed on Compendex (a comprehensive engineering index) yielded eight results. Of the eight results found, two were particularly applicable to the research discussed here. In the first, Fodor and Redfield [6] investigate the use of resistance controlled semi-active damping to improve sprung mass isolation while also reducing suspension stroke. They presented experimental results performed on a 1/30 scale 2-DOF quarter-car model and showed that the experimental results are comparable to computer simulation results. In the second paper, by Palkovics and El-Gindy [7], the authors investigate the use of different control strategies for the improvement of the handling characteristics of a 5-axle tractor-semitrailer. One of the control strategies examined involves the use of controllable dampers at the fifth-wheel joint for torque control. The control strategy used was a RLQR/H-Infinity approach, to try to ensure the vehicle's performance in the presence of parametric uncertainty. The effectiveness of this control strategy was investigated in response to a severe path-follow lane-change maneuver.

1.2.2 Keyword: Semiactive

A search for the keyword semiactive performed on Compendex yielded 198 results. Of the 198 results found, many applied to structural (rather than vehicular) vibration. Thirty eight of the remaining articles were found to be applicable. The first article, by Heo, Park, and Hwang [8] recognizes that semi-active suspension systems are being adopted into passenger vehicles based on their ability to improve ride comfort. The authors examined several control strategies and concluded (based on simulation results) that the semi-active systems are able to improve ride comfort without sacrificing driving safety.

In another article, Ursi, Ursi, Sireteanu, and Stammers [9] examined the development of control laws for semiactive suspension systems using artificial intelligence. The results of their study are based on the use of a 2-DOF quarter-car model. A different study by Fang, Chen, Wu, Wang, Fan, and Li [10] applied a fuzzy control strategy to a 4-DOF vehicle model and developed a useful control strategy. The authors performed road testing of the actual system in addition to presenting simulation results. The results (which are in approximate agreement) indicate that the performance of their semi-active suspension exceeds that of a traditional passive suspension, in terms of ride comfort. Authors Lieh and Li [11] also investigated the performance of a semi-active suspension with a fuzzy control rule, based on a quarter car model. In a similar study, authors Nicolas, Landaluze, Castrillo, Gaston, and Reyero [12] investigated (both in terms of simulation and on-road testing) the effectiveness of two fuzzy approaches to the control of a semi-active suspension system. They found that their fuzzy control approach can yield performance results similar to other control algorithms with a smaller number of required sensors, and therefore less cost. In another similar study, authors Hashiyama, Furuhashi, and Uchikawa [13] presented a new method in which a genetic algorithm is used to generate fuzzy controllers. They showed the effectiveness of their approach by generating fuzzy controllers for semi-active suspension systems. Authors Al-Holou, Sung Joo, and Shaout [14] also developed a fuzzy logic based controller for a semi-active suspension system. Their model was developed based on suspension and body velocity, and shows a major improvement over passive suspensions and a minor improvement over skyhook control.

Authors Hodmann and Holle [15] examined the use of different control algorithms for a semi-active suspension to improve the driving safety and ride comfort of a delivery truck, while Ahmadian [16] examined the effectiveness of a semi-active suspension at improving the ride of a class 8 truck. Ahmadian found that the semi-active system yielded an improved ride as compared to the passive suspension. Additionally, he found that this result could be achieved by using controllable dampers at only four of the six damper locations. A study by Margolis and Nobles [17] addressed the application of semi-active suspension systems for the heave and roll control of large off-road vehicles, and presented evidence that a properly designed semi-active suspension can result in an overall system superior to a passive system.

Giua, Seatzu, and Usai [18] presented a two-phase design technique for developing semi-active suspension control algorithms. In the first phase of their design technique, they computed a target active control law that can be implemented by Optimal Gain Switching, and then, in the second phase, they approximated this target by controlling the variable damping coefficient of the semi-active suspension. They showed (by way of simulation results) that the performance of the semi-active suspension is close to the performance of the ideal active suspension. Saxon, Meldrum, and Bonte [19] confirmed that ride quality and stability are the greatest advantages of using a semi-active suspension through field-testing. Authors Nakai, Yoshida, Ohsaku, and Motozono [20] focused on the design of a practical observer for use with a semiactive suspension, and showed a method that reduces the quantity of computation generally inherent in the use of observers. Their results are verified through simulations and experiments. In the area of semi-active suspension analysis, authors Hwang, Heo, Kim, and Lee [21] developed a semi-active control algorithm using a “hardware-in-the-loop” approach (based on a ¼ car model). They compared simulation results for passive, on/off and continuously controlled dampers. Leigh [22] develops the controller for a semi-active damper from second-order equations and compared the simulated performance with that of a full-state system, again based on a quarter car model. He also investigated the effects of high damping levels and control valve switching time on the ride performance. Gordon and Best [23] utilized a suspension ride model incorporating actuator dynamics and damper compliance to compare the performance of a number of semi-active control laws. Their analysis focused on the effectiveness of clipped linear controllers and was restricted to the response of the model to initial condition disturbances. A paper by Venhovens, Van Der Knapp, Savkoor, and Van Der Weiden [24] examined the relation between vertical and lateral dynamics with respect to suspension control, as well as the interaction between the suspensions at each of the four wheels of a passenger car. Their analysis is based on a full-vehicle model. In a similar paper, Venhovens, Van Der Knapp, and Pacejka [25] examined using semi-actively generated compensation forces to prevent a car from rolling in curves and pitching during braking or accelerating. They found that the performance of their control strategy was commensurate with the performance of a fully active suspension system.

Leih [26] showed that the switching time of a controllable damper used as part of a semi-active suspension can have an appreciable effect on the vehicle ride, suspension travel, and tire deflection. These conclusions are based on an analysis performed on a passenger car model with a full car body and four wheel-axle assemblies. Redfield [27] also investigated the performance of low-bandwidth semi-active damping concepts. Yi and Hedrick [28] investigated the effectiveness of semi-active suspension systems at controlling dynamic tire forces. Their investigation was carried out using a laboratory test vehicle equipped with controllable dampers, accelerometers, and a computer. Their study shows that the performance of the semi-active system is close to that of the best passive system for all frequency ranges. In another study, Leigh [29] addressed the effect of the slope of the controllable damper saturation nonlinearities on the performance of a semi-active system, including the effect on high frequency wheel hop. Miller and Nobles [30] developed methods for eliminating jerk and noise in semi-active suspensions by reducing the magnitude of force discontinuities that can result from both on-off and continuous semi-active control policies.

Crolla and Abdel-Hady [31] studied various control laws for semi-active suspension and achieve their best results by making use of the fact that the input to the rear wheels of the vehicle can be previewed by measuring the input to the front wheels of the vehicle. The delay between the input to the front wheels and the rear wheels can be calculated from the vehicle speed and wheelbase. They found that a semi-active system that makes use of this feed-forward information can achieve performance superior to the performance of a fully active system that does not make use of this information.

1.2.3 Literature Search Summary

Though there has been significant research in the areas of semiactive suspension systems and controllable dampers, there are still areas in which significant research is missing. The most obvious failing of research previously performed in this area is that researchers have not completed whole studies. That is, have not performed studies in which the expected performance of semiactive suspension is investigated by way of multiple approaches. Past studies have investigated aspects of performance via testing or simulation, but only in very rare instances have researchers investigated both aspects. The study presented in this document is an investigation encompassing multiple approaches. This complete approach provides a more complete analysis, and therefore a more complete understanding of the application of semiactive suspensions for passenger vehicles. Additionally, this study extends the body of work in this area by proposing additionally, non-standard control approaches which are then investigated, and characterized.

1.3 Objective

The primary objectives of this study are to:

1. investigate the effectiveness of semiactive suspensions for improving vehicle roll dynamics, particularly as it pertains to sport utility vehicles;
2. evaluate, both analytically and experimentally, various semiactive control policies that can provide improved roll dynamics, as compared to conventional passive suspensions, without degradation of the vehicle ride comfort;
3. provide a thorough on-the-vehicle comparison between passive suspensions and the commonly used semiactive suspensions control policies, such as skyhook control, and other semiactive policies proposed in this study; and

4. provide recommendations to automotive suspension designers on the practical merits of different semiactive control methods and how they perform in different vehicle configurations, in particular as related to changes in vehicle load.

1.4 Approach

This investigation will have three distinct phases, as follows:

1. Phase I: The first phase involves simulating the performance of an SUV class vehicle with a semiactive suspension operated according to different control strategies. The effectiveness of the different strategies will be compared to the performance of the stock suspension, as well as to each other. The simulations will be based on a roll-plane model so that we can address the vehicle's roll dynamics.
2. Phase II: The second phase involves performing the same kind of investigations on an actual vehicle in a laboratory setting. This allows us to isolate the effect of the changes made in the control strategy of the semiactive suspension. The laboratory setting will also allow us to take a more complete set of data pertaining to the suspension performance than is practical in a road-testing environment.
3. Phase III: The third and final phase is the testing of the different control strategies developed in the earlier phases on a vehicle during controlled driving experiments. This is the ultimate test of the effectiveness of these control strategies. The result of this research will be a clear understanding of the effectiveness of the semiactive control strategies investigated.

CHAPTER 2

NUMERICAL MODEL

This section discusses the motivation behind the development of a numerical model, as well as the development of the model itself. Additionally, the development of the different system inputs that are to be used with this model will also be highlighted. The results of the use of the model will also be detailed. These results will be presented section by section and will be summarized at the end of this chapter.

2.1 Numerical Model Motivation

The numerical model developed for this study is used for three purposes:

- To develop and tune different semiactive control policies,
- To compare the effectiveness of the selected semiactive control policies with conventional passive suspensions, and
- To determine how variation of vehicle parameters may influence the effectiveness of the different semiactive policies.

The possession of a valid numerical model capable of simulating the response of the system to an arbitrary input can be an invaluable tool in this investigation. The use of the model allows the researchers to examine many times the number of cases than can be reasonably examined in a physical system. Of course, it is the performance of the actual physical system that ultimately determines the effectiveness of any of the control systems examined here, but the use of a model of the system is no less valuable because of this. There are a number of considerations that have to be taken into account during the development of the numerical model.

2.2 Numerical Model Development

Some of the most important aspects of the numerical model used for simulating the response of the system include:

- The mathematical development of, and the coding of the model,
- Determining accurate vehicle model parameters,
- The development and coding of various controllers to be used in conjunction with the model,
- Developing inputs to be used for simulation, and
- Decisions regarding what aspects of the simulation output have the greatest relevance in evaluating the relative merits of the different control strategies.

2.2.1 Mathematical Model

In order to be useful, the mathematical model must be sufficiently complex to accurately include the dynamics of the vehicle, yet be reasonably simple to manipulate. In order to examine the roll dynamics of a vehicle, the simplest model that can be used is a two-degree-of-freedom roll plane model, shown in Figure 2.1.

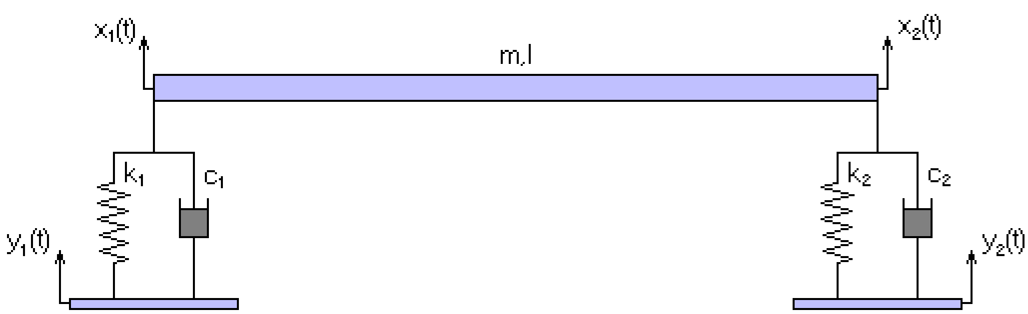

Figure 2.1. Two-Degree-of-Freedom Roll Plane Model

In this model, a bar of specified mass, moment of inertia, and length represents the vehicle body. The two-degrees-of-freedom (x_1 and x_2) represent the vertical motion of either side of the vehicle. In this two-degree-of-freedom model, the inputs (y_1 and y_2) represent the motion of the two sides of an axle of the vehicle. The suspension system parameters are c_1, c_2, k_1, and k_2. This model, however, does not include the tire/axle dynamics and may not sufficiently characterize the vehicle dynamics in the roll plane. Incorporating the dynamics of the tire/axle into the model results in a four-degree-of-freedom model, shown in Figure 2.2.

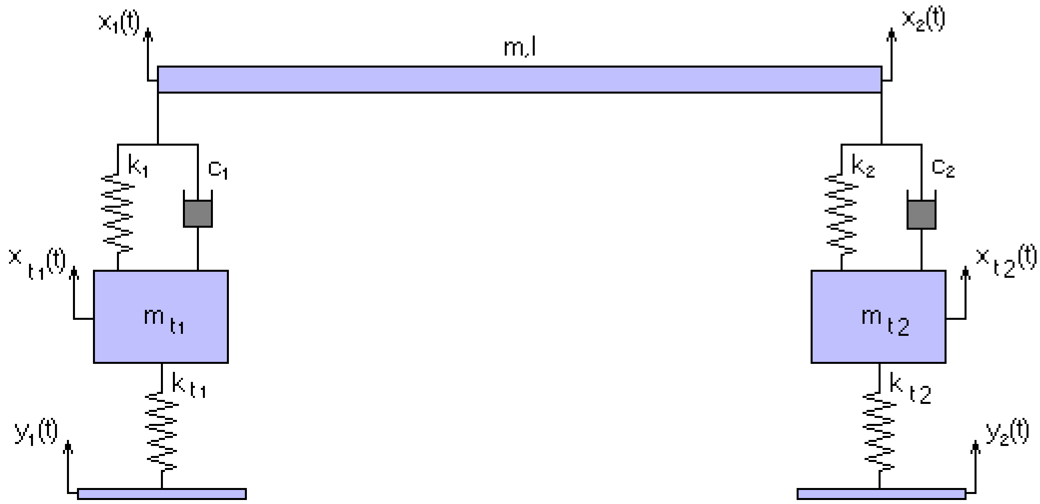

Figure 2.2. Four Degree of Freedom Roll Plane Model

In this model, a bar of specified mass, moment of inertia, and length again represents the body of the vehicle. Likewise, x_1 and x_2 represent the vertical motion of either side of the vehicle. The spring constants of the primary suspension of the vehicle are represented by k_1 and k_2, while the damping rates of the primary suspension are represented by c_1 and c_2. The mass of the wheel/axle on either side is represented by m_{t1} and m_{t2}, while the position of either tire is represented by x_{t1} and x_{t2}. The vertical stiffness of each of the vehicle wheels are represented by k_{t1} and k_{t2}. The inputs to this system are now the road profile under each of the two vehicle wheels (y_1 and y_2). By incorporating these additional degrees of freedom into the model, we now capture the dynamics of the vehicle wheel/axle, which better captures the true dynamic situation.

The governing equations for the model in Figure 2.2 can be easily derived as:

$$\frac{m}{2}(\ddot{x}_2+\ddot{x}_1)+k_1(x_1-x_{t1})+k_2(x_2-x_{t2})=c_1(\dot{x}_{t1}-\dot{x}_1)+c_2(\dot{x}_{t2}-\dot{x}_2) \tag{2.2a}$$

$$\frac{I}{l}(\ddot{x}_2-\ddot{x}_1)+\frac{k_2 l}{2}(x_2-x_{t2})-\frac{k_1 l}{2}(x_1-x_{t1})=\frac{c_1 l}{2}(\dot{x}_1-\dot{x}_{t1})-\frac{c_2 l}{2}(\dot{x}_2-\dot{x}_{2t}) \tag{2.2b}$$

$$m_{t1}\ddot{x}_{t1}+k_1(x_{t1}-x_1)+c_1(\dot{x}_{t1}-\dot{x}_1)=k_{t1}(y_1-x_{t1}) \tag{2.2c}$$

$$m_{t2}\ddot{x}_{t2}+k_2(x_{t2}-x_2)+c_2(\dot{x}_{t2}-\dot{x}_2)=k_{t2}(y_2-x_{t2}) \tag{2.2d}$$

Rewriting the equations in a matrix form results in:

$$\begin{bmatrix} \frac{m}{2} & \frac{m}{2} & 0 & 0 \\ \frac{-I}{l} & \frac{I}{l} & 0 & 0 \\ 0 & 0 & m_{t1} & 0 \\ 0 & 0 & 0 & m_{t2} \end{bmatrix} \begin{Bmatrix} \ddot{x}_1 \\ \ddot{x}_2 \\ \ddot{x}_{t1} \\ \ddot{x}_{t2} \end{Bmatrix} + \begin{bmatrix} k_1 & k_2 & -k_1 & -k_2 \\ \frac{-k_1 l}{2} & \frac{k_2 l}{2} & \frac{k_1 l}{2} & \frac{-k_2 l}{2} \\ -k_1 & 0 & k_1+k_{t1} & 0 \\ 0 & -k_2 & 0 & k_2+k_{t2} \end{bmatrix} \begin{Bmatrix} x_1 \\ x_2 \\ x_{t1} \\ x_{t2} \end{Bmatrix} = \tag{2.3}$$
$$\begin{bmatrix} -c_1 & -c_2 & c_1 & c_2 \\ \frac{c_1 l}{2} & \frac{-c_2 l}{2} & \frac{-c_1 l}{2} & \frac{c_2 l}{2} \\ c_1 & 0 & -c_1 & 0 \\ 0 & c_2 & 0 & -c_2 \end{bmatrix} \begin{Bmatrix} \dot{x}_1 \\ \dot{x}_2 \\ \dot{x}_{t1} \\ \dot{x}_{t2} \end{Bmatrix} + \begin{bmatrix} 0 & 0 & 0 & 0 \\ 0 & 0 & 0 & 0 \\ 0 & 0 & k_{t1} & 0 \\ 0 & 0 & 0 & k_{t2} \end{bmatrix} \begin{Bmatrix} 0 \\ 0 \\ y_1 \\ y_2 \end{Bmatrix}$$

Pre-multiplying by the inverse of the mass matrix, we develop the following matrix, we have:

$$[I]\begin{Bmatrix} \ddot{x}_1 \\ \ddot{x}_2 \\ \ddot{x}_{t1} \\ \ddot{x}_{t2} \end{Bmatrix} + \begin{bmatrix} \frac{k_1}{m}+\frac{k_2 l^2}{4I} & \frac{k_2}{m}-\frac{k_2 l^2}{4I} & \frac{-k_1}{m}-\frac{k_2 l^2}{4I} & \frac{-k_2}{m}+\frac{k_2 l^2}{4I} \\ \frac{k_1}{m}-\frac{k_2 l^2}{4I} & \frac{k_2}{m}+\frac{k_2 l^2}{4I} & \frac{-k_1}{m}+\frac{k_2 l^2}{4I} & \frac{-k_2}{m}-\frac{k_2 l^2}{4I} \\ \frac{-k_1}{m_{t1}} & 0 & \frac{k_1+k_{t1}}{m_{t1}} & 0 \\ 0 & \frac{-k_2}{m_{t2}} & 0 & \frac{k_2+k_{t2}}{m_{t2}} \end{bmatrix} \begin{Bmatrix} x_1 \\ x_2 \\ x_{t1} \\ x_{t2} \end{Bmatrix} = \tag{2.4}$$
$$\begin{bmatrix} \frac{-c_1}{m}-\frac{c_2 l^2}{4I} & \frac{-c_2}{m}+\frac{c_2 l^2}{4I} & \frac{c_1}{m}+\frac{c_2 l^2}{4I} & \frac{c_2}{m}-\frac{c_2 l^2}{4I} \\ \frac{-c_1}{m}+\frac{c_2 l^2}{4I} & \frac{-c_2}{m}-\frac{c_2 l^2}{4I} & \frac{c_1}{m}-\frac{c_2 l^2}{4I} & \frac{c_2}{m}+\frac{c_2 l^2}{4I} \\ \frac{c_1}{m_{t1}} & 0 & \frac{-c_1}{m_{t1}} & 0 \\ 0 & \frac{c_2}{m_{t2}} & 0 & \frac{-c_2}{m_{t2}} \end{bmatrix} \begin{Bmatrix} \dot{x}_1 \\ \dot{x}_2 \\ \dot{x}_{t1} \\ \dot{x}_{t2} \end{Bmatrix} + \begin{bmatrix} 0 & 0 & 0 & 0 \\ 0 & 0 & 0 & 0 \\ 0 & 0 & \frac{k_{t1}}{m_{t1}} & 0 \\ 0 & 0 & 0 & \frac{k_{t2}}{m_{t2}} \end{bmatrix} \begin{Bmatrix} 0 \\ 0 \\ y_1 \\ y_2 \end{Bmatrix}$$

These equations can now be used to develop a Simulink block diagram such as shown in Figure 2.3.

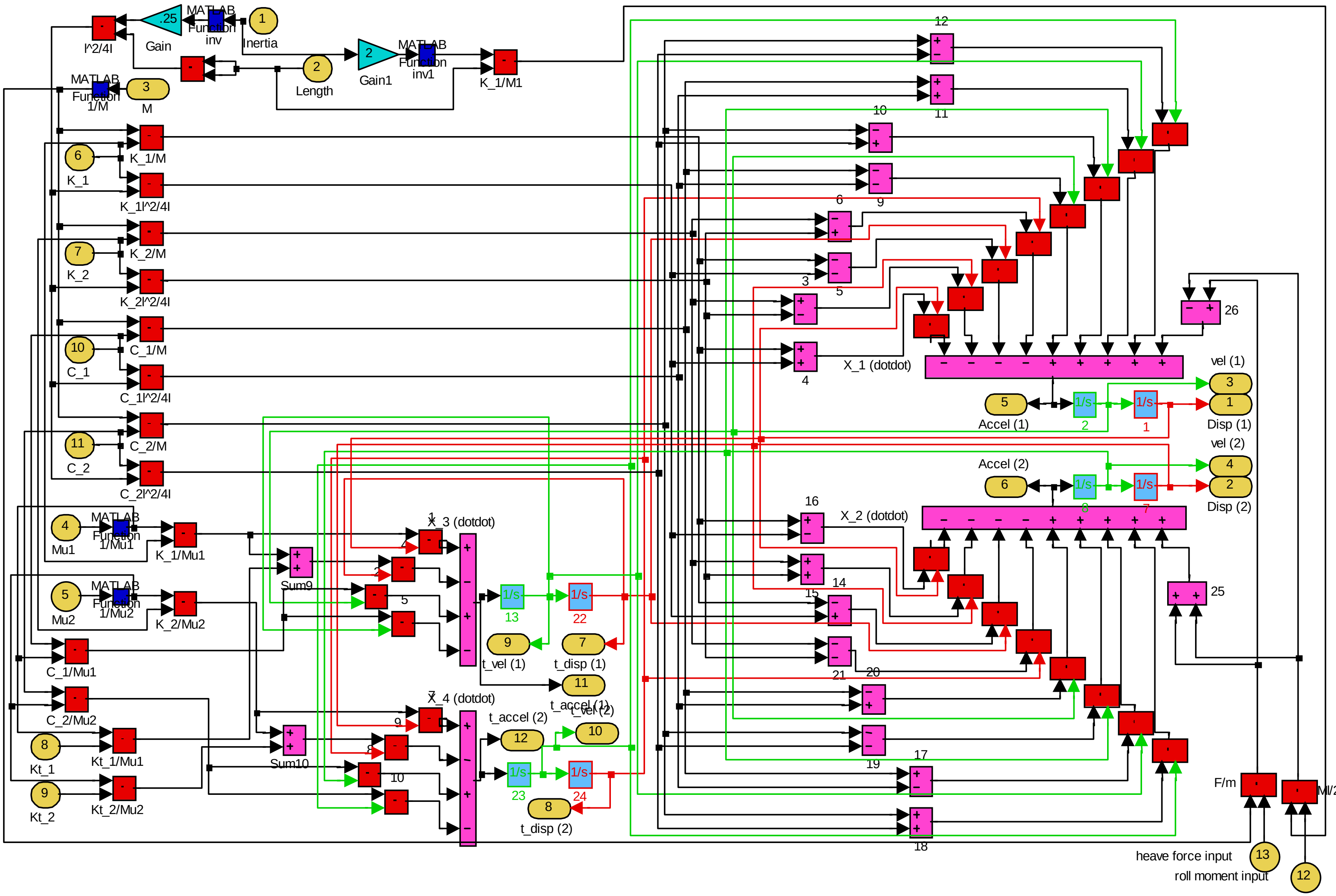

Figure 2.3. SIMULINK Block Diagram for a Four-Degree-of-Freedom Vehicle Roll-Plane Model

The Simulink model shown in Figure 2.3, simulates the response of a passive four-degree-of-freedom system to two road inputs, and is meant to be an example of the type of model used in this study, but is not by any means to be taken as the extent of the code developed.

2.2.2 Vehicle Model Parameters

The parameters shown in Table 2.1 are determined to be representative of the class of vehicle studied.

Table 2.1. Vehicle Parameters (Baseline Model) Simulation

Parameter	Description	Value
$\omega_{n,heave}$	Heave natural frequency	1.3 Hz (8.17 rad/s)
$\omega_{n,roll}$	Roll natural frequency	3.0 Hz (18.84 rad/s)
m_{tire}	Mass of the tire/axle	36.26 kg (80 lb)
R	The mass ratio m^*/m_t	8
$\zeta_{passive}$	Passive damping ratio	0.15
L	Vehicle track	1.524 m (60 in)
k_t	Tire vertical stiffness	96319.76 N/m (550 lb/in)

Additionally, the parameters in Table 2.2 are derived from those in Table 2.1, for the purpose of our simulation.

Table 2.2. Derived Parameters for Vehicle Simulation

Derived Parameter	Description	Value
M	Mass of ½ car	580 kg (1280 lb)
K	Spring stiffness	19357.2 N/m (110.4 lb/in)
I	Rotational Inertia of ½ car	63.3316 kg-m^2 (6726.4 slug-in^2)
c	Damping constant	710.79 N-2/m (4.06 lb-s/in)

2.3 Controller Development

Though more complicated feedback control strategies offer great possibilities in many situations, it is predicted that significant performance gains can be realized with basic control strategies arising from optimal control theory. In the initial phases of the numerical part of this study, two basic strategies were examined:

- Velocity skyhook control, and
- Displacement skyhook control

2.3.1 Velocity Skyhook Control

In velocity skyhook control, the system's controllable damping constant is adjusted so that the damper's force emulates the damper force that would be present if the damper was arranged in a skyhook configuration. The ideal velocity skyhook configuration is shown in Figure 2.4.

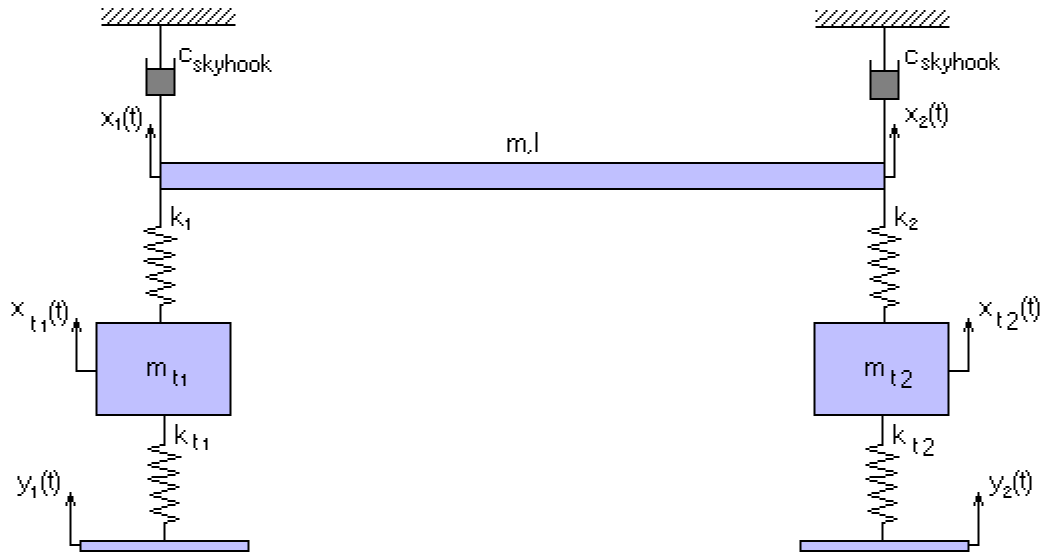

Figure 2.4. Four-Degree-of-Freedom System With Ideal Velocity Skyhook Configuration

This implies that the ideal velocity skyhook damper force can be calculated as:

$$
\begin{aligned}
c_1 &= \frac{c_{skyhook}\dot{x}_1}{\dot{x}_1 - \dot{x}_{t1}} \\
c_2 &= \frac{c_{skyhook}\dot{x}_2}{\dot{x}_2 - \dot{x}_{t2}}
\end{aligned}
\qquad (2.5)
$$

Of course, even though the damper is controllable, it still has the same limitations of a conventional damper, the damper constants c_1, and c_2 are limited by the physical parameters of the damper. This means that not only can neither c_1 or c_2 be negative, but also that there are both upper and lower bounds on both, i.e., both c_1 and c_2 saturate at both their upper and lower bounds. This formulation bypasses the conventional switching logic common to skyhook control systems.

2.3.2 Displacement Skyhook Control

In displacement skyhook control, the system's controllable damping constant is adjusted so that the damper's force emulates the force that would be present from a spring connected directly from the sprung mass to ground. The ideal displacement skyhook configuration is shown in Figure 2.5.

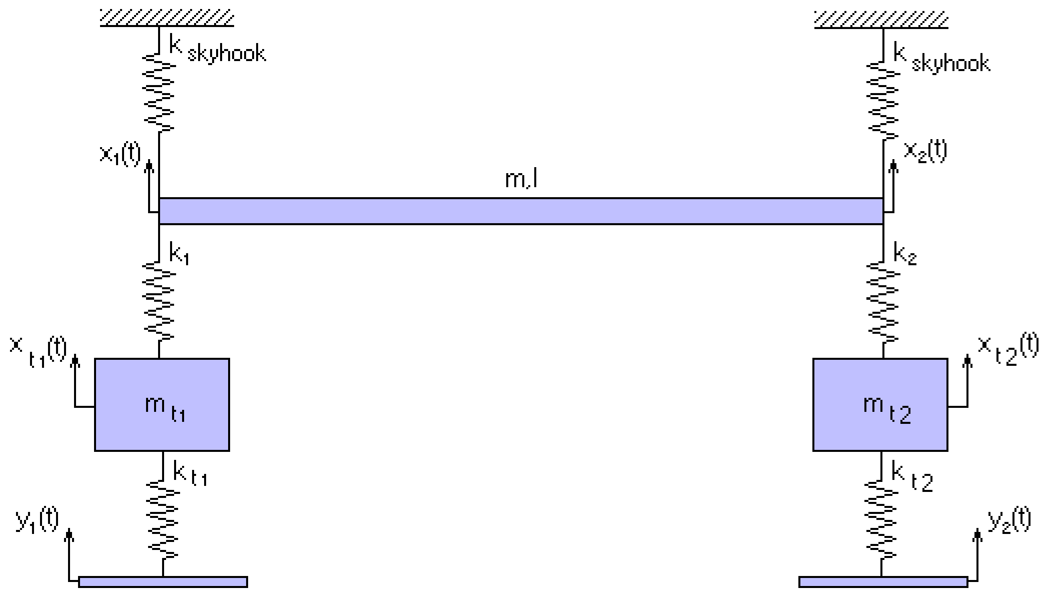

Figure 2.5. Four-Degree-of-Freedom System With Ideal Displacement Skyhook Configuration

This model implies that the ideal displacement skyhook damper force can be calculated as:

$$c_1 = \frac{k_{skyhook} x_1}{\dot{x}_1 - \dot{x}_{t1}}$$
$$c_2 = \frac{k_{skyhook} x_2}{\dot{x}_2 - \dot{x}_{t2}} \quad (2.6)$$

Like the velocity skyhook configuration, the damper still has the same limitations on the values that c_1 and c_2 can take. That is, the damper constants c_1, and c_2 are still limited by the physical parameters of the damper meaning that not only can neither c_1 or c_2 be negative, but also that there are both upper and lower bounds on both. This formulation likewise bypasses the conventional switching logic common to skyhook control systems.

2.4 *Simulation Inputs*

In order to pursue control system development and system design, it is necessary to create system inputs which can be used to test the effectiveness of the various configurations investigated. To this end, three basic inputs are examined. They are:

- A heave type input,
- A sinusoidal type input,
- And a moment (force) type input.

2.4.1 *Heave Input*

A heave type input was created in order to investigate the response of the system to this type of input. The input created has an amplitude of 0.1 m and a duration of three seconds. The profile of the input is a half-sine. This input was applied to both wheels (y_1 and y_2) one second out of phase so as to excite both heave and roll modes. A profile of the input is shown in Figure 2.6.

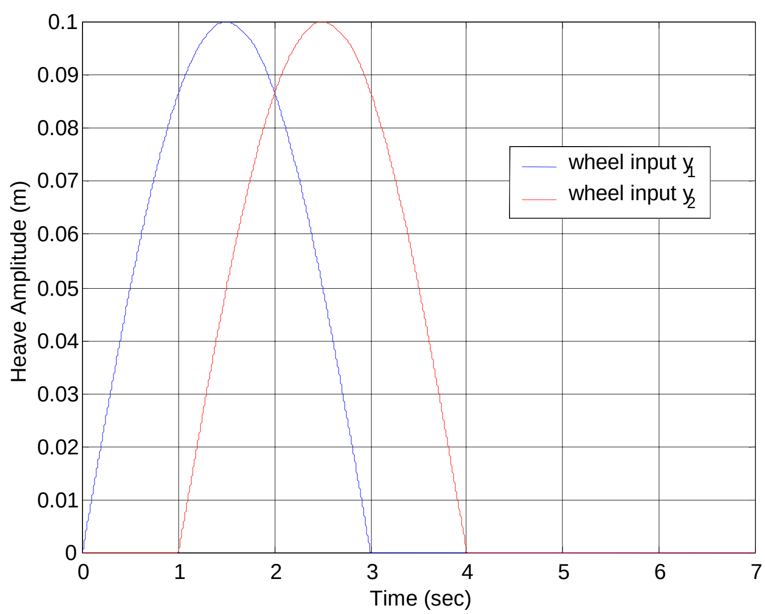

Figure 2.6. Heave Input

2.4.2 Sinusoidal Input

A sinusoidal type input was created in order to investigate the response of the system to this type of input. The input created consisted of the summation of two sine waves. The two waves had frequencies of 1.3 and 3.0 Hz, and amplitudes of 0.025 and 0.05 m, respectively. This was done in order to excite both the heave and roll modes of the system. This input was applied to both wheels (y_1 and y_2) 0.25 seconds out of phase so as to excite both heave and roll modes. A profile of the input is shown in Figure 2.7.

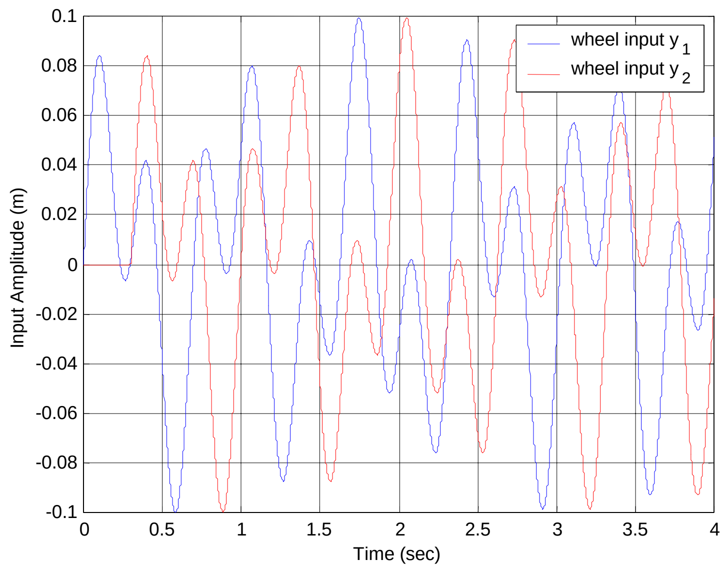

Figure 2.7. Sinusoidal Input

2.4.3 Moment (Force) Input

A moment type input was created in order to investigate the response of the system to this type of input. The input created consisted of a half sine wave with an amplitude of 500 N-m and a duration of 4 seconds. This input is meant to emulate the cornering force that is applied to the body of a vehicle as it negotiates a turn. This input was applied directly to the body of the vehicle. A profile of the input is shown in Figure 2.8.

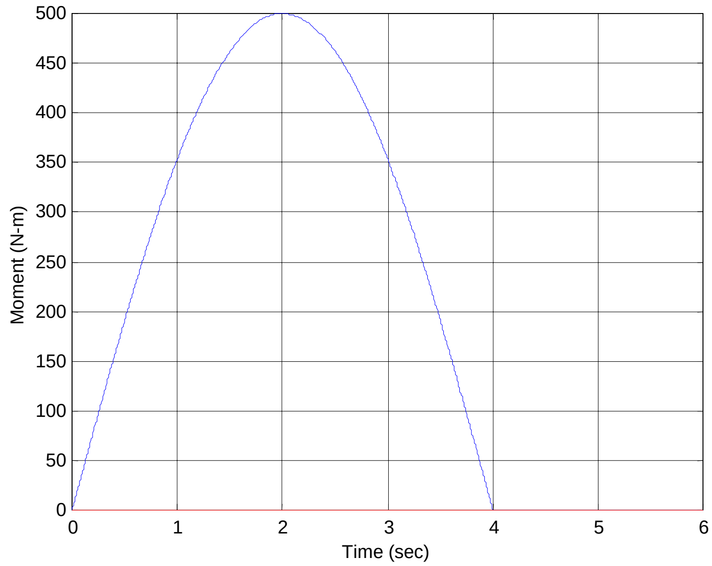

Figure 2.8. Moment (Force) Input

2.5 Data Reduction

In order for the simulation to be useful, it is necessary to characterize the output. Though time traces can be exceedingly informative in a case by case basis, it is not possible to develop useful information from a large quantity of them without first processing them into a meaningful form. To this end, the output of a number of variables pertaining to the model were recorded during simulation and then processed. The outputs measured are:

- Body displacements x_1 and x_2,
- Tire deflections x_{1t} and x_{2t},
- Body accelerations $\ddot{x}_1$ and $\ddot{x}_2$, and
- Tire accelerations $\ddot{x}_{1t}$ and $\ddot{x}_{2t}$.

For each simulation, eight time traces were recorded. Then, two additional (derived) measurements were generated. These are the difference between x_1 and x_2, and the difference between $d^2/dt^2(x_1)$and $d^2/dt^2(x_2)$; these being measures of vehicle roll and vehicle roll acceleration respectively. In order to make these time series more manageable, certain characteristics of each were then calculated. These characteristics are the peak value of each trace, as well as the average value of the absolute value of the trace (a measurement similar to finding the Root Mean Squared (RMS) value of the trace;

equal to the area under the curve divided by the length). Graphically, these quantities are shown in Figure 2.9.

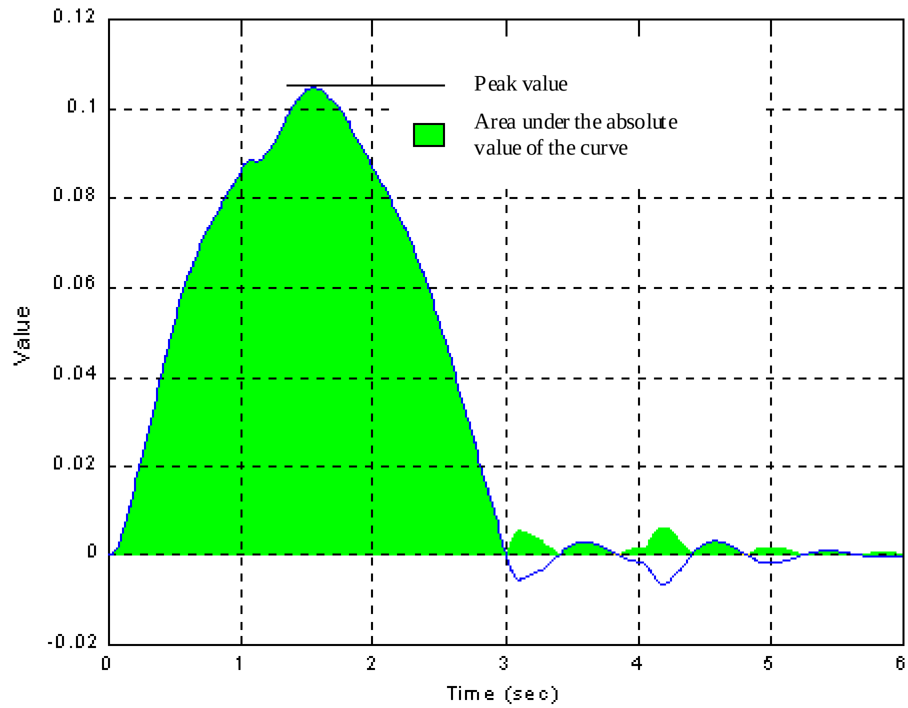

Figure 2.9. Sample Time Trace Showing Peak and Area Under the Curve Measurements

The results that will be presented in the following sections are reduced according to the above method.

2.6 Control Policy Tuning and Development

In order to get the best possible performance from any semiactive control policy it is first necessary to determine what "best" means, and what measures are used to define "best". The design objectives of this study are two fold: 1) to increase the safety of the vehicle by improving its stability, and 2) providing modest improvements (or minimal deterioration) of vehicle comfort. To this end, we relate different measurements from the model to stability, comfort, or neither, as listed in Table 2.3.

Table 2.3. Measurement Safety/Comfort Correlations

Measurement	x_1 disp. trace area	x_2 disp. trace area	x_1-x_2 disp. trace area	x_1 disp. trace peak	x_2 disp. trace peak
Correlation	stability	stability	stability	stability	stability
Measurement	x_1 accel. trace area	x_2 accel. trace area	x_1-x_2 accel. trace area	x_1 accel. trace peak	x_2 accel. trace peak
Correlation	neither	neither	neither	comfort	comfort
Measurement	x_1-x_2 disp. trace peak	x_{1t} disp. trace area	x_{2t} disp. trace area	x_{1t}-x_{2t} disp. trace area	x_{1t} disp. trace peak
Correlation	stability	stability	stability	stability	stability
Measurement	x_1-x_2 accel. trace peak	x_{1t} accel. trace area	x_{2t} accel. trace area	x_{1t}-x_{2t} accel. trace area	x_{1t} accel. trace peak
Correlation	neither	neither	neither	neither	neither

For the control policies investigated here, it was necessary to determine two parameters of the controllable damper. These parameters are c_{on} and c_{off}. Together, they determine the range in which the controllable damper can operate, as shown in Figure 2.10.

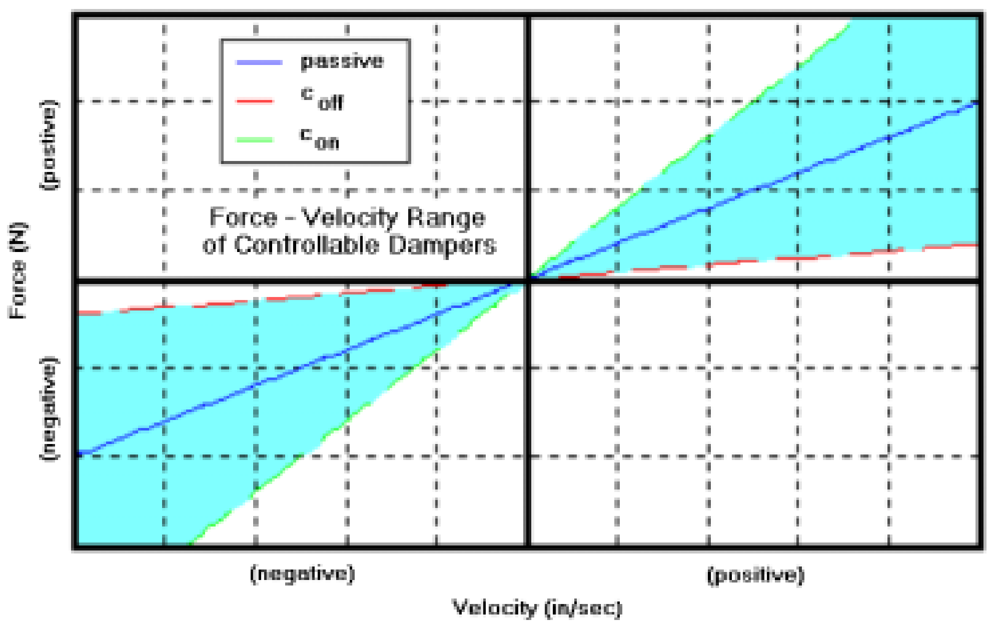

Figure 2.10. Controllable Damper Operating Range

In order to verify that changing the damping rates of the system would have a significant effect on the system's response to the inputs in question, the stock passive system was simulated and the response investigated for damping rate factors ranging from 0.2 to 1.8.

The damping rate factor is the level of damping in the system given as a multiplicative factor to be used with the nominal level of damping. A system with a damping rate factor of 0.5 will have half the damping of the original system. Figure 2.11 shows the results of testing with different damping rate factors, in terms of displacement and Figure 2.12 shows them in terms of Acceleration.

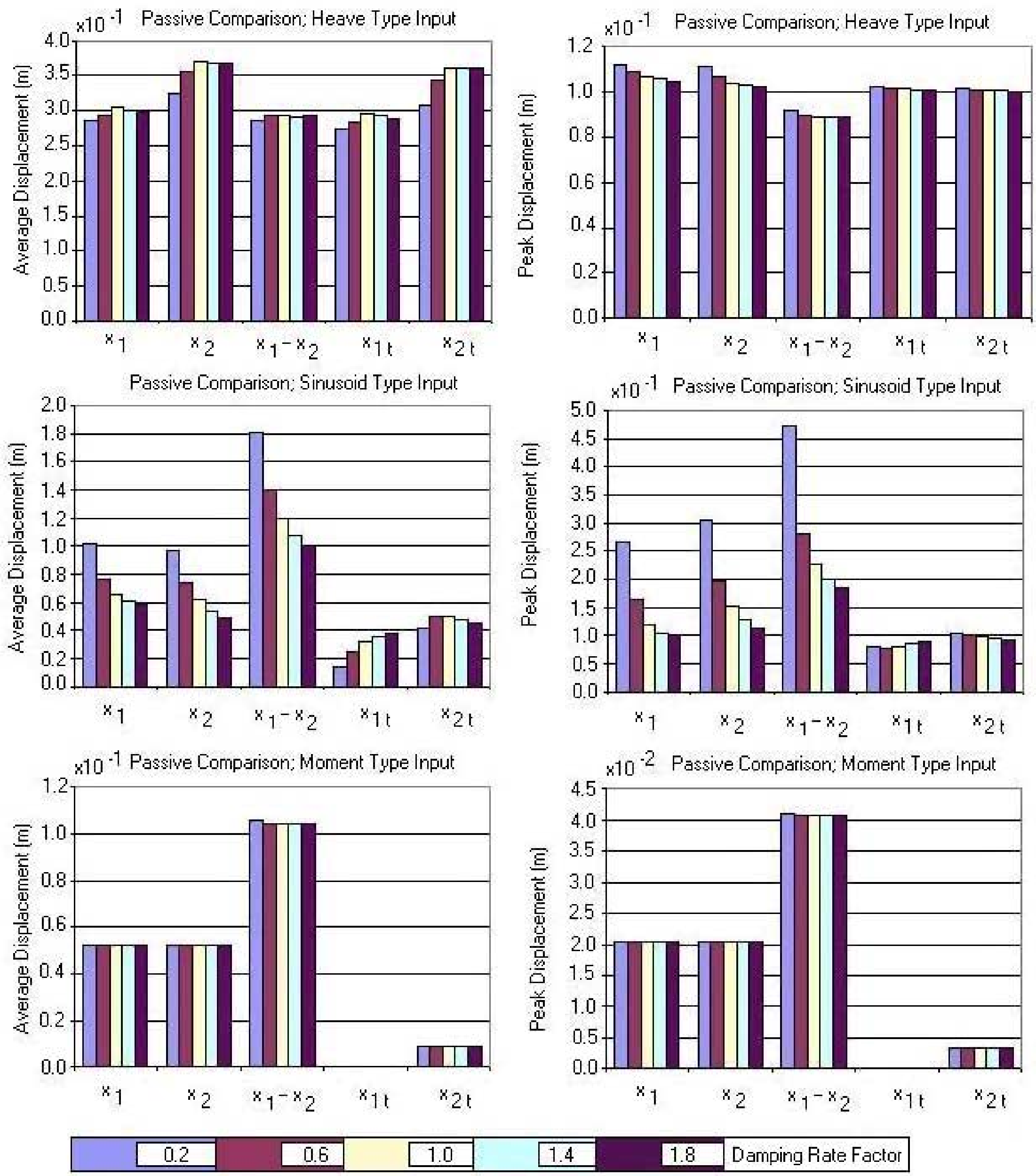

Figure 2.11. Passive Damper Comparison Shown in Terms of Displacement Outputs

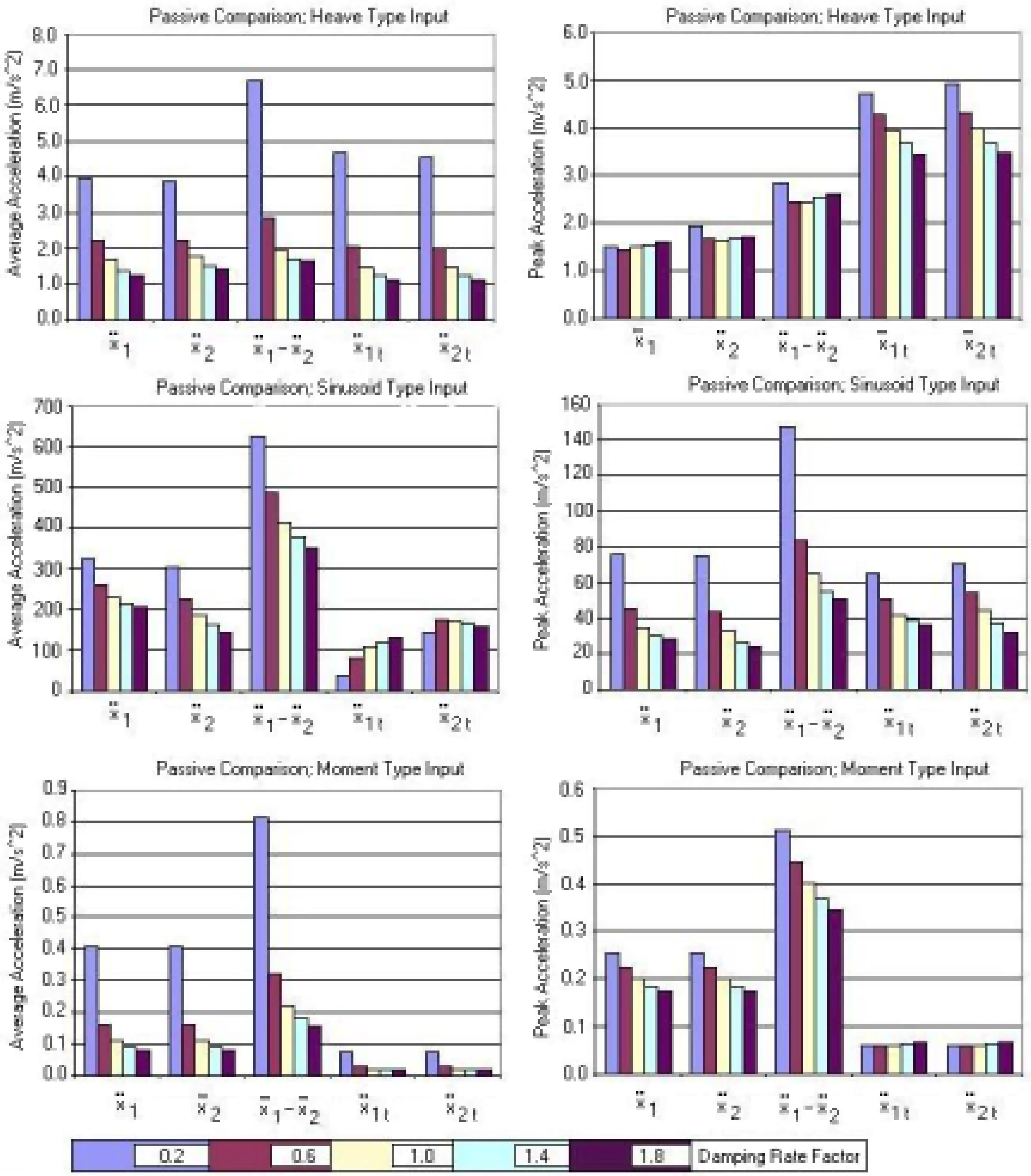

Figure 2.12. Passive Damper Comparison Shown in Terms of Acceleration Outputs

These figures clearly show that it is possible to influence the system outputs by varying the level of damping present in the system. The semiactive control policies developed subsequently can only control within the envelope defined by the above plots.

Since there are two parameters that are varied, it made sense to examine the results in terms of surface plots. By doing this, it is possible to determine how each of the aforementioned relevant parameters varies with these two variables. An example of this is shown in Figure 2.13.

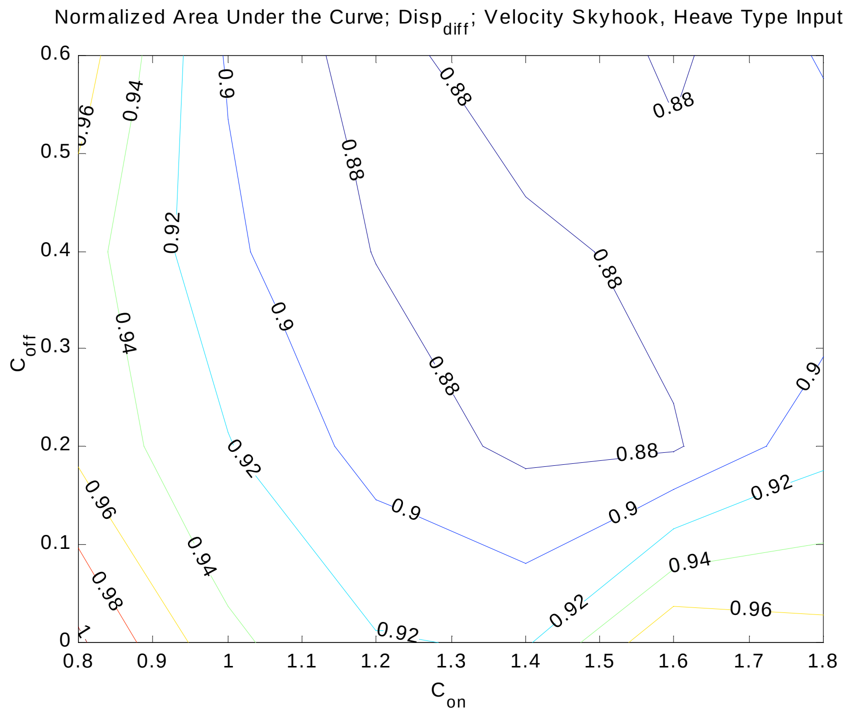

Figure 2.13. Sample Surface Plot Showing the Variation of the Area Under the x_1-x_2 Trace with c_{off} and c_{on}

In the above sample plot, the values of the contours have been normalized to those of the passive case with the same input. This allows for simple visual confirmation of the effectiveness of the policy. For example: a contour of 0.9 indicates a 10% decrease from the passive case. Plots such as the one above were generated for each of the measurement positions, as well as for each of the three different inputs. This was also repeated for each of the different control policies. The above contour plot shows that if the objective were solely to reduce the area under the x_1-x_2 trace in response to a heave type input, then the controllable damper parameters c_{off} and c_{on} should be set at 0.3 and 1.4 (times the nominal damping value) respectively. Of course when different inputs are looked at, as well as different measurement positions, this result varies.

2.6.1 *Velocity Skyhook Damper Tuning Results*

After generating all the relevant contour plots for the case of velocity skyhook control in response to the three inputs the results (optimal c_{off} and c_{on} values; in terms of their multiplication factor compared to the nominal value) were concatenated as shown in Table 2.4.

Table 2.4. Velocity Skyhook Optimal Results

Input:	Heave Displacement		Sinusoid Displacement		Moment (force)	
Measurement	Coff	Con	Coff	Con	Coff	Con
X1 Disp Area	0.3	1.4	0	1.8	0.6	1.8
X1 Disp Peak	0.6	1.8	0	1.8	0.6	1.8
X2 Disp Area	0.3	1.4	0	1.8	0.6	1.8
X2 Disp Peak	0.6	1.8	0.6	1.8	0.2	1.3
X1-X2 Disp Area	0.3	1.4	0	1.8	0.6	1.8
X1-X2 Disp Peak	0.6	1.8	0	1.8	0.6	1.8
X1t Disp Area	0.5	1.2	0.4	0.8	0.6	1.8
X1t Disp Peak	0.6	1.8	0.6	0.8	0.6	0.8
X2t Disp Area	0.3	1.5	0	0.8	0.6	1.8
X2t Disp Peak	0.6	1.8	0	1.8	0.2	1.3
X1 Accel Peak	0.3	1.7	0.6	1.8	0.6	1.4
X2 Accel Peak	0.6	1.8	0	1.8	0.6	1.4
X1-X2 Accel Peak	0.6	1.8	0	1.8	0.6	1.4
X1 Accel Area	0.6	1.8	0	1.8	0.6	1.8
X2 Accel Area	0.6	1.8	0	1.8	0.6	1.8
X1-X2 Accel Area	0.6	1.8	0	1.8	0.6	1.8
X1t Accel Area	0.6	1.8	0.6	1.8	0.6	0.8
X1t Accel Peak	0.6	1.8	0.6	1.8	0.6	0.8
X2t Accel Area	0.6	1.8	0.8	0.6	0.6	0.8
X2t Accel Peak	0.6	1.8	0.6	1.8	0.6	0.8

Stability	Comfort	Neither

The above table provides a good starting point for determining optimal values for the on and off state damping levels. However, since some of the outputs (peak accelerations and displacements) are particularly sensitive to variations in on and off damping states (an example of an insensitive case is shown in Figure 2.14), the above numbers are not equally weighted.

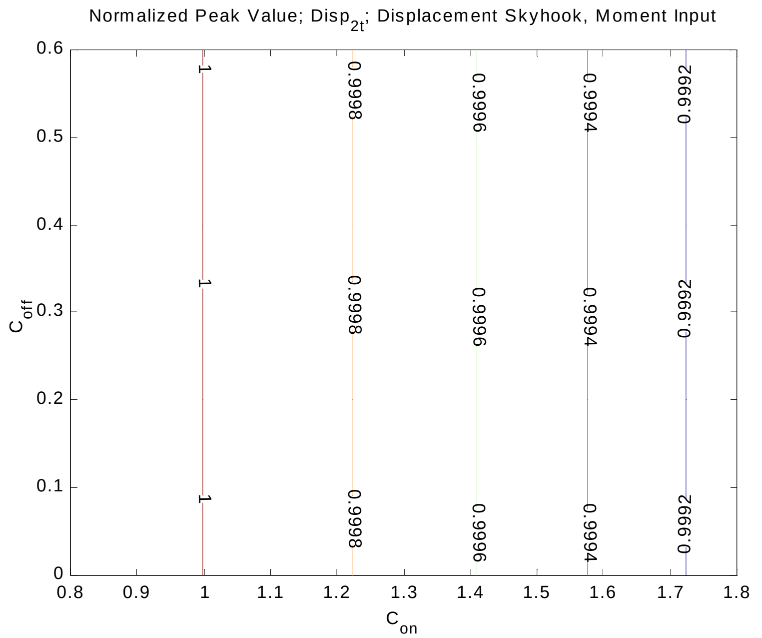

Figure 2.14. Contours Showing Insensitivity to c_{off} and c_{on}

The best judgment can be made by simultaneously examining all the contour plots for each type of control, and then determining what the best values for ($c_{off,}$ c_{on}) are. In the case of velocity skyhook control, the optimal values are (0.6, 1.8) when designing for safety and (0.6, 1.8) when designing for comfort. Thus the overall velocity skyhook policy is determined to have ($c_{off,}$ c_{on}) equal to (0.6, 1.8) for optimum performance.

2.6.2 Displacement Skyhook Damper Tuning Results

After generating all the relevant contour plots for the case of displacement skyhook control in response to the three inputs the results (optimal c_{off} and c_{on} values; in terms of their multiplication factor compared to the nominal value) were concatenated as shown in Table 2.5.

Table 2.5. Displacement Skyhook Optimal Results

Input:	Heave Displacement		Sinusoid Displacement		Moment (force)	
Measurement	Coff	Con	Coff	Con	Coff	Con
X1 Disp Area	0.6	1.8	0.6	1.8	0.6	1.6
X1 Disp Peak	0.6	1.8	0.6	1.8	0.6	1.8
X2 Disp Area	0.6	1.8	0.6	1.8	0.6	1.6
X2 Disp Peak	0.6	1.8	0.6	1.8	0.6	1.8
X1-X2 Disp Area	0.6	1.8	0.6	1.8	0.6	1.6
X1-X2 Disp Peak	0	1.4	0.6	1.8	0.6	1.8
X1t Disp Area	0.6	0.8	0.3	0.8	0.6	1.8
X1t Disp Peak	0.6	1.8	0.6	0.8	0.6	1.8
X2t Disp Area	0.6	1..8	0.6	0.8	0.6	1.8
X2t Disp Peak	0.6	1.8	0.6	1.8	0.6	1.8
X1 Accel Peak	0.2	0.8	0.6	1.8	0.6	0.8
X2 Accel Peak	0.4	1	0.6	1.8	0.6	0.8
X1-X2 Accel Peak	0	0.8	0.6	1.8	0.6	0.8
X1 Accel Area	0.6	1.8	0.6	1.8	0.6	1.8
X2 Accel Area	0.6	1.8	0.6	1.8	0.6	1.8
X1-X2 Accel Area	0.6	1.8	0.6	1.8	0.6	1.8
X1t Accel Area	0.6	1.8	0.6	0.8	0.6	0.6
X1t Accel Peak	0.6	1.8	0.6	1.8	0.6	0.6
X2t Accel Area	0.6	1.8	0.6	1.8	0.6	0.6
X2t Accel Peak	0.4	1.1	0.6	1.8	0.6	0.6

Stability	Comfort	Neither

As in the previous case where we were concerned with velocity skyhook control, the above table again provides a good starting point for determining optimal values for the on and off state damping levels. Once again, since some of the outputs (peak accelerations and displacements) are more sensitive than others to variations in the off and on state damping levels, the above numbers are not equally weighted. The best judgment can again be made by simultaneously examining all the contour plots for each type of control, and then determining what the best values for ($c_{off,}$ c_{on}) are. In the case of displacement skyhook control, the optimal values are (0.6, 0.8) when designing for safety and (0.6 1.3) when designing for comfort. Thus the overall velocity skyhook policy is determined to have ($c_{off,}$ c_{on}) equal to (0.6, 1.0) for optimum performance.

2.6.3 *Tuning Summary*

The results of the tuning for the velocity and displacement skyhook controllers are summarized in Table 2.6.

Table 2.6. Velocity and Displacement Skyhook Controller Tuning Results

	Velocity Skyhook				Displacement Skyhook			
	Safety		Comfort		Safety		Comfort	
Input	Coff	Con	Coff	Con	Coff	Con	Coff	Con
Heave:	0.3	1.4	0.6	1.8	0.6	1.8	0.4	1.1
Sinusoid:	0.6	1.8	0.6	1.8	0.6	1.1	0.6	1.1
Moment:	0.6	1.8	0.6	1.4	0.6	1.3	0.6	0.8
Overall:	0.6	1.8	0.6	1.8	0.6	1.3	0.6	0.8
Compromise:	Coff=0.6, Con=1.8				Coff=0.6, Con=1.0			

The performance of these "optimized" velocity and skyhook controllers is illustrated in Figure 2.15.

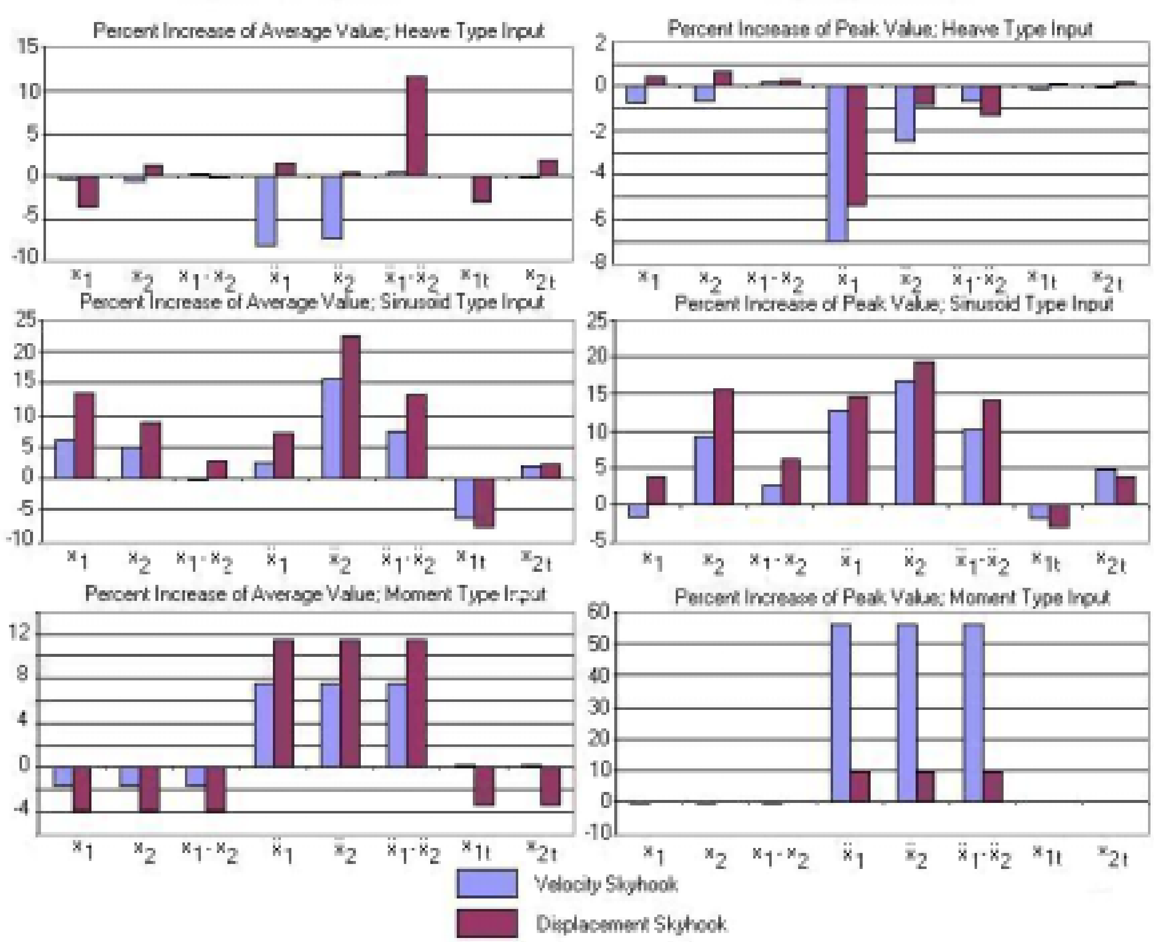

Figure 2.15. Tuned Velocity and Displacement Skyhook Controller Results

Although it is evident that significant gains can be realized through the use of this type of control policy, and that performance gains can also be realized through other closed loop control policies, these methodologies do not make use of the wealth of information that is already available on the vehicle. Some of this information includes vehicle speed, steering wheel angle, brake pressure, and throttle position. In order to achieve significant performance gains, this information (all or some) can be used to as inputs into the damper's controller. The most important effect of driver input on the dynamics of the vehicle lies in situations where roll is induced. The most common scenario in which this is a factor lies in the situation where the driver undergoes a swerve maneuver.

2.6.4 Development of the Swerve Input

Since the model does not allow for the operator to work with parameters such as steering wheel angle or speed, it is necessary to develop another way to apply these conditions to the model. To do this, we look at the combined effect of changing the steering wheel angle, while at a constant speed. The maneuver that will be investigated is shown in Figure 2.16.

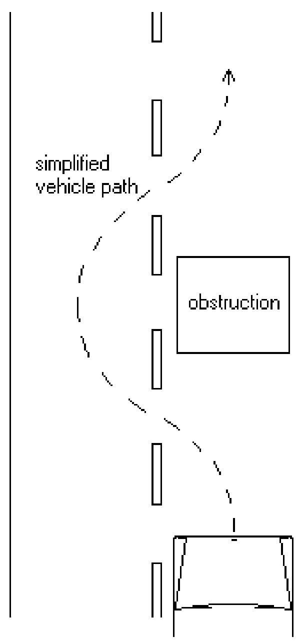

Figure 7.16. Vehicle Swerve Maneuver

This maneuver may represent either an obstruction avoidance maneuver, or a high speed passing maneuver. In either instance, the result of the changing vehicle trajectory is to create a moment to be applied to the body (about its center of gravity), which must be counteracted by the vehicle suspension. If the suspension is not able to successfully counteract the moment caused by the maneuver, the vehicle will roll, causing damage and possibly loss of life. Clearly, the vehicle dynamics in this situation must be improved in order to successfully state that a particular semiactive suspension system will have positive gains in vehicle safety. In order to examine the response of the vehicle to this type of "driver-induced" input, we apply the effect of the input to the system. That is, the body of the vehicle sees an applied moment as shown in Figure 2.17.

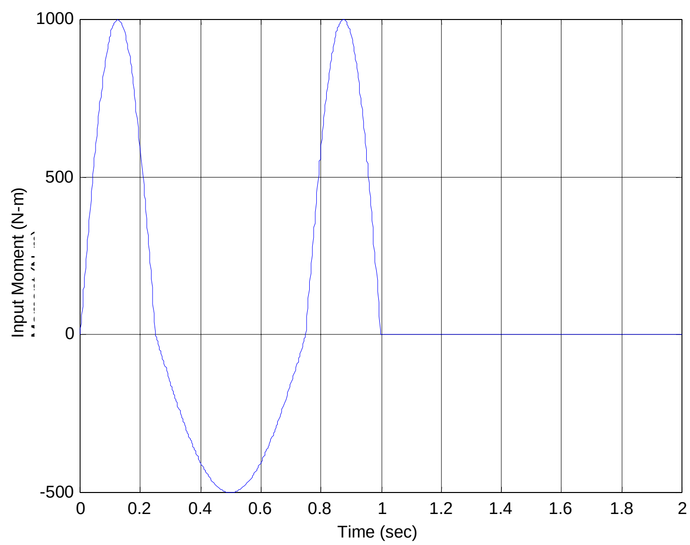

Figure 2.17. Moment Applied to Vehicle Body During Swerve Maneuver

2.6.5 Development of Force Control

When the vehicle is undergoing a maneuver such as the swerve type maneuver discussed, better performance is achieved when the suspension is stiff. Clearly, a stiff suspension is desirable whenever the steering wheel is turned, nor is it desirable whenever the vehicle speed reaches some nominal threshold. Instead, it is the combination of these two factors that determines whether or not it is desirable to have the suspension be stiff. In other words, it is the combination of these two factors that determines the magnitude of the moment that is applied to the vehicle body. In a very basic sense, the control strategy discussed here can be looked at as one that causes the suspension to be stiff when there is a significant applied moment to the body of the vehicle (provided that the moment is the result of a steering input). The response of this Force Control strategy being used in response to the swerve input is very positive, as shown in Figure 2.18.

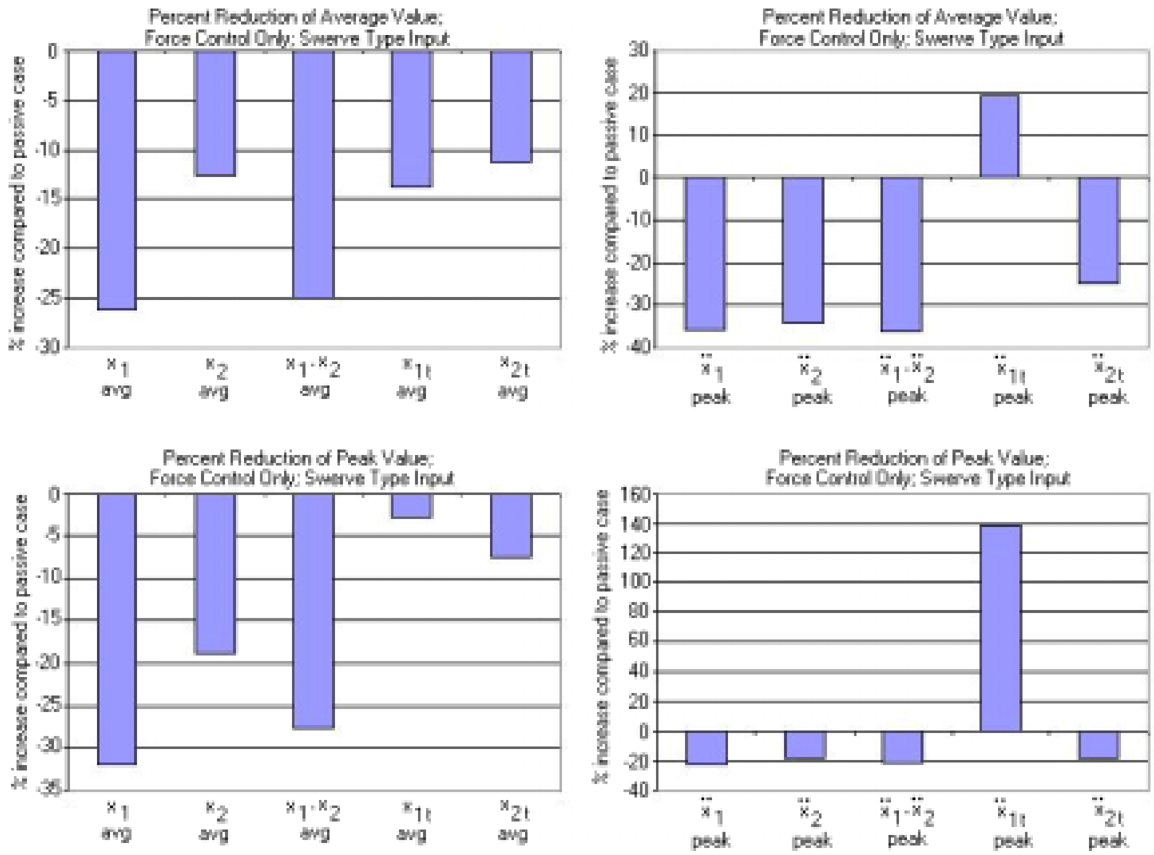

Figure 2.18. Summary of Force Control Only With Swerve Input Response

The values shown represent percent increase in comparison to the passive case (negative numbers indicate that the force control is allowing less motion than the passive case). Though these results indicate that the force control is effective at limiting the response of the vehicle in response to this class of driver induced input, it does not address the issue of road excitation. The solution is to piggyback the two control policies. That is, the system will be controlled according to either velocity or displacement skyhook, but will revert to force control in the presence of a driver-induced input.

2.6.6 Time Traces

In order to fully understand the results, it is necessary to not only examine the type of summary information mentioned previously, but also to look at some of the original time traces and therefore verify that the conclusions indicated do make physical sense. Time traces for the Displacements x_1 and x_2 as well as x_{1t} and x_{2t} are shown in Figure 2.19.

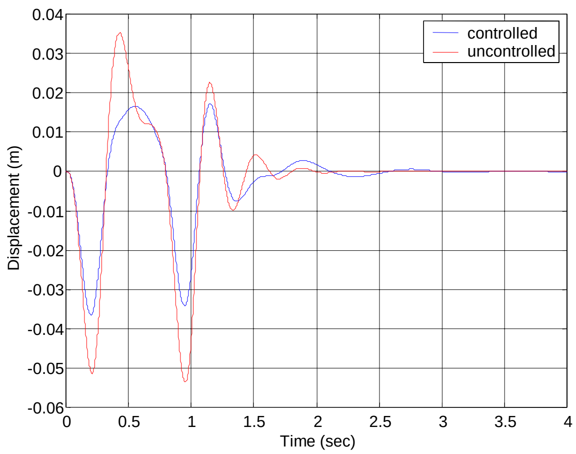

(a) Body Displacement – Side 1

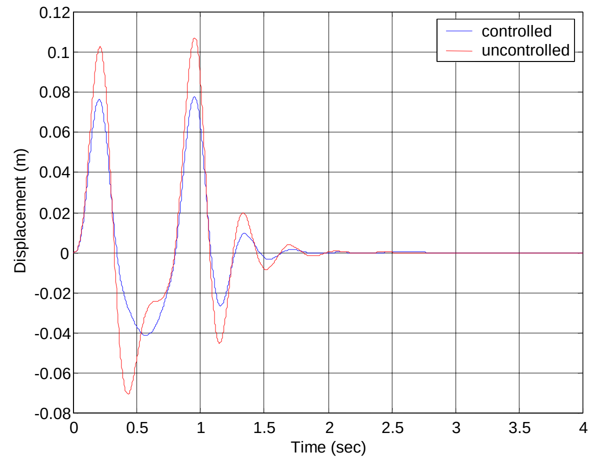

(b) Body Displacement - Side 2

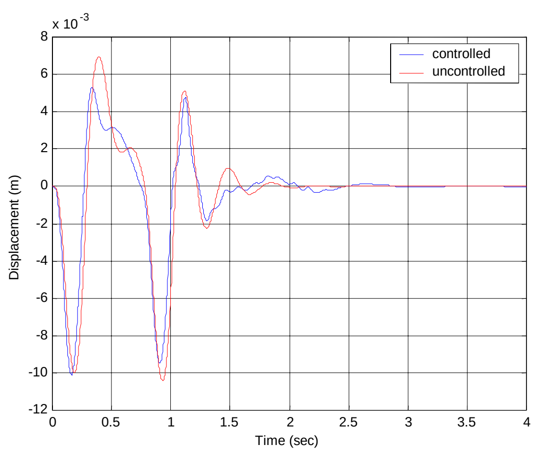

(c) Tire Deflection – Side 1

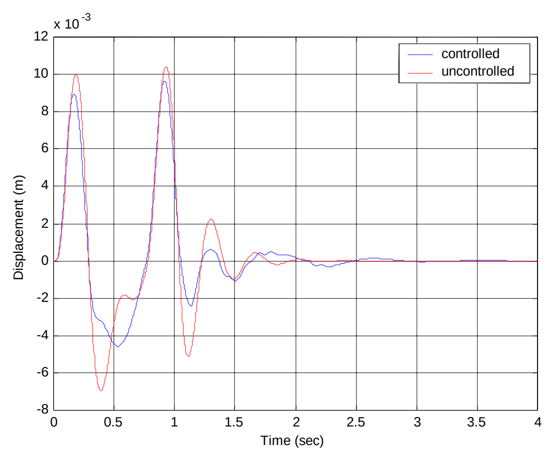

(d) Tire Deflection – Side 2

Figure 2.19. Velocity Skyhook With Force Control Swerve Input Response Time Traces

2.7 Investigation of the Effect of Mass Variation on the Controlled Response

In order to be able to determine that there will be significant benefits to using semiactive suspension in practice, it is necessary that simulations not only show significant gains for vehicle modeled, but also that the gains are still present after parameters of the vehicle are changed, as they may change in the real world. The most basic vehicle parameter that changes during real day-to-day driving conditions is the mass of the vehicle. This quantity may change with events ranging from filling up the gas tank, to having a number of passengers, to hauling lumber. Obviously, these are frequent driving situations, the effect of which must therefore be investigated. In order to determine that the effectiveness of the different semiactive policies investigated here are not diminished by changes in the vehicle mass, the effect of three levels of added vehicle mass were added (70, 140, and 210 kg). In each case, the performance of the semiactive system with the various control systems was contrasted with the performance of the passive system, with the same added mass. The results are shown for velocity skyhook control in Figure 2.20 (average values) and Figure 2.21 (peak values); for displacement skyhook control in Figure 2.22 (average values) and Figure 2.23 (peak values); for force control with and without both velocity and displacement skyhook control in Figure 2.24 (average values) and Figure 2.25 (peak values).

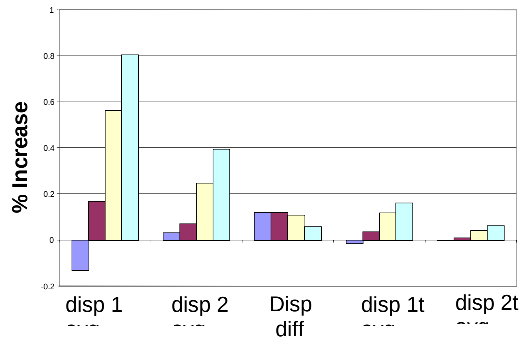

(a) Heave Type Input

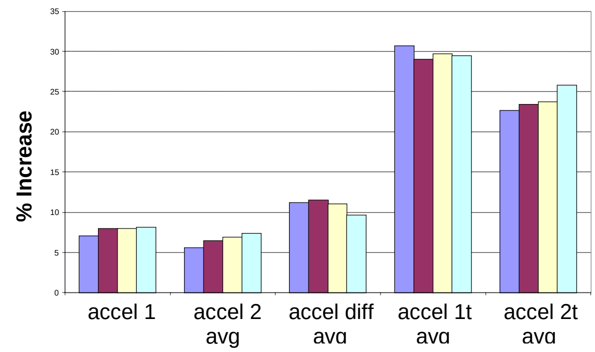

(b) Heave Type Input

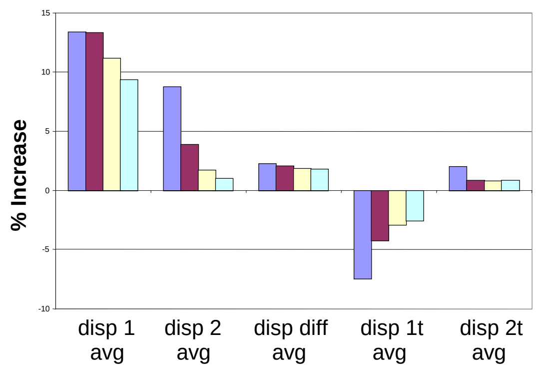

(c) Sinusoid Type Input

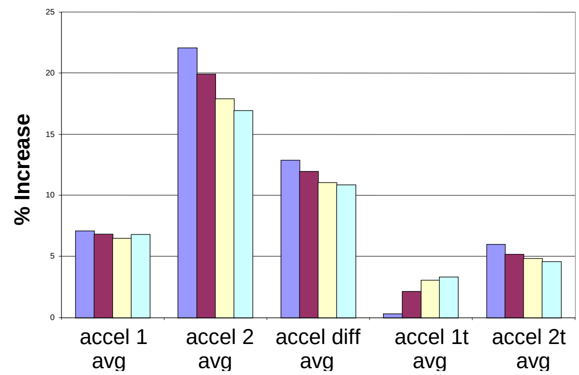

(d) Sinusoid Type Input

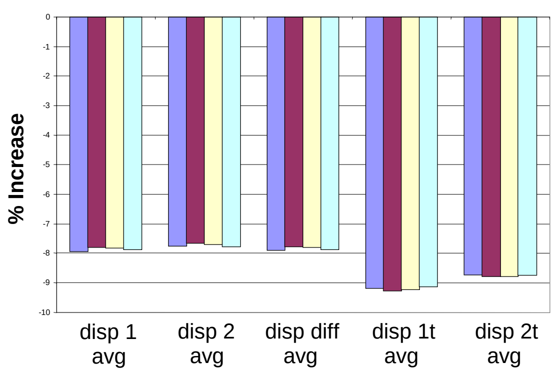

(e) Swerve Type Input

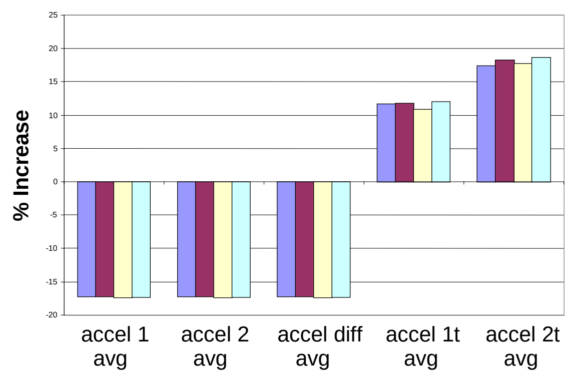

(f) Swerve Type Input

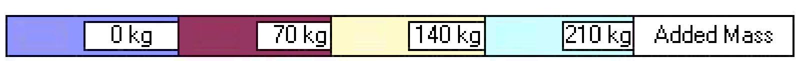

Figure 2.20. Performance of Velocity Skyhook System With Added Mass (Average Values)

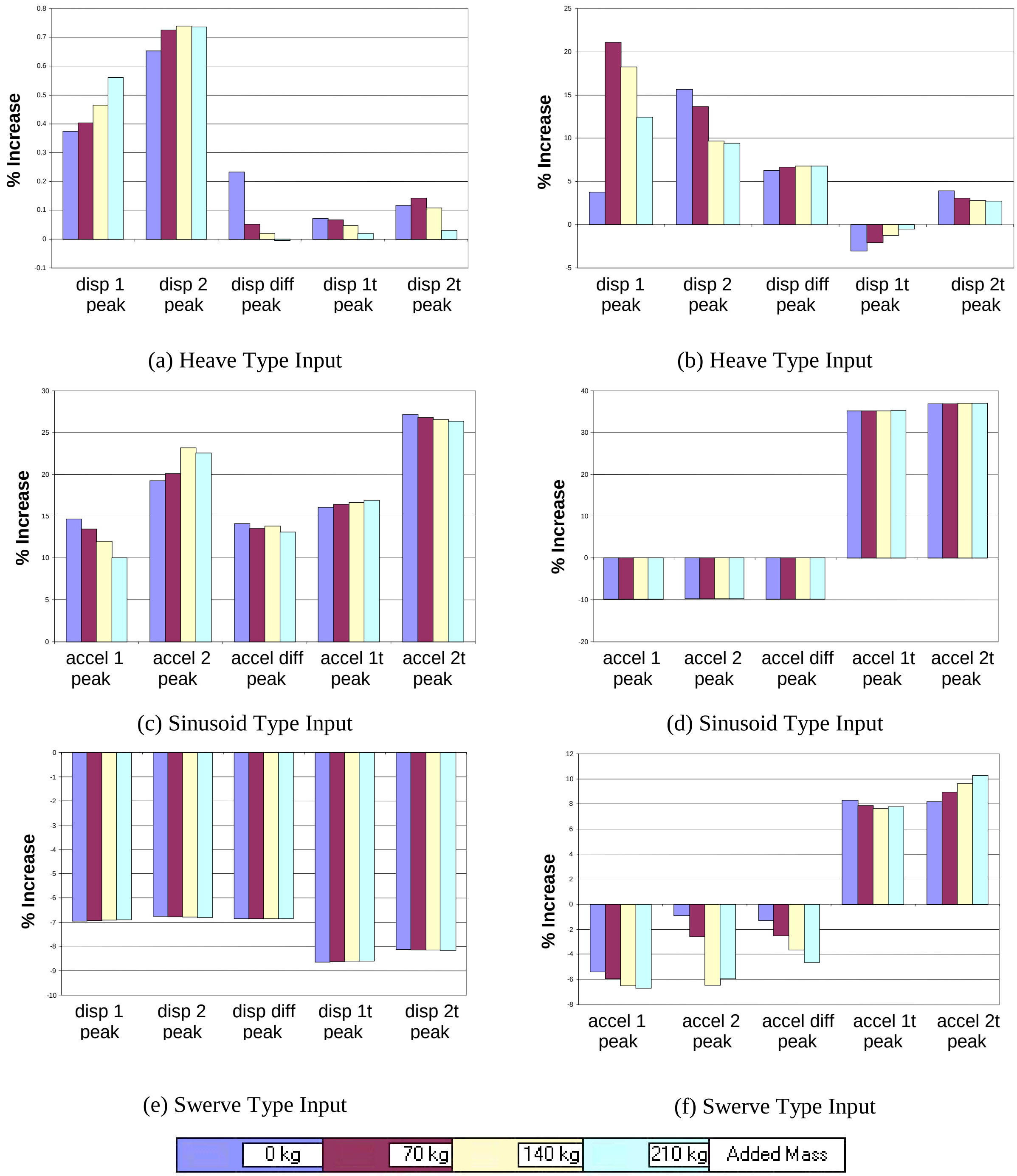

(a) Heave Type Input

(b) Heave Type Input

(c) Sinusoid Type Input

(d) Sinusoid Type Input

(e) Swerve Type Input

(f) Swerve Type Input

Figure 2.21. Performance of Velocity Skyhook System With Added Mass (Peak Values)

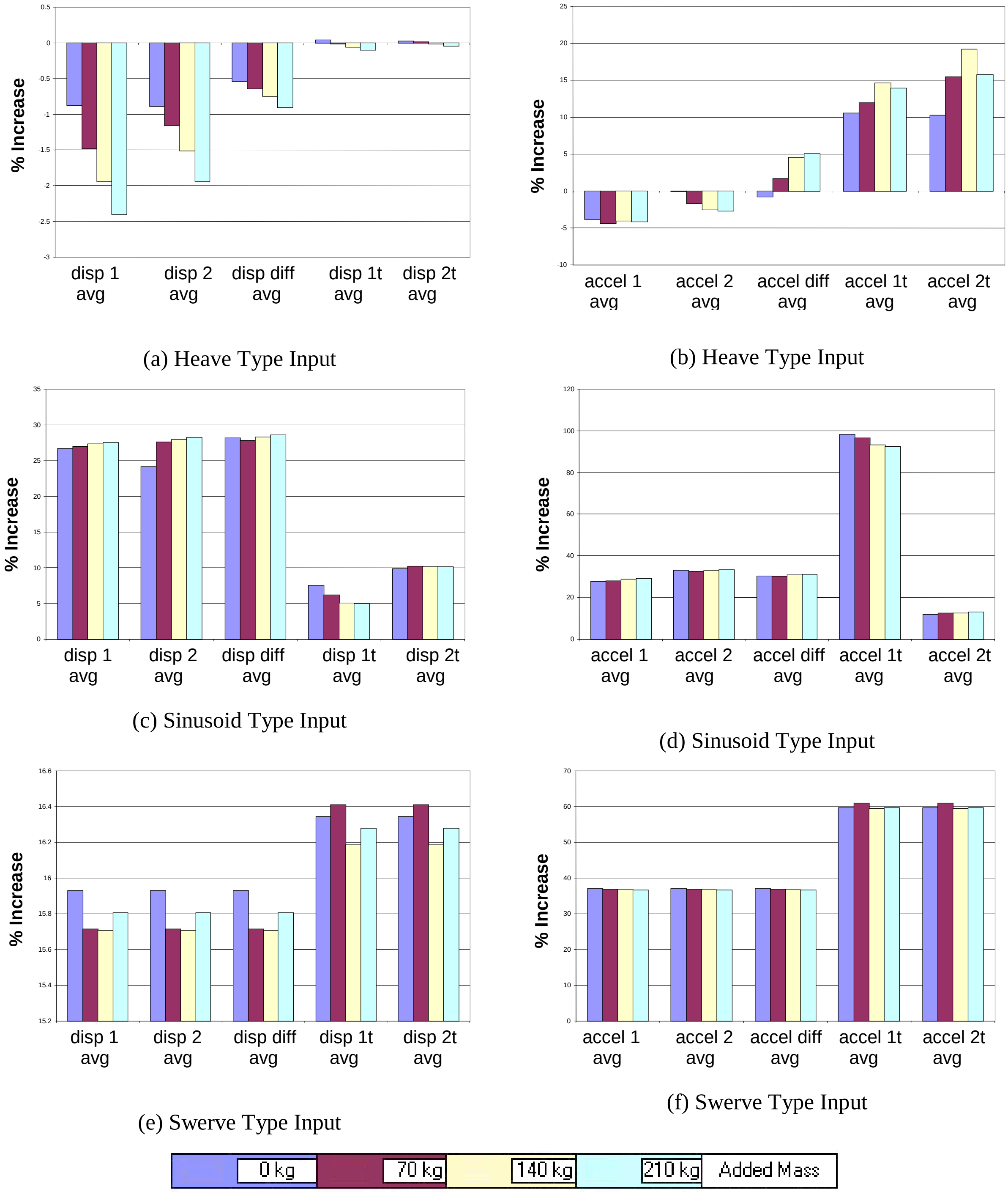

(a) Heave Type Input

(b) Heave Type Input

(c) Sinusoid Type Input

(d) Sinusoid Type Input

(e) Swerve Type Input

(f) Swerve Type Input

Figure 2.22. Performance of Displacement Skyhook System With Added Mass (Average Values)

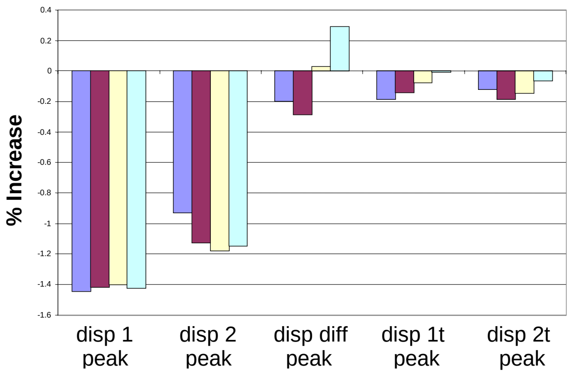

(a) Heave Type Input

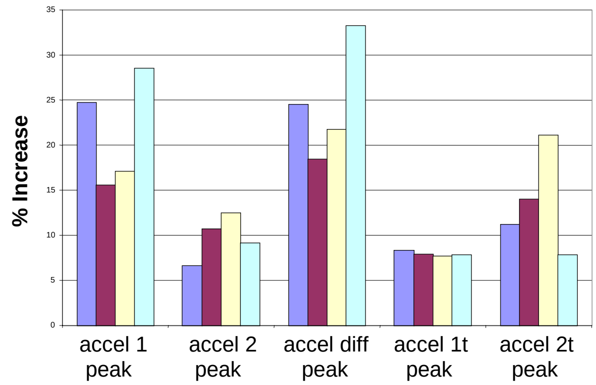

(b) Heave Type Input

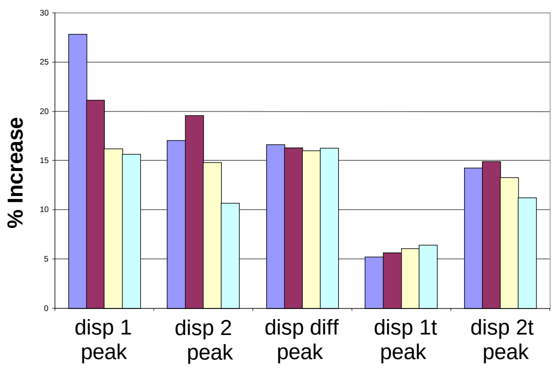

(c) Sinusoid Type Input

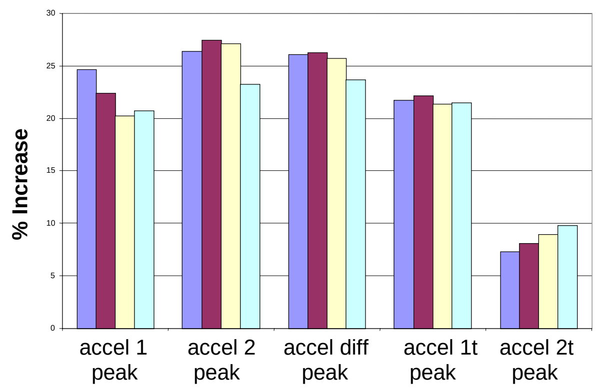

(d) Sinusoid Type Input

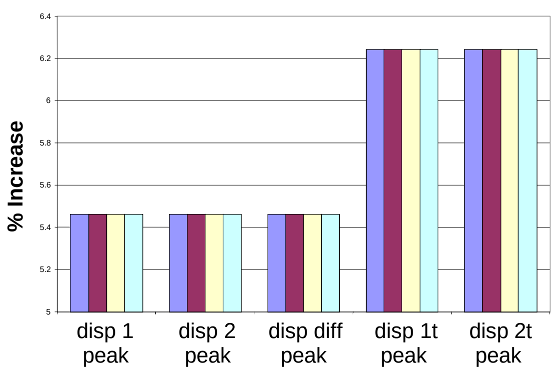

(e) Swerve Type Input

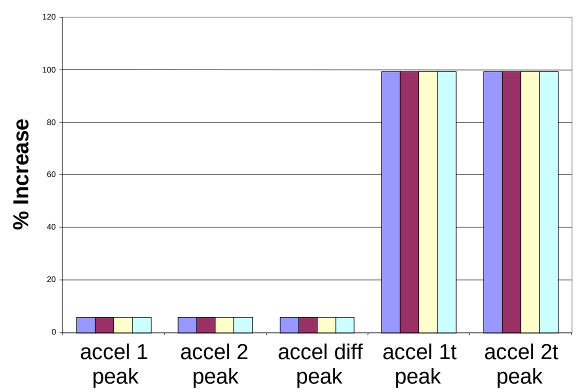

(f) Swerve Type Input

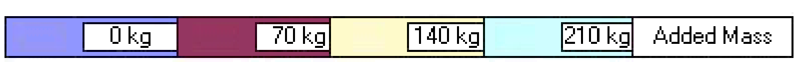

Figure 2.23. Performance of Displacement Skyhook System With Added Mass (Peak Values)

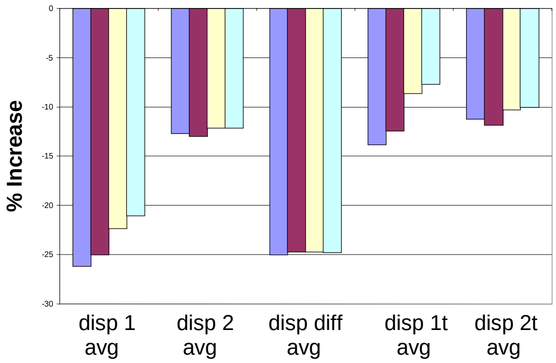

(a) Force Control Only

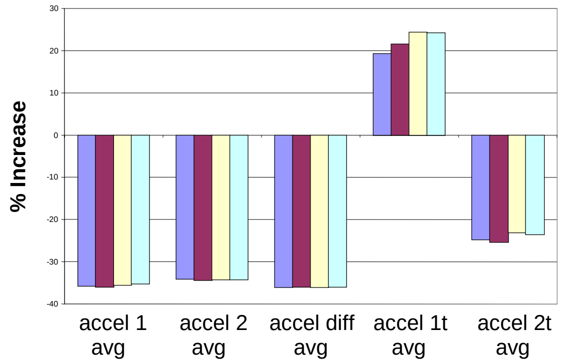

(b) Force Control Only

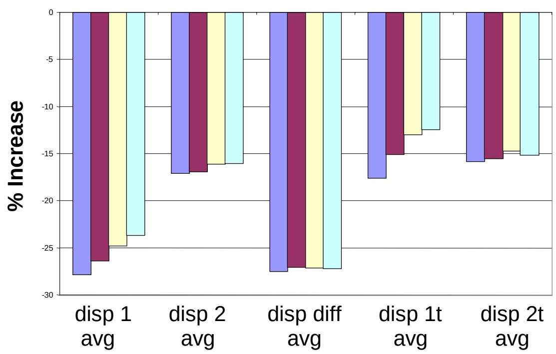

(c) Velocity Skyhook w/Force Control

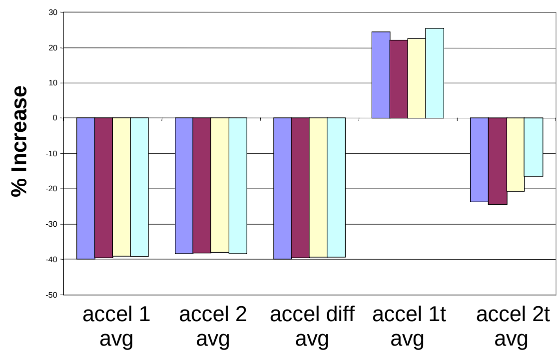

(d) Velocity Skyhook w/Force Control

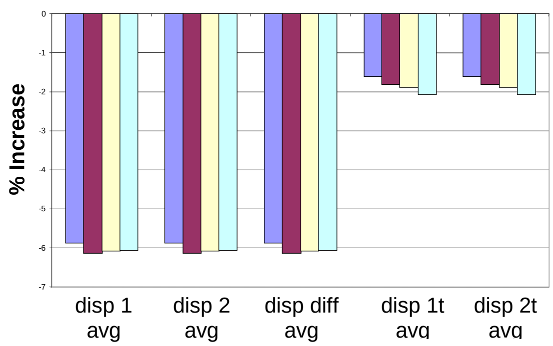

(e) Displacement Skyhook w/Force Control

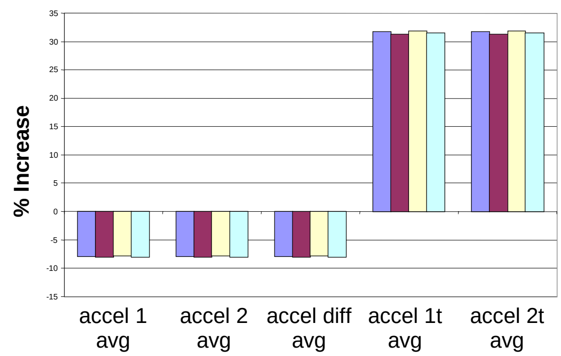

(f) Displacement Skyhook w/Force Control

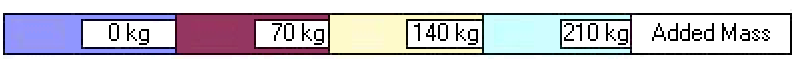

Figure 2.24. Performance of Force Control to Swerve Type Input, With and Without Skyhook Policies, with Added Mass (Average Values)

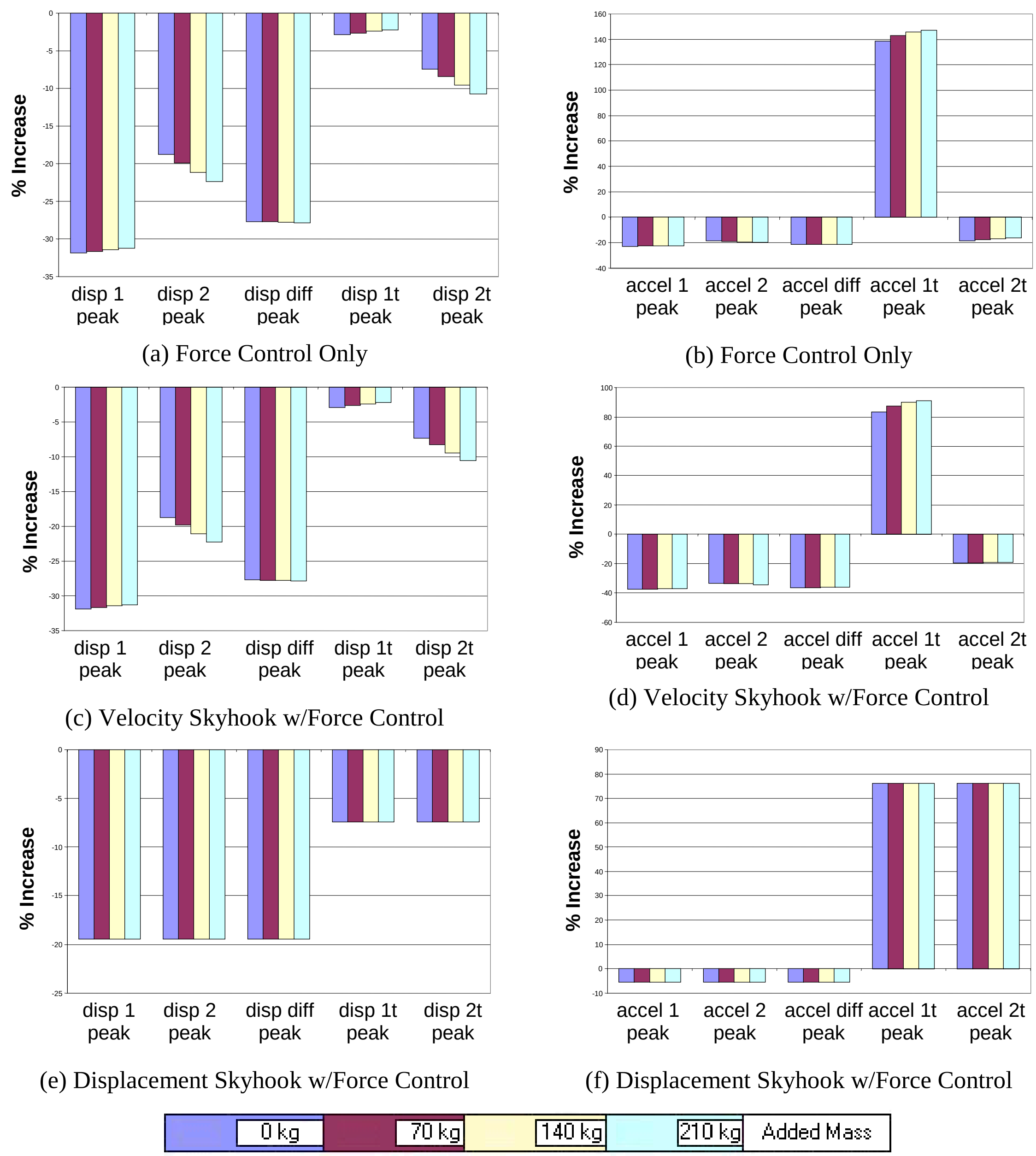

(a) Force Control Only

(b) Force Control Only

(c) Velocity Skyhook w/Force Control

(d) Velocity Skyhook w/Force Control

(e) Displacement Skyhook w/Force Control

(f) Displacement Skyhook w/Force Control

Figure 2.25. Performance of Force Control to Swerve Type Input, With and Without Skyhook Policies, with Added Mass (Peak Values)

The figures show that added mass (load) generally has a minimal impact on the performance of the various semiactive control systems investigated here, though it is apparent that it is important in some cases. At this point, trends in the results are not apparent. This will be investigated further in later phases of this study.

2.8 Simulation Results Observations

Because of the tradeoffs inherent in the design of a vehicle suspension, it is necessary for designers to look beyond traditional passive systems in order to address today's handling and safety requirements. This need is particularly apparent in larger, higher center of gravity passenger vehicles, such as Sport Utility Vehicles (SUVs). This phase of the study provides the findings resulting from the use of a numerical model to examine the effectiveness of different control strategies that can be used with semiactive suspensions. The effectiveness of two common semiactive control strategies, namely velocity based skyhook control and displacement based skyhook control, were investigated, which led to the proposal of two new semiactive strategies referred to as "Velocity Skyhook with Force Control" and "Displacement Skyhook with Force Control" for the purpose of this study. The four control strategies were simulated using a four degree-of-freedom vehicle roll-plane model and the results indicate that the performance achievable with each of the different control strategies was heavily dependent on the controllable damper's high and low state damping levels.

A tuned controllable damper was developed (numerically) for each of the control policies, then the performance of the tuned policies were compared both with each other and the conventional passive dampers. This comparison was performed for multiple inputs, each representing a road input or a vehicle maneuver. This phase of the study indicates that a velocity based skyhook control policy with force control will be most effective at controlling both road induced vibration and driver induced roll. Additionally, in order to investigate the effectiveness of the control policies for different vehicle configurations, most notably vehicle weight variations, we evaluated the performance of each of the semiactive systems compared to the simulated performance of a passive system with the same added weight. It was found that the performance of velocity skyhook control showed either very little change or improvement (based on the measure used) as weight was added to the vehicle. The performance of displacement skyhook control also generally showed increased effectiveness with added vehicle weight. The performance of force control degraded as weight was added to the vehicle. The performance of the control strategy incorporating both force control and velocity skyhook control degraded as weight was added to the vehicle, though the amount of degradation was small. The performance of the control strategy incorporating both force control and displacement skyhook control improved slightly as weight was added to the vehicle, although, the amount of improvement was slight. The performance change of both of the combination policies (as weight was added) was as low or lower than the performance change of the individual control strategies.

The results presented here imply that control strategies involving a combination of skyhook and force control will yield the best performance when used on a real vehicle. This result is expected to be particularly apparent in terms vehicle roll resulting from driver input, without degradation of the response to general road inputs. The phases of this study presented in the remainder of this document relate to experimental research performed on a Ford Expedition and the results ultimately determine which semiactive control policies are most effective for controlling vehicle roll dynamics without negatively affecting the vehicle comfort.

CHAPTER 3

VEHICLE LABORATORY TESTING

Vehicle testing performed in a lab setting is important for a number of reasons. In the lab, real world driving situations can be accurately emulated, while allowing greater opportunities for data collection and analysis, as well as higher repeatability than road testing. Furthermore, specific inputs can be repeated, often as other aspects of the test are varied. Among other advantages, this allows the specific effect of changes in specific vehicle parameters to be isolated. Additionally, in the lab it is possible to investigate the response of the vehicle to pure-tone inputs; something not possible during road testing. Testing performed in a lab setting is an important part of the complete analysis of the performance of a vehicle; it not only bridges the gap between numerical simulation and road testing, but allows a more complete understanding of the dynamics involved than either one of the other methods individually.

In this study, lab testing is performed using a tire-coupled two-post actuator system designed and assembled specifically for this purpose. The test rig is part of the facilities of the Advanced Vehicle Dynamics Lab (AVDL) at Virginia Tech and is housed at the Virginia Tech Transportation Institute (Figure 3.1); the governing body of Virginia Tech's Smart Road.

Figure 3.1. The Virginia Tech Transportation Institute

The test vehicle used for this study is a 2000 Ford Expedition (shown in Figure 3.2) that was made available by Visteon Corporation for the purpose of this study.

Figure 3.2. 2000 Ford Expedition Test Vehicle

The test vehicle (VIN # 1FMRU17L5YLA24995) is a rear-wheel drive model and is equipped with a load leveling rear suspension, which remained disabled for the duration of our lab testing.

3.1 Test Setup

The tire-coupled two-post actuator system used in this study has five main components (with the exclusion of the data collection system). The five components are:

- Two Material Testing Systems (MTS) model 248.03 hydraulic actuators,
- an MTS model 505.20 hydraulic power unit,
- two wheel stands,
- an asymmetric vehicle lift by Benwill,
- and an MTS model 458 controller in conjunction with D-Space and Matlab Products.

3.1.1 Actuators

The MTS model 248.03 hydraulic actuators, shown in Figure 3.3, can exert up to 5.5 kip, have a 6 inch stroke, and include 15 GPM servovalves (model # 252.22).

Figure 3.3. MTS Model 248.03 Hydraulic Actuator

Additionally, because they incorporate hydrostatic bearings, they are able to support side loads. These features make them ideal for vehicle testing use. In order to accommodate vehicles with different track widths, it was necessary to design our test setup, such that the actuators can be easily repositioned. This was accomplished by building elevated stands for the actuators. These stands allow the actuators to be repositioned using a pallet jack, as is shown in Figure 3.4.

Figure 3.4. Pallet Jack Repositioning Hydraulic Actuators

The tire of the test vehicle sits on a wheel pan, shown in Figure 3.5, which is bolted onto the hydraulic actuator.

Figure 3.5. Wheel Pan Attached to Hydraulic Actuator

The wheel pans incorporate both a raised lip and nylon webbing to keep the test vehicle in place.

The actuators are supplied hydraulic fluid by an MTS model 505.20 Hydraulic Power Unit, This unit, shown in Figure 3.6, supplies 20 GPM of hydraulic fluid at 3000 PSI of pressure.

Figure 3.6. MTS Model 505.20 Hydraulic Power Unit

While the actuators support the front of the vehicle, it is necessary to support the rear of the vehicle. This is accomplished through the use of two custom manufactured wheel stands, one of which is shown in Figure 3.7.

Figure 3.7. Wheel Stands

Each stand is 38.25 in. tall. The base of the stands are made of 0.75 in. thick steel, the uprights are made from 4 in. x 4 in. x 0.25 in. box tubing, and the wheel pan is made of 0.5 in. thick steel. The heights of the stands match the height of the actuator wheel pans at mid stroke. The stands are designed to be moved with a pallet jack, in the same manner as the actuators

As shown in Figure 3.8, an asymmetric vehicle lift (manufactured by Benwill) is used to raise the vehicle, so that the actuators and stands can be positioned under the tires.

Figure 3.8. Benwill Asymmetric Vehicle Lift

The test system is controlled with an MTS model 458 Controller, which is shown in Figure 3.9, in conjunction with a dSpace Autobox.

Figure 3.9. MTS Model 458 Controller Used For Lab Testing

Inputs and outputs are programmed in Matlab's Simulink, then compiled and downloaded onto the dSpace Autobox shown in Figure 3.10.

Figure 3.10. D-Space Autobox

The Autobox is equipped for eight outputs and twenty inputs. During Testing, all twenty channels of input data can be viewed and the eight outputs controlled using a software package called Control Desk by dSpace. A screen shot of this control software is shown in Figure 3.11.

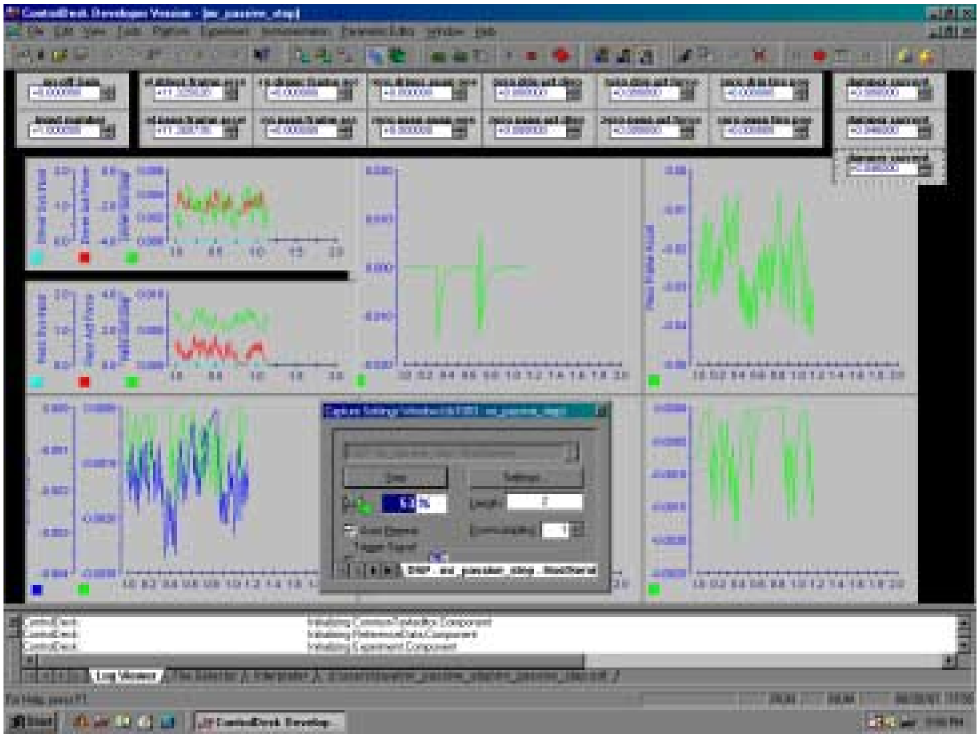

Figure 3.11. Control Desk Software

3.1.2 Safety Considerations

Due to the nature of our work, it is necessary to make special safety considerations. During testing, the vehicle is supported by two actuators and two stands. Since in many instances, testing consists of vigorously shaking the vehicle, it is necessary to constrain the vehicle such that it will remain on the stands. In order to do this, we used nylon webbing, as shown in Figure 3.12, which is attached over each of the wheels of the vehicle and secured to the stands.

Figure 3.12. Nylon Webbing on Rear Stand

Although the straps constrain the motion of the tire and can slightly affect the wheel-axle dynamics, we took special care to make sure that the degree to which the results are influenced is minimized

The staps and the presence of lips built onto the front and back of each wheel pan keep the vehicle securely in place during testing. A safety chain, shown in Figure 3.13, was added to the test setup to provide a safety cushion in the event of hydraulic power failure.

Figure 3.13. Safety Chain Shown Affixed to Test Vehicle

Since the zero position of the test setup is designated to be the mid stroke position of the actuators, were hydraulic power to fail, the front end of the vehicle would drop a distance equal to one half of the stroke of the actuators. In such an event, the safety chain insures that the vehicle stands would not tip, nor would the vehicle roll forward towards the front of the actuators by constraining the rear of the vehicle in the fore-aft direction. The geometry of the safety chain allows the front end of the test vehicle to move vertically, while limiting forward motion.

3.1.3 Putting the Test Vehicle onto the Test Stand

There are ten steps that must be performed for getting the test vehicle ready at the beginning of each test session. They are as follows:

1. The vehicle must be placed onto the lift and raised to a height sufficient to maneuver the actuators and stands under the vehicle.
2. The stands and actuators are positioned below the wheels of the test vehicle. Care is taken to insure that they are centered to maximize the stability of the test stand.
3. The actuators are moved into their mid-stroke position using the MTS model 458 controller.
4. The vehicle is lowered until the wheels are touching the stands, but the weight is still supported by the lift.
5. The nylon straps are secured around each of the four wheels, but not tightened.
6. The vehicle is then lowered until it's entire weight is supported by the actuators and stands.
7. The safety chain is loosely attached between the rear of the vehicle and the floor.
8. The nylon webbing is then uniformly tightened until snug.
9. The test vehicle is shifted into neutral and the parking brake released.
10. The safety chain is tightened.

Now, the vehicle is positioned on the test rig as shown in Figure 3.14, and is ready for testing.

Figure 3.14. Test Vehicle on Test Stand, Ready for Testing

3.1.4 Vehicle Instrumentation

In order to characterize the performance of a vehicle suspension, it is necessary to record dynamic measurements of the vehicle in motion. The choice of what measurements are recorded depends on the suspension parameters of interest. For example, if rattle space is of concern, a designer will find it necessary to measure the displacement across the primary suspension. This can be done directly using a linear voltage differential transformer (LVDT), or indirectly; by measuring the absolute position of the tire/hub and of the body and then calculating the difference between the two. In general, it is desirable to measure quantities of interest directly. For our study, we have recorded fourteen channels of data during testing. The sensors used to measure the suspension performance include:

- Differential pressure sensors and displacement transducers embedded on the actuator, to measure input force and displacement
- LVDTs to measure the displacement and velocity across both the vehicle tire, and the vehicle suspension
- Accelerometers to measure acceleration at different points on the vehicle

The usage and placement of each of these sensors will be discussed next in more detail.

3.1.4.1 Actuator Force and Displacement

Each of the MTS model 248 actuators is equipped with a differential pressure sensor, which measures the pressure differential across the actuator piston. This reading, together with the piston area is then converted to force. Time traces of actuator force are particularly useful in studies examining the effect of different suspensions on road bed wear as this reading represents the force applied by the vehicle on the surface of the road. Actuator force was recorded for both the driver and passenger side actuators. The displacement of each of the actuators was also recorded. This signal was recorded to verify that the actual signal being applied to the system was the same as the control signal as well as to develop transmissibility plots between road inputs and certain characteristics of the response of the test vehicle.

3.1.4.2 *LVDT's*

In this study, we used four LVDT's to measure the displacement across various parts of the vehicle. The velocimeters/displacement transducers used are Unimeasure model VP510-10 (sensitivity of 999.98 mV/in, 196.37 mV/inch/sec), and are shown in Figure 3.15.

Figure 3.15. Unimeasure Model VP510-10 Transducers

Two of the LVDT's are used to measure the displacement and velocity across the vehicle's front tires, as shown in Figure 3.16.

Figure 3.16. Tire Deflection/Velocity Transducer

This measurement correlates directly to the size of the tire's contact patch; an accepted measure of stability. It is also a measurement necessary for the enactment of skyhook control. Two more of the LVDT's are used to measure the displacement and velocity across the suspension of the vehicle, as shown in Figure 3.17.

Figure 3.17. Suspension Rattle/Velocity Transducer

This is a direct measurement of how much of the available rattle space the suspension is utilizing; an important measure for suspension packaging. Additionally, it is also needed for the use of skyhook control.

3.1.4.3 *Accelerometers*

Four PCB model U352C65 ICP accelerometers (sensitivities ranging from 84.1 to 111.4 mV/g) were used in this study. These accelerometers were positioned to measure the tire/wheel acceleration and the frame acceleration at the top and bottom of the front suspension dampers, as shown in Figures 3.18 and 3.19.

Figure 3.18. Frame Mounted PCB Accelerometer

Figure 3.19. Tire/Wheel Mounted PCB Accelerometer

The acceleration measurement is conditioned using a PCB signal conditioner (shown in Figure 3.20), and gained by a factor of one hundred (a factor of ten in the conditioner and a factor of 10 in the acquisition software).

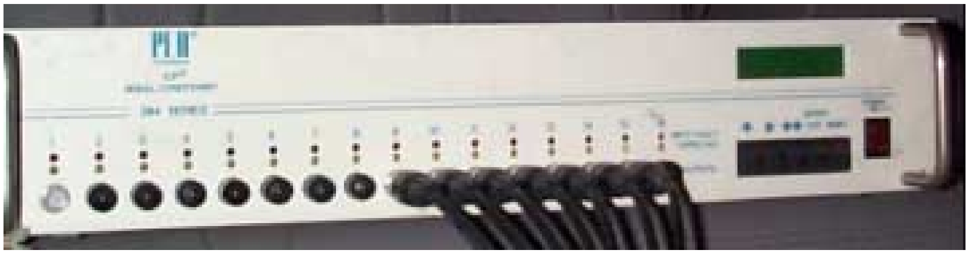

Figure 3.20. PCB Signal Conditioner

The use of the tenfold gain at the signal conditioner stage preserves a good signal to noise ratio. These signals are used both to develop acceleration transmissibility, and as a measure of the comfort of the vehicle.

All the system's inputs and outputs come through a custom built junction box located within the test vehicle, as shown in Figure 3.21.

Figure 3.21. Junction Box Located Within the Test Vehicle

3.2 Vehicle Testing

The testing of the vehicle progressed in a natural and organic manner. The first tests performed had the goal of developing elementary information regarding the dynamic characteristics of the test vehicle. Subsequent testing determined the effectiveness of different control methodologies. The first of the tests involved using pure tone system input.

3.2.1 Pure Tone Testing

The first stage of vehicle testing consisted of measuring the response to pure tone inputs. The goal of the pure tone testing was to measure the transmissibility between inputs at the wheel and outputs at different measurement positions. Doing this with sine waves makes it easy to determine when steady state has been reached. Once it is apparent that the output is at steady state, the output amplitude is recorded. This testing was performed frequency by frequency for the range 0 to 6 Hz. The data can then be used to develop transmissibility plots, which pinpoint the frequencies associated with various vehicle modes. This type of testing was performed for the vehicle in stock configuration, as well as for the vehicle with the stock roll bar removed. The roll bar was removed in order to determine how much of an effect it has on the vehicle's suspension characteristics; in particular its roll dynamics.

Using in-phase actuator input signals with amplitude +/- 0.25 inch, the transmissibility between the input and both supension rattle (rattle space), and frame acceleration were measured. The results of this testing is shown in Figure 3.22.

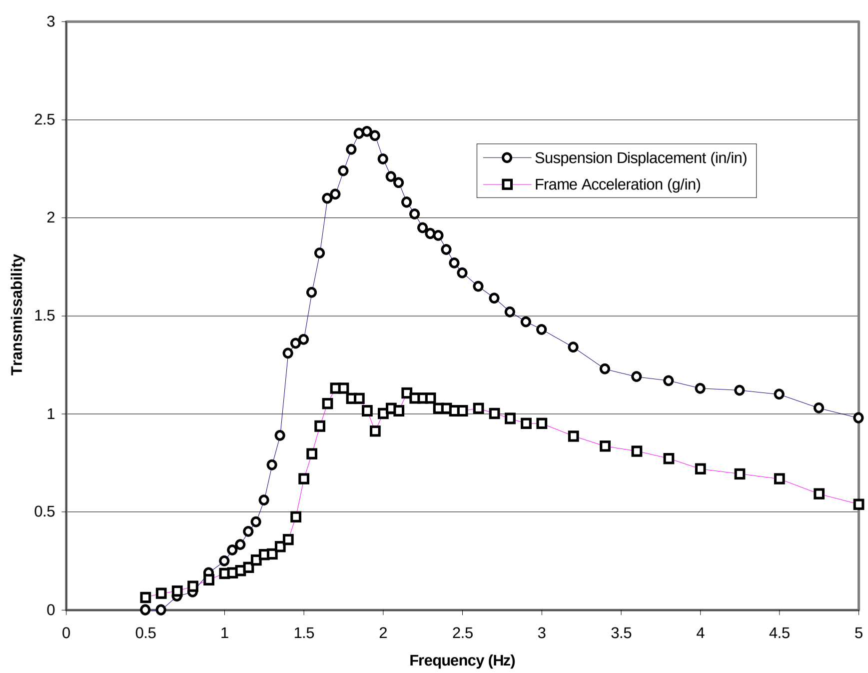

Figure 3.22. Supension rattle and Frame Acceleration Transmissibility with Respect to Road Displacement Input for a Ford Expedition.

The data in Figure 3.22 represents averaged readings from the driver and passenger sides, and clearly shows the presence of dominant heave modes at 1.9 Hz.

Using out-of-phase actuator input signals with amplitude of +/- 0.2 in., the transmissibility between an out-of-phase road input and the quantities suspension roll displacement and frame roll acceleration were measured. Suspension roll displacement is a measure of the difference in the displacement across the suspension of the vehicle from one side to the other; it is the amount of displacement that the vehicle's roll bar tries to counteract. Frame roll acceleration is the difference in the measured acceleration on the frame of the vehicle between the driver and passenger sides. The results of this testing are shown in Figure 3.23.

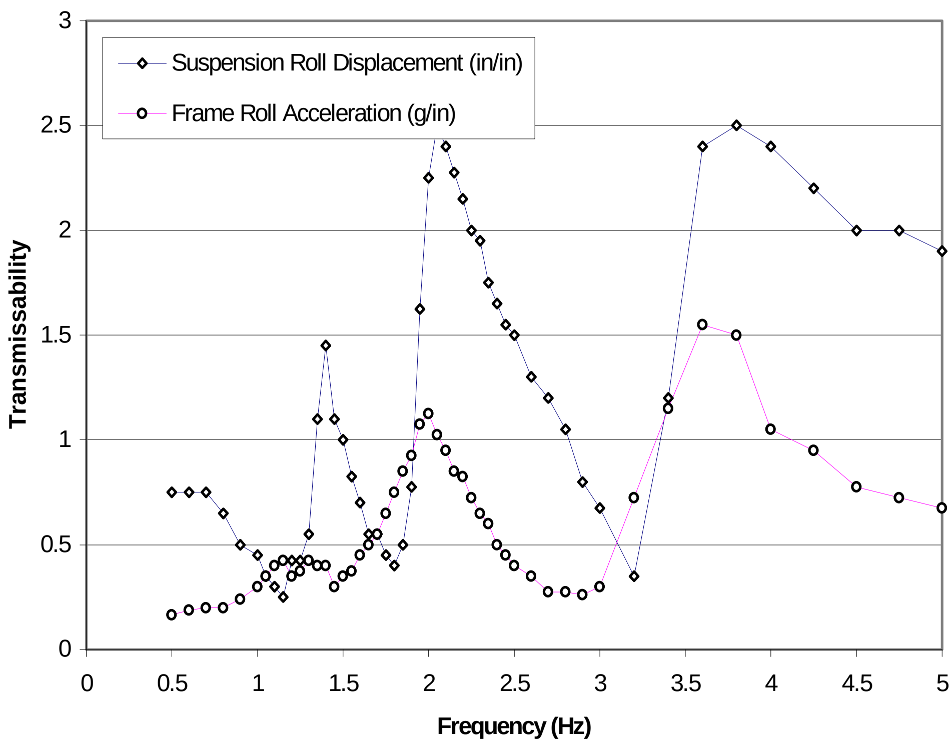

Figure 3.23. Suspension Roll Displacement and Frame Roll Acceleration Transmissibility with Respect to Road Displacement Input for a Ford Expedition.

The data in Figure 3.23 clearly shows the presence of roll modes at 1.4, 2.2, and 4 Hz. After examining the data taken on the vehicle in its completely stock configuration, the roll bar was removed. This was performed in order to investigate how much of an effect the roll bar had on the vehicle's heave dynamics. The results of testing with an heave sine wave are shown in Figures 3.24 and 3.25.

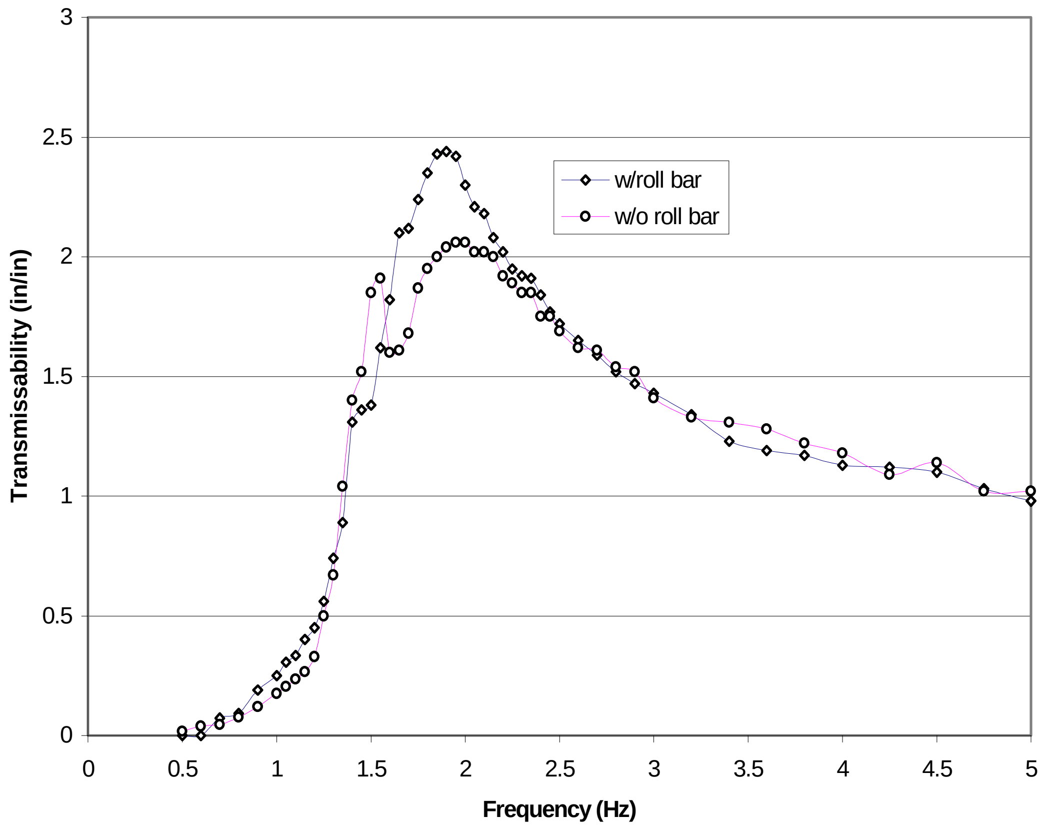

Figure 3.24. Supension rattle Transmissibility with Respect to Road Displacement Input for a Ford Expedition; With and Without Roll Bar

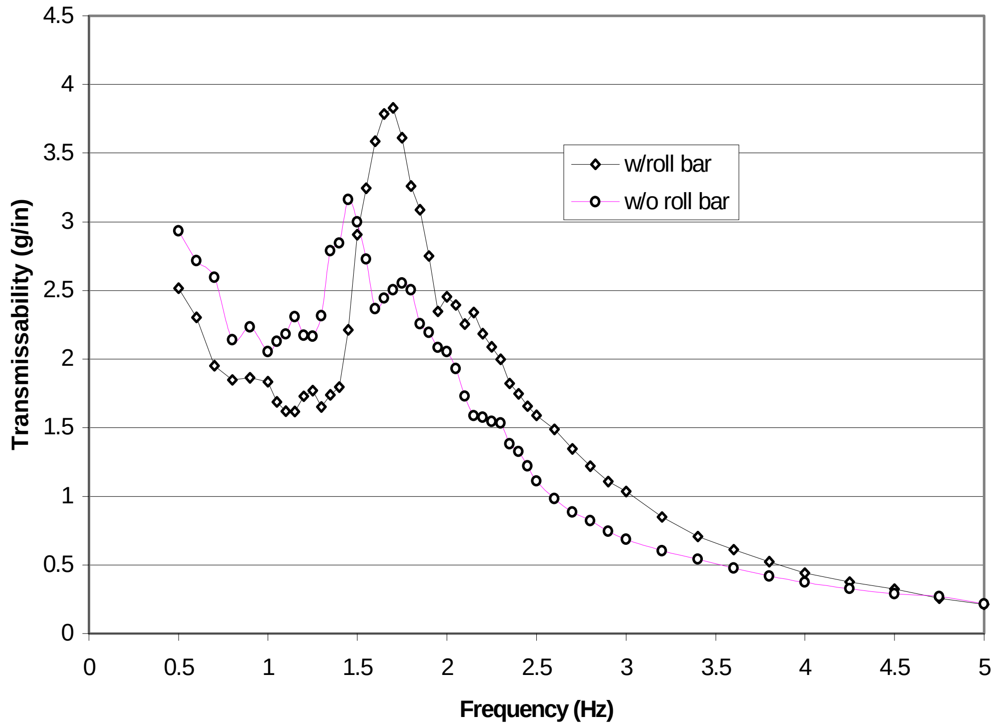

Figure 3.25. Frame Acceleration Transmissibility with Respect to Road Displacement Input for a Ford Expedition; With and Without Roll Bar

Both figures show that the presence of the roll bar does have an effect on the vehicle's heave modes. In both cases, the main effect of removing the vehicle roll bar is to cause a slight shift in the frequencies associated with maximum transmissibility, and to reduce the transmissibility ratio between the road input and both supension rattle and frame acceleration at those frequencies. It is also evident that although the presence of the vehicle roll bar does have an effect on the vehicle heave dynamics, the effect is slight and the basic nature of the dynamics is not determined by the roll bar. The same test was then repeated, this time exciting the vehicle's roll modes by using an out of phase sine wave as the system input. The results of this testing are shown in Figures 3.26 and 3.27.

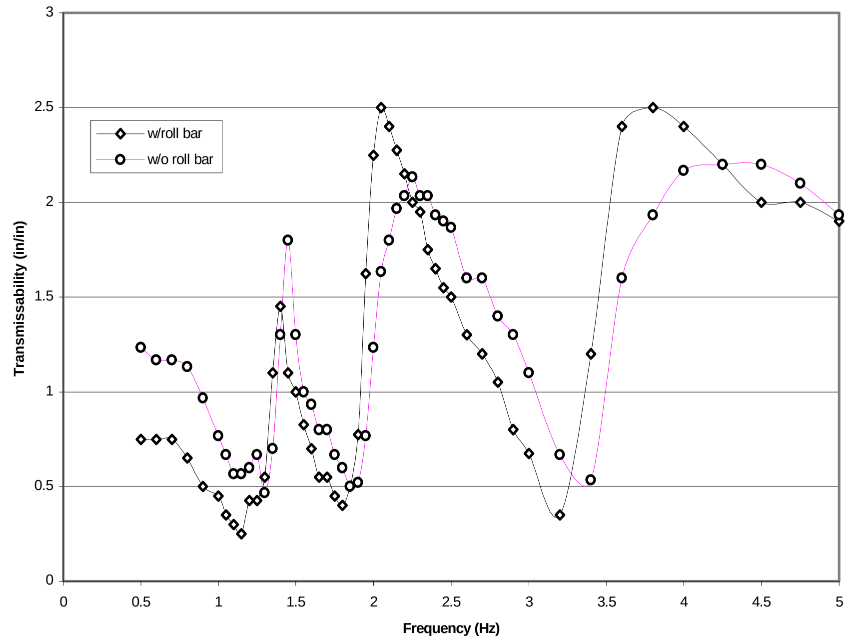

Figure 3.26. Suspension rattle Transmissibility with Respect to an Roll Road Displacement Input for a Ford Expedition; With and Without Roll Bar

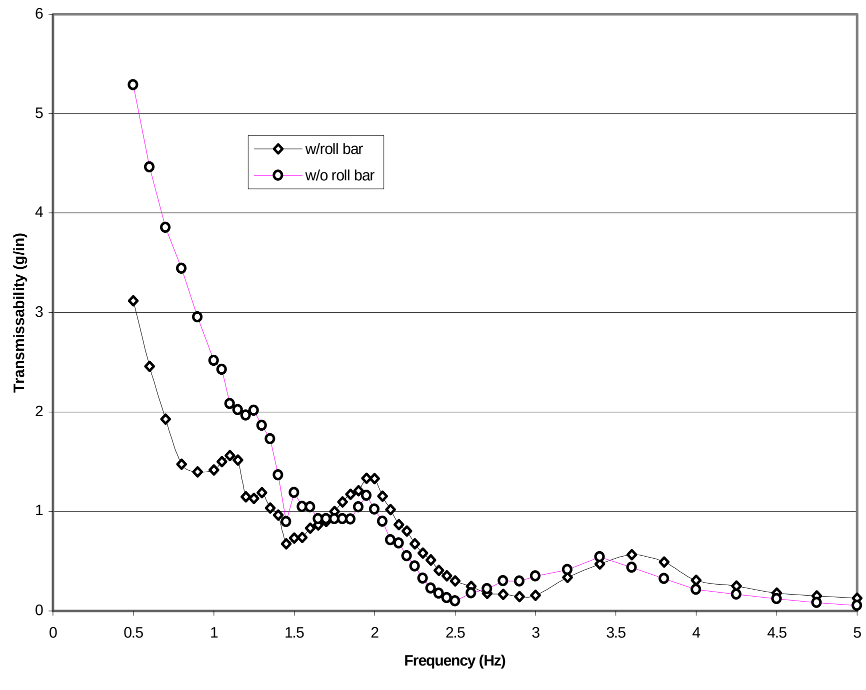

Figure 3.27. Frame Acceleration Transmissibility with Respect to an Roll Road Displacement Input for a Ford Expedition; With and Without Roll Bar

Both figures show that the presence of the roll bar does have an effect on the vehicle's roll modes. In both cases, the main effect of removing the vehicle roll bar is to cause both a decrease in the transmissibility ratio at low frequencies, as well as an increase in the transmissibility ratio at higher frequencies. From the previous figures, it is apparent that the roll bar is effective at controlling roll for frequencies below 1.8 Hz.

3.2.2 *Test Signal Development*

In order to characterize the response of the vehicle, it is necessary to use different test signals that can excite the dominant dynamics of the vehicle, as well as to examine the response corresponding to inputs that represent those applied to the vehicle in a real driving situation. For this study, three types of inputs (five inputs total) are used to investigate the vehicle dynamics. The first of these inputs is a multi-Sine input.

3.2.2.1 *Multi-Sine Input*

A multi-sine input consisting of a concatenation of six sine waves has been developed. These six waves combined together according to Eq. (3.1) excite both vehicle heave and roll.

$$\begin{gathered}y_{dr}(t) = \sin(\omega_{h1}t) + \sin(\omega_{h2}t) + \sin(\omega_{h3}t) + \sin(\omega_{r1}t) + \sin(\omega_{r2}t) + \sin(\omega_{r3}t) \\ y_{ps}(t) = \sin(\omega_{h1}t) + \sin(\omega_{h2}t) + \sin(\omega_{h3}t) - \sin(\omega_{r1}t) - \sin(\omega_{r2}t) - \sin(\omega_{r3}t) \\ \left| \begin{array}{l} \omega_{h1} = 2\times\pi\times 1.18, \quad \omega_{h2} = 2\times\pi\times 1.95, \quad \omega_{h3} = 2\times\pi\times 3.45 \\ \omega_{r1} = 2\times\pi\times 1.43, \quad \omega_{r2} = 2\times\pi\times 2.15, \quad \omega_{r3} = 2\times\pi\times 4.0 \end{array} \right.\end{gathered} \tag{3.1}$$

The amplitude of the resulting waves is multiplied by an overall gain of 0.1 prior to sending to the hydraulic controller. A time trace of the multi-sine input used in this study is shown in Figure 3.28.

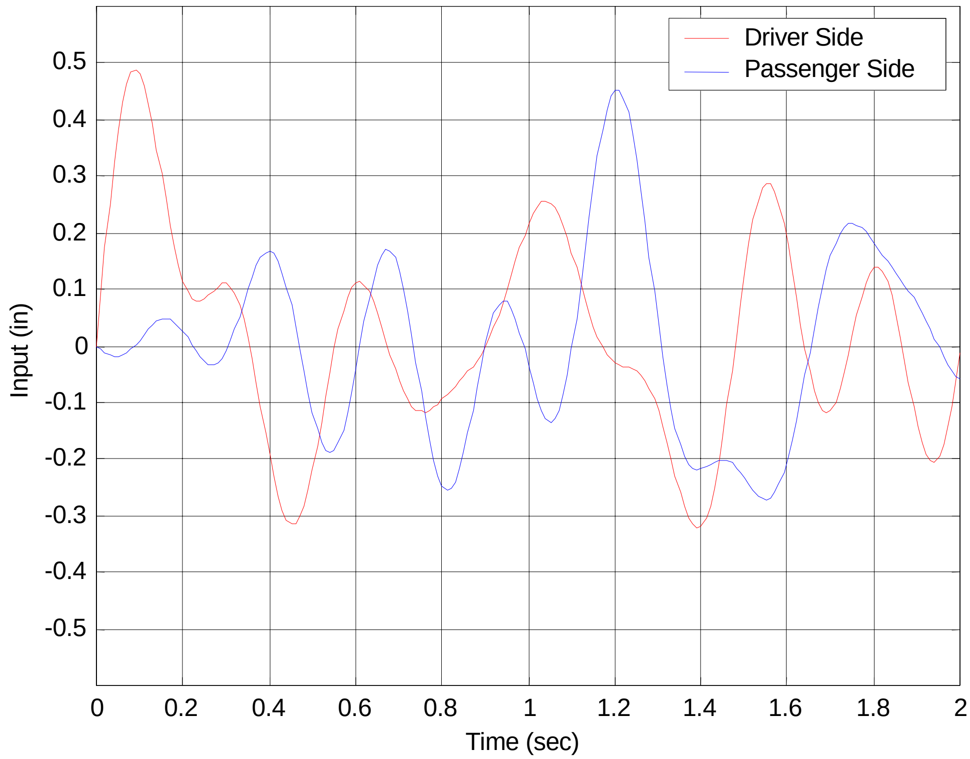

Figure 3.28. Multi-Sine Road Displacement Inputs for Vehicle Testing

The six frequencies that comprise the multi-sine input are not arbitrary, rather they correspond to significant aspects of the response of the vehicle. The three heave frequencies (subscripts h1, h2, and h3) are chosen to match the vehicles dominant (within the frequency range investigated) heave mode (1.95 Hz) and to have input components both above and below (in terms of frequency) the dominant heave mode. The three roll frequencies (subscripts r1, r2, and r3) are chosen to match the first three heave modes of the vehicle.

3.2.2.2 *Step Inputs*

Step inputs were used to investigate the transient response of the vehicle. The step inputs were applied to both front wheels of the vehicle, both in and out-of-phase. The in phase step input (heave) simultaneously raised and then lowered both wheels by 1.0 inch, while the out-of-phase step input (roll) raised one wheel by 0.5 inch while dropping the other by 0.5 inch. Both the heave and roll step inputs are shown in Figure 3.29.

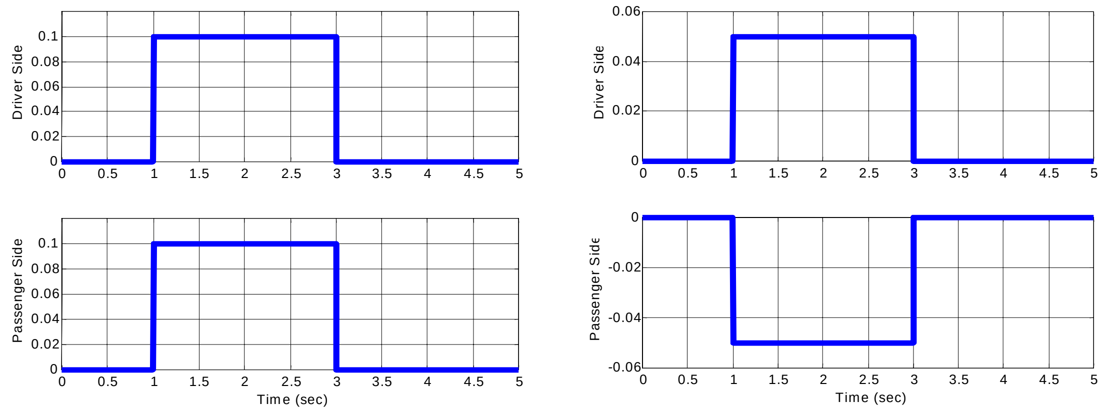

(a) Heave Step Input

(b) Roll Step Input

Figure 3.29. Heave and Roll Road Displacement Step Inputs for Vehicle Testing

3.2.2.3 Chirp Inputs

Chirp inputs were also used to characterize the dynamics of the test vehicle. Chirp inputs covering a frequency range of 0.5 to 6.0 Hz were applied to both sides of the vehicle, both in (heave) and out of phase (roll). These inputs are shown in Figure 3.30.

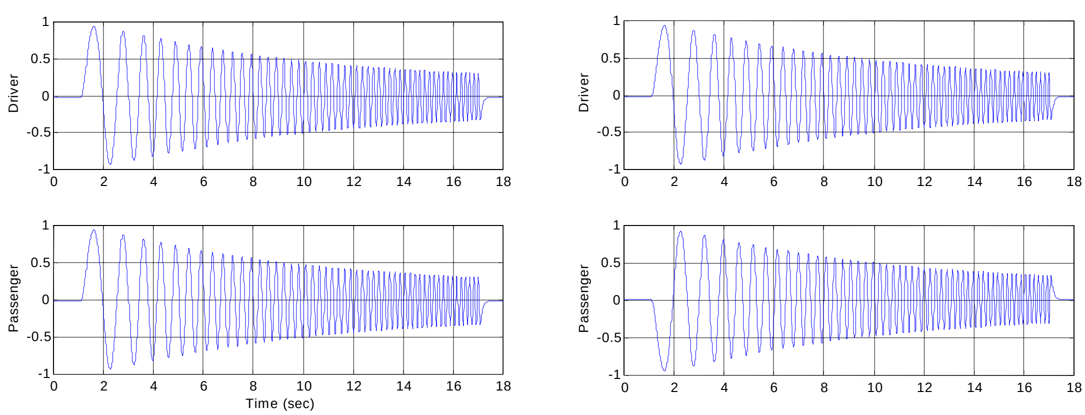

(b) Roll Chirp Input

(a) Heave Chirp Input

Figure 3.30. Heave and Roll Road Displacement Chirp Inputs for Vehicle Testing

This input allows us to get a feel for the frequency response of the vehicle without the complexity or time expenditure involved with pure-tone testing.

3.2.3 *Stock Vehicle Response Data*

The response of the test vehicle to each of the five inputs discussed earlier was measured. This testing was performed for the vehicle in stock configuration, with the roll bar removed, and with the stock dampers removed. Figure 3.31 shows the vehicle with the stock roll bar and stock damper.

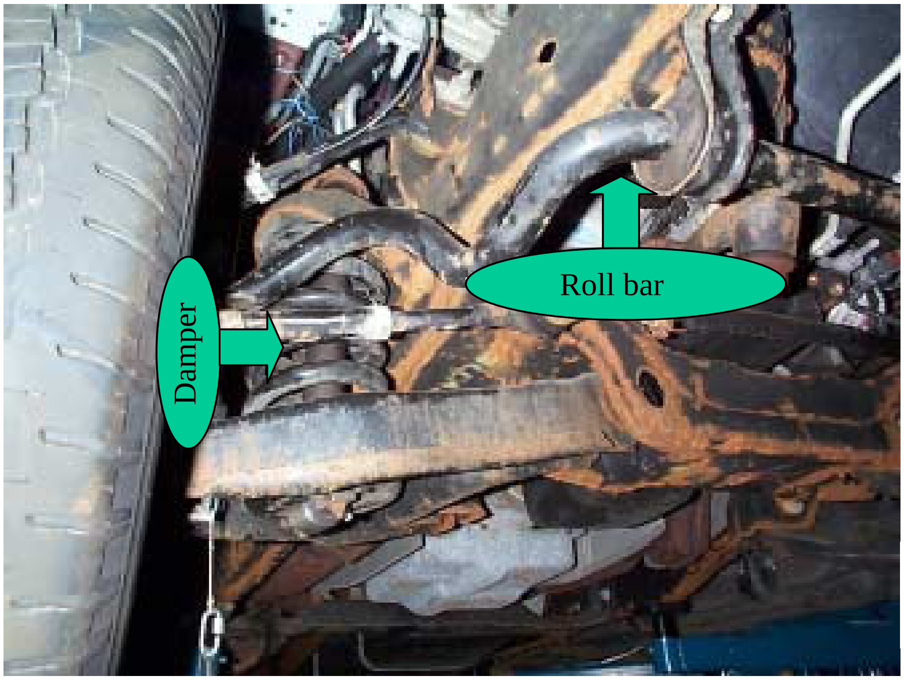

Figure 3.31. Ford Expedition With Stock Roll Bar and Stock Damper

In order to verify that the trends evident with a specific input amplitude hold true for other amplitude inputs, four overall gains (0.4, 0.6, 0.8, and 1.0) were applied to the multi-sine input and the response measured. In each case, time traces were recorded and relevant numbers (peak value and the average of the absolute value of the trace) were calculated. These numbers are plotted in Figure 3.32 (in terms of displacement) and Figure 3.33 (in terms of acceleration), for six of the measurement positions (vehicle with and without the roll bar).

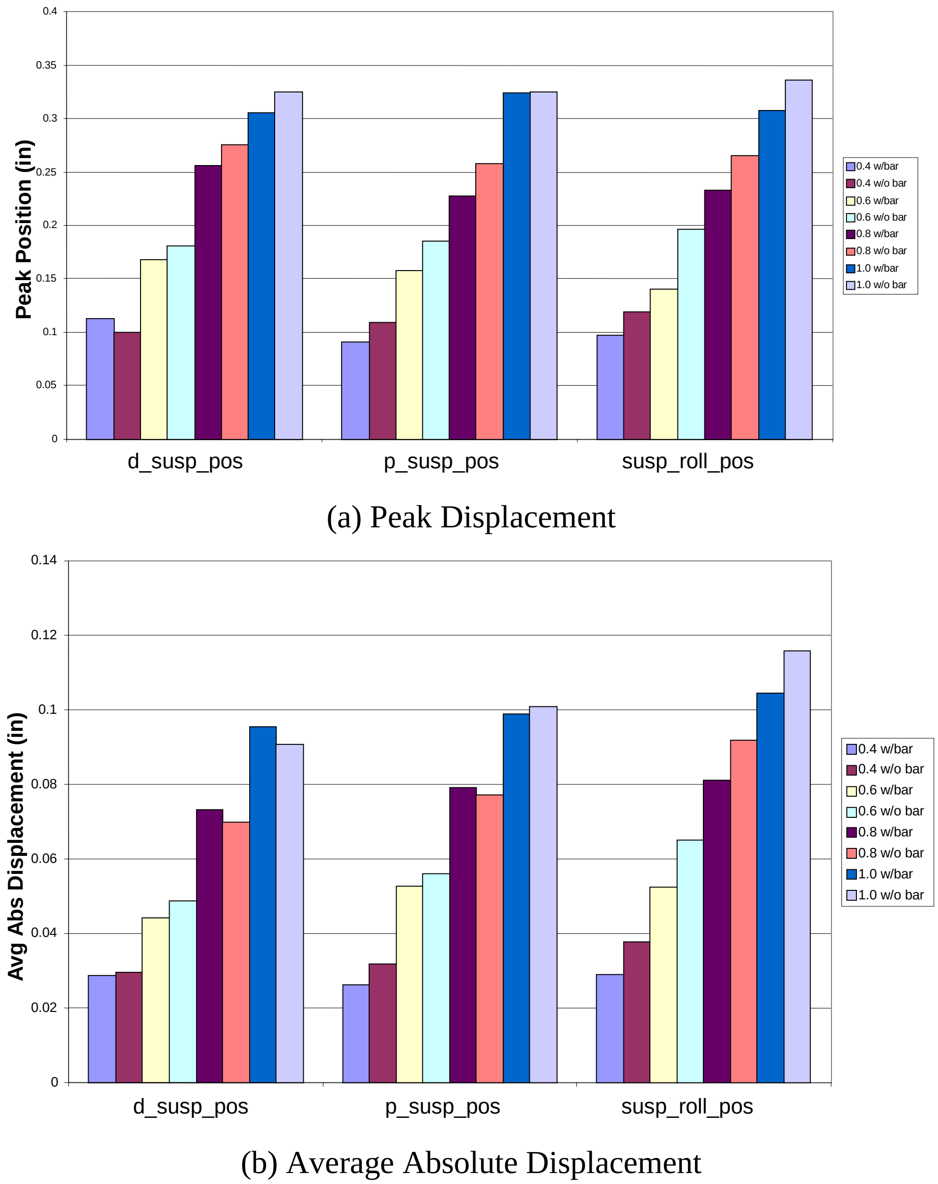

Figure 3.32. Stock Ford Expedition Displacement Response to Multi-Sine Road Displacement Input (Multiple Gains; With and Without Roll Bar)

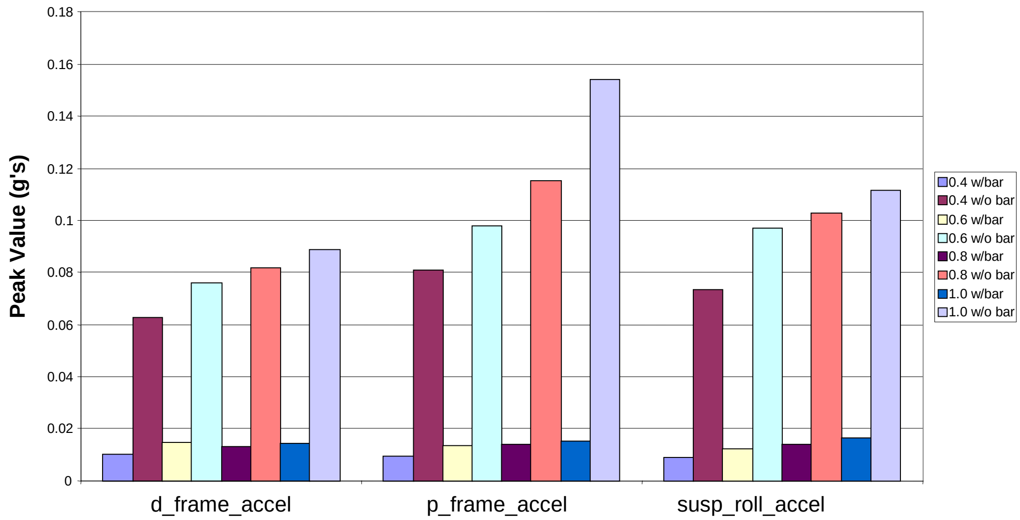

(a) Peak Acceleration

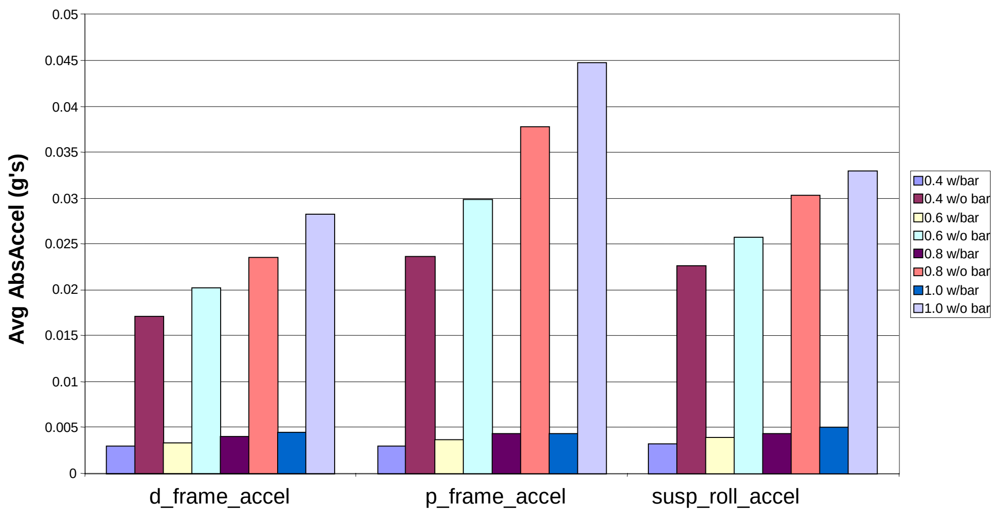

(b) Average Absolute Acceleration

Figure 3.33. Stock Ford Expedition Acceleration Response to Multi-Sine Road Displacement Input (Multiple Gains; With and Without Roll Bar)

Figures 3.32 and 3.33 show that the presence of the roll bar on the vehicle decreases both the peak and average absolute supension rattle (rattle space). The figure also shows that the presence of the roll bar dramatically reduces the acceleration transmitted to the frame of the vehicle. Figures 3.34 and 3.35 show, in terms of displacement and acceleration respectively, the results of testing the vehicle (with and without the stock damper) with the multi-sine input and an overall gain of 1.0.

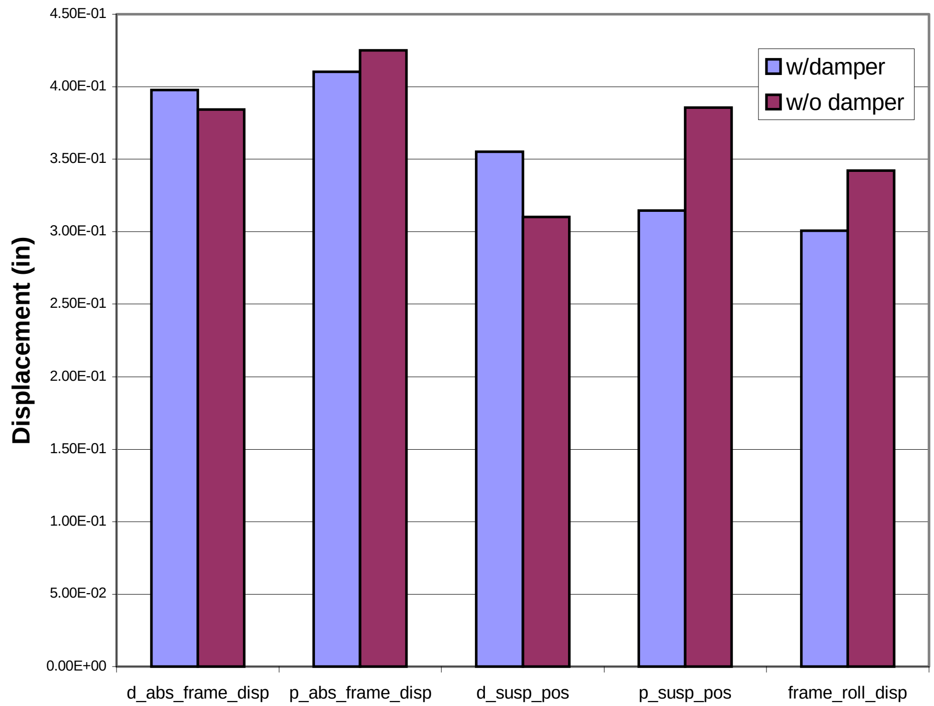

(a) Peak Displacement

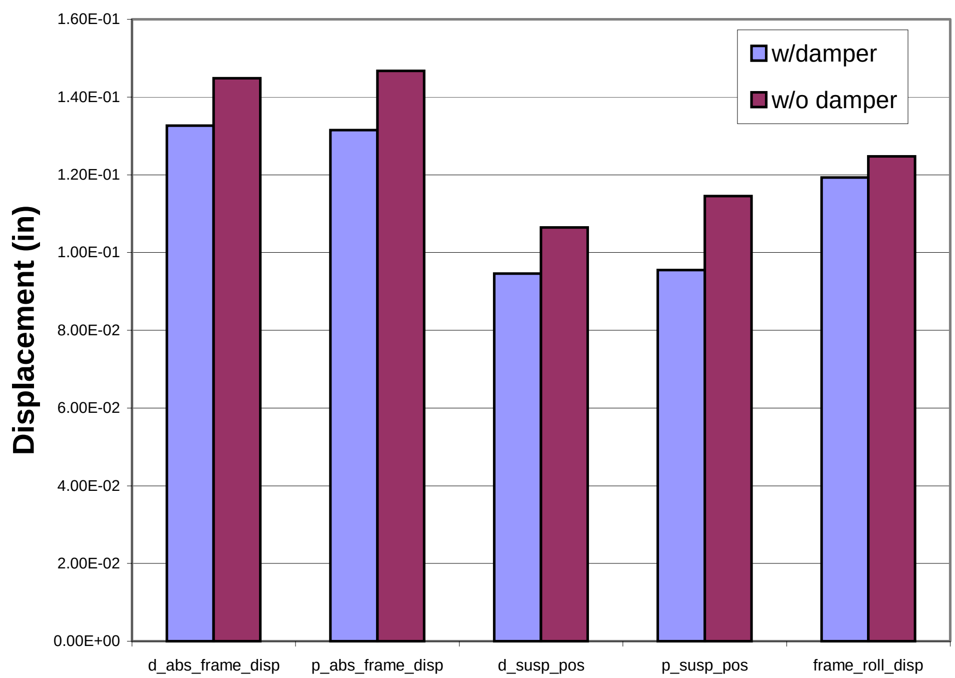

(b) Average Absolute Displacement

Figure 3.34. Stock Ford Expedition Displacement Response to Multi-Sine Road Displacement Input (With and Without Damper)

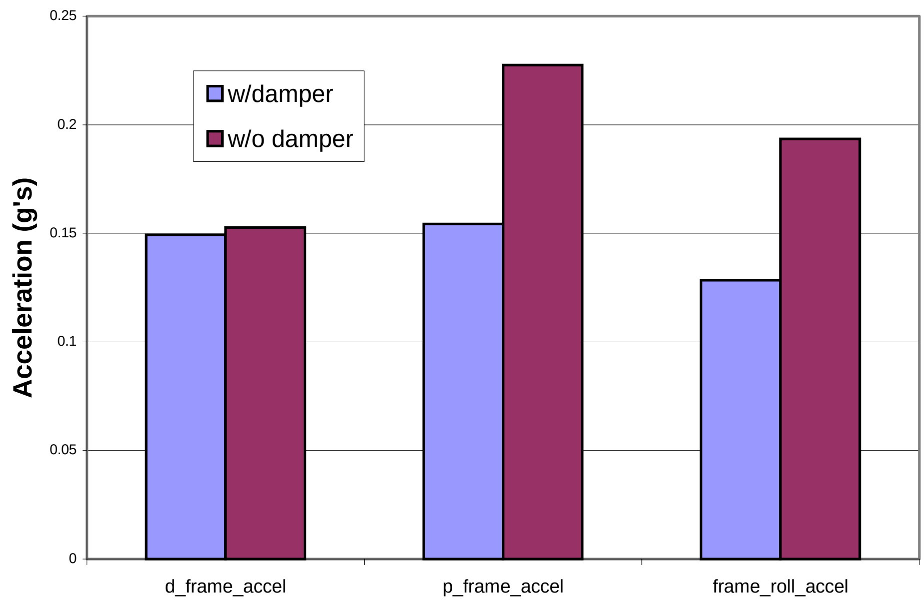

(a) Peak Acceleration

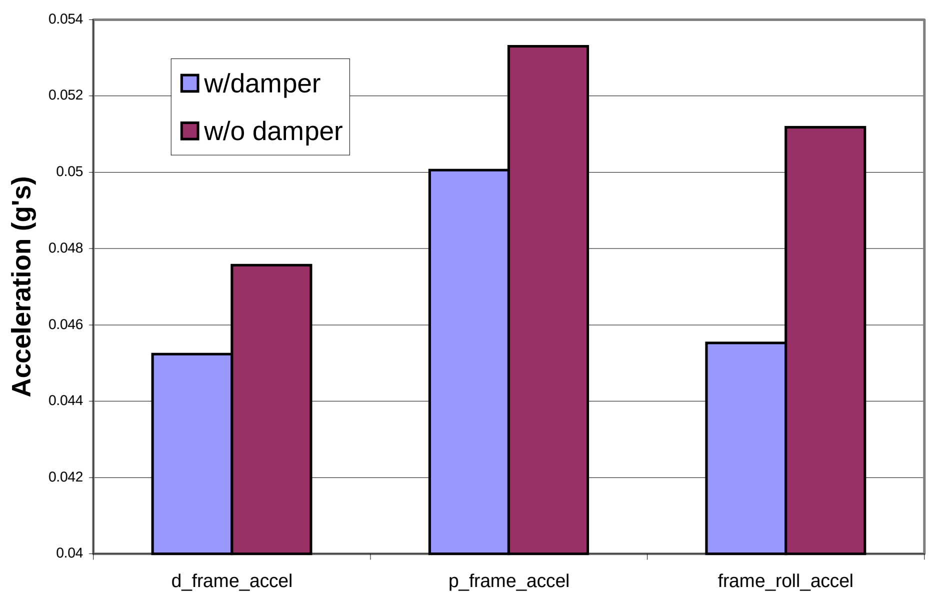

(b) Average Absolute Acceleration

Figure 3.35. Stock Ford Expedition Acceleration Response to Multi-Sine Road Displacement Input (With and Without Damper)

These figures show that the damper is generally effective at controlling the acceleration of the frame of the test vehicle in terms of both peak and average absolute values. Generally the displacement measures are also reduced with the inclusion of the damper. This is important in that if the stock damper was determined to not have a measurable effect on the dynamics of the vehicle, then it is unlikely that significant performance gains could be realized by using controllable dampers in their place.

The time responses from this testing can also be examined in terms of their frequency content, as shown in Figures 3.36-38 for the two cases we tested.

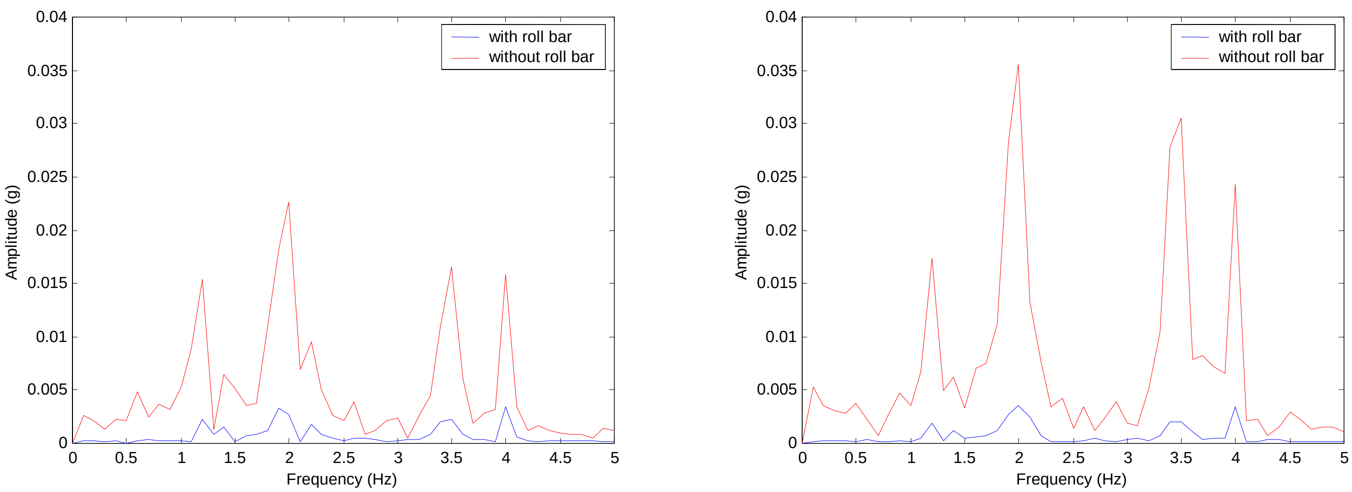

(a) Driver Frame Acceleration (b) Passenger Frame Acceleration

Figure 3.36. FFTs of Stock Vehicle Acceleration Response to Multi-Sine Road Displacement Input (With and Without Roll Bar)

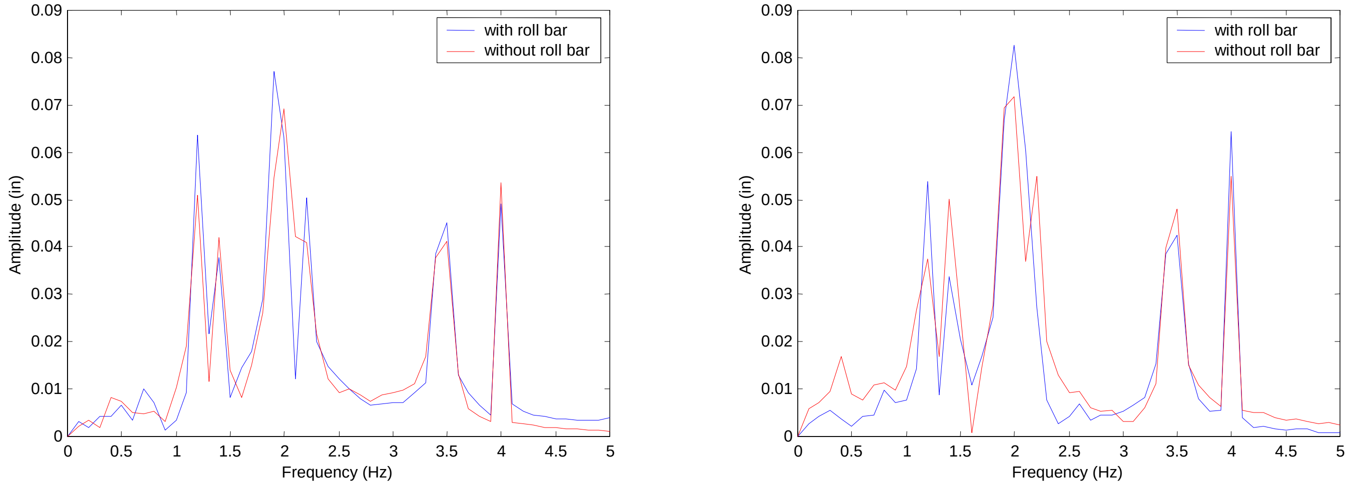

(a) Driver Suspension Rattle (b) Passenger Suspension Rattle

Figure 3.37. FFTs of Stock Vehicle Displacement Response to Multi-Sine Road Displacement Input (With and Without Roll Bar)

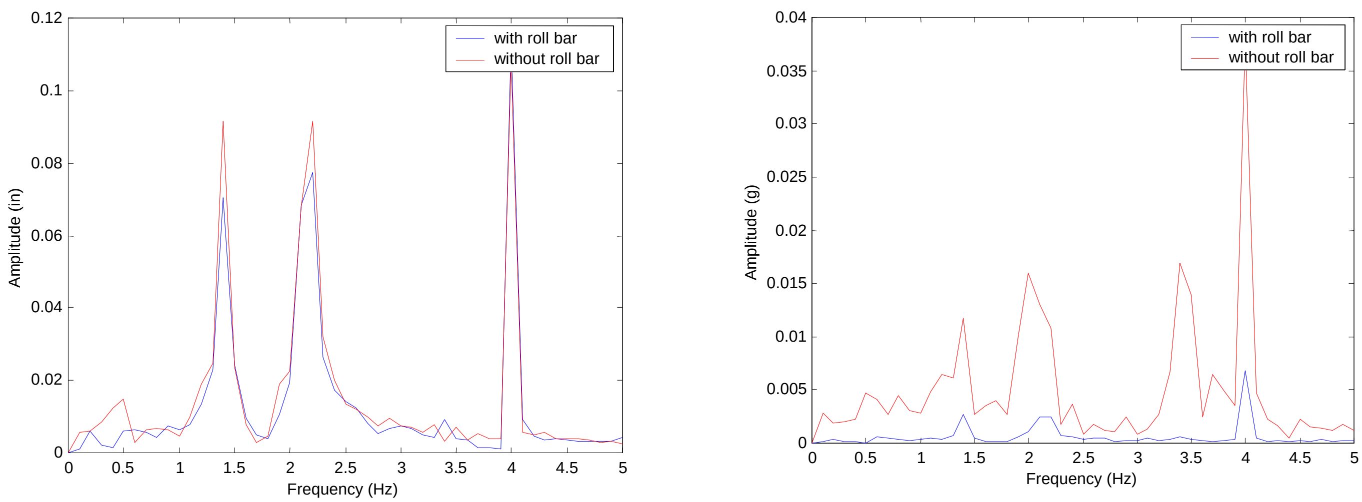

(e) Suspension Roll Displacement (f) Suspension Roll Acceleration

Figure 3.38. FFTs of Stock Vehicle Response to Multi-Sine Road Displacement Input (With and Without Roll Bar)

Figures 3.36-38 again show that the presence of the roll bar dramatically reduces the acceleration transmitted to the frame of the vehicle. This result is not as apparent in terms of displacement across the suspension. The figure shows that the roll bar is moderately effective at controlling motion at frequencies not corresponding to natural frequencies of the vehicle, and is not effective at frequencies that do correspond to the vehicle's natural frequencies. Figures 3.39-43 shows these results with and without the stock damper.

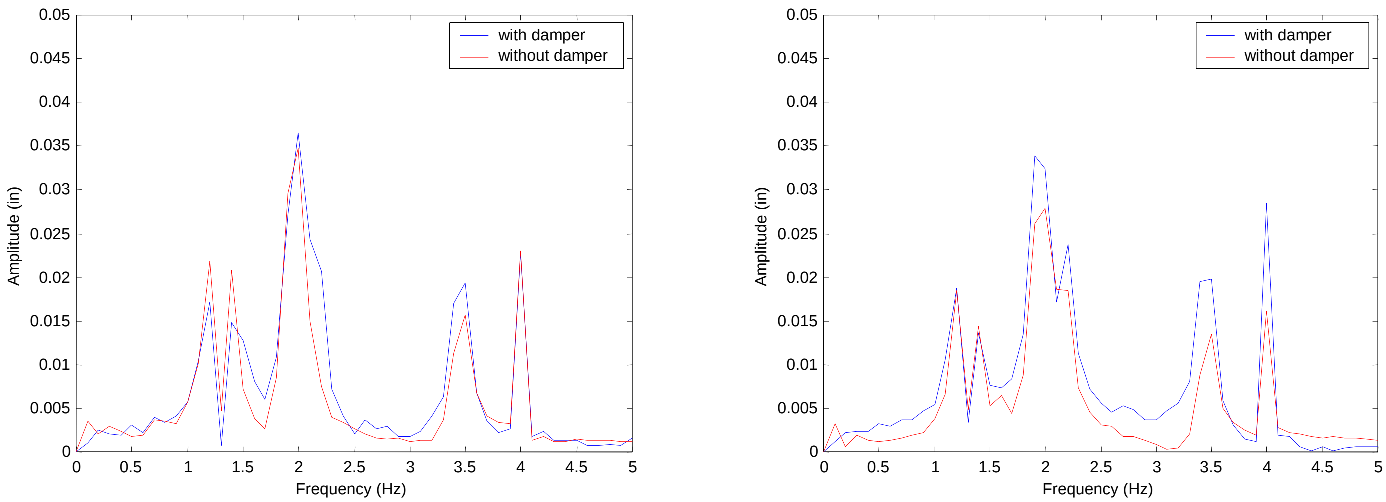

(a) Driver Tire Deflection (b) Passenger Tire Deflection

Figure 3.39. FFTs of Stock Vehicle Tire Deflection Response to Multi-Sine Road Displacement Input (With and Without Roll Bar)

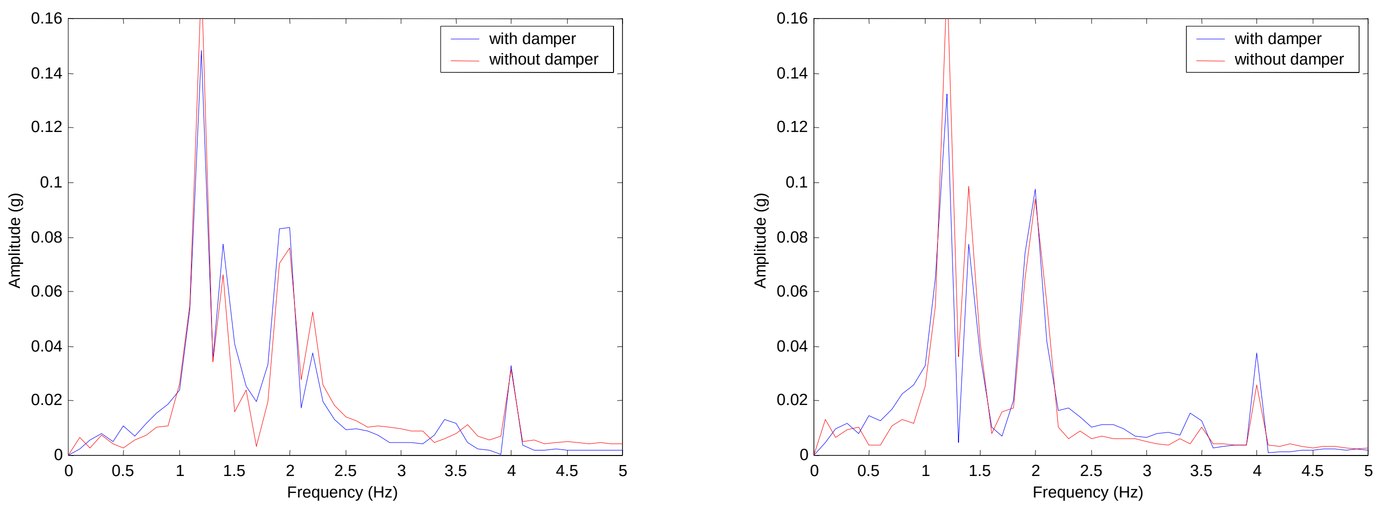

(a) Driver Absolute Frame Position (b) Passenger Absolute Frame Position

Figure 3.40. FFTs of Stock Vehicle Absolute Frame Position Response to Multi-Sine Road Displacement Input (With and Without Roll Bar)

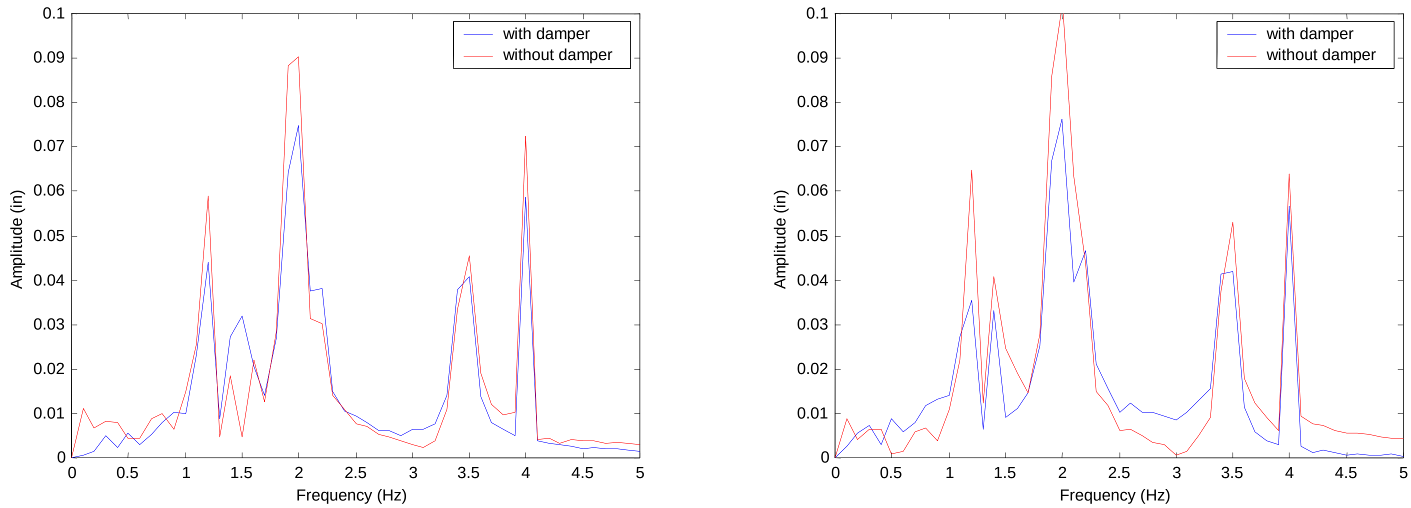

(a) Driver Suspension Rattle (b) Passenger Suspension Rattle

Figure 3.41. FFTs of Stock Vehicle Suspension Rattle Response to Multi-Sine Road Displacement Input (With and Without Roll Bar)

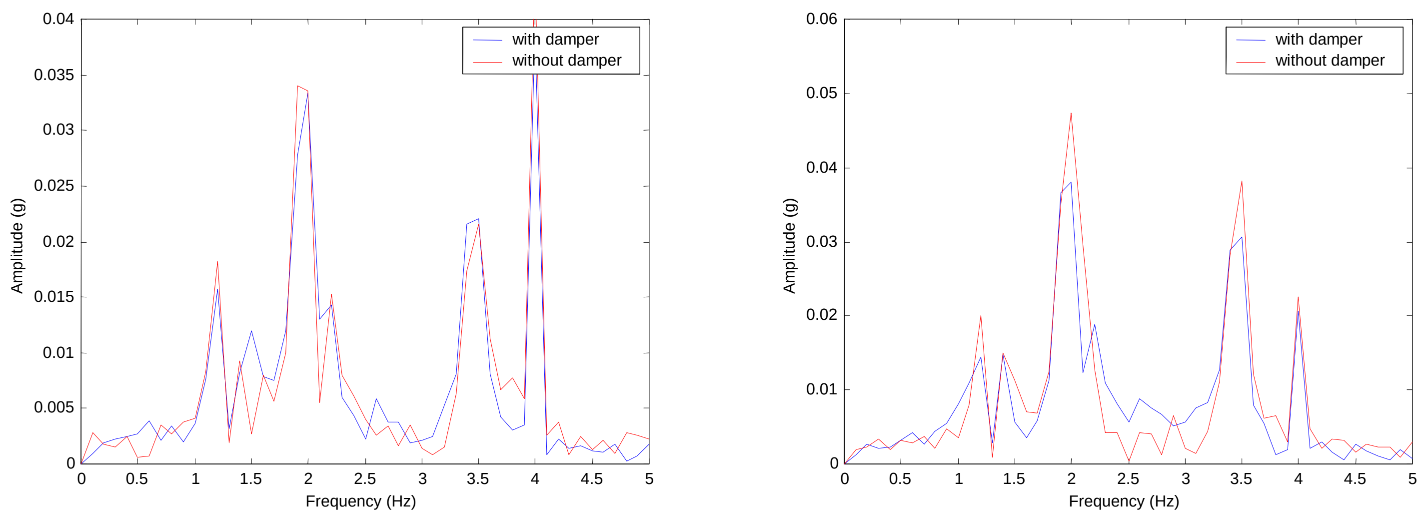

(a) Driver Frame Acceleration (b) Passenger Frame Acceleration

Figure 3.42. FFTs of Stock Vehicle Frame Acceleration Response to Multi-Sine Road Displacement Input (With and Without Roll Bar)

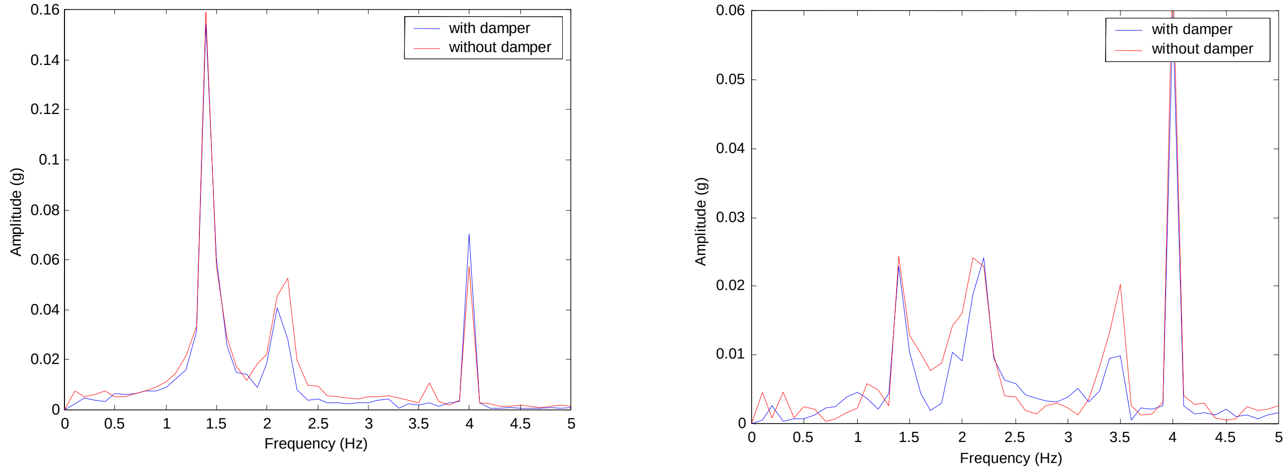

(a) Frame Roll Displacement

(b) Frame Roll Acceleration

Figure 3.43. FFTs of Stock Vehicle Roll Response to Multi-Sine Road Displacement Input (With and Without Roll Bar)

This figure shows that the damper is effective at controlling the displacement across the suspension, particularly in terms of the response to the 1.95 Hz input component. It is less effective at controlling the acceleration of the frame, and not effective at controlling the absolute displacement of the frame.

The response of the vehicle to the step input (both heave and roll) was also measured. Time traces of the response to the heave step input are shown in Figures 3.44-47 (with and without the roll bar) and in Figure 3.48-51 (with and without the damper).

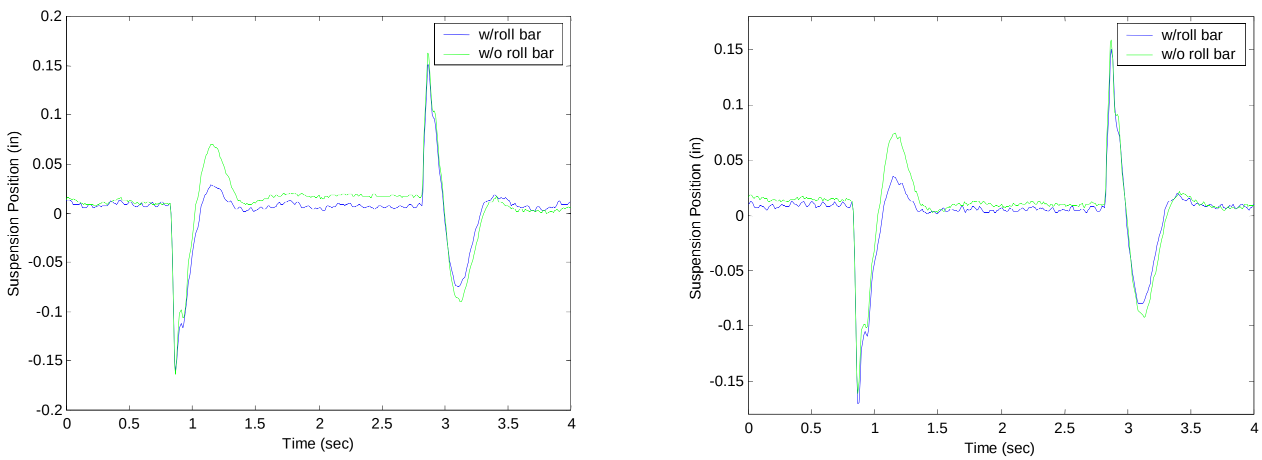

(a) Driver Suspension Rattle

(b) Passenger Suspension Rattle

Figure 3.44. Heave Road Displacement Step Input Suspension Rattle Response (With and Without Roll Bar)

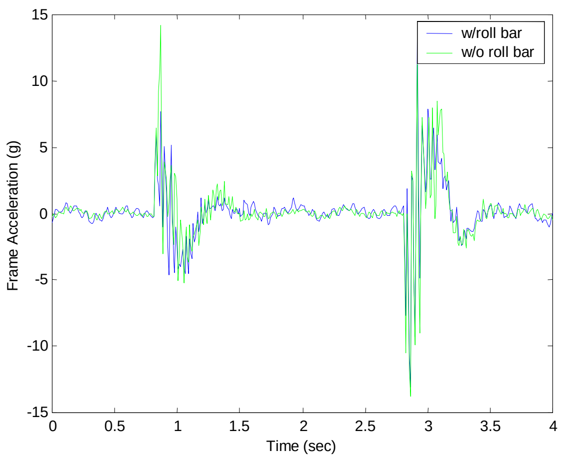

(a) Driver Frame Acceleration

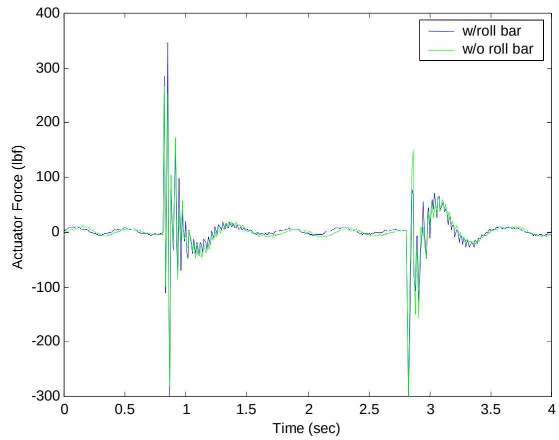

(b) Passenger Frame Acceleration

Figure 3.45. Heave Road Displacement Step Input Frame Acceleration Response (With and Without Roll Bar)

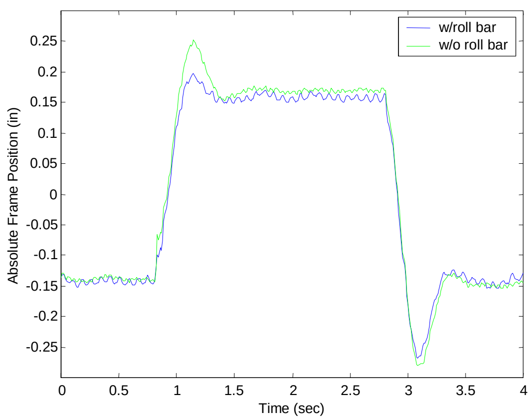

(a) Driver Absolute Frame Position

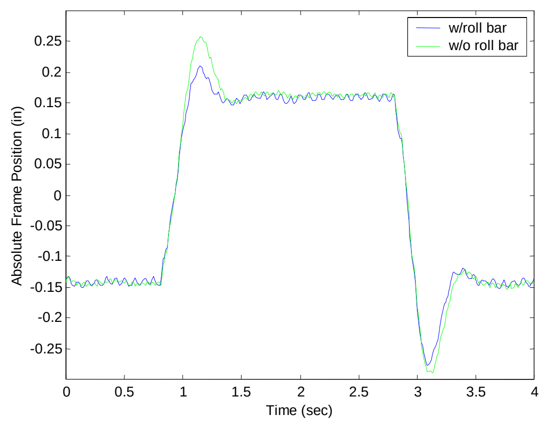

(b) Passenger Absolute Frame Position

Figure 3.46. Heave Road Displacement Step Input Absolute Frame Position Response (With and Without Roll Bar)

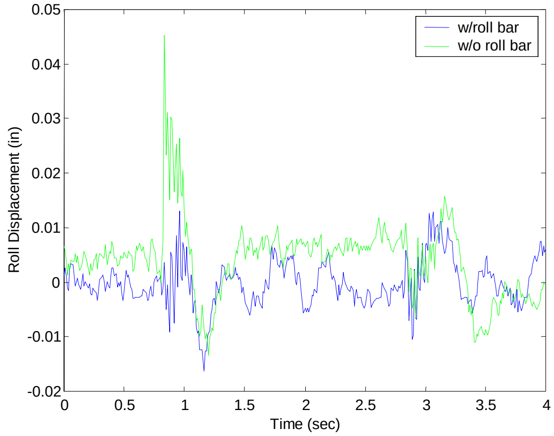

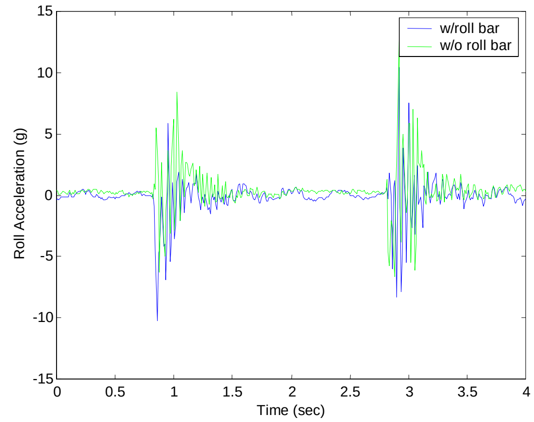

(a) Frame Roll Displacement

(b) Frame Roll Acceleration

Figure 3.47. Heave Road Displacement Step Input Roll Response (With and Without Roll Bar)

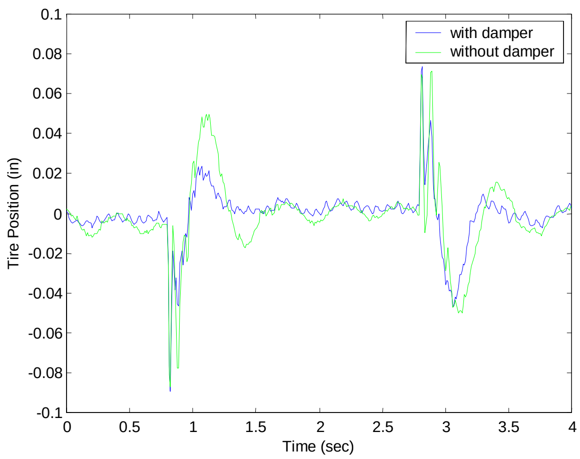

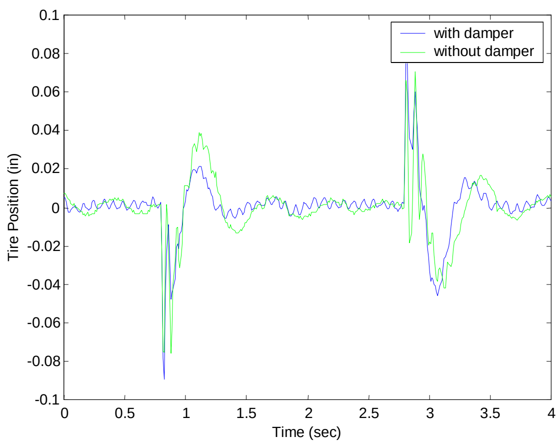

(a) Driver Tire Deflection

(b) Passenger Tire Deflection

Figure 3.48. Heave Road Displacement Step Input Tire Deflection Response (With and Without Damper)

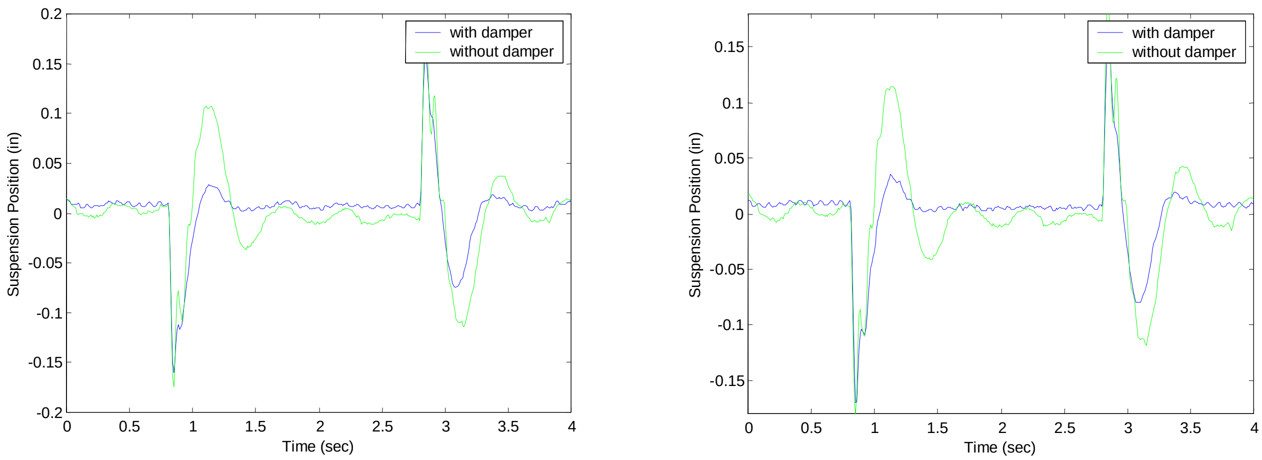

(a) Driver Supension rattle (d) Passenger Supension rattle

Figure 3.49. Heave Road Displacement Step Input Suspension Rattle Response (With and Without Damper)

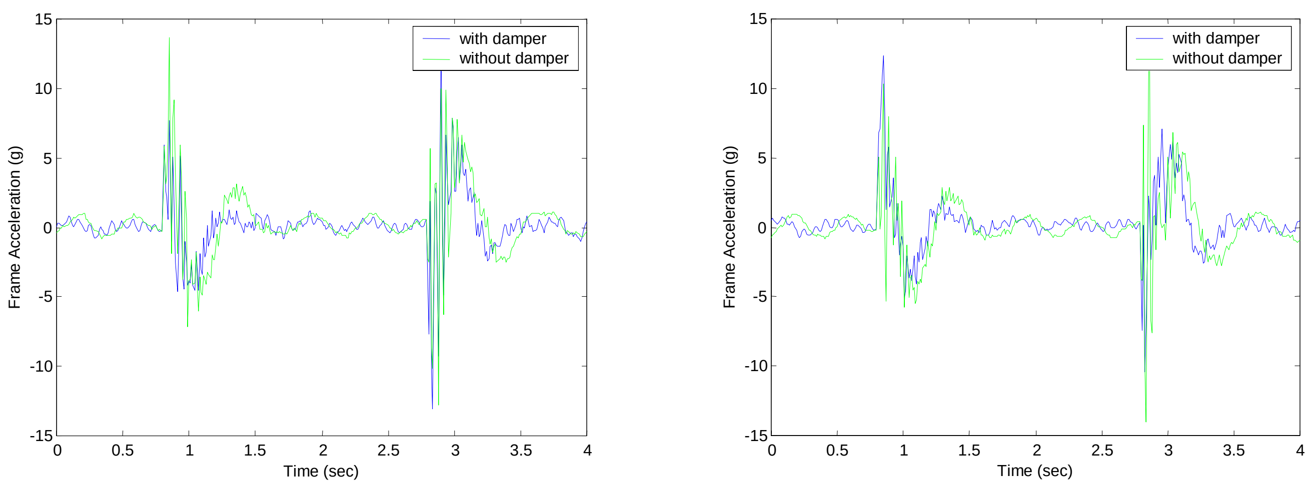

(a) Driver Frame Acceleration (b) Passenger Frame Acceleration

Figure 3.50. Heave Road Displacement Step Input Frame Acceleration Response (With and Without Damper)

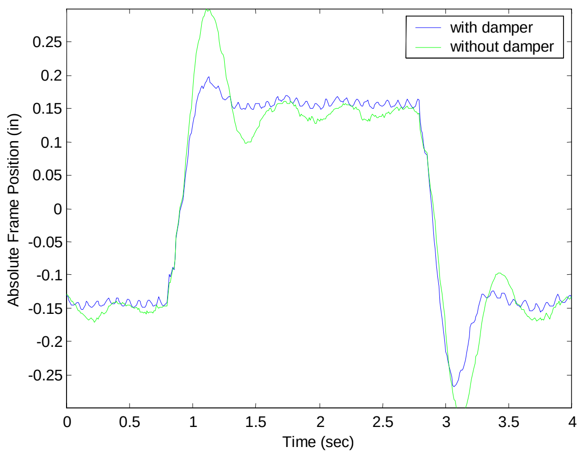

(a) Driver Absolute Frame Position (b) Passenger Absolute Frame Position

Figure 3.51. Heave Road Displacement Step Input Absolute Frame Position Response (With and Without Damper)

The data from the heave step input shows that the roll bar is very effective at limiting the acceleration of the frame of the vehicle, and less effective at limiting the supension rattle. It also shows that the damper is particularly effective in terms of attenuating supension rattle, tire deflection and the absolute displacement of the frame. The time traces of the response to the roll step input are shown in Figure 3.52-56 (with and without the roll bar) and in Figure 3.57-61 (with and without the damper).

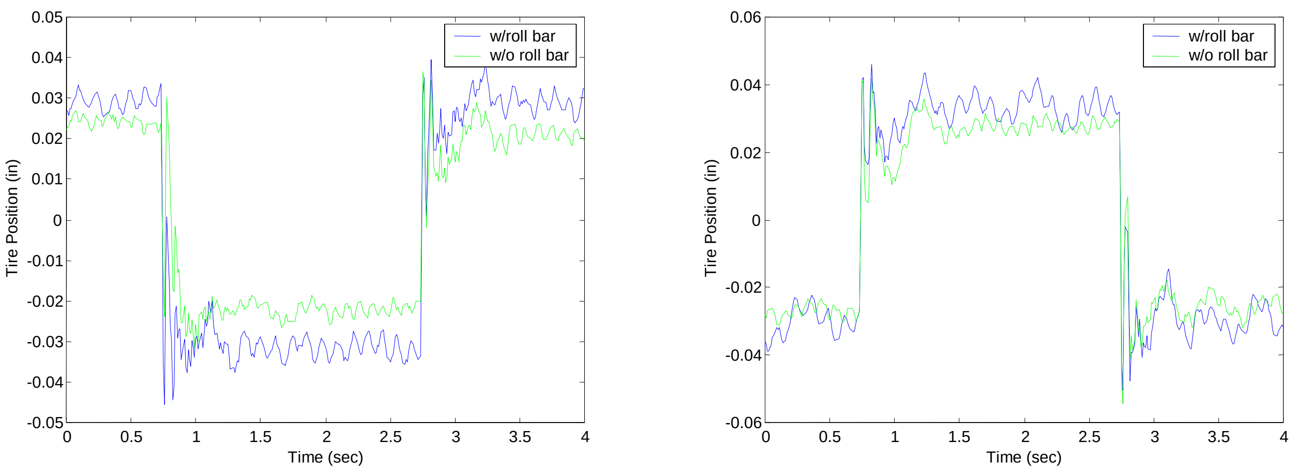

(a) Driver Tire Deflection (b) Passenger Tire Deflection

Figure 3.52. Roll Road Displacement Step Input Tire Deflection Response (With and Without Roll Bar)

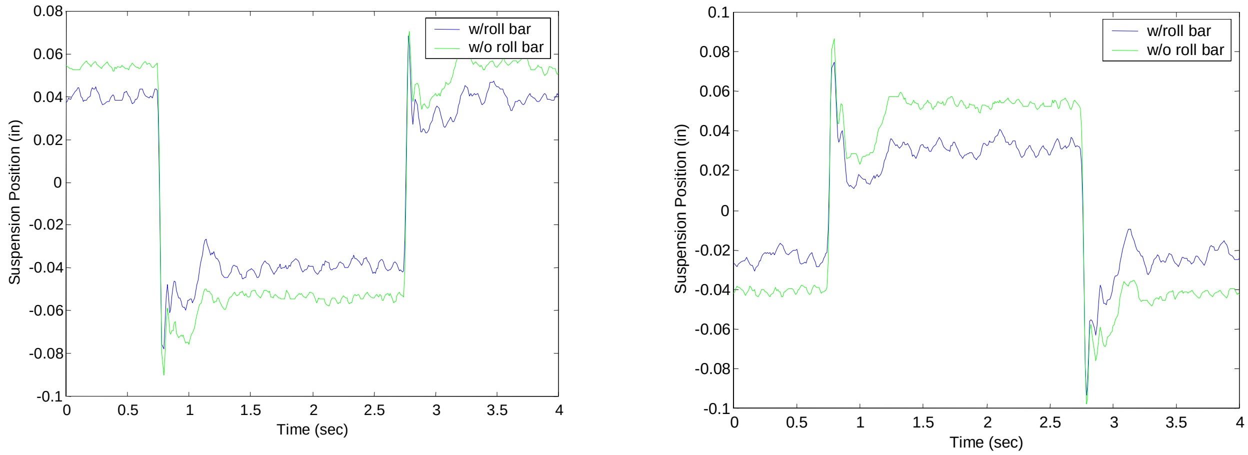

(a) Driver Suspension Rattle

(b) Passenger Suspension Rattle

Figure 3.53. Roll Road Displacement Step Input Suspension Rattle Response (With and Without Roll Bar)

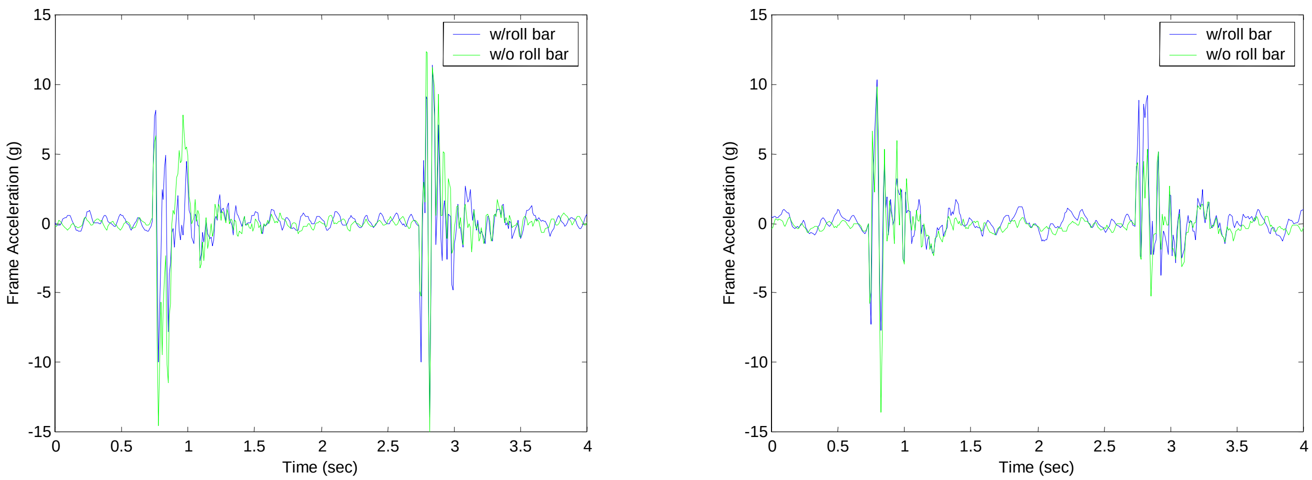

(a) Driver Frame Acceleration

(b) Passenger Frame Acceleration

Figure 3.54. Roll Road Displacement Step Input Frame Acceleration Response (With and Without Roll Bar)

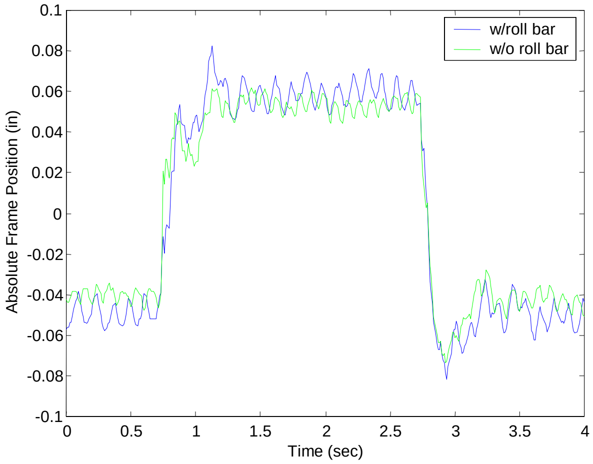

(a) Driver Absolute Frame Position

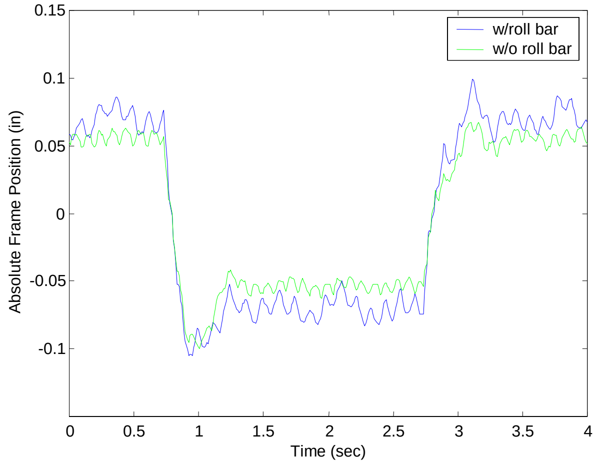

(b) Passenger Absolute Frame Position

Figure 3.55. Roll Road Displacement Step Input Absolute Frame Position Response (With and Without Roll Bar)

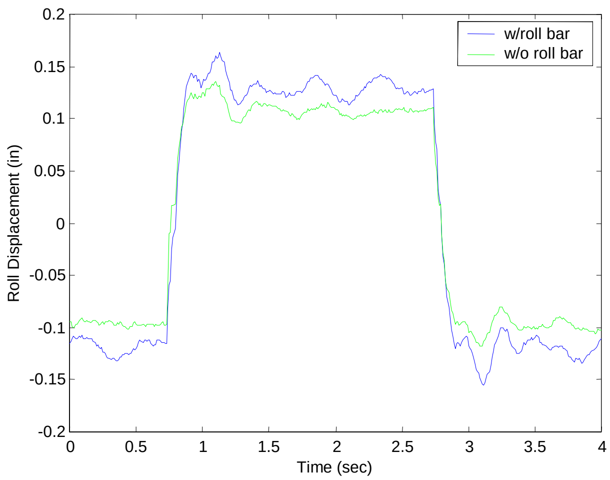

(a) Frame Roll Displacement

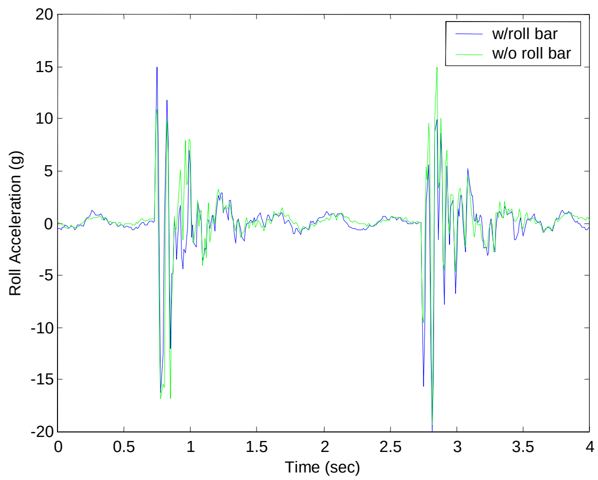

(b) Frame Roll Acceleration

Figure 3.56. Roll Road Displacement Step Input Roll Response (With and Without Roll Bar)

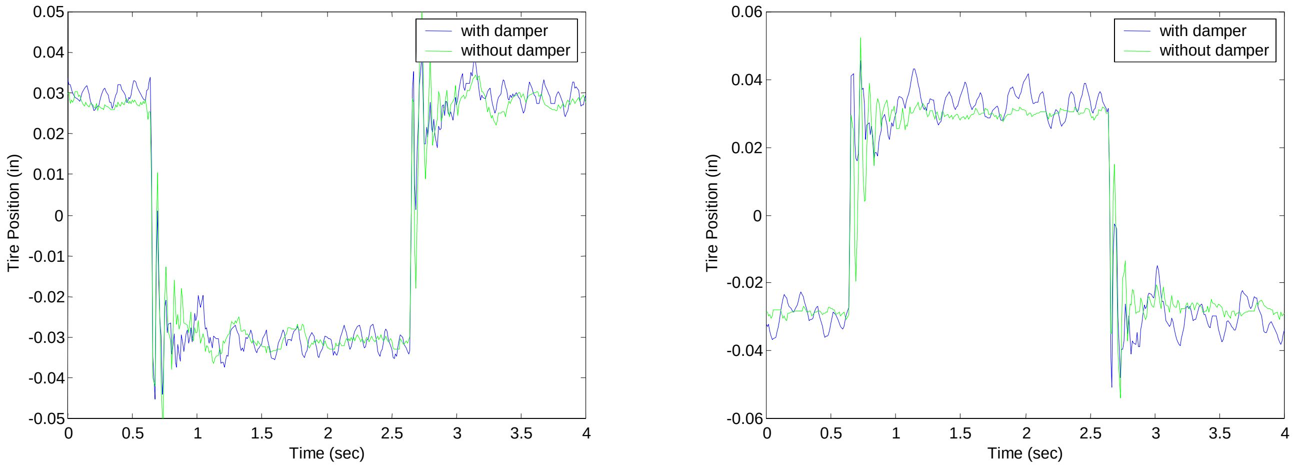

(a) Driver Tire Deflection

(b) Passenger Tire Deflection

Figure 3.57. Roll Road Displacement Step Input Tire Deflection Response (With and Without Damper)

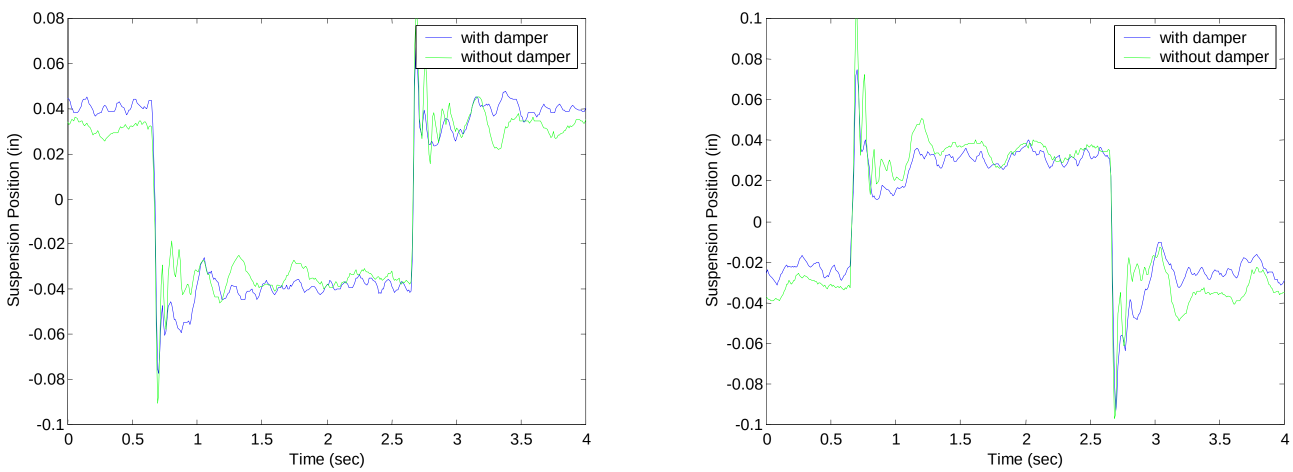

(a) Driver Suspension Rattle

(b) Passenger Suspension Rattle

Figure 3.58. Roll Road Displacement Step Input Suspension Rattle Response (With and Without Damper)

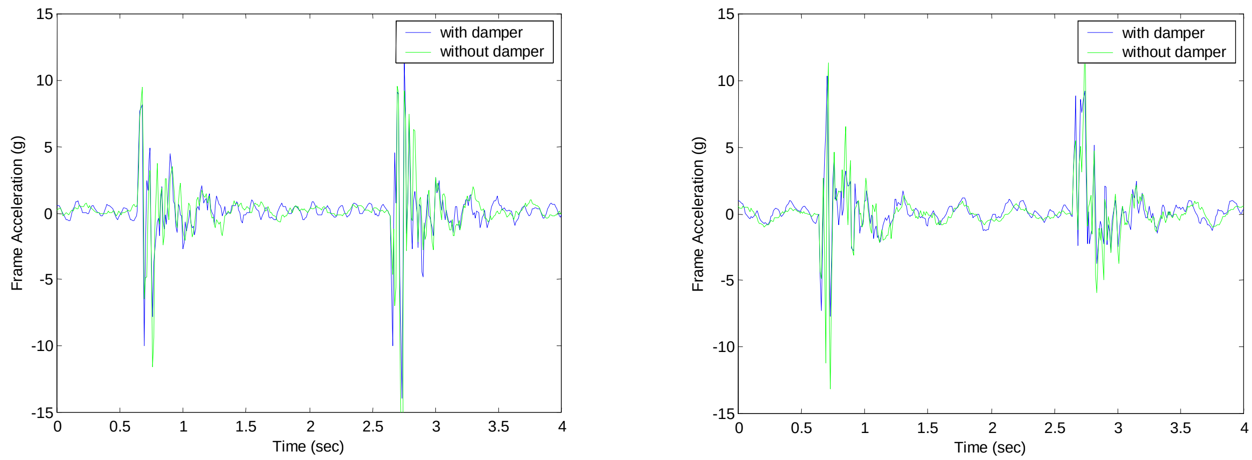

(a) Driver Frame Acceleration

(b) Passenger Frame Acceleration

Figure 3.59. Roll Road Displacement Step Input Frame Acceleration Response (With and Without Damper)

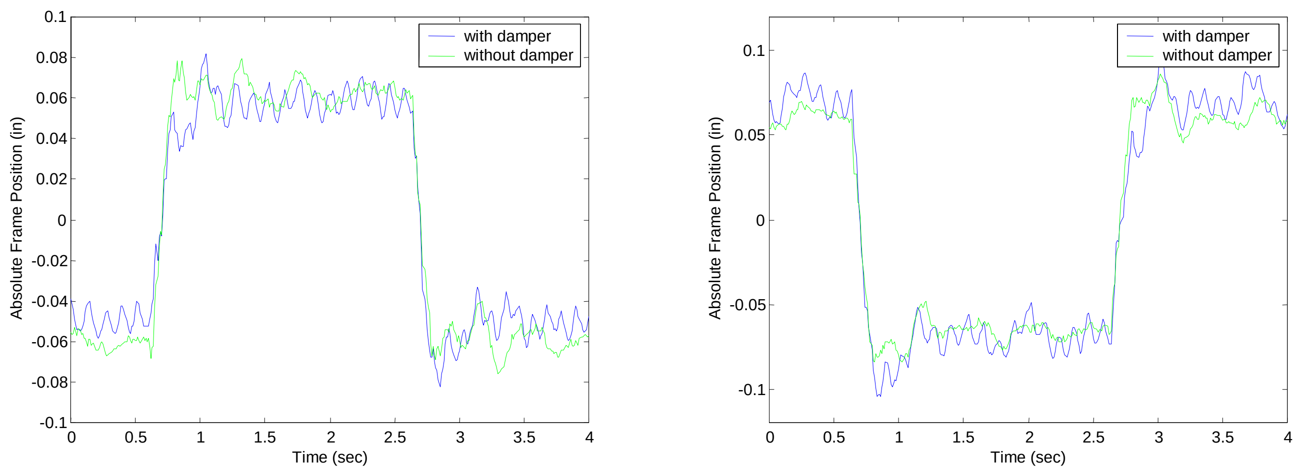

(a) Driver Absolute Frame Position

(b) Passenger Absolute Frame Position

Figure 3.60. Roll Road Displacement Step Input Absolute Frame Position Response (With and Without Damper)

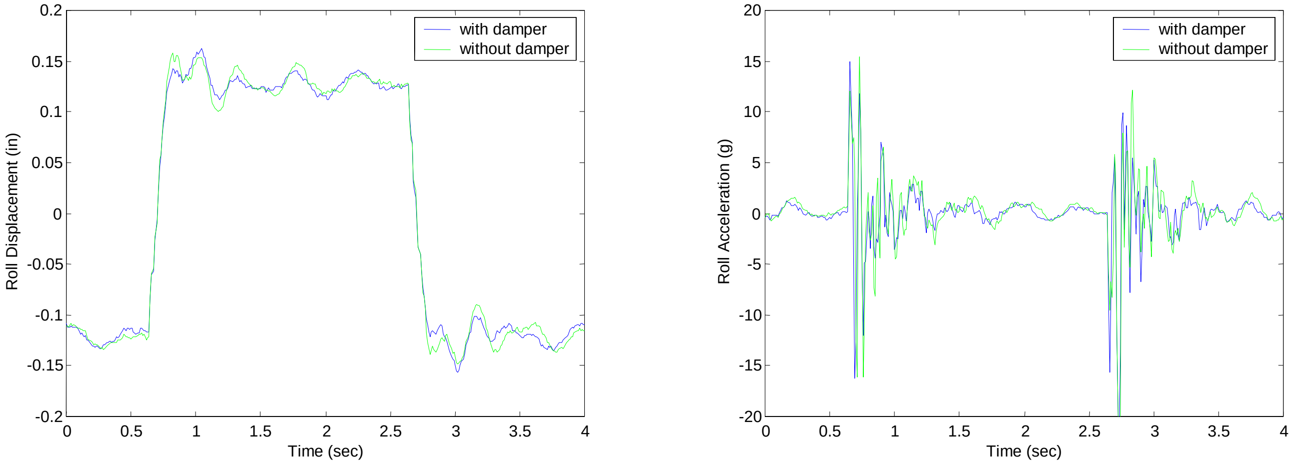

(a) Frame Roll Displacement (b) Frame Roll Acceleration

Figure 3.61. Roll Road Displacement Step Input Roll Response (With and Without Damper)

The data from the roll step input shows that the roll bar is moderately effective at reducing the roll of the frame of the vehicle as well as the displacement across the vehicle's suspension. It is, however, not effective at limiting either the acceleration of the frame or the deflection of the tire. The data also shows that the damper is not very effective at attenuating the response to a roll input.

The chirp input was also applied (to excite both heave and roll modes) to the test vehicle. This was performed for the vehicle in its stock configuration, the vehicle with the roll bar removed, and for the vehicle with the stock dampers removed. The results (in both time and frequency domains) of the in-phase chirp input are shown in Figures 3.62-65 and Figures 3.66-70.

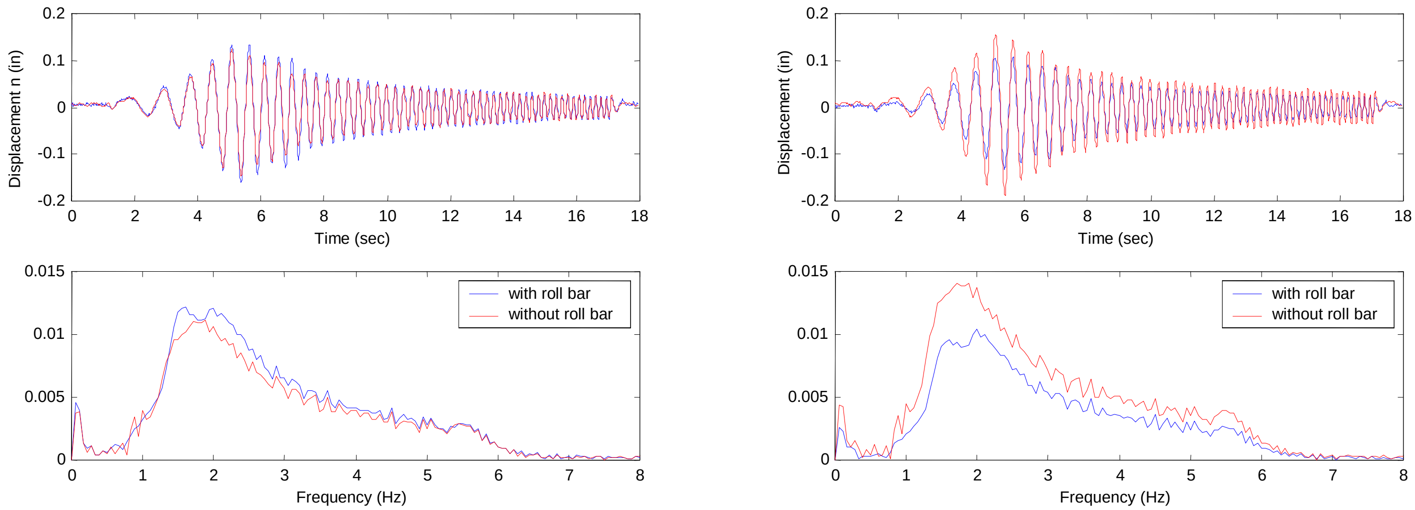

(a) Driver Tire Deflection (b) Passenger Tire Deflection

Figure 3.62. Heave Chirp Input Tire Deflection Response w/wo Roll Bar

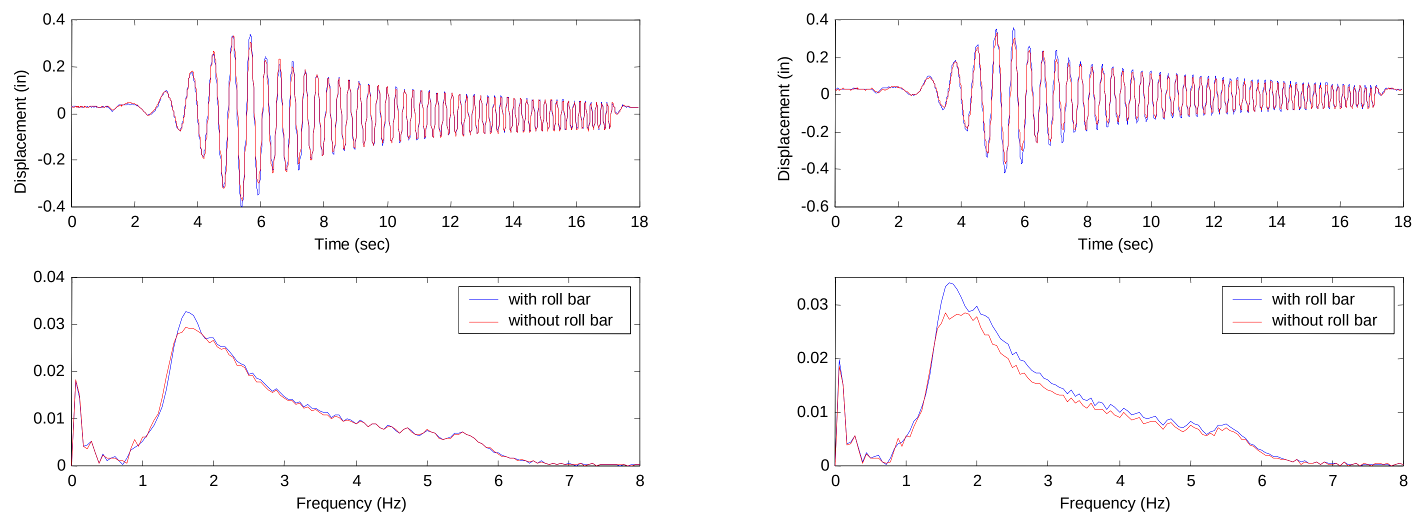

(a) Driver Suspension Rattle (b) Passenger Suspension Rattle

Figure 3.63. Heave Chirp Input Suspension Rattle Response w/wo Roll Bar

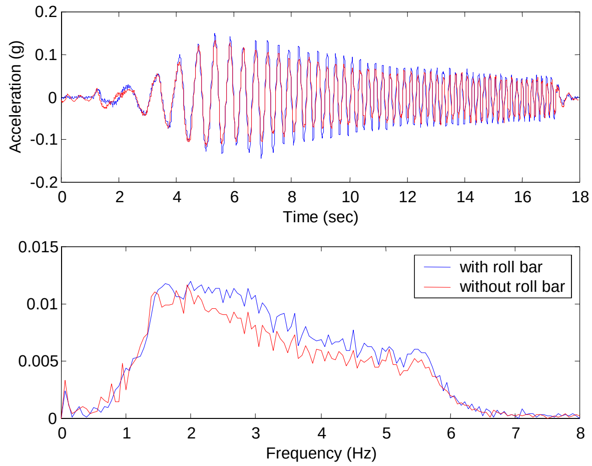

(a) Driver Frame Acceleration

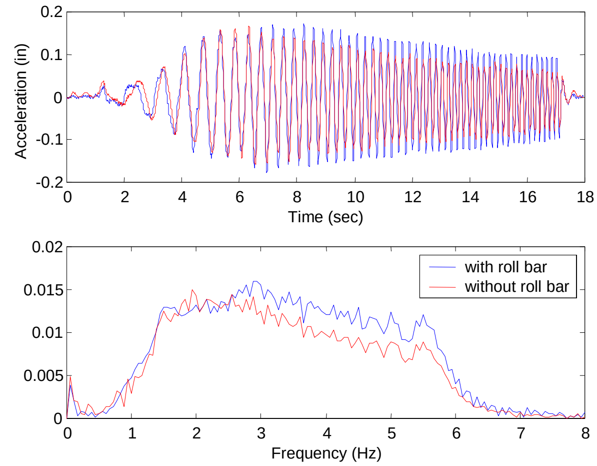

(b) Passenger Frame Acceleration

Figure 3.64. Heave Chirp Input Frame Acceleration Response w/wo Roll Bar

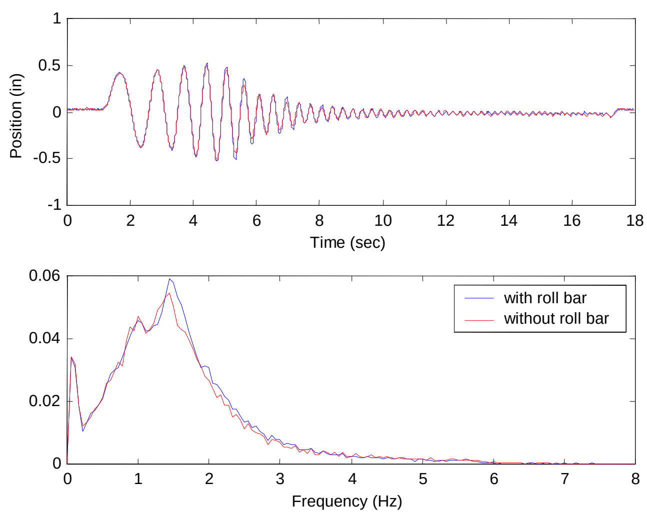

(a) Driver Absolute Frame Position

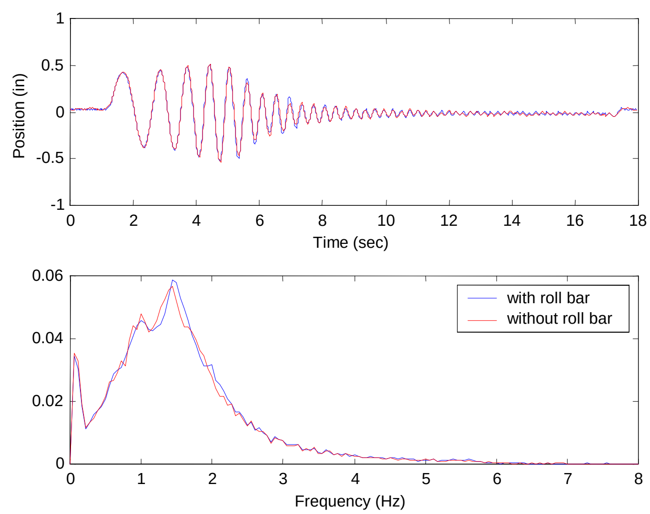

(b) Passenger Absolute Frame Position

Figure 3.65. Heave Chirp Input Absolute Frame Position Response w/wo Roll Bar

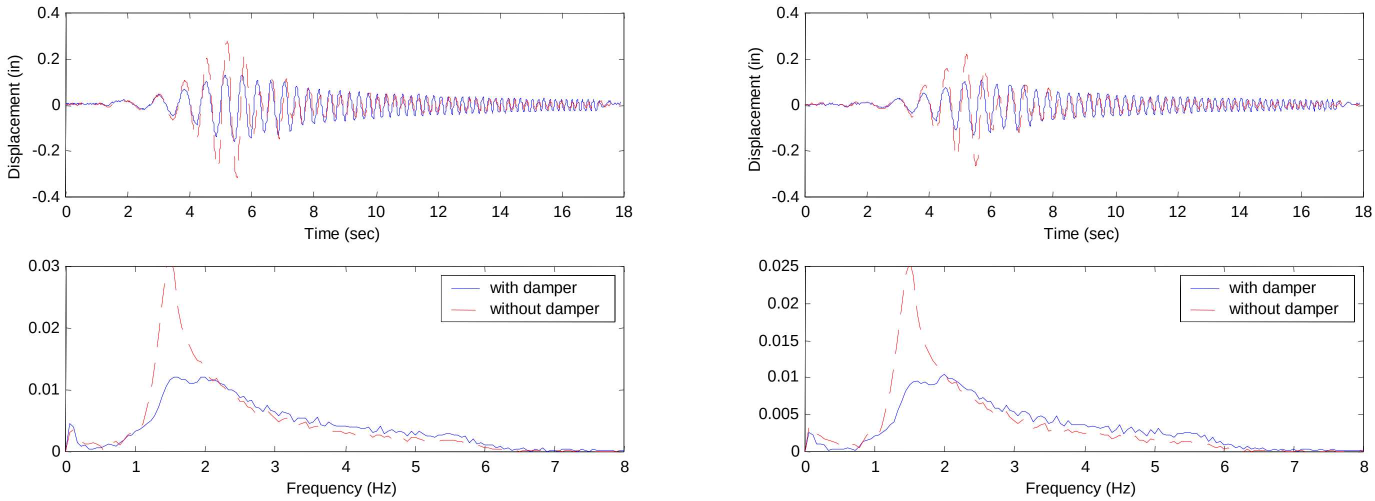

(a) Driver Tire Deflection (b) Passenger Tire Deflection

Figure 3.66. Heave Road Displacement Chirp Input Tire Deflection Response (With and Without Damper)

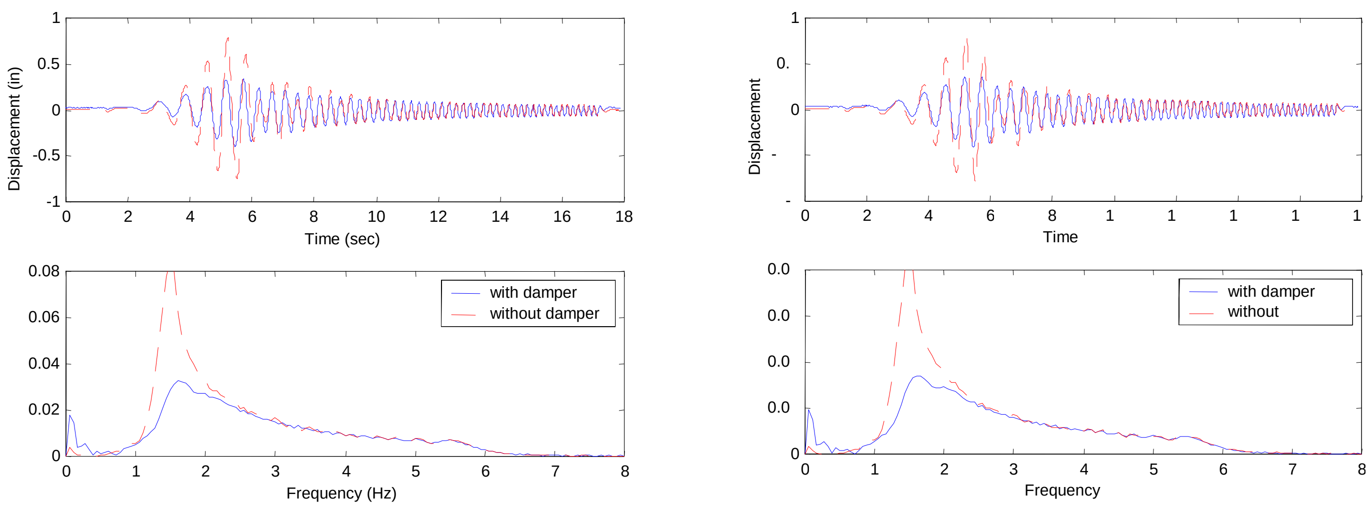

(a) Driver Suspension Rattle (b) Passenger Suspension Rattle

Figure 3.67. Heave Road Displacement Chirp Input Suspension Rattle Response (With and Without Damper)

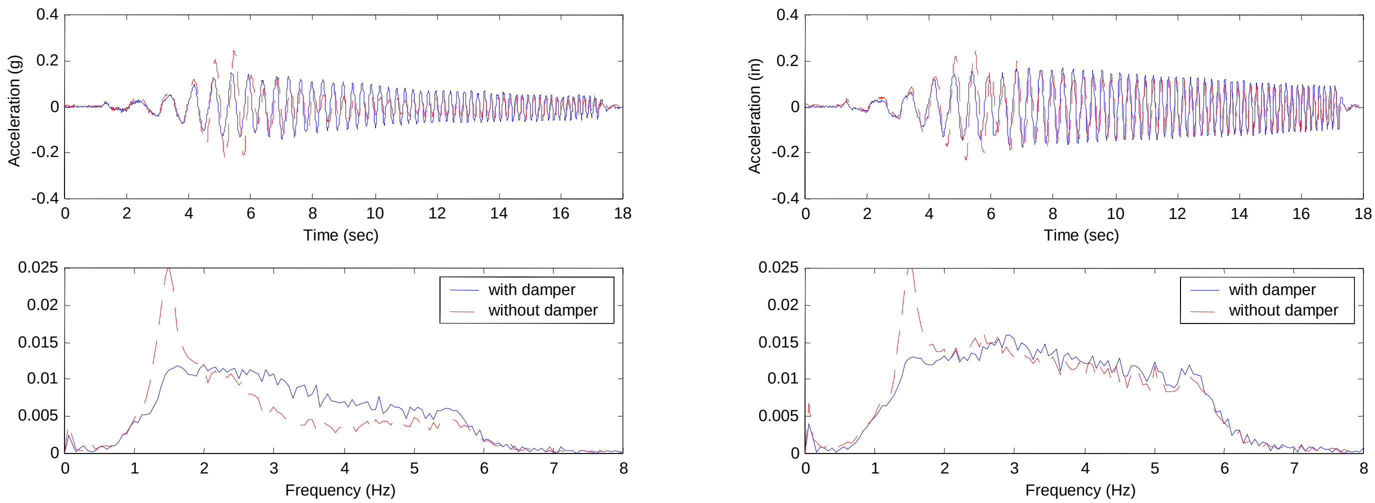

(a) Driver Frame Acceleration (b) Passenger Frame Acceleration

Figure 3.68. Heave Road Displacement Chirp Input Frame Acceleration Response (With and Without Damper)

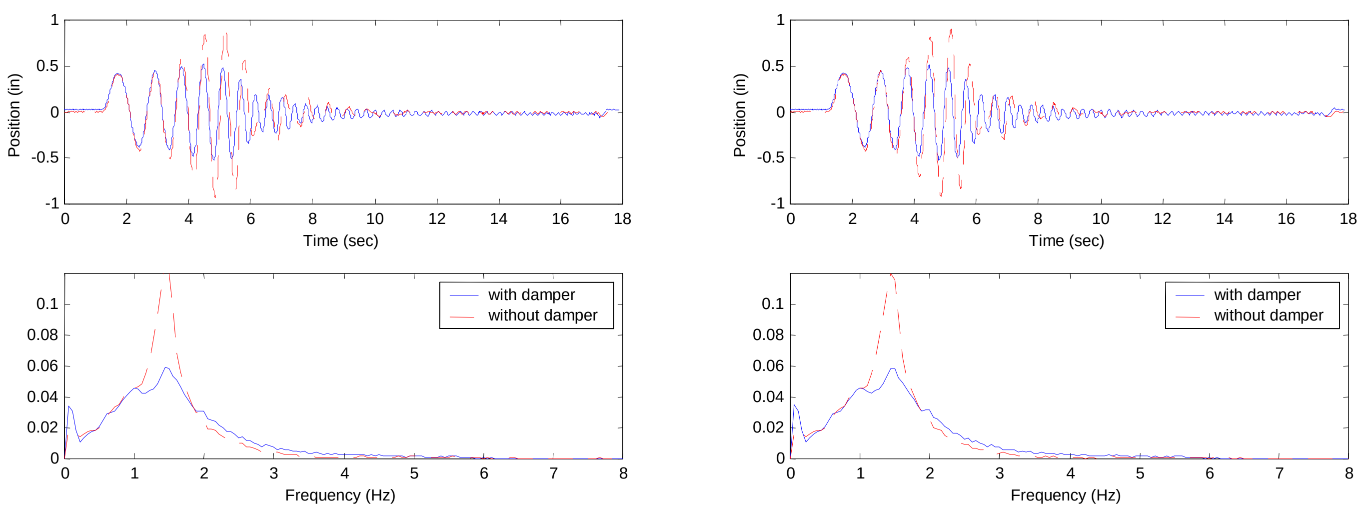

(a) Driver Absolute Frame Position (b) Passenger Absolute Frame Position

Figure 3.69. Heave Road Displacement Chirp Input Absolute Frame Position Response (With and Without Damper)

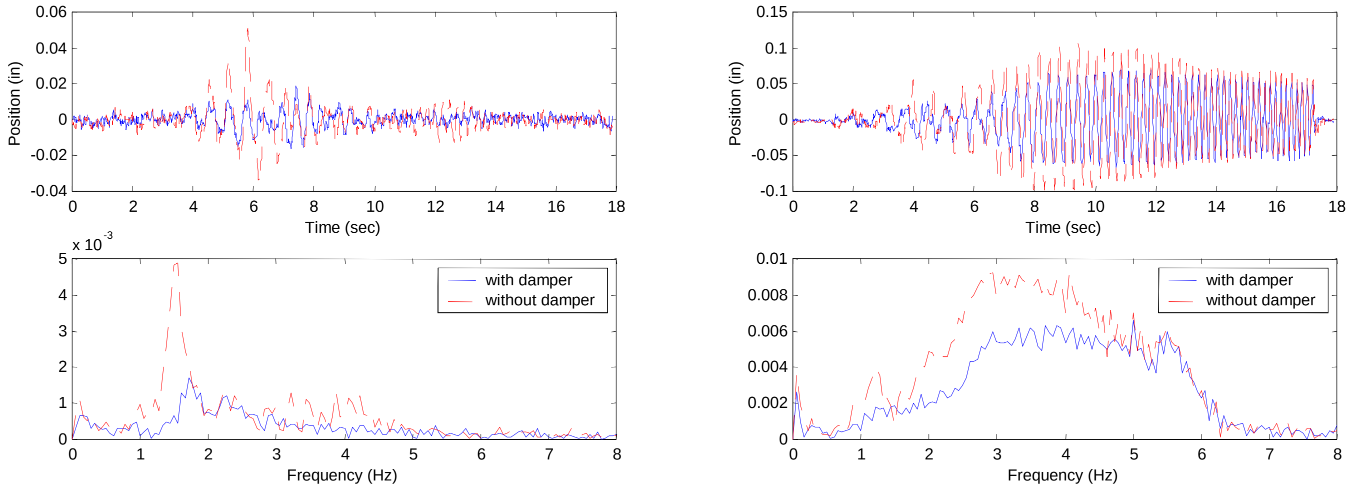

(a) Frame Roll Displacement

(b) Frame Roll Acceleration

Figure 3.70. Heave Road Displacement Chirp Input Roll Response (With and Without Damper)

The heave chirp data shows (for most of the frequencies of interest) a slight increase in the acceleration of the frame, tire deflection, supension rattle, and absolute displacement of the frame with the inclusion of the roll bar. It also shows that for all measurements made, the presence of the damper causes a large reduction in the vibration in the 1 to 2 Hz range. As the low frequency response is, from a dynamics perspective, more important than the response at higher frequencies, this is a very important result. The results (in both time and frequency domains) for the roll input are shown in Figures 3.71-74 and Figures 3.75-78.

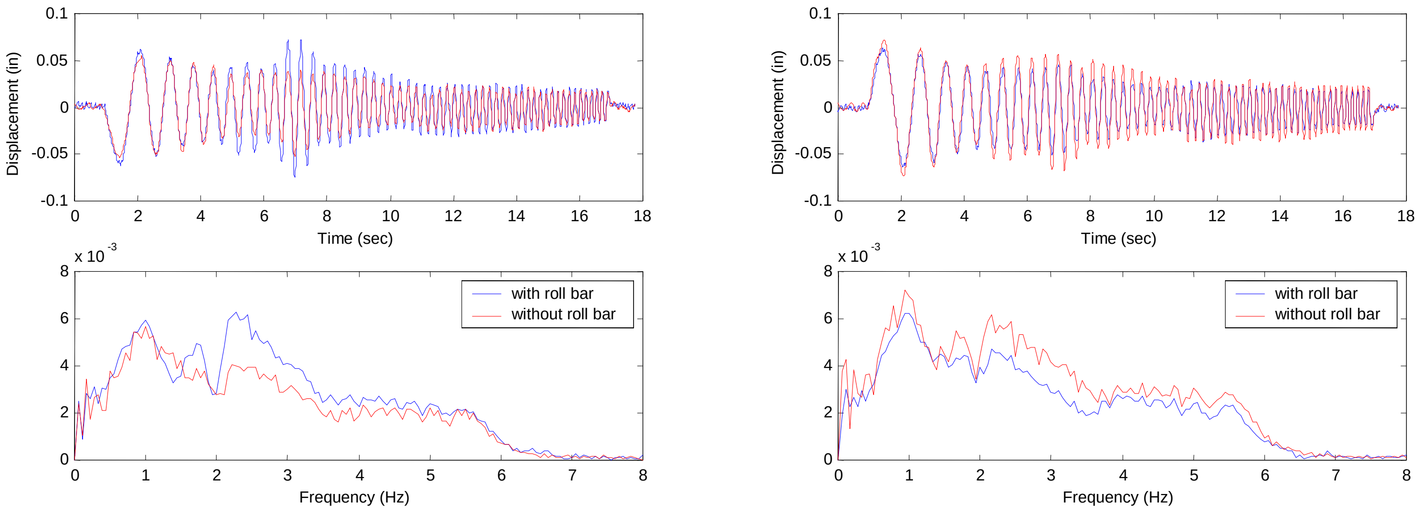

(a) Driver Tire Deflection

(b) Passenger Tire Deflection

Figure 3.71. Roll Road Displacement Chirp Input Tire Deflection Response (With and Without Roll Bar)

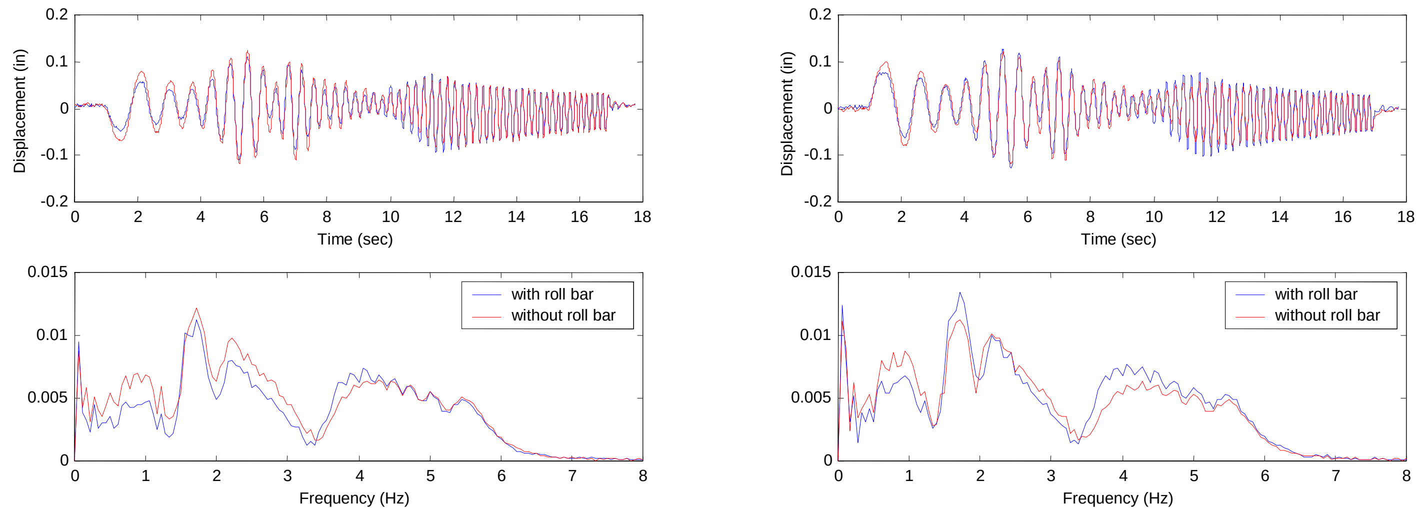

(a) Driver Suspension Rattle

(b) Passenger Suspension Rattle

Figure 3.72. Roll Road Displacement Chirp Input Suspension Rattle Response (With and Without Roll Bar)

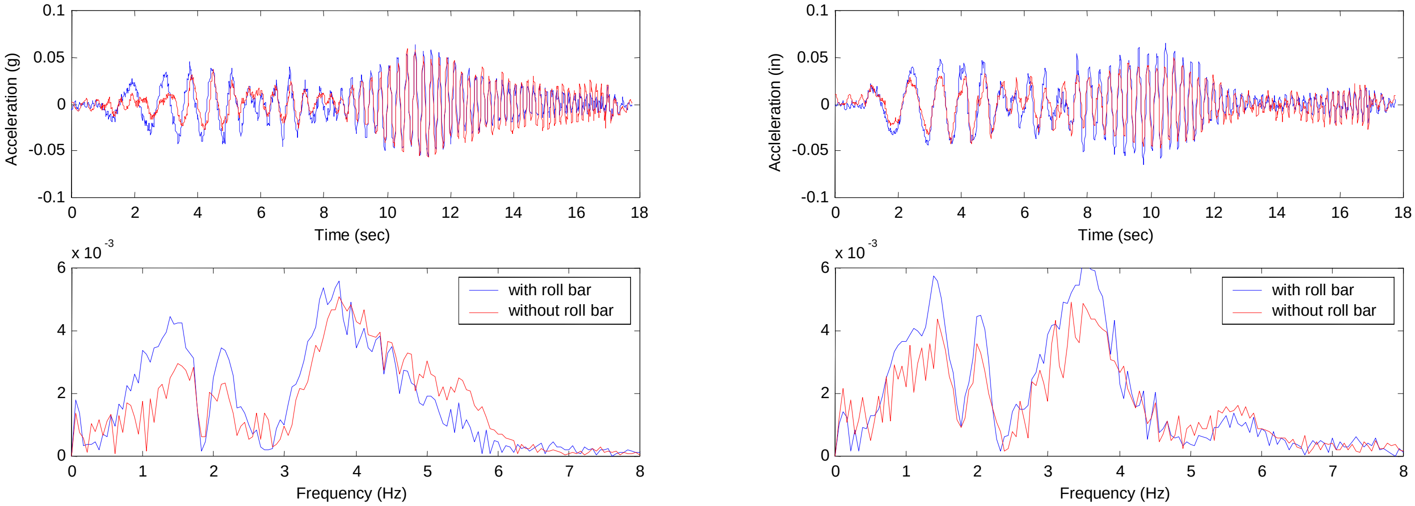

(a) Driver Frame Acceleration (b) Passenger Frame Acceleration

Figure 3.73. Roll Road Displacement Chirp Input Frame Acceleration Response (With and Without Roll Bar)

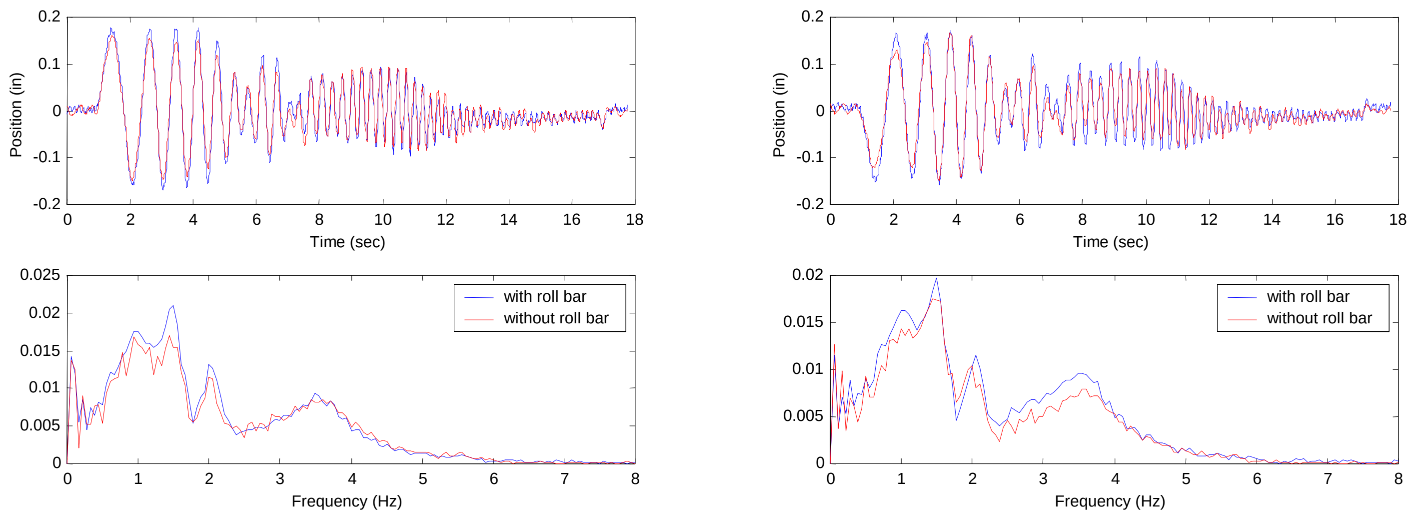

(a) Driver Absolute Frame Position (b) Passenger Absolute Frame Position

Figure 3.74. Roll Road Displacement Chirp Input Absolute Frame Position Response (With and Without Roll Bar)

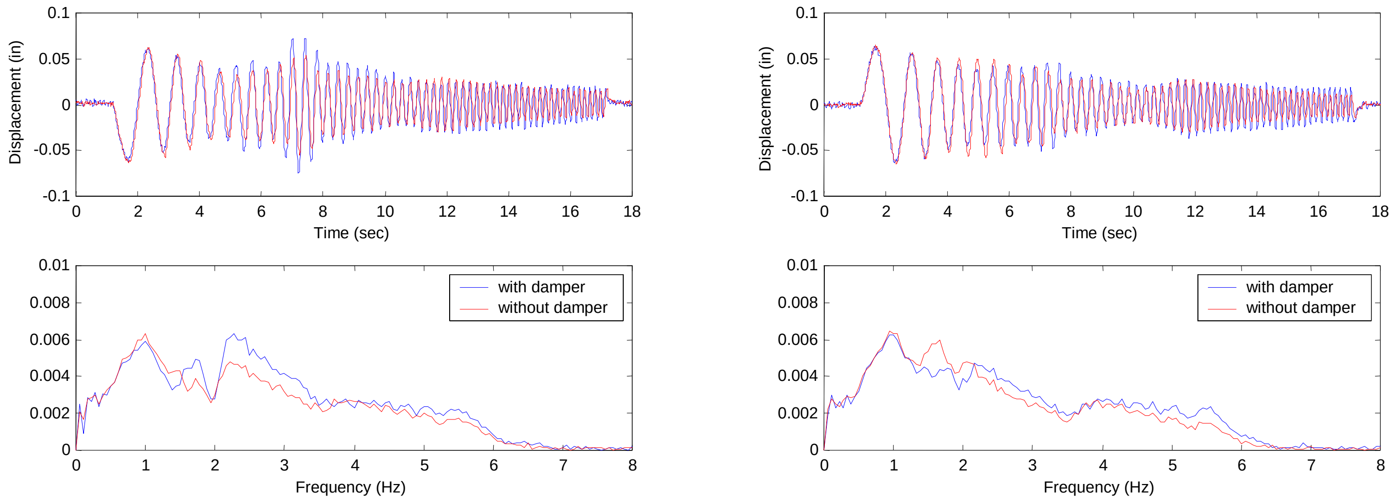

(a) Driver Tire Deflection (b) Passenger Tire Deflection

Figure 3.75. Roll Road Displacement Chirp Input Tire Deflection Response (With and Without Damper)

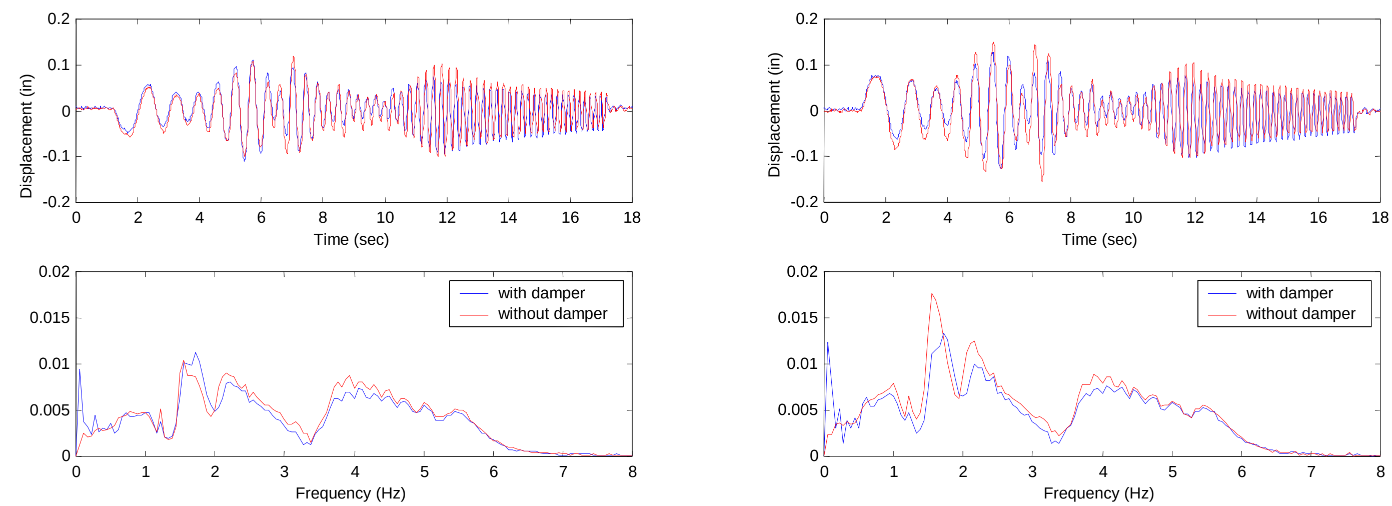

(a) Driver Suspension Rattle (b) Passenger Suspension Rattle

Figure 3.76. Roll Road Displacement Chirp Input Suspension RattleResponse (With and Without Damper)

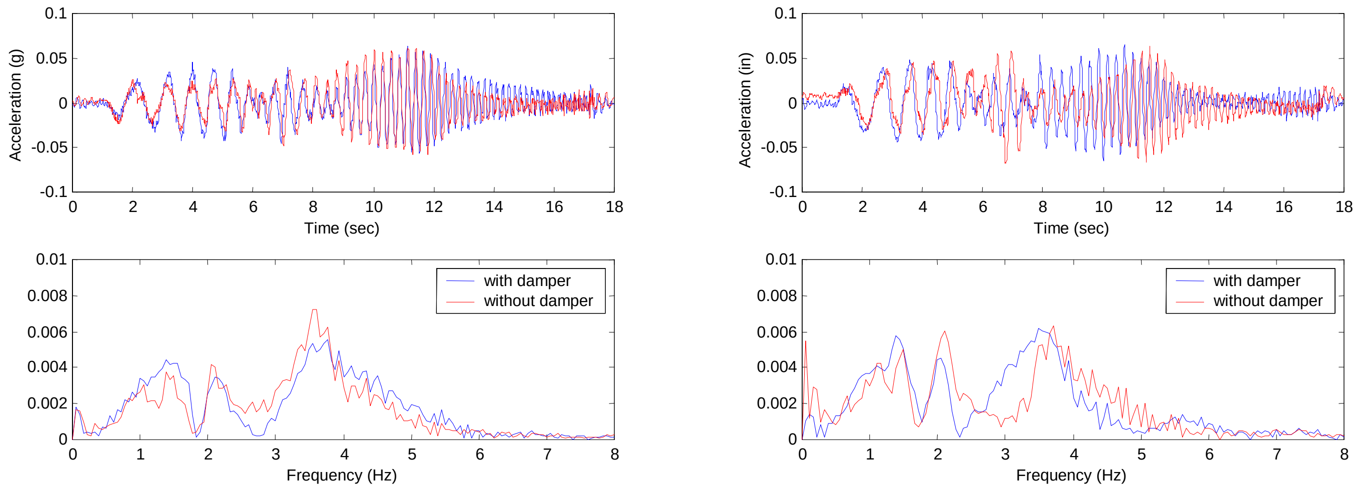

(a) Driver Frame Acceleration (b) Passenger Frame Acceleration

Figure 3.77. Roll Road Displacement Chirp Input Frame Acceleration Response (With and Without Damper)

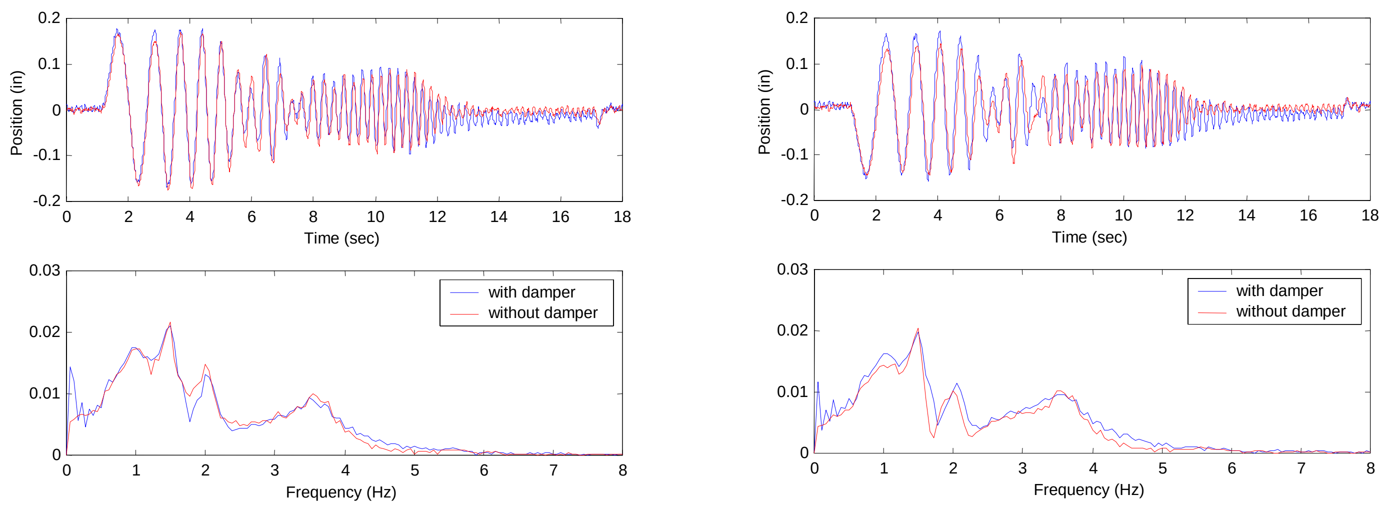

(a) Driver Absolute Frame Position (b) Passenger Absolute Frame Position

Figure 3.78. Roll Road Displacement Chirp Input Absolute Frame Position Response (With and Without Damper)

The roll chirp data shows a slight increase in frame acceleration with the inclusion of the roll bar. The driver side supension rattle and passenger side tire deflection both increase with the addition of the roll bar, while the passenger side supension rattle and driver side tire deflection both decrease for the same case. This is not contradictory as the roll bar acts to equalize motion from side to side. The data also shows that the inclusion of the damper has an effect on the vibration of the vehicle that varies with different input frequencies.

The more surprising result of the roll chirp testing is that in the frequency band of interest, the addition of the roll bar increases both frame roll displacement and frame roll acceleration, as shown in Figure 3.79.

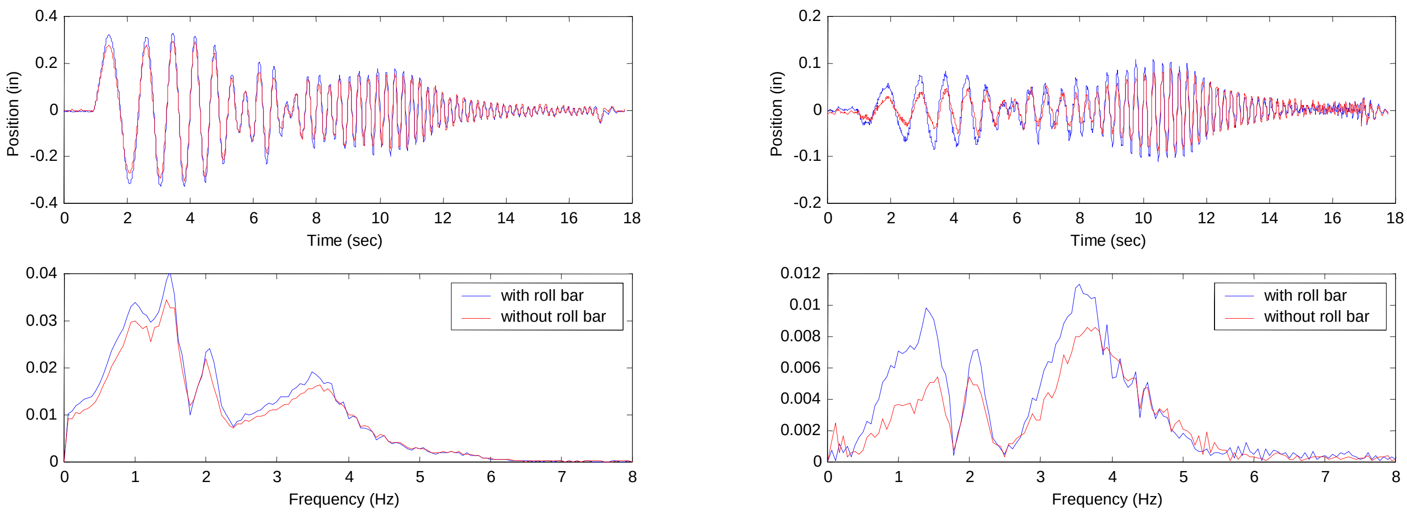

(a) Frame Roll Displacement (b) Frame Roll Acceleration

Figure 3.79. Frame Roll Measures; Roll Road Displacement Chirp Input Response (With and Without Roll Bar)

The inclusion of the damper, likewise increases both measures of roll, as shown in Figure 3.80.

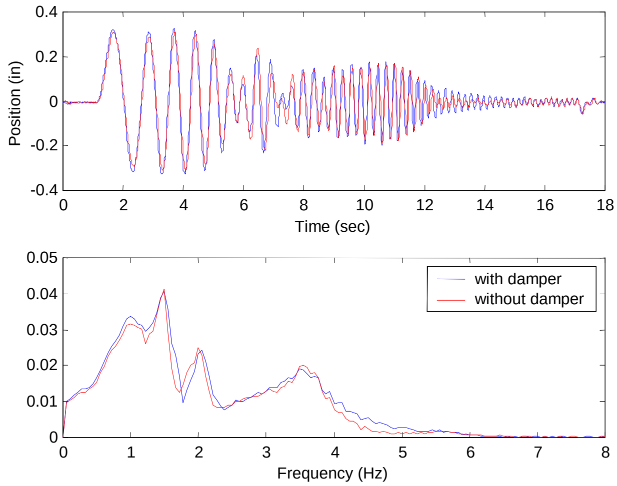

(a) Frame Roll Displacement

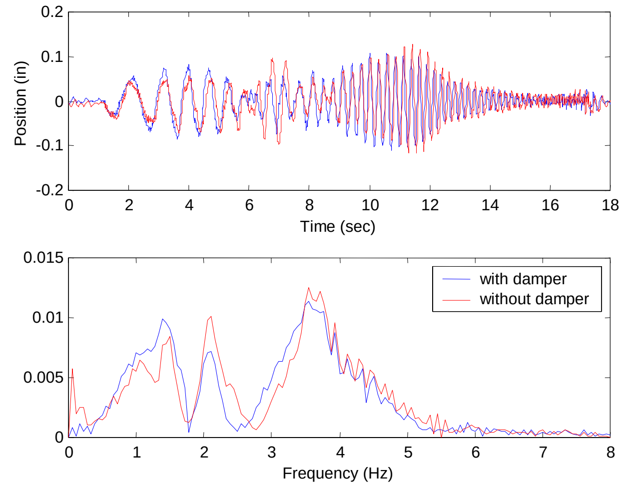

(b) Frame Roll Acceleration

Figure 3.80. Frame Roll Measures; Roll Road Displacement Chirp Input Response (With and Without Dampers)

This is not a surprising result as the presence of the damper increases the amount of coupling between the sprung and unsprung bodies and therefore more of the input (a roll input in this case) will be transmitted.

3.2.4 Passive Damper Data

In order to develop controllable MR dampers that will be useful in controlling the dynamics of the test vehicle, it is first necessary to characterize the stock dampers, shown in Figures 3.81 and 3.82.

Figure 3.81. Stock Front Ford Expedition Dampers [32]

Figure 3.82. Stock Rear Ford Expedition Damper [32]

Physically, the overall dimensions of the MR damper must match those of the stock damper being replaced. It must have the same mounting hardware, the same uncompressed length, and the same stroke. Additionally, it must have a similar diameter in order to fit in the stock damper's mounting location (on the front of the vehicle, the mounting position is within the coil spring). The overall dimensions of the stock dampers are listed in Table 3.1.

Table 3.1. Stock Front Ford Expedition Damper Overall Dimensions

Dimension	Value (front/rear)
Extended Length	14.75/20.0
Stroke	4.375/6.125
Diameter	2.875/3.25
Upper Mounting Configuration	stud/eye
Lower Mounting Configuration	eye/eye

Additionally, the force/velocity characteristics of the stock dampers must be known in order to determine the range of force the controllable MR damper must have. In order to determine these curves, the stock damper was removed from the vehicle and installed on a Material Testing System (MTS) rig shown in Figure 3.83. The damper was encased in a water jacket to provide cooling during testing in order to ensure a constant temperature throughout the test for more accurate characterization of the damper.

Figure 3.83. Test Vehicle Damper on MTS Load Frame With Water Jacket [32]

With the damper on the load frame, it was possible to cycle the damper and record the applied force. In order to perform the testing, the damper was cycled with a sine wave of fixed frequency and adjustable amplitude. The peak velocity in one cycle can be found by multiplying the amplitude (maximum displacement) by the excitation frequency (in rad/sec). The maximum force (read off of the force display), together with the corresponding peak velocity yields one point on the desired force/velocity plot. The force/velocity plot developed in this manner is shown in Figure 3.84.

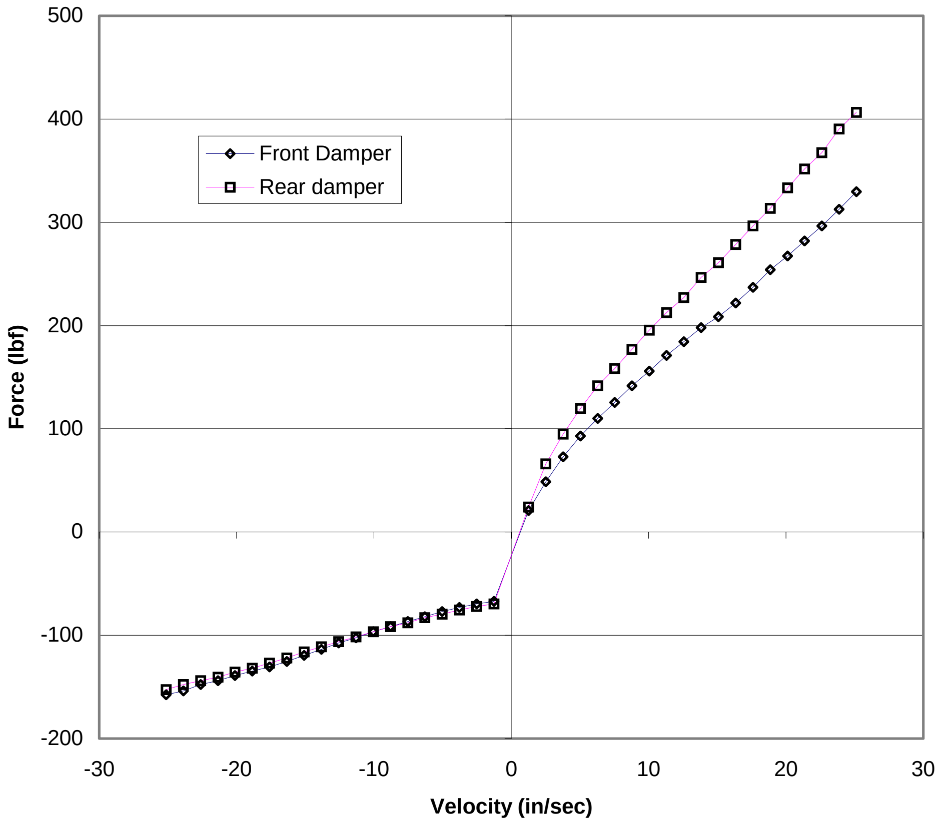

Figure 3.84. Force/Velocity Curves; Ford Expedition Stock Dampers

Figure 3.50 shows a force/velocity curve that is much higher in extension than in compression. This is a common characteristic of conventional dampers. Additionally, the extension side (positive velocity) is a bilinear curve. This change from a high slope at low velocities to a lower slope at higher velocities is again a common characteristic of conventional dampers and is meant to increase ride comfort without sacrificing vehicle stability. The characteristics of the force/velocity plot that are most important in the design of an MR damper are the maximum and minimum values. These values (in the velocity range tested) are 406.5 lbf in extension and 157.5 lbf in compression.

3.2.5 MR Damper Development

The MR damper designed for this study is a monotube damper; the piston travels in a single cylinder that contains a fluid chamber and pressurized air chamber. A floating piston is used to separate the fluid and air chambers. The air chamber is used to accommodate the change in the fluid chamber volume, due to the volume of the piston rod entering the chamber. This is necessary to prevent the creation of a vacuum as the piston extends. If a vacuum is created in the fluid chamber, then the fluid will cavitate as it passes through the damper piston and the damping effect will be significantly diminished. The damping force is the result of viscous friction arising from the passage of the working fluid through an orifice. The damping force is a function of properties of both the orifice and the fluid rheology. The size and shape of the orifice as well as the viscosity of the fluid determine how easy it is for the fluid to pass through the orifice. In order to make a controllable damper without mechanically changing the character of the internal orifices, it is necessary to vary the properties of the working fluid. The fluid itself must be able to change from a low viscosity, free flowing fluid to a high viscosity, semisolid in a brief time span. The class of fluids whose characteristics can be externally varied in this manner are called controllable fluids. A controllable fluid is a fluid whose rheology can be externally controlled, typically by the application of either an electric or a magnetic field. Fluids that can be controlled by the application of a magnetic field are called Bingham magnetic fluids or magnetorheological (MR) fluids and were initially developed in the 1940's by Rabinow [8].

The MR damper designed for this study includes many innovative design features which are detailed in [32]. One of the more relevant (within the scope of this study) design feature of the MR dampers used here is that they incorporate a modular piston assembly with two coils would in parallel. Each of the two coils consists of 48 turns of 24-gauge magnet wire, and has a resistance of 0.36Ω. Therefore, the overall resistance of the damper is 0.18Ω. Furthermore, in this design, the ground side of the electric circuit is the body of the damper itself. This design feature necessitates that the dampers be electrically isolated from the test vehicle. Also, of importance is that the damper's accumulators are charged to 160 psi to prevent cavitation of the MR fluid when the damper is in extension. The force/velocity curves of the MR dampers developed for this study are shown in Figure 3.85.

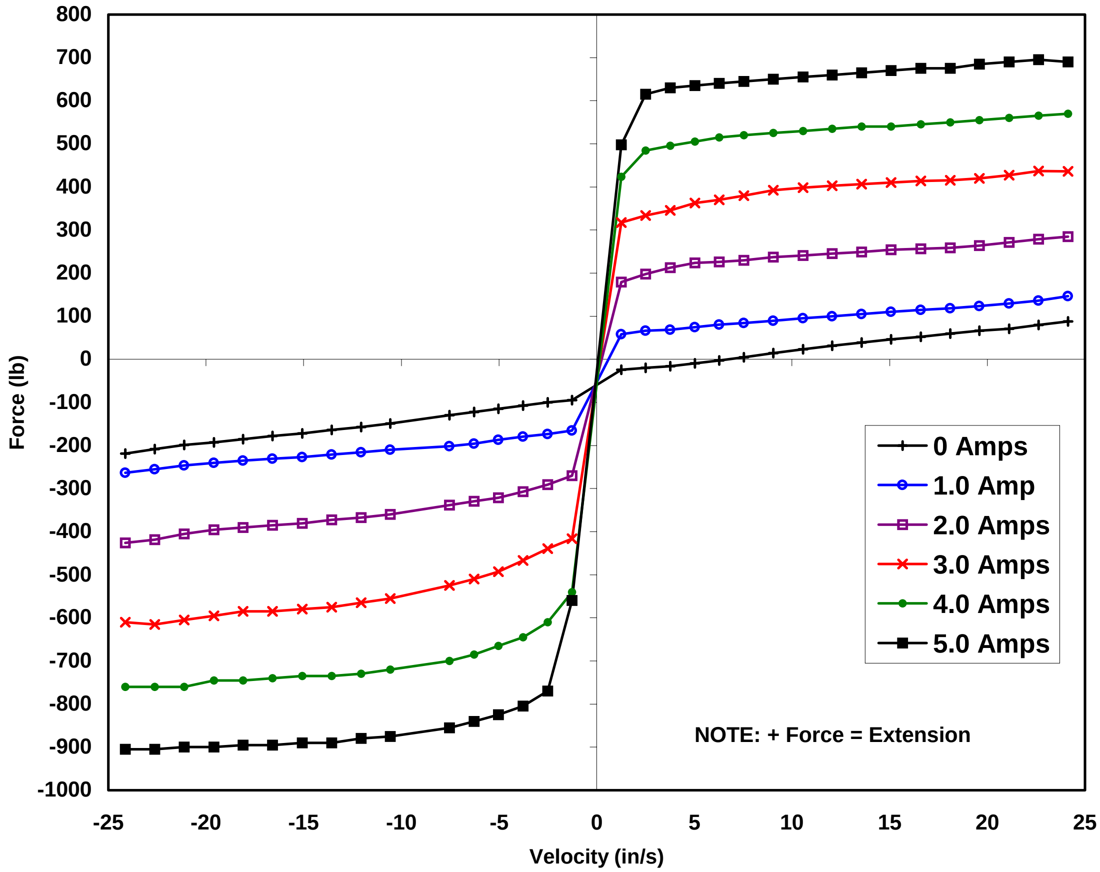

Figure 3.85. MR Damper Force/Velocity Curves

Figure 3.86 clearly shows that the force/velocity curves of the stock dampers fall predominately within the envelope described in Figure 3.85.

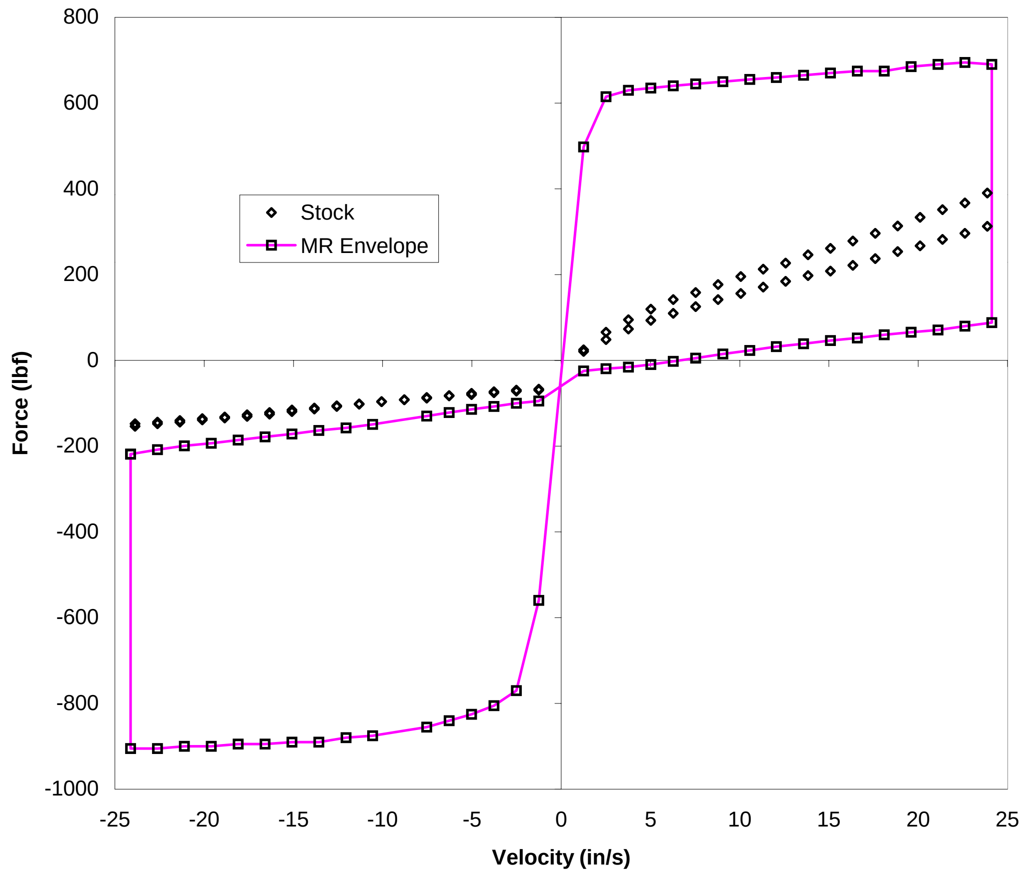

Figure 3.86. MR Damper Force/Velocity Envelope and Stock Damper Curves

It is evident that the level of damping exhibited by the stock damper in extension is well within the envelope described by the MR damper. However, in extension, the off state of the MR damper is not lower than the stock damper it is meant to replace. This may limit the amount of ride comfort that can be achieved by the MR dampers.

3.2.6 MR Damper Quarter Car Rig Testing (Uncontrolled)

The first step towards testing the utility of the MR dampers was to install them onto a quarter car rig and verify that changing the level of current supplied to the dampers changes the dynamics of the rig. The quarter car rig used for this testing is shown with the MR damper in place in Figure 3.87.

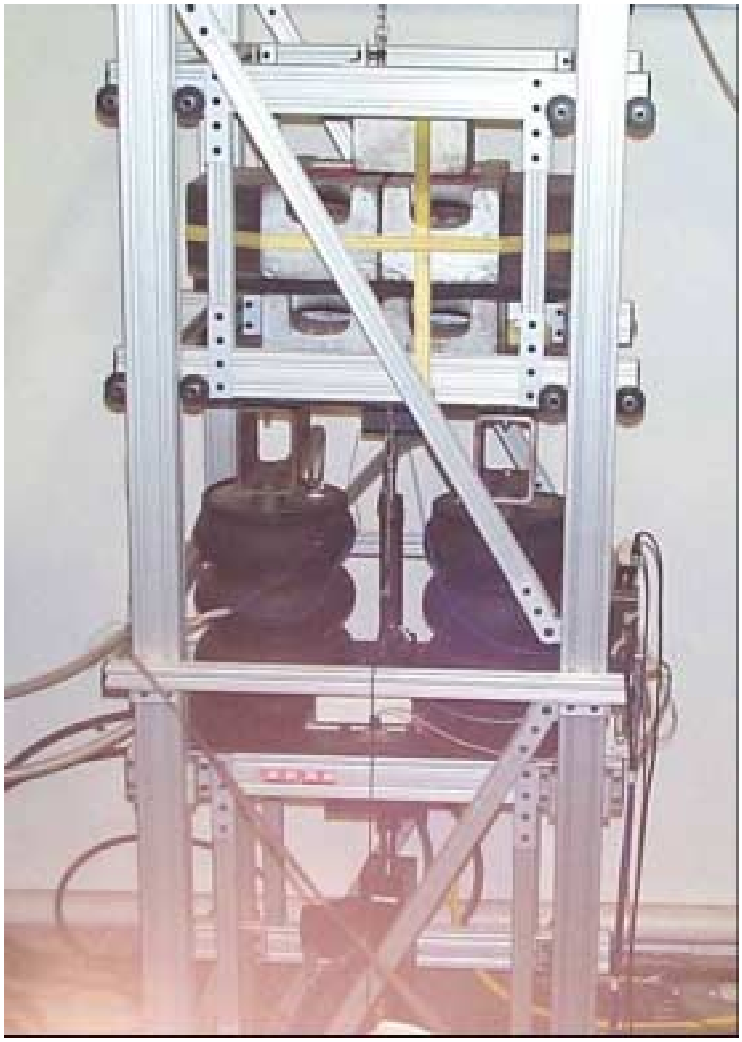

Figure 3.87. Quarter Car Rig with MR Damper in Place [33]

In this test, a chirp input (the same as has been used in the stock vehicle testing) was applied to quarter car rig, and the response measured. One of the advantages of testing with the quarter car rig is that it is possible to measure the force exerted by the damper. The results of this testing are shown in Figure 3.88.

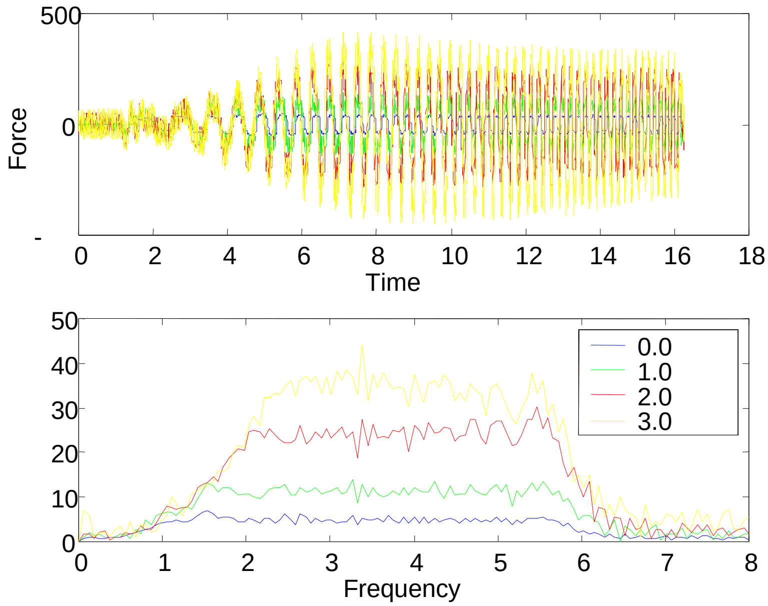

Figure 3.88. Quarter Car Testing; Damper Force Response to Chirp Input

This figure clearly shows that as the level of current supplied to the damper is increased the force likewise increases. Figure 3.89 shows that increasing the level of current also successfully limits the motion of both the tire and body.

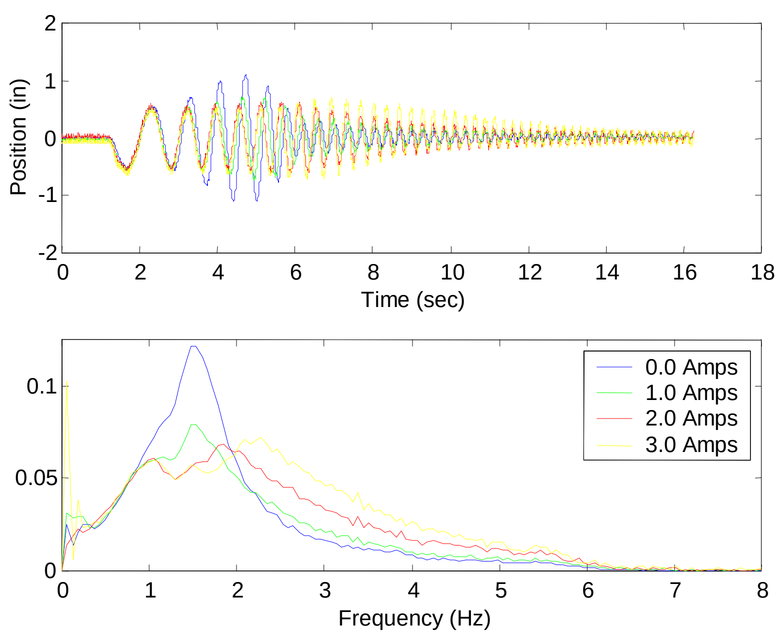

Figure 3.89. Quarter Car Testing; Chirp Input Body Position Response

This testing is meant solely to verify that the MR dampers and current supply hardware are working as expected. The data shows that this is the case.

3.2.7 MR Damper Vehicle Testing (Uncontrolled)

The next step towards testing the utility of the MR dampers for the chosen application was to install them on the test vehicle and supply them with a range of constant current while applying various inputs at the wheels. This was performed in order to develop an impression of the working performance envelope that can be achieved with the MR dampers. It should be restated that deteriorated performance with respect to comfort is expected due to the damper's relatively high off state damping levels.

The response of the test vehicle equipped with the MR dampers and powered with constant current was measured for each of the five inputs previously discussed. The first input that will be examined is the multi-sine input. To do this, the time response to the multi-sine input was measured and relevant numbers calculated. As before, the relevant numbers include the peak value and the average of the absolute value of the trace. This testing was performed for six constant current settings (0, 1, 2, 3, 4, and 5 Amps) These numbers are plotted in Figure 3.90 for eight of the measurement positions.

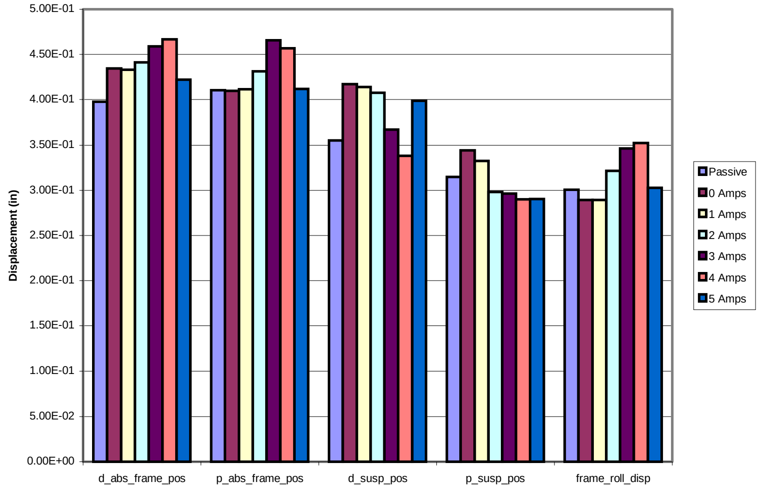

(a) Maximum Displacement

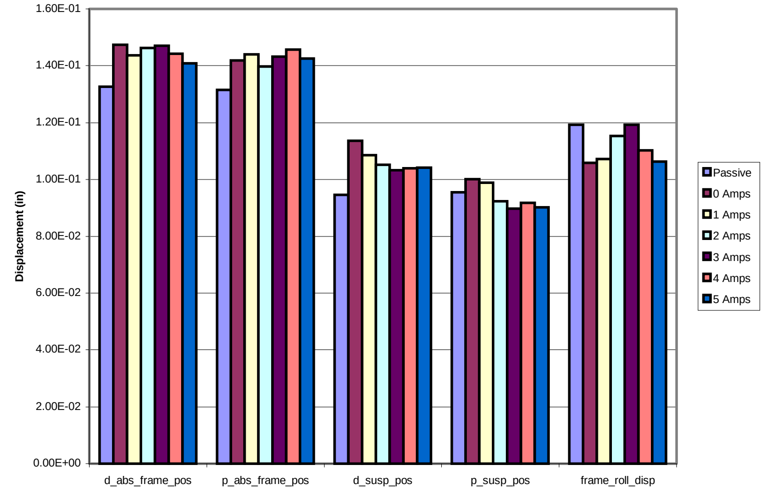

(b) Average Absolute Displacement

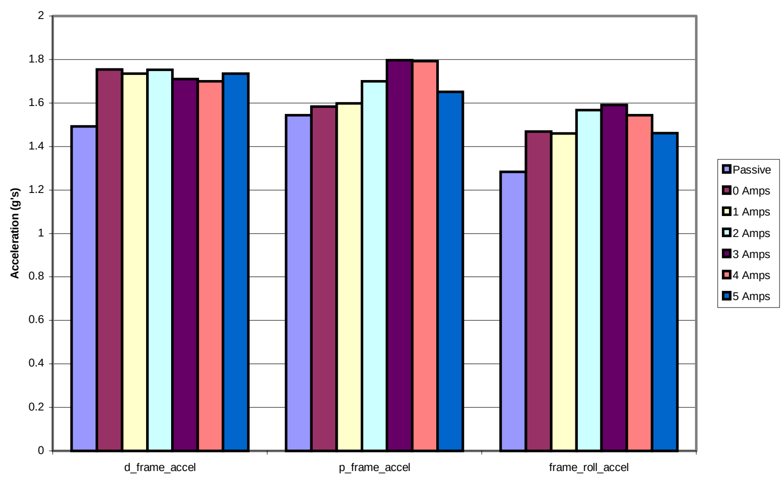

(c) Maximum Acceleration

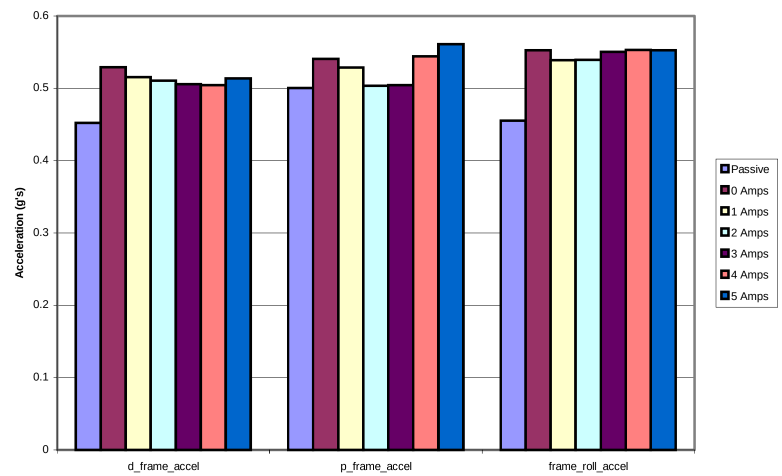

(d) Average Absolute Acceleration

Figure 3.90. Vehicle Response to Multi-Sine Road Displacement Input (MR Dampers; Constant Current)

This figure shows that by changing the level of current supplied to the damper, we are able to influence the dynamics of the system. This is an expected result. What is surprising is the disparity between trends evident at different measurement positions. The time responses from this testing can also be examined in terms of their frequency content. This has been performed and the results are presented in Figures 3.91-95.

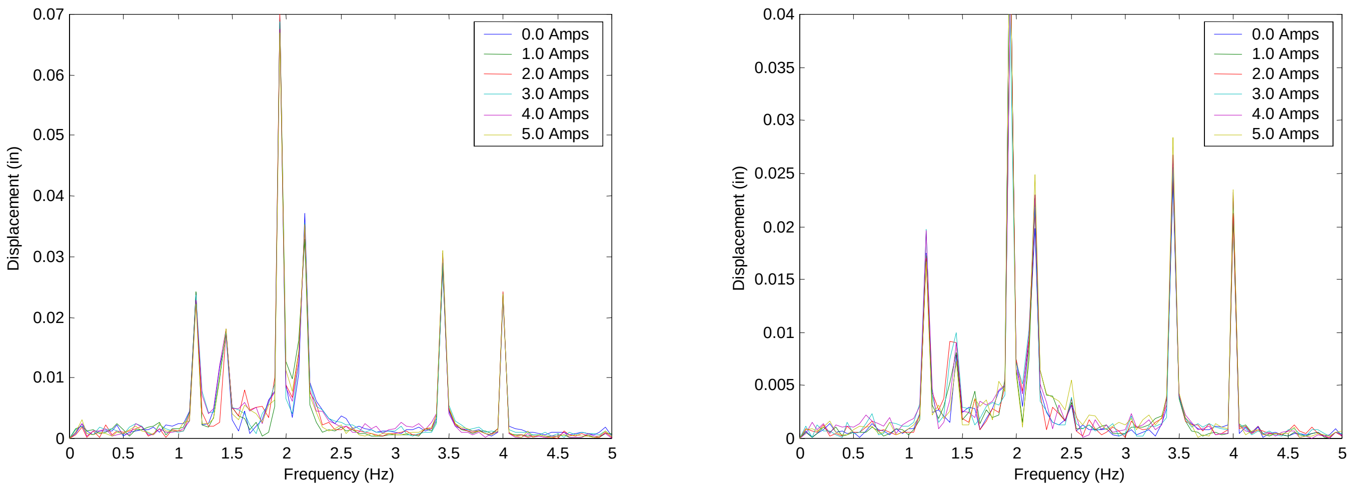

(a) Driver Tire Deflection (b) Passenger Tire Deflection

Figure 3.91. FFTs of Vehicle Tire Deflection Response to Multi-Sine Road Displacement Input (MR Dampers; Constant Current)

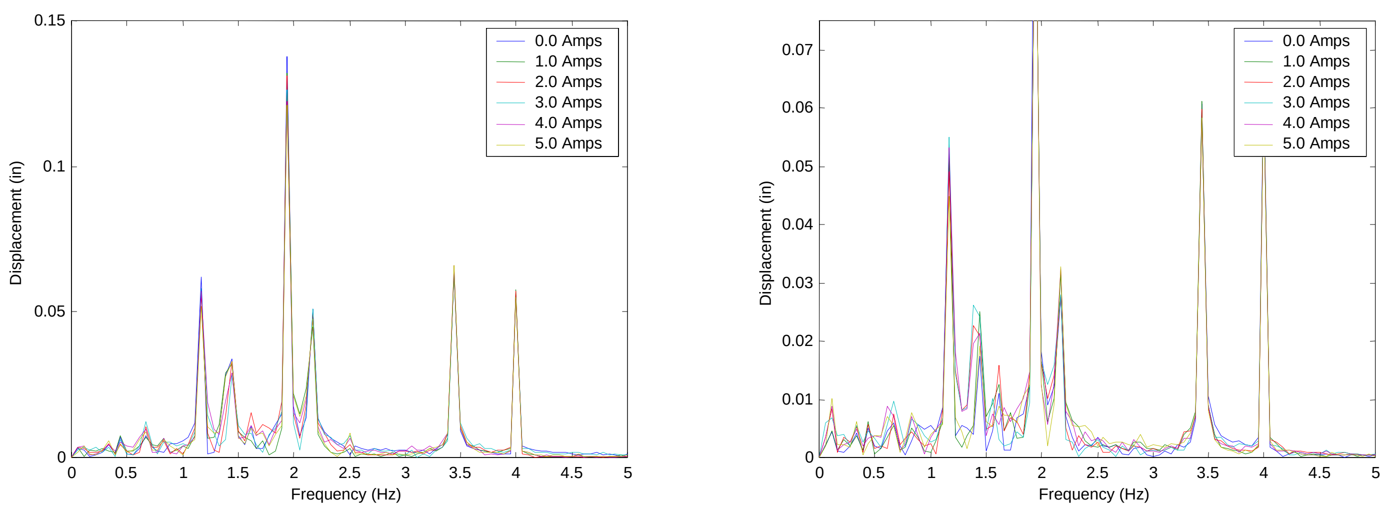

(a) Driver Suspension Rattle (b) Passenger Suspension Rattle

Figure 3.92. FFTs of Vehicle Suspension Rattle Response to Multi-Sine Road Displacement Input (MR Dampers; Constant Current)

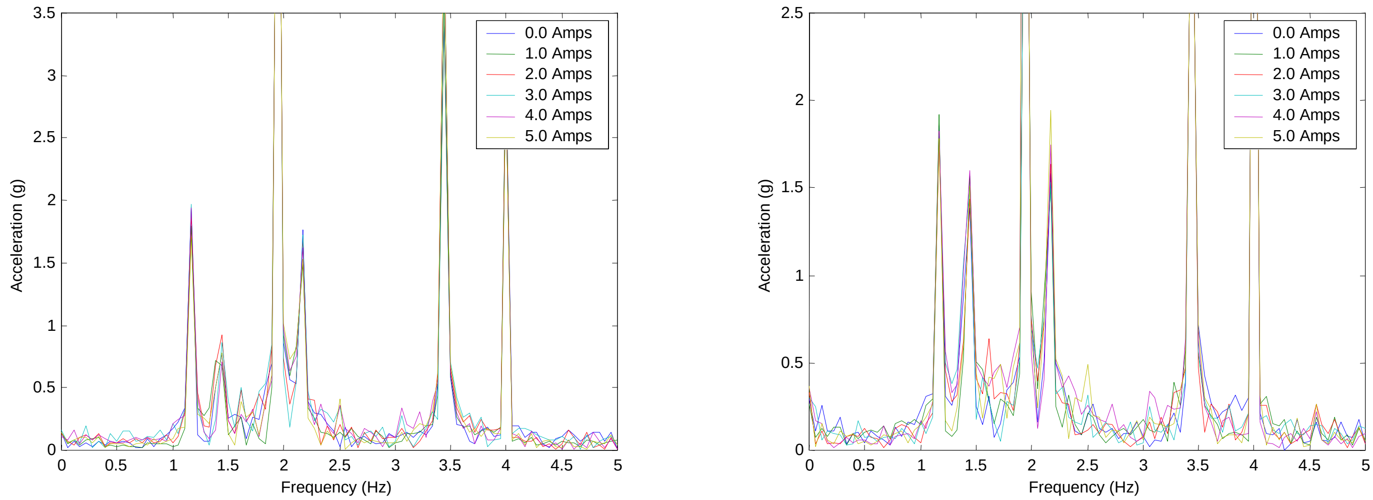

(a) Driver Frame Acceleration (b) Passenger Frame Acceleration

Figure 3.93. FFTs of Vehicle Frame Acceleration Response to Multi-Sine Road Displacement Input (MR Dampers; Constant Current)

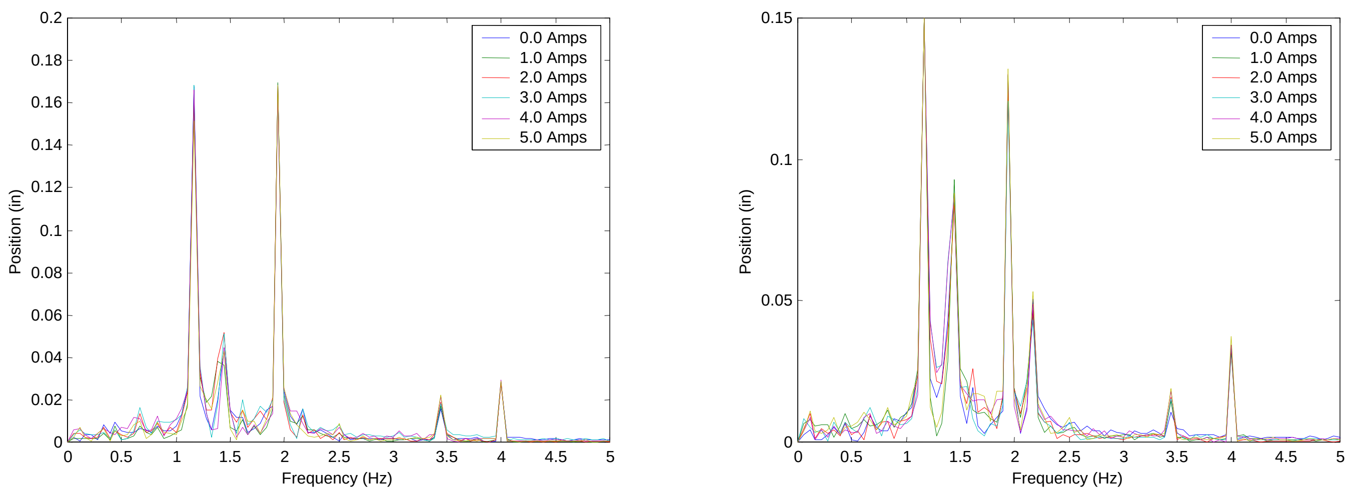

(a) Driver Absolute Frame Position (b) Passenger Absolute Frame Position

Figure 3.94. FFTs of Vehicle Absolute Frame Position Response to Multi-Sine Road Displacement Input (MR Dampers; Constant Current)

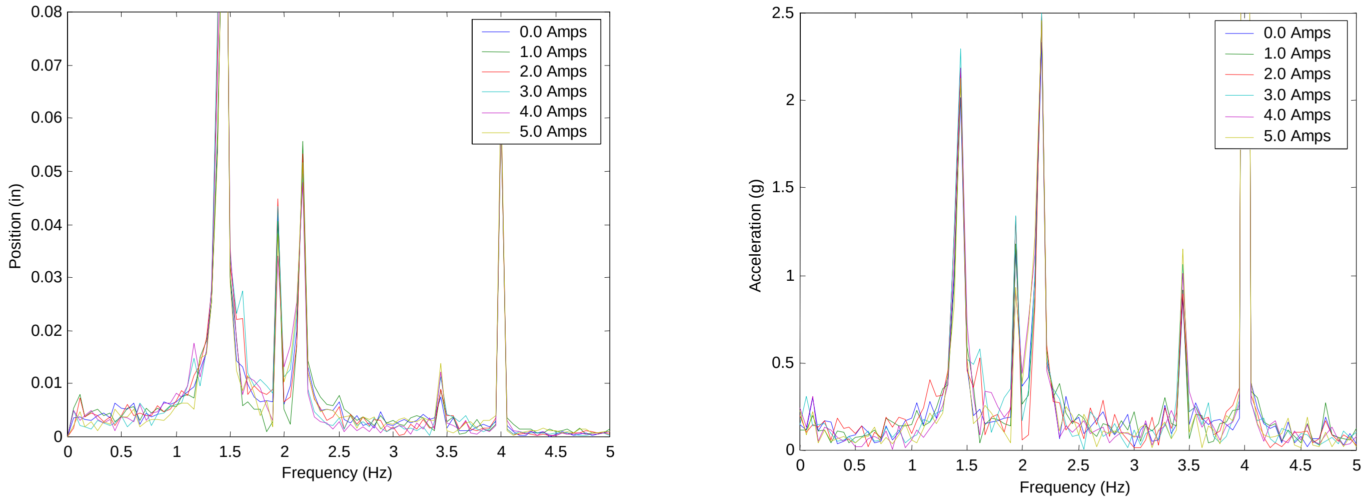

(a) Frame Roll Displacement

(b) Frame Roll Accleration

Figure 3.95. FFTs of Vehicle Roll Response to Multi-Sine Road Displacement Input (MR Dampers; Constant Current)

These figures show slight differences between the responses as the damper current is varied. The response of the vehicle (equipped with the MR dampers and supplied with three levels of constant current) to the step input (both heave and roll) was also measured. The time traces resulting from the heave step input are shown in Figures 3.96-99.

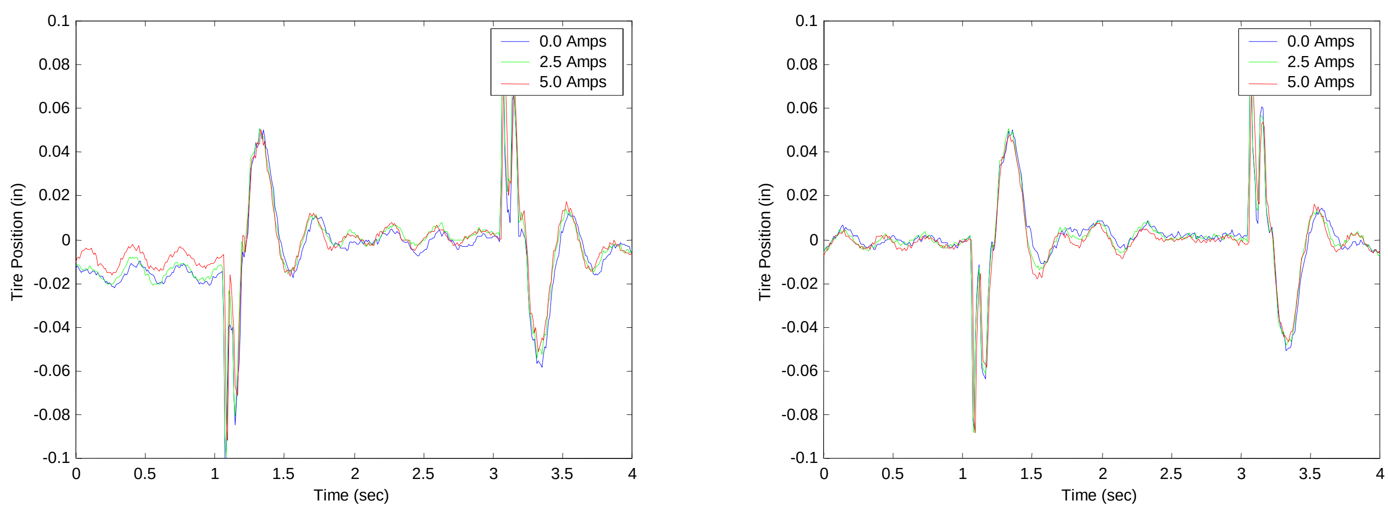

(a) Driver Tire Deflection

(b) Passenger Tire Deflection

Figure 3.96. Heave Road Displacement Step Input Vehicle Tire Deflection Response (MR Dampers; Constant Current)

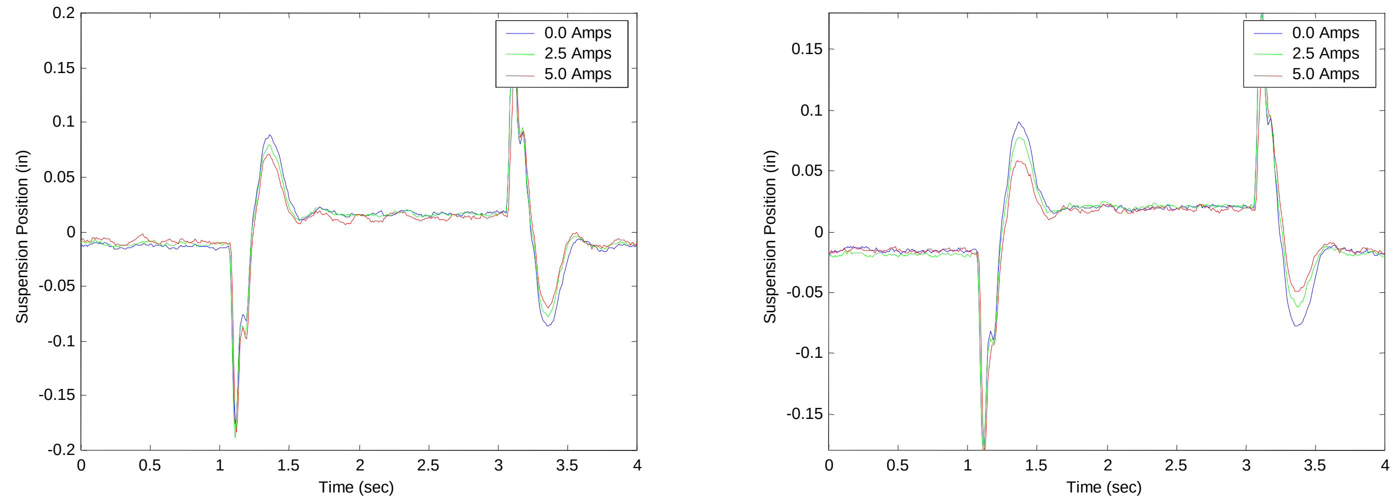

(a) Driver Suspension Rattle (b) Passenger Suspension Rattle

Figure 3.97. Heave Road Displacement Step Input Vehicle Suspension Rattle Response (MR Dampers; Constant Current)

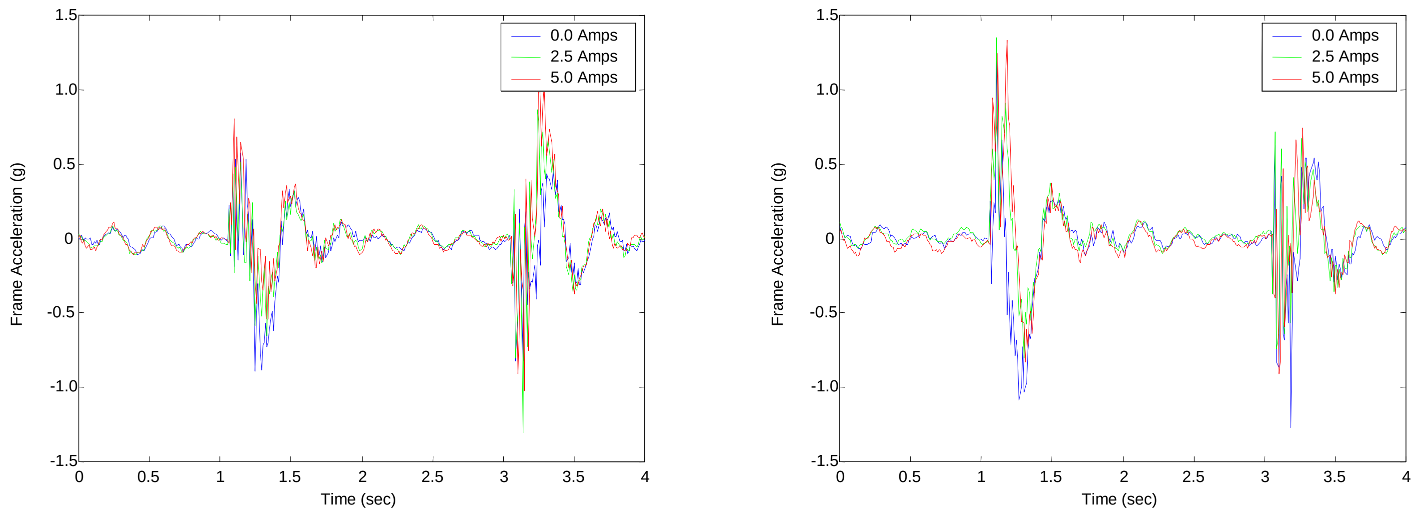

(a) Driver Frame Acceleration (b) Passenger Frame Acceleration

Figure 3.98. Heave Road Displacement Step Input Vehicle Frame Acceleration Response (MR Dampers; Constant Current)

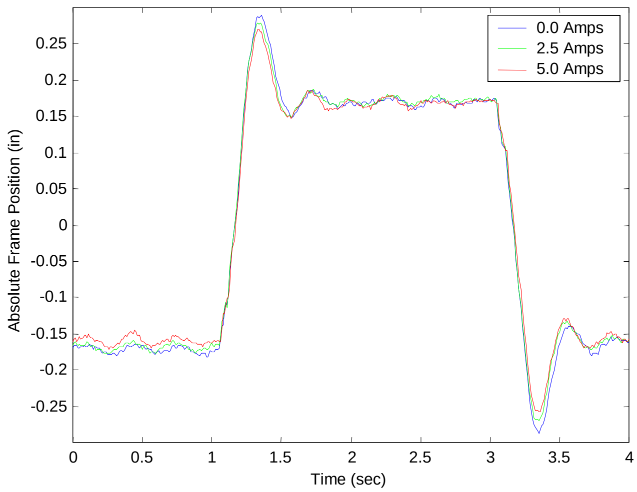

(a) Driver Absolute Frame Position

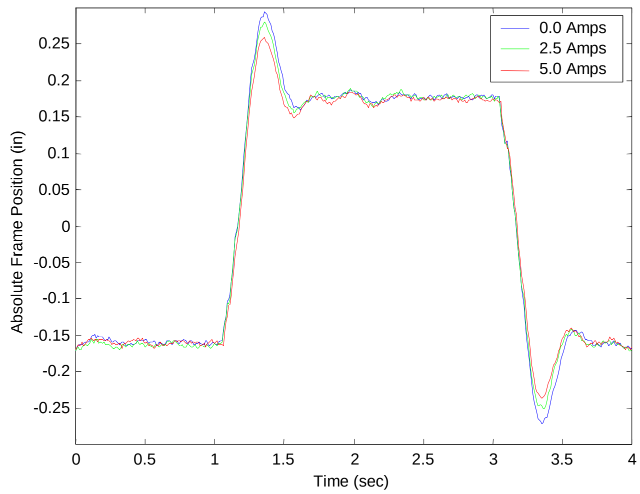

(b) Passenger Absolute Frame Position

Figure 3.99. Heave Road Displacement Step Input Vehicle Absolute Frame Position Response (MR Dampers; Constant Current)

The data from the heave step input shows that the MR dampers can be effective at attenuating suspension rattle as well as the absolute displacement of the frame. The time traces resulting from the roll step input are shown in Figures 3.100-104 (with the MR dampers supplied with three levels of constant current.

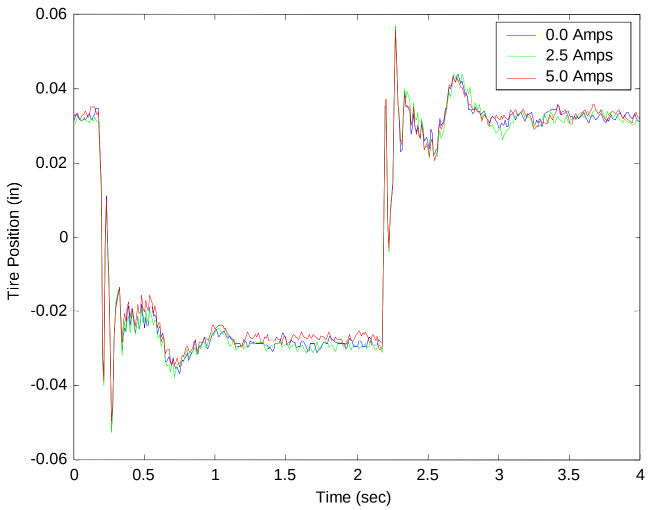

(a) Driver Tire Deflection

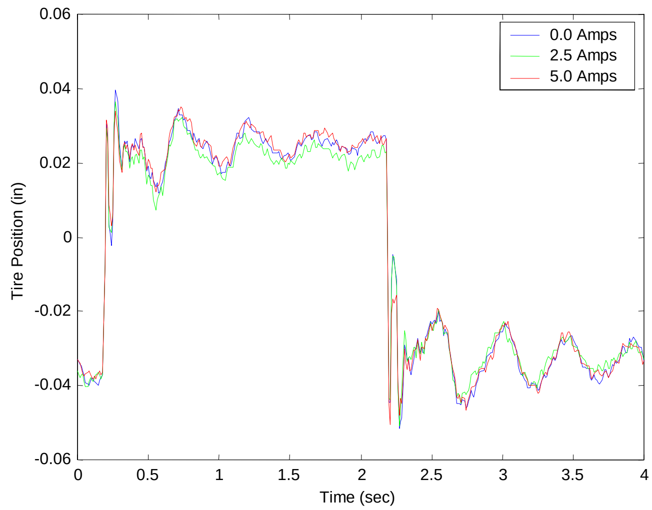

(b) Passenger Tire Deflection

Figure 3.100. Roll Road Displacement Step Input Vehicle Tire Deflection Response (MR Dampers; Constant Current)

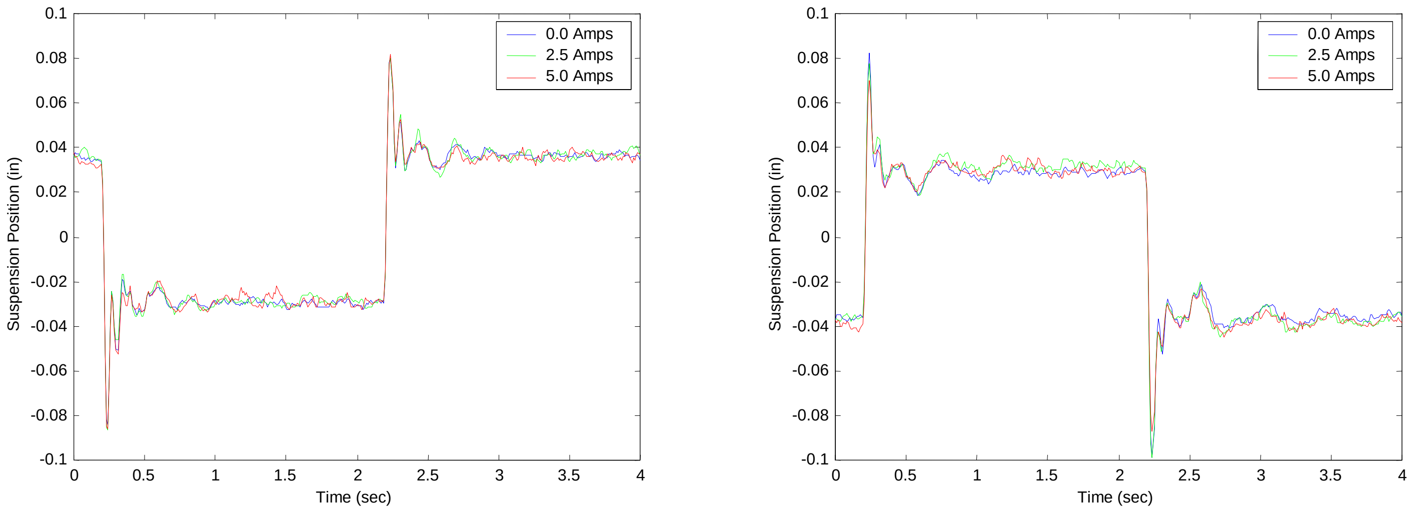

(a) Driver Suspension Rattle (b) Passenger Suspension Rattle

Figure 3.101. Roll Road Displacement Step Input Vehicle Suspension Rattle Response (MR Dampers; Constant Current)

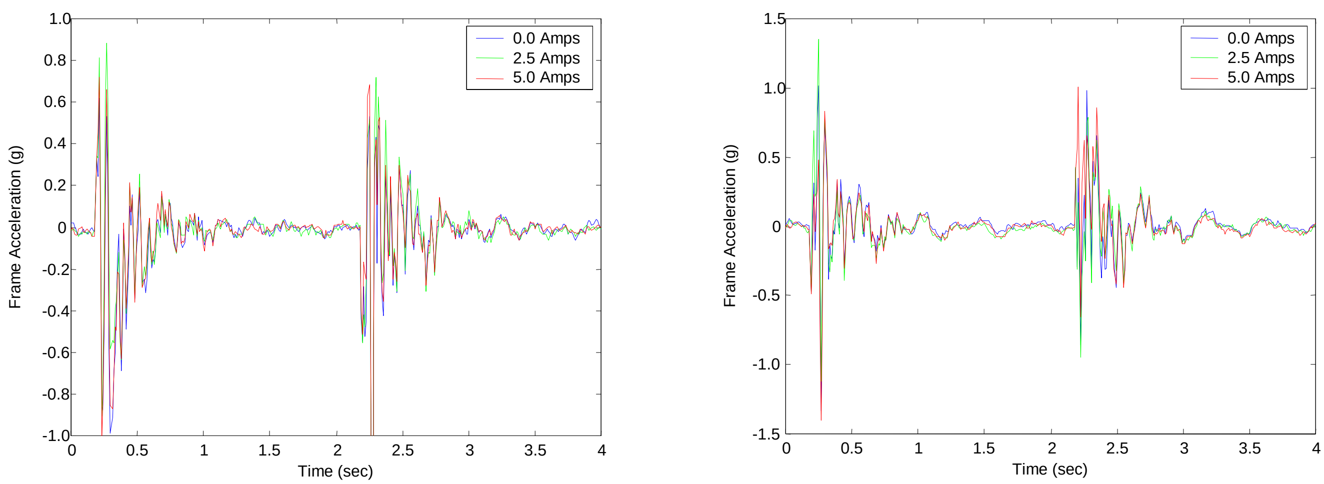

(a) Driver Frame Acceleration (b) Passenger Frame Acceleration

Figure 3.102. Roll Road Displacement Step Input Vehicle Frame Acceleration Response (MR Dampers; Constant Current)

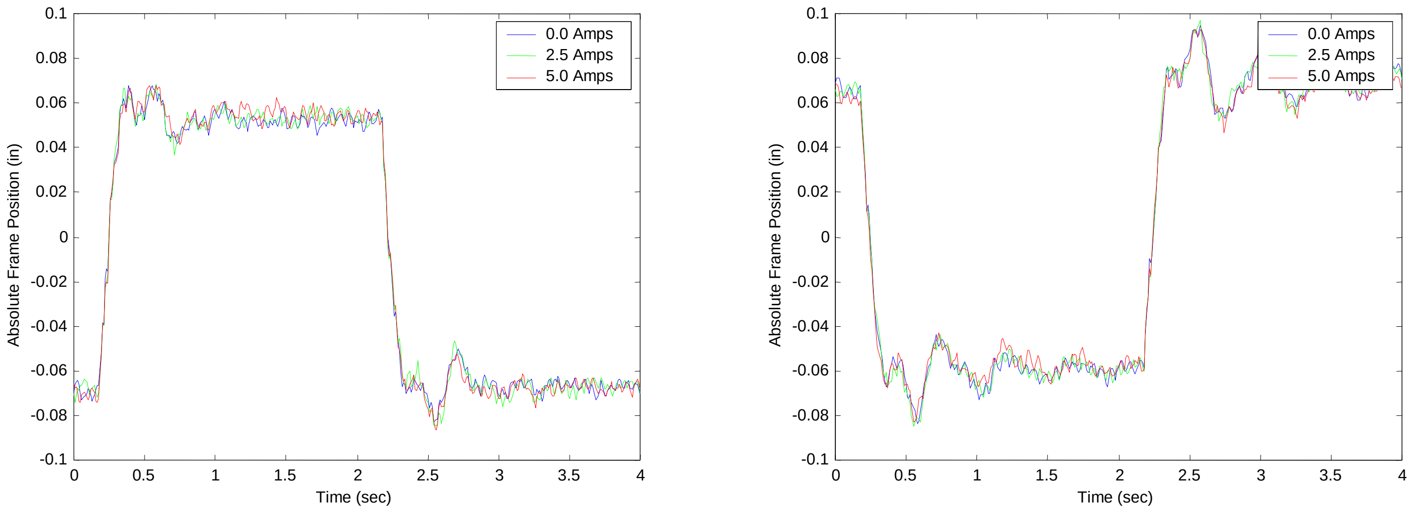

(a) Driver Absolute Frame Position (b) Passenger Absolute Frame Position

Figure 3.103. Roll Road Displacement Step Input Vehicle Absolute Frame Position Response (MR Dampers; Constant Current)

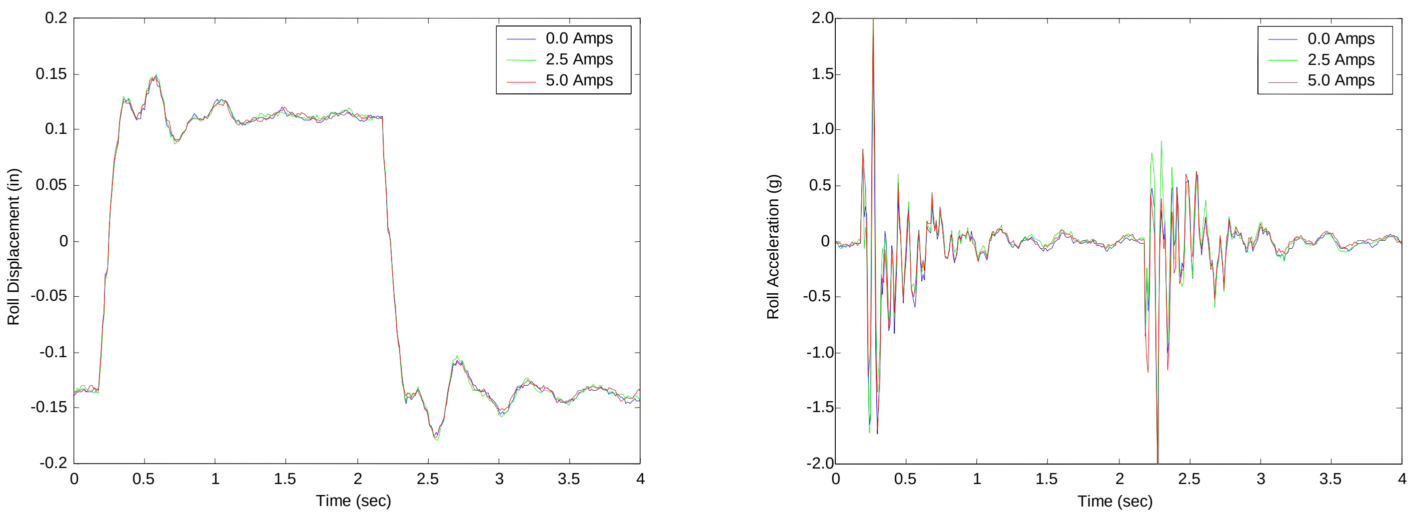

(a) Frame Roll Displacement (b) Frame Roll Acceleration

Figure 3.104. Roll Road Displacement Step Input Vehicle Response (MR Dampers; Constant Current)

This data shows that regardless of the level of current supplied to the MR damper, the response to the roll input is not significantly attenuated. This is not a surprising result as earlier testing showed that the dampers do not greatly effect the roll response of the vehicle.

The chirp input was also applied (both heave and roll) to the test vehicle. This was performed for with multiple levels of constant current supplied to the MR dampers. The results for the heave chirp input are shown in Figures 3.105-108, in both time and frequency domains.

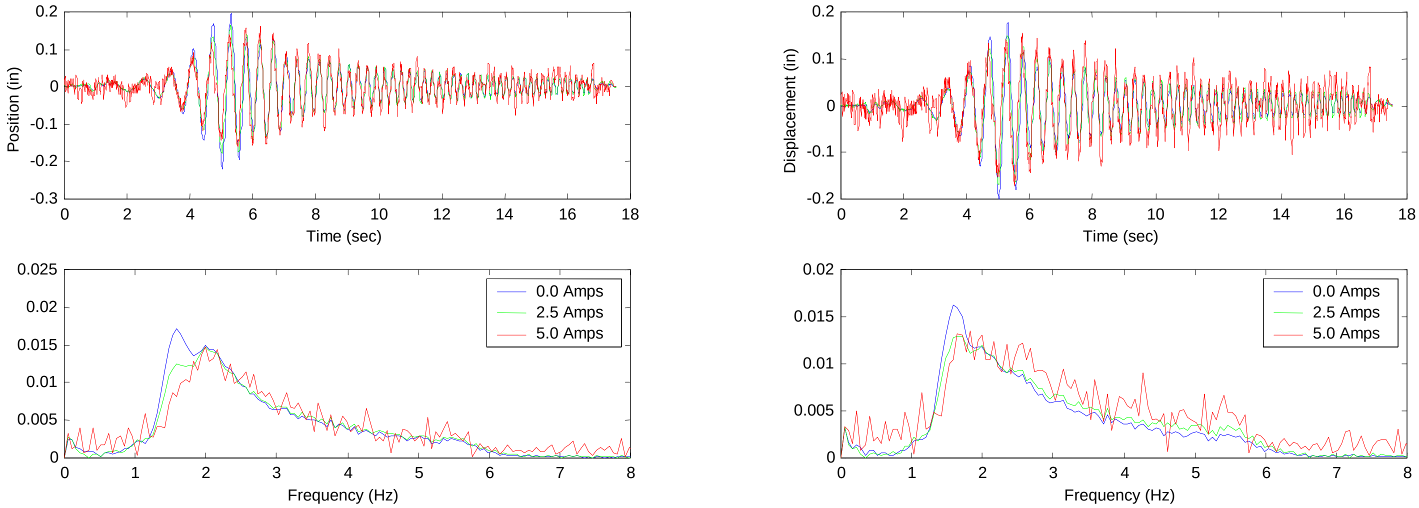

(a) Driver Tire Deflection (b) Passenger Tire Deflection

Figure 3.105. Heave Road Displacement Chirp Input Vehicle Tire Deflection Response (MR Dampers; Constant Current)

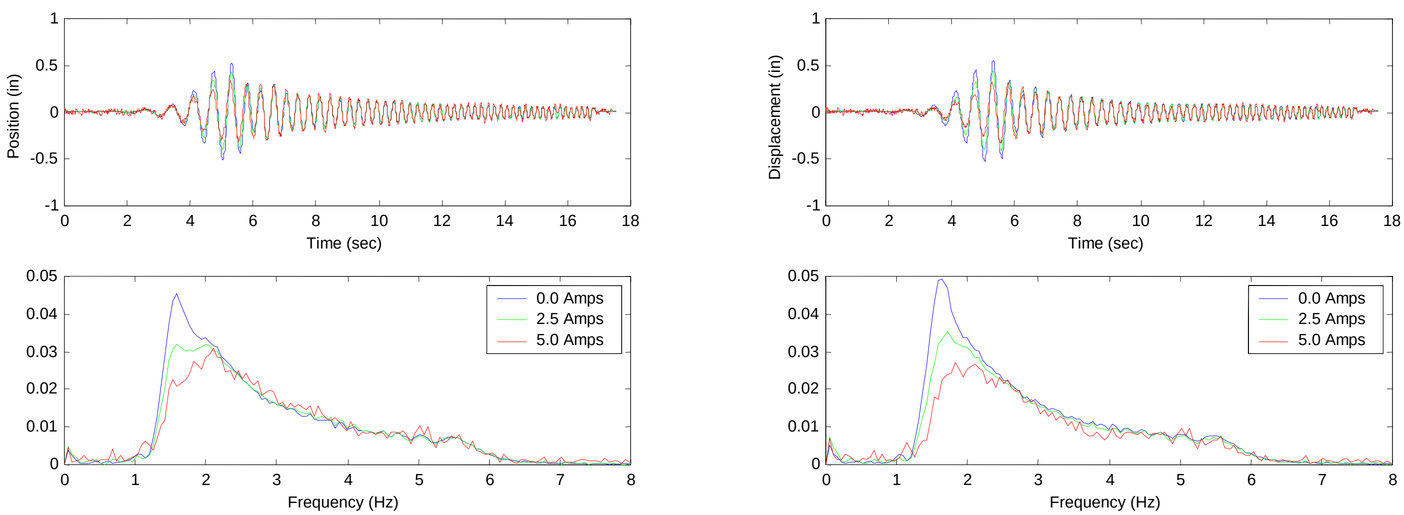

(a) Driver Suspension Rattle (b) Passenger Suspension Rattle

Figure 3.106. Heave Road Displacement Chirp Input Vehicle Suspension Rattle Response (MR Dampers; Constant Current)

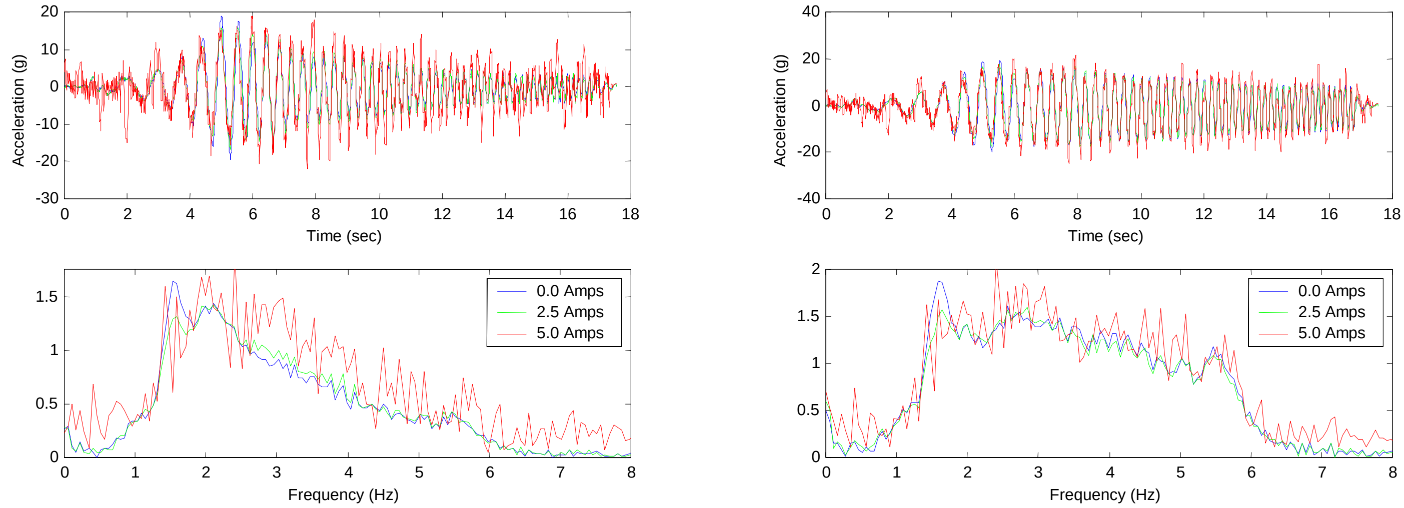

(a) Driver Frame Acceleration (b) Passenger Frame Acceleration

Figure 3.107. Heave Road Displacement Chirp Input Vehicle Frame Acceleration Response (MR Dampers; Constant Current)

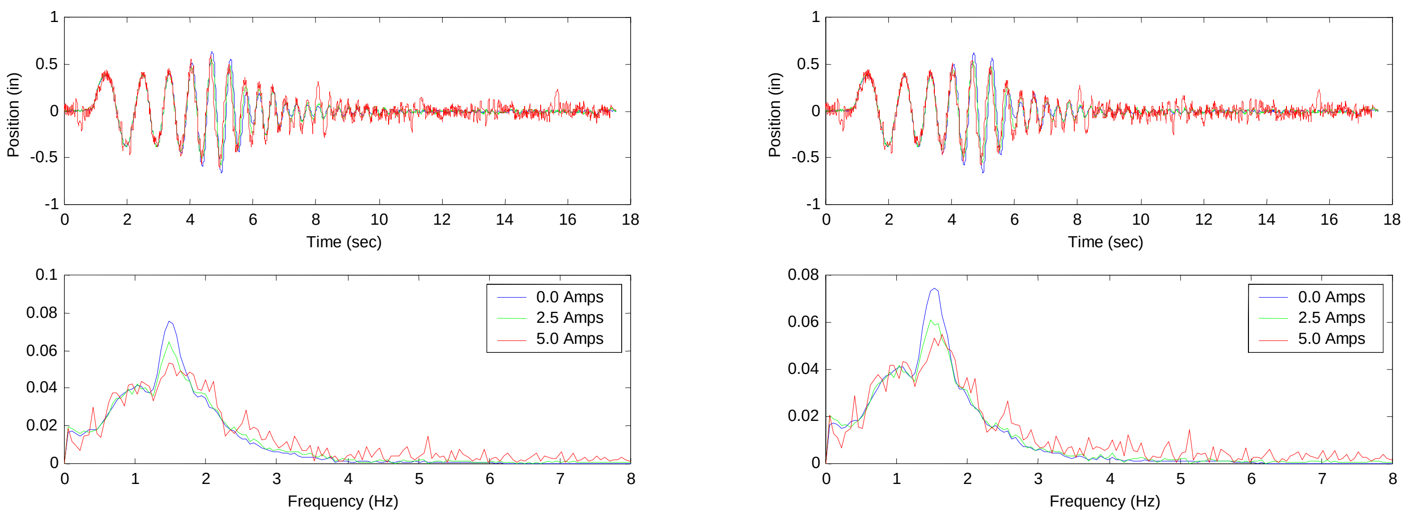

(a) Driver Absolute Frame Position (b) Passenger Absolute Frame Position

Figure 3.108. Heave Road Displacement Chirp Input Vehicle Absolute Frame Position Response (MR Dampers; Constant Current)

The heave chirp data shows that the MR dampers have only a slight effect on the acceleration transmitted to the frame of the vehicle. In terms of other measures, however, the MR dampers have a large influence. This is particularly evident in the frequency response of the supension rattle, tire deflection, and absolute frame position chirp response time traces. The results (in both time and frequency domains) for the roll chirp input are shown in Figure 3.109-113.

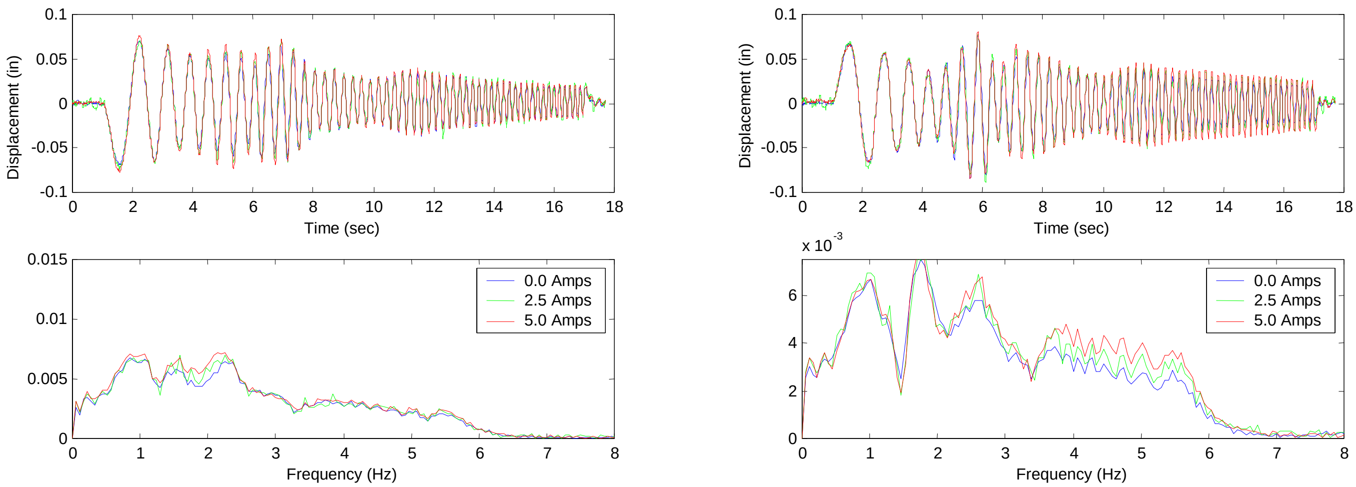

(a) Driver Tire Deflection (b) Passenger Tire Deflection

Figure 3.109. Roll Road Displacement Chirp Input Vehicle Tire Deflection Response w/wo Roll Bar

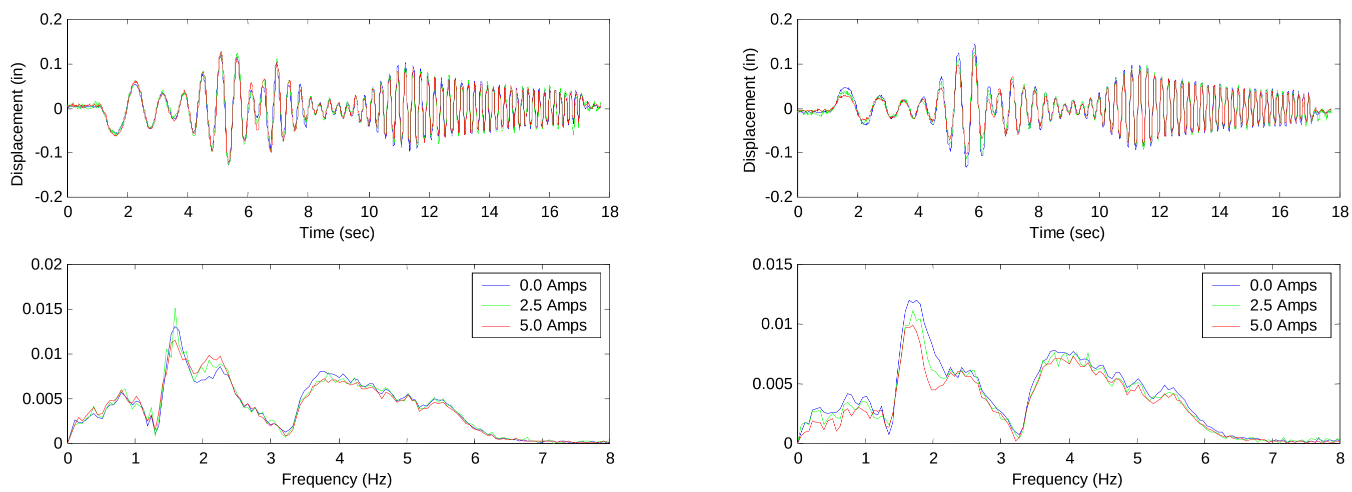

(a) Driver Suspension Rattle (b) Passenger Suspension Rattle

Figure 3.110. Roll Road Displacement Chirp Input Vehicle Suspension Rattle Response w/wo Roll Bar

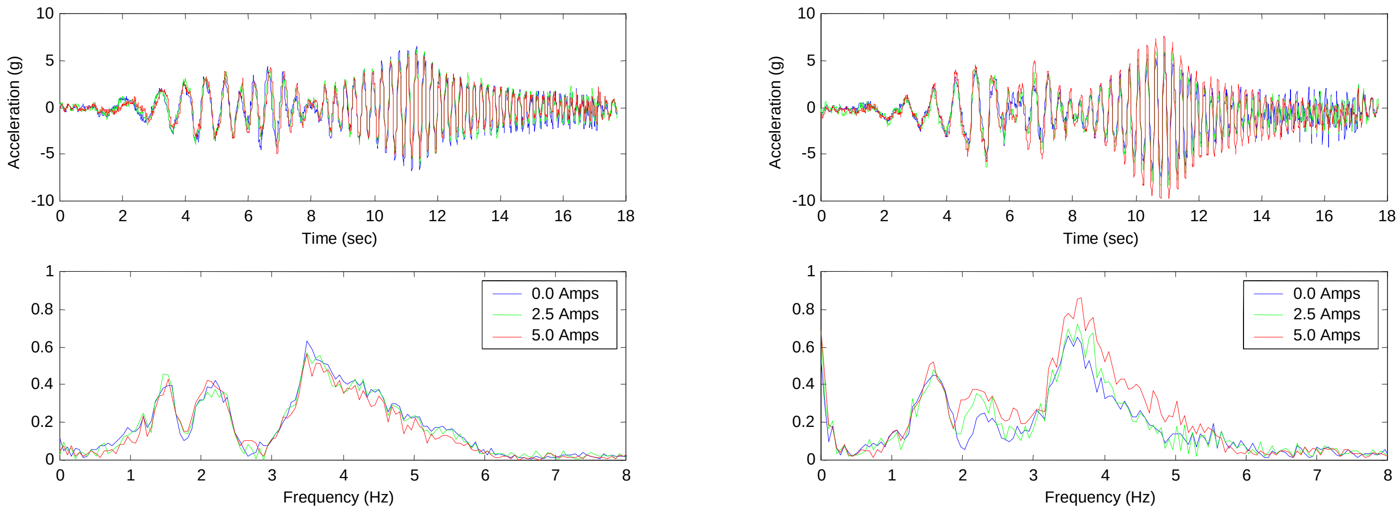

(a) Driver Frame Acceleration (b) Passenger Frame Acceleration

Figure 3.111. Roll Road Displacement Chirp Input Vehicle Frame Acceleration Response w/wo Roll Bar

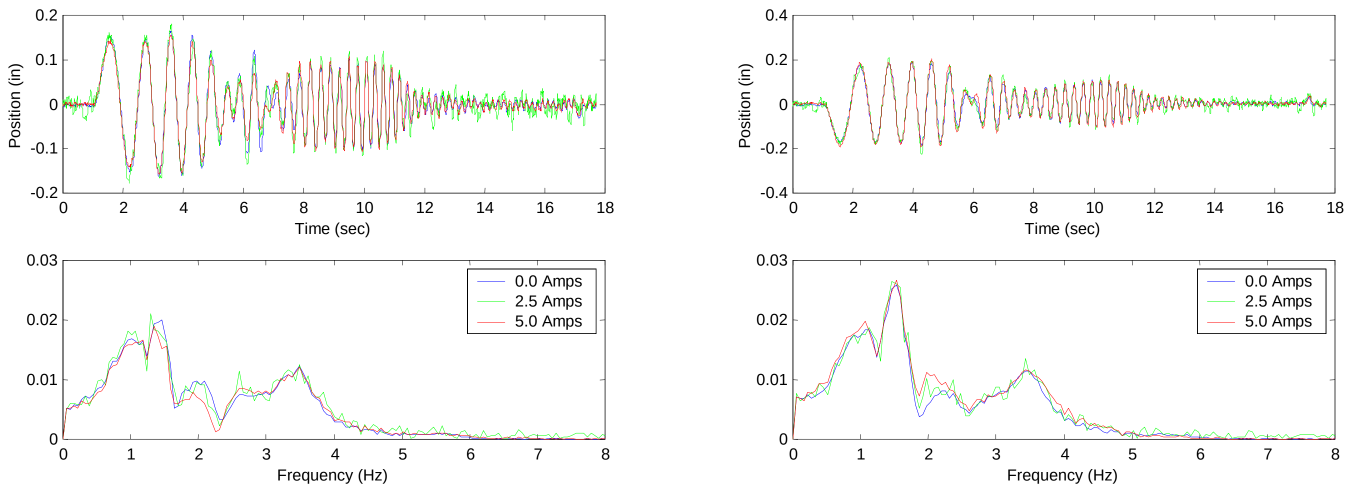

(a) Driver Absolute Frame Position (b) Passenger Absolute Frame Position

Figure 3.112. Roll Road Displacement Chirp Input Vehicle Absolute Frame Position Response w/wo Roll Bar

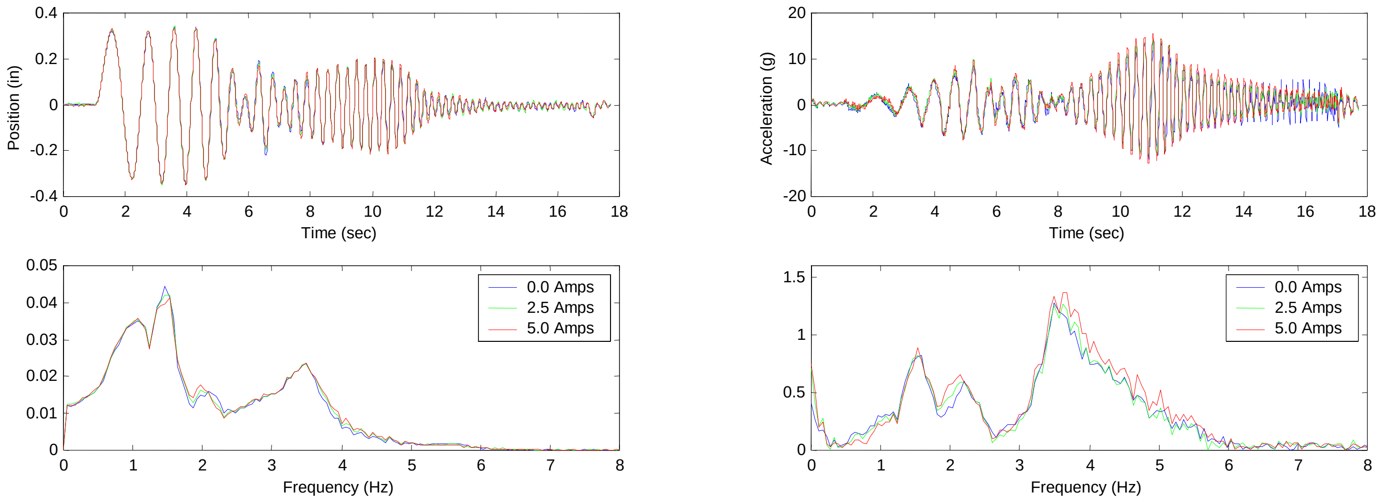

(a) Frame Roll Displacement (b) Frame Roll Acceleration

Figure 3.113. Roll Road Displacement Chirp Input Vehicle Roll Response w/wo Roll Bar

The roll chirp input data shows that changing the level of constant current supplied to the MR dampers does not significantly change the roll dynamics of the vehicle. Again, this is an expected result as data from the vehicle with and without the damper implied the same result.

3.2.8 Controller Implementation

In order to successfully control the MR dampers on the vehicle, it is necessary to develop both circuitry and a relationship between the force prescribed by the control policy and the voltage supplied to the circuitry, which then supplies current to the damper.

3.2.8.1 Circuit Development

The circuitry developed for this application must be capable of supplying up to five Amps of current to each of the MR dampers, corresponding to an input of less than five Volts. Additionally, as it will be used in an automotive environment, it must be resistant to vibration damage. A schematic of the electrical circuit used for this purpose is shown in Figure 3.114.

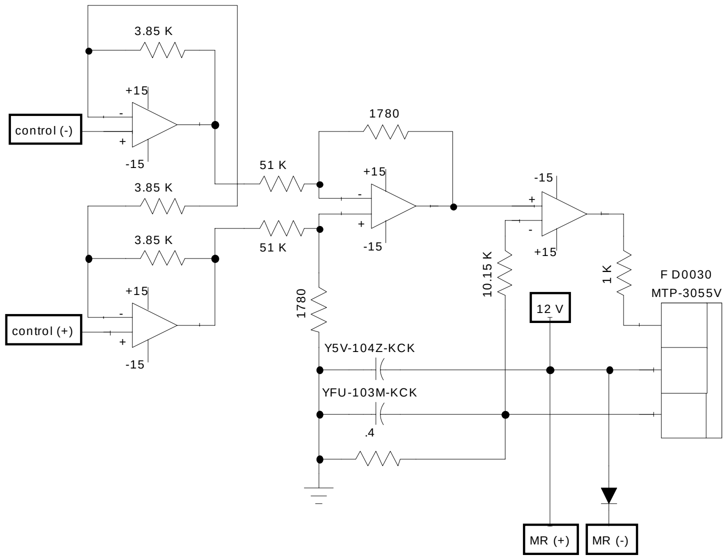

Figure 3.114. Electrical Circuit used to Power MR Dampers Schematic

The circuit shown in only capable of supplying 2.8 Amps of current to the dampers, so two circuits have been bridged together for each damper. This allows up to 5.6 Amps to be supplied to each damper. The two circuits (for each damper) have been built into boxes (as shown in Figure 3.115) to facilitate their use.

(a) Open (b) Closed

Figure 3.115. Circuit Box Used to Power MR Dampers

In order to determine that the control boxes are suitable for the control of the MR dampers, it was necessary to prove that they are able to deliver current that follows the input velocity without significant time lag. This was proven by recording the output

(Amps) to a pulse train input (Volts). The results have been scaled (the current measured went from 0 to 2 Amps) to aid comparisons between the voltage and current time traces, and are shown in Figure 3.116.

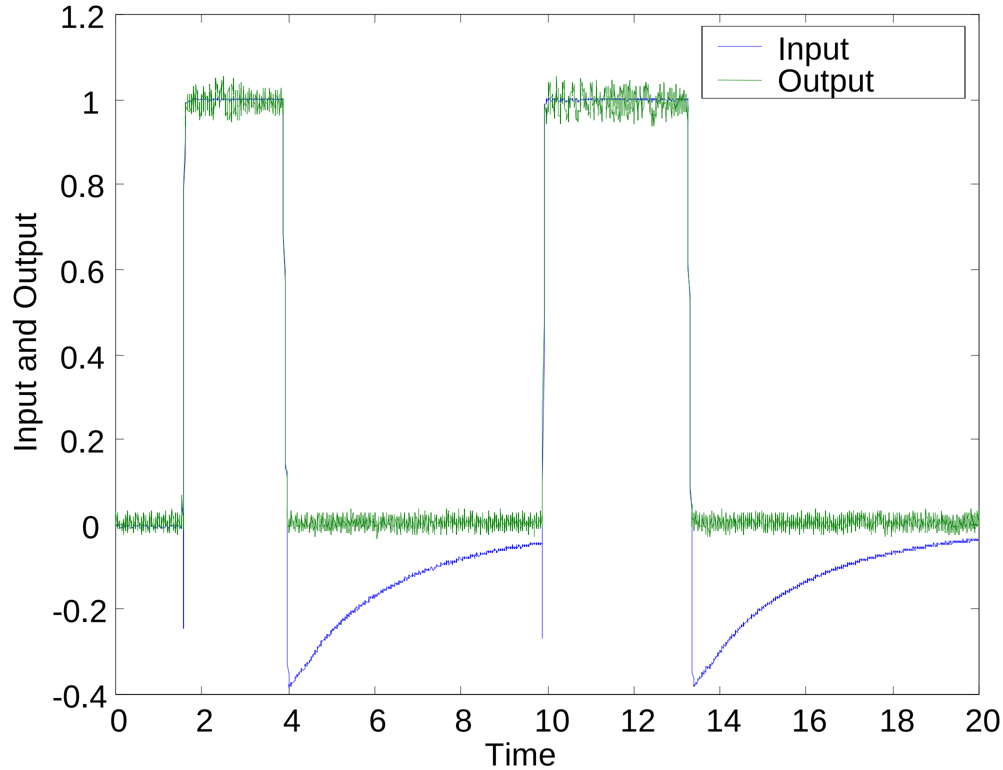

Figure 3.116. Control Circuit Scaled Output Current Response to a Step Input Voltage

This figure clearly shows that the amount of delay between the applied input and measured output is insignificant.

3.2.8.2 Control Policy Development

The control policies investigated in this part of the research consist of the displacement based skyhook and velocity based skyhook policies discussed previously. Despite the workings of the control policy being clear, there are a number of issues that must be addressed before a real system can be controlled. The skyhook policies tell us how much force would be exerted on the sprung mass for a given sprung mass absolute velocity. Since the MR damper is connected between the sprung and unsprung masses, the force applied depends on the relative velocity across the suspension as well as the current supplied to the damper. In order for the force (as determined by the skyhook policy) to be applied to the sprung mass, it is necessary to supply the MR damper with a current corresponding to both the force needed and the relative velocity across the damper. In other words, based on a desired force and an existing relative velocity, the current supplied to the MR damper must be determined. If for a given desired force, the relative velocity changes, then the current supplied to the MR damper must likewise change. Developing an equation relating force and relative velocity to current has solved this problem.

In order to develop this equation, it was necessary to create a fit to the original MR damper force velocity curves. In order to do this, it was necessary to use a shape function to model the MR damper force/velocity curves. Numerous functions were investigated and the hyperbolic tangent function was found to be the most applicable. The relationship derived is given in equation (3.2) and the results plotted in Figure 3.117.

$$force = \{126.63 \times i_{damper} + 52.595\} \times \{\tanh(1.1 \times v_{relative}) + .008 \times v_{relative} - .21\} \qquad (3.2)$$

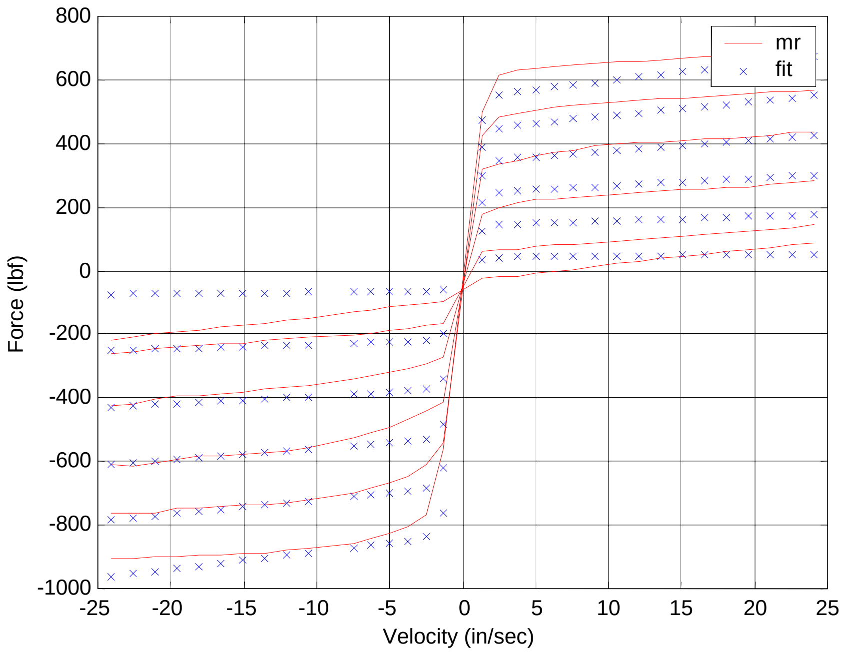

Figure 3.117. Force, Velocity, and Current Tanh Relation

The current that must be supplied to the damper for a prescribed force and a given relative velocity can now be calculated. In velocity based skyhook control, the force applied to the sprung mass is equal to the skyhook damping constant times the absolute velocity of the sprung mass. Using equation (3.2), the current supplied to the damper can be calculated as:

$$i_{Velocity\_Skyhook} = \frac{\left[\dfrac{c_{skyhook} \times v_{spung\_mass}}{\{\tanh(1.1 \times v_{relative}) + .008 \times v_{relative} - .21\}} - 52.595\right]}{126.63} \qquad (3.3)$$

Of course, there are physical limitations on the value of $i_{velocity\_skyhook}$. In our case, the upper limit is determined by the control circuit hardware and is taken to be 5 Amps despite the true limit of the circuits being 5.6 Amps. The lower limit is zero.

In displacement based skyhook control, the force applied to the sprung mass is equal to the skyhook spring stiffness times the absolute displacement of the sprung mass. Using equation (3.2), the current that should be supplied to the damper can be calculated as:

$$i_{Displacement\_Skyhook} = \frac{\left[\dfrac{k_{skyhook} \times disp_{spung\_mass}}{\{\tanh(1.1 \times v_{relative}) + .008 \times v_{relative} - .21\}} - 52.595\right]}{126.63} \qquad (3.4)$$

The same limitations that apply to $i_{velocity\_skyhook}$, also apply to $i_{displacement\_skyhook}$.

3.2.9 Control Policy Tuning

In order for there to be a valid comparison between the different control policies investigated here, it is necessary that each policy individually yield the best performance possible. In order for this to be true, it is necessary to tune each policy. For each control policy, there are three parameters that can be adjusted. One parameter is the off state of the controllable damper. This parameter is best adjusted during the damper construction phase, but can be retroactively adjusted by limiting the current supplied to the damper to be greater than zero on the low side. This type of adjustment can raise, but cannot lower the effective off state of the damper. Since the off state of the controllable dampers investigated here are already slightly higher (in compression) than the stock dampers they are replacing, adjustment of this parameter was not investigated. Another parameter that can be adjusted in the same manner is the upper limit on the supplied current. The effect of variation of this parameter on the expected performance will be investigated by examining two values. The last parameter that can be tuned is the value of either $c_{skyhook}$ or $k_{skyhook}$ (depending on whether it is velocity or displacement based skyhook being investigated). A range of values for each of these parameters will be investigated. The tuning will be based on the response of the system to the heave step input and the heave chirp input.

3.2.9.1 Velocity Skyhook Control Policy Tuning

In order to start the tuning process for velocity skyhook control, it is necessary to have a starting point for $c_{skyhook}$. In this case, that starting point was taken to be the nominal damping coefficient of the stock damper. The calculation of this nominal value is shown in Figure 3.118.

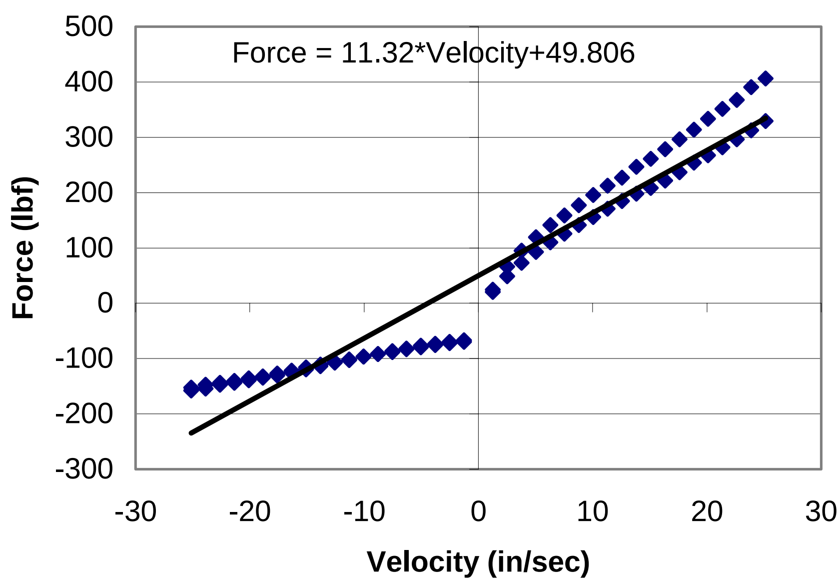

Figure 3.118. Stock Damper Curve Fit Developing Nominal Stock Damping Coefficient

The slope of the curve fit determined the nominal value of $c_{skyhook}$ to be 11.0 lbf-sec/in. A range of 6.0 to 20.0 lbf-sec/in was chosen for testing. This range varies from roughly half to double the nominal value. The upper limit on the current supplied to the damper was taken to be 5 Amps for this testing.

Both the heave step input and the heave chirp input were used to determine the optimum value of $c_{skyhook}$. For each input, a time trace of the output was recorded. For the step input, the maximum value of the response immediately following the step was recorded, as well as the average of the absolute value of the response were recorded. For the chirp input, the maximum magnitude and the average magnitude of the FFT of the time trace in the frequency band 1-1.6 Hz were recorded. Since, in this case, the inputs are both in phase, the results from measurement positions on either side of the vehicle have been averaged together. The results were then normalized to the stock case and presented as percent increase relative to stock (therefore a negative value represents a decrease relative to stock). Figure 3.119 shows the results for frame acceleration, suspension rattle, tire deflection, and absolute frame position.

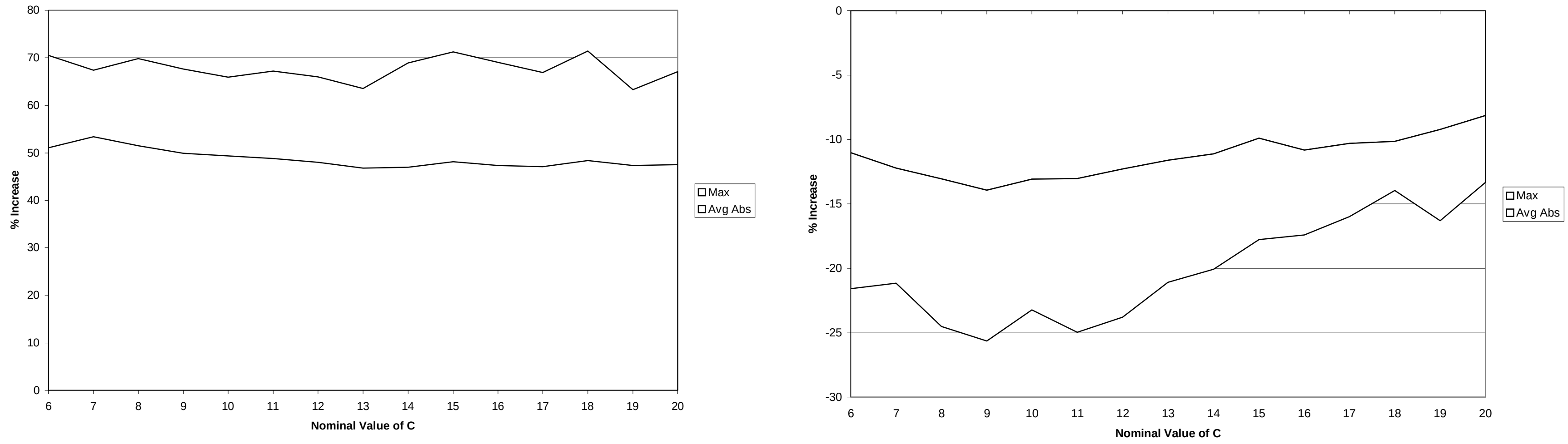

(a) Step Input

(b) Chirp Input

Figure 3.119. Velocity Skyhook Frame Acceleration Percent Increase Relative to Stock (5A Limit)

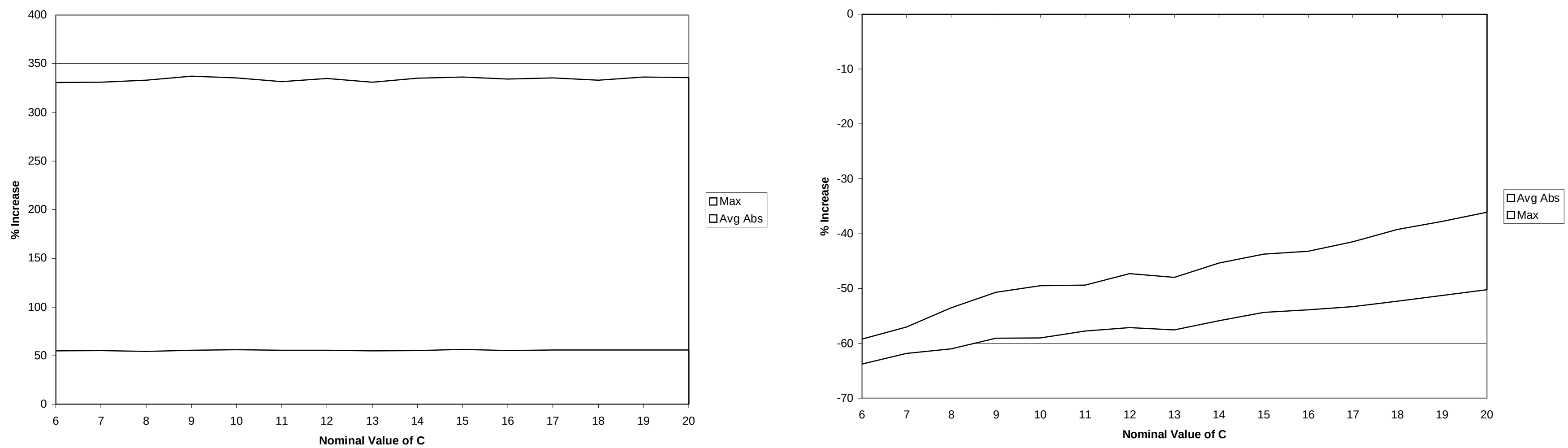

(a) Step Input

(b) Chirp Input

Figure 3.120. Velocity Skyhook Suspension Rattle Percent Increase Relative to Stock (5A Limit)

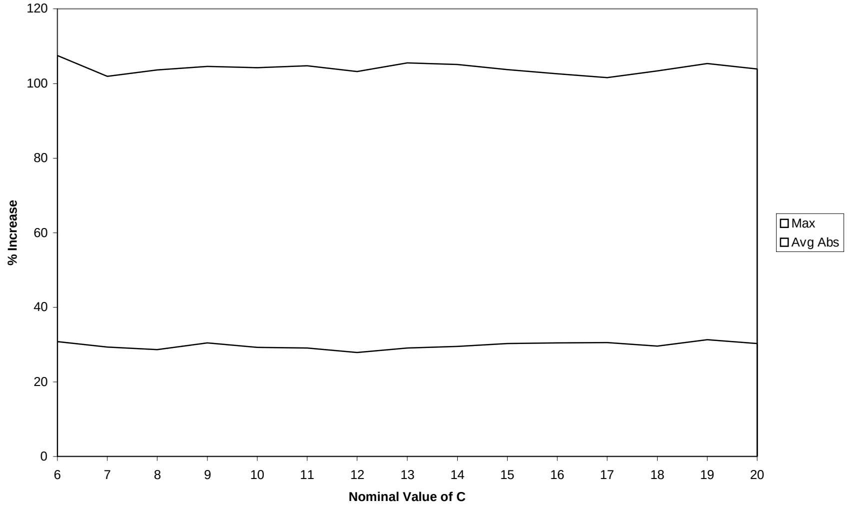

(a) Tire deflection; Step Input

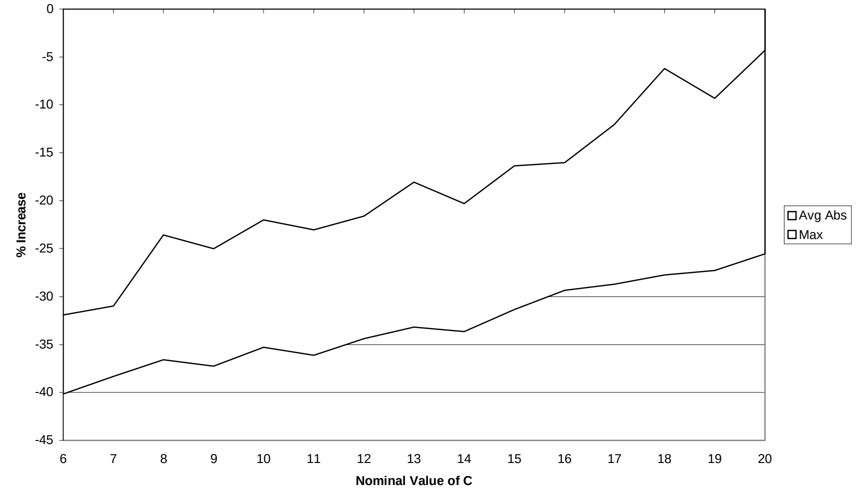

(b) Tire deflection; Chirp Input

Figure 3.121. Velocity Skyhook Percent Increase Relative to Stock (5A Limit)

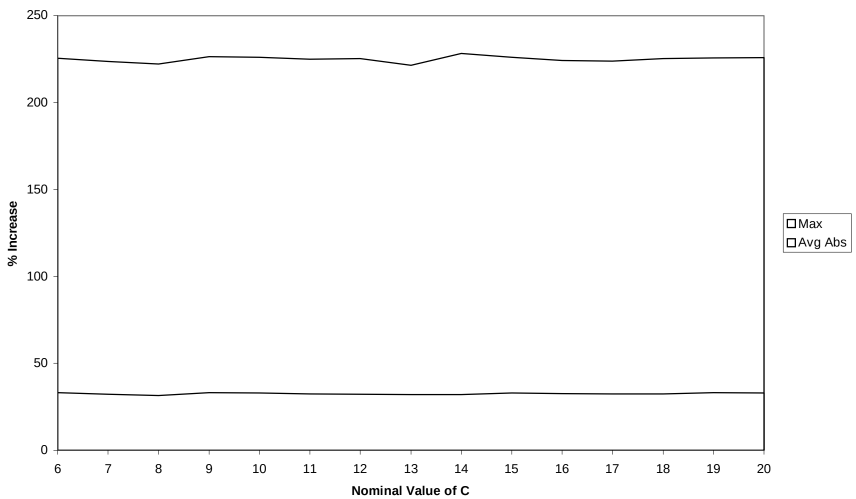

(a) Absolute Frame Position; Step Input

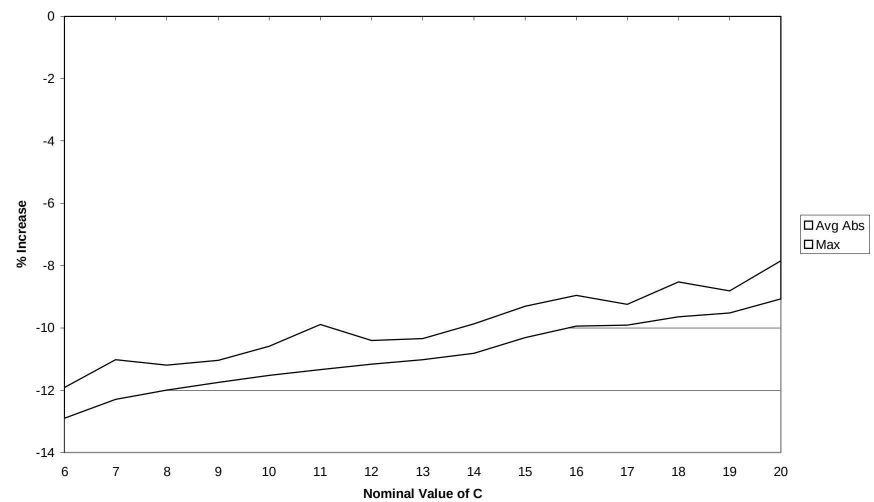

(b) Absolute Frame Position; Chirp Input

Figure 3.122. Velocity Skyhook Percent Increase Relative to Stock (5A Limit)

This data can now be used to tune $c_{skyhook}$. By examining the frame acceleration results, it is apparent that the optimal value of $c_{skyhook}$ is 9.0 lbf-sec/in. It is not as easy to make such a judgment based on the other measures. The frame acceleration response to the step input shows a slight dependence on $c_{skyhook}$, with larger values yielding marginally better performance. By other measures, however, the response to the step input is independent of the value of $c_{skyhook}$. Based on measurements of supension rattle, tire deflection, and absolute frame position, the response to the chirp input imply that lower values of $c_{skyhook}$ yield the best performance. Based on these results, it was decided that a value of $c_{skyhook}$ equal to 9.0 lbf-sec/in will be taken as the ideal value for the velocity based skyhook control.

In order to further validate the results of our velocity skyhook tuning, the response of the system with a 5 Amp limit on the current supplied to the MR damper is compared to the response attained with a 3 Amp limit on the current supplied to the damper. This comparison is shown in Figure 3.123.

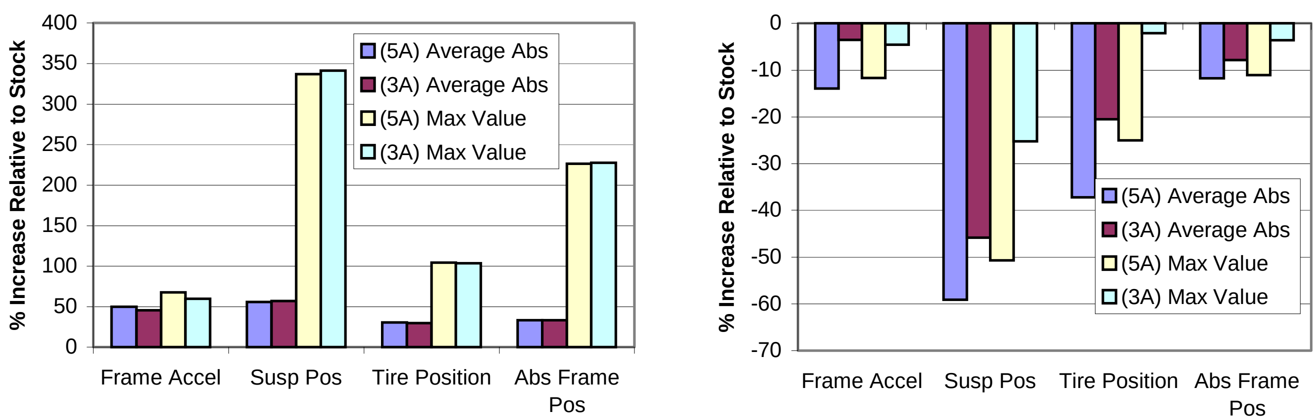

(a) Step Input Response

(b) Chirp Input Response

Figure 3.123. 3 and 5 Amp Velocity Skyhook Result Comparison

The response to the heave step input shows little dependence on the upper limit of the current supplied to the damper. The response to the heave chirp input, however, exhibits a large dependence on this value, and clearly shows that the 5 Amp limit yields improved performance over the 3 Amp limit.

3.2.9.2 Displacement Skyhook Control Policy Tuning

In order to start the tuning process displacement skyhook control, it is necessary to have a starting point for $k_{skyhook}$. In this case, that starting point was found based on the nominal value of $c_{skyhook}$ chosen. $k_{skyhhok}$ was chosen such that the maximum force applied in response to an applied 2 Hz displacement will be the same as the force applied by $c_{skyhook}$. This is expressed in (3.5)

$$k_{skyhook} A \sin(2\pi ft) = c_{skyhook} 2\pi fA \sin(2\pi ft) \tag{3.5}$$

for:

$$f = 2Hz$$

$$c_{skyhook} = 9.0 \frac{lbfx \sec}{in}$$

we get:

$$k_{skyhook} = 138.23 \approx 140.0 \frac{lbf}{in}$$

Based on the nominal value of $k_{skyhook}$ of 140.0 lbf /in, it was decided that a range of 100.0 to 240.0 lbf/in would be investigated. This range roughly corresponds to the nominal value –30% to the nominal value +70%. The upper limit on the current supplied to the damper was taken to be 5 Amps for this testing.

As was performed when investigating velocity based skyhook control, both the heave step input and the heave chirp input were used to determine the optimum value of $k_{skyhook}$, and for each input, a time trace of the output was recorded. The same numbers that were recorded when investigating velocity based skyhook are recorded here as well, and the results from measurement positions on either side of the vehicle have been averaged together. The results were then normalized and presented as percent increase relative to stock dampers. Figures 3.124-127 show the results for frame acceleration, supension rattle, tire deflection, and absolute frame position.

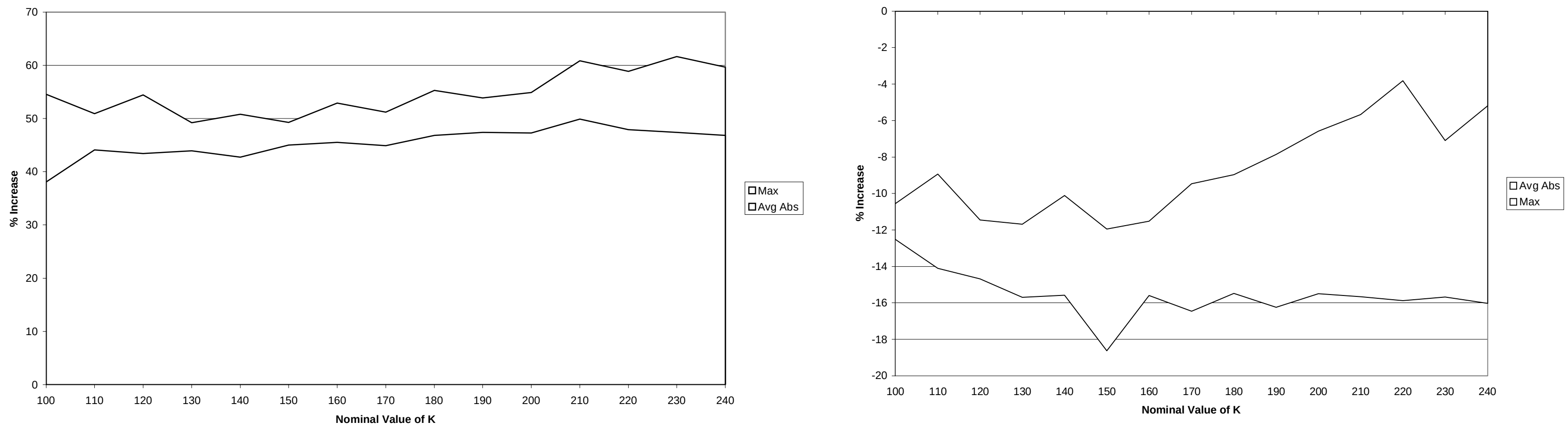

(a) Frame Acceleration; Step Input

(b) Frame Acceleration; Chirp Input

Figure 3.124. Displacement Skyhook Frame Acceleration Percent Increase Relative to Stock (5A Limit)

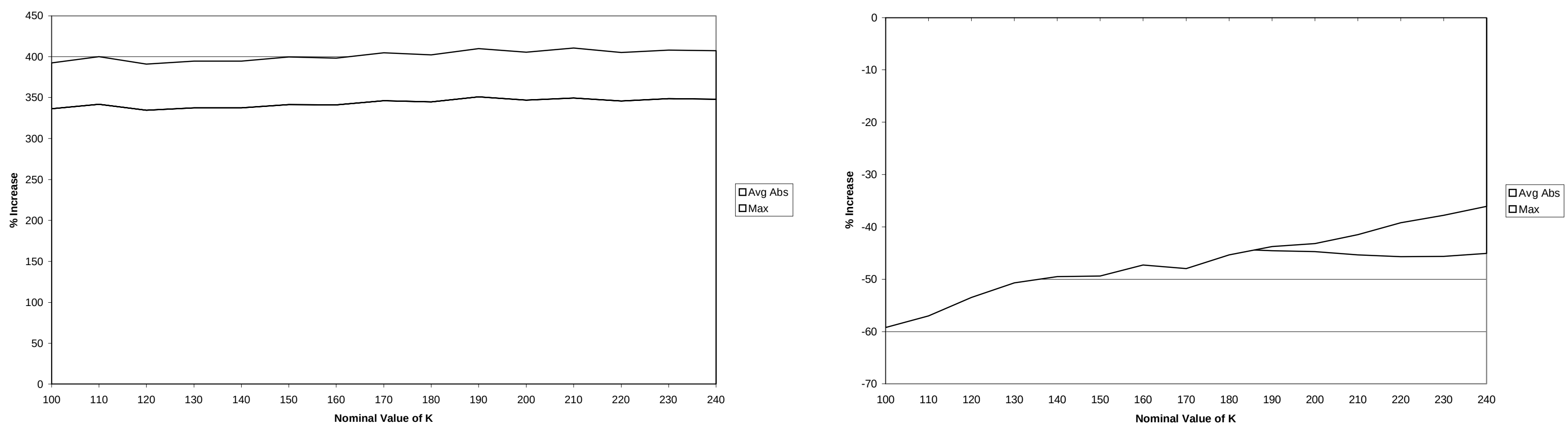

(a) Step Input

(b) Chirp Input

Figure 3.125. Displacement Skyhook Suspension Rattle Percent Increase Relative to Stock (5A Limit)

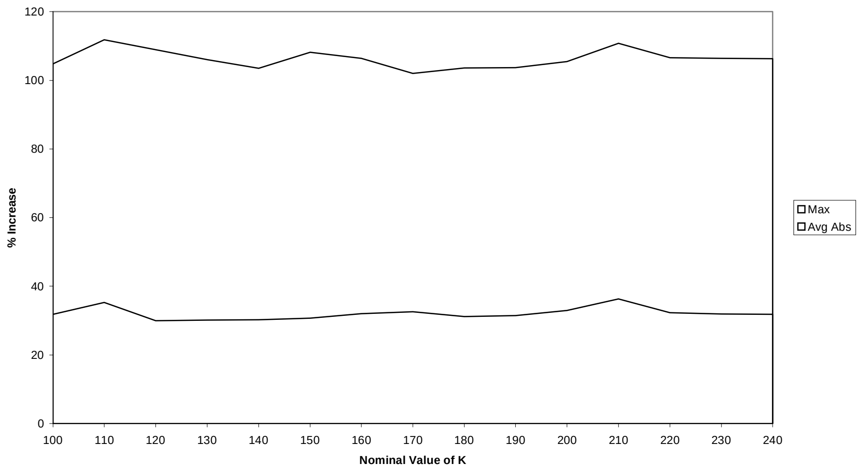

(a) Step Input

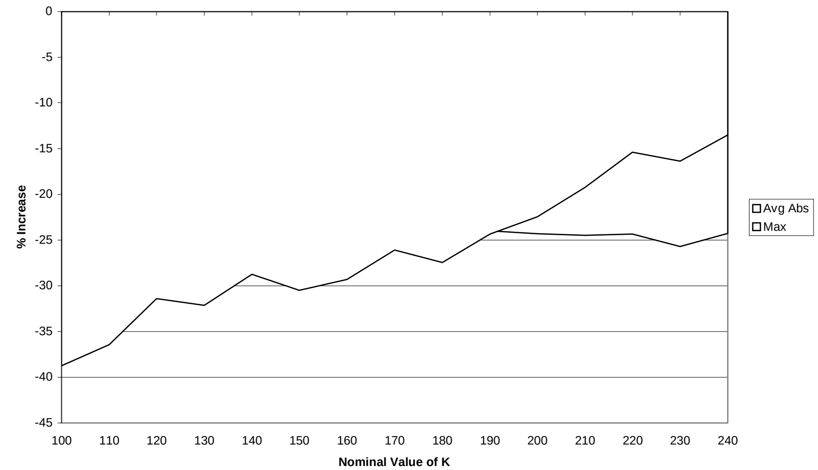

(b) Chirp Input

Figure 3.126. Displacement Skyhook Tire Deflection Percent Increase Relative to Stock (5A Limit)

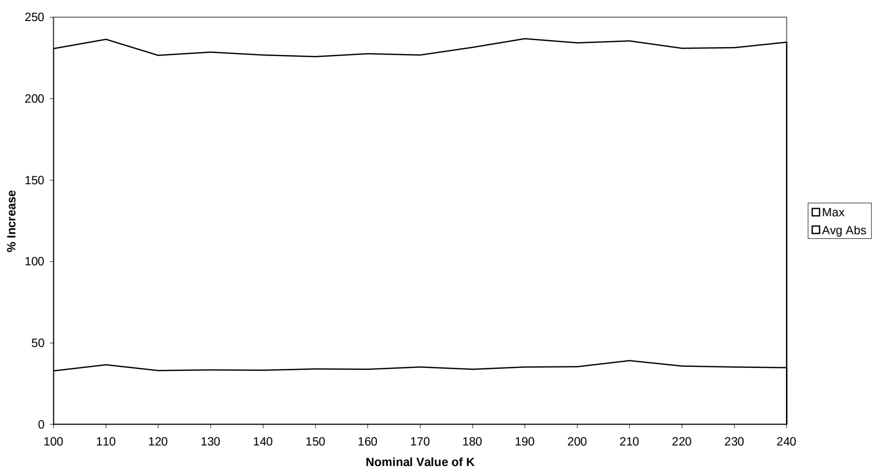

(a) Step Input

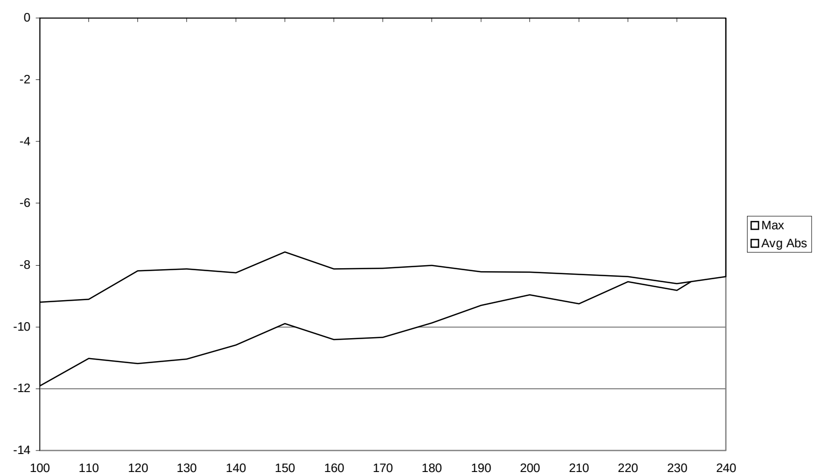

(b) Chirp Input

Figure 3.127. Displacement Skyhook Absolute Frame Position Percent Increase Relative to Stock (5A Limit)

This data can now be used to tune $k_{skyhook}$. By examining the frame acceleration results, it is apparent that the optimum value of $k_{skyhook}$ is 150.0 lbf/in. It is not as easy to make such a judgment based on the other measures. The maximum value as well as the average absolute value of the response to the step input both appear to be relatively independent of $k_{skyhook}$. Additionally, the average value of the magnitude of the FFT of the response to the chirp input, in the frequency band 1-1.6 Hz, appears to be independent of $k_{skyhhok}$ as well. The maximum value of the magnitude of the FFT of the response to the chirp input implies that better performance is achieved with lower values of $k_{skyhook}$. Based on these results, it was decided that a value of $k_{skyhook}$ equal to 140.0 lbf/in will be taken as the ideal value for the displacement based skyhook control.

The results of the displacement skyhook tuning were also investigated in terms of changing the upper limit of the current supplied to the MR damper. The response of the tuned system with 3 and 5 Amp limits on the current supplied to the MR damper are shown in Figure 3.128.

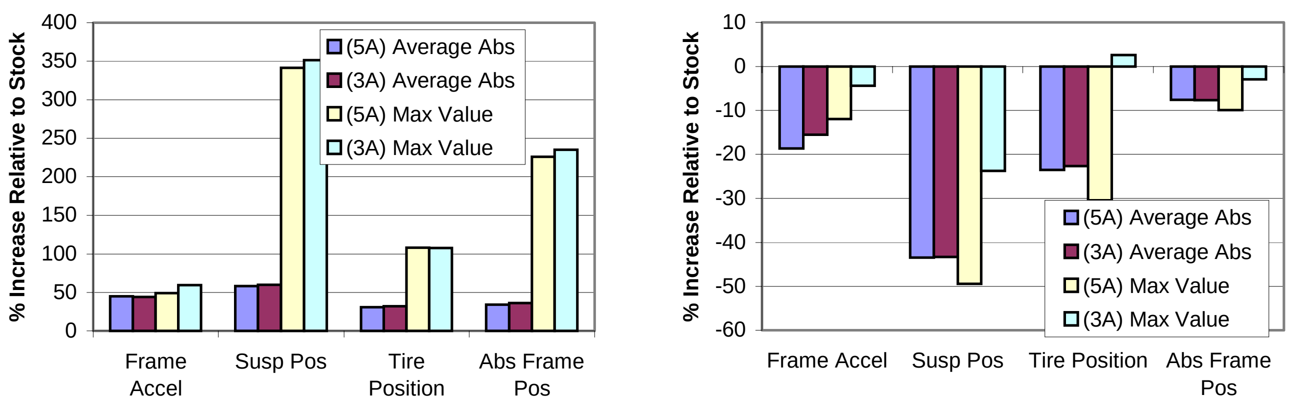

(a) Step Input Response

(b) Chirp Input Response

Figure 3.128. 3 and 5 Amp Displacement Skyhook Result Comparison

The response to the heave step input shows a slight dependence on the upper limit of the current supplied to the damper. This dependence indicates that marginally improved performance is achieved with the lower current limit. The response to the heave chirp input, however, exhibits a large dependence on this value, and clearly shows that the 5 Amp limit yields improved performance over the 3 Amp limit.

3.3 MR Damper Vehicle Testing (Controlled)

After the best values of $c_{skyhook}$ and $k_{skyhook}$ were determined, both the velocity and displacement based skyhook policies were tested for the five inputs. The first one examined is the heave step input.

3.3.1 Heave Step Input

The heave step input was applied to the passive system, the system with velocity based skyhook control, and the system with displacement based skyhook control. The resulting time traces are shown in Figure 3.129.

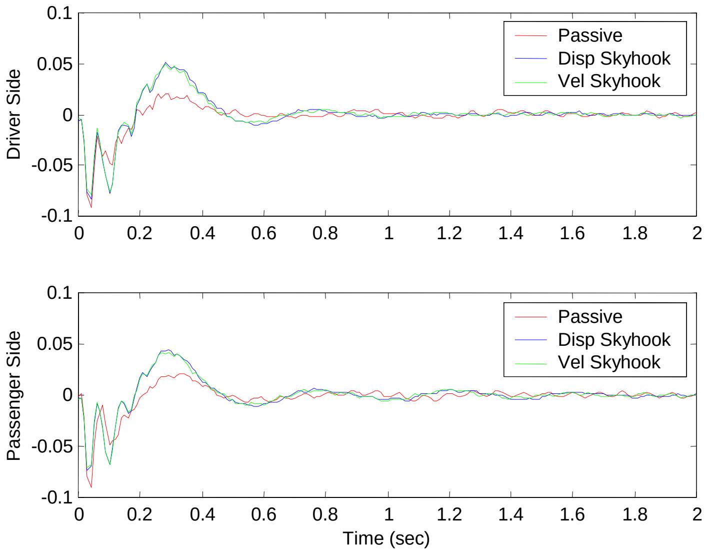

(a) Tire Deflection

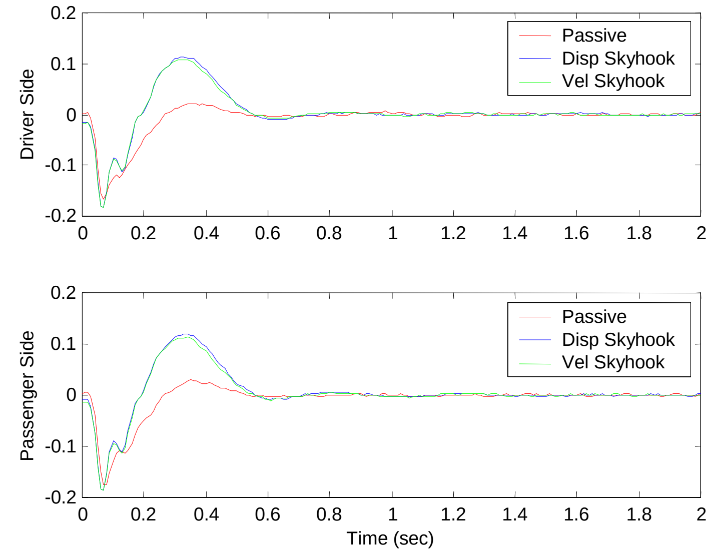

(b) Suspension Rattle

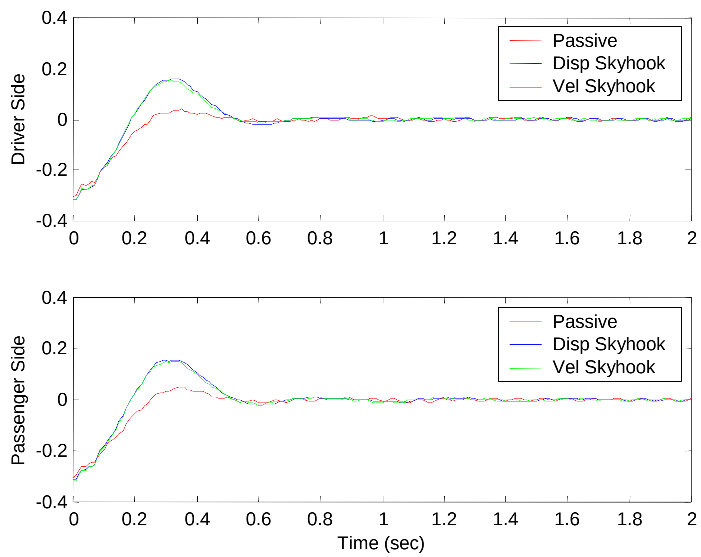

(c) Absolute Frame Position

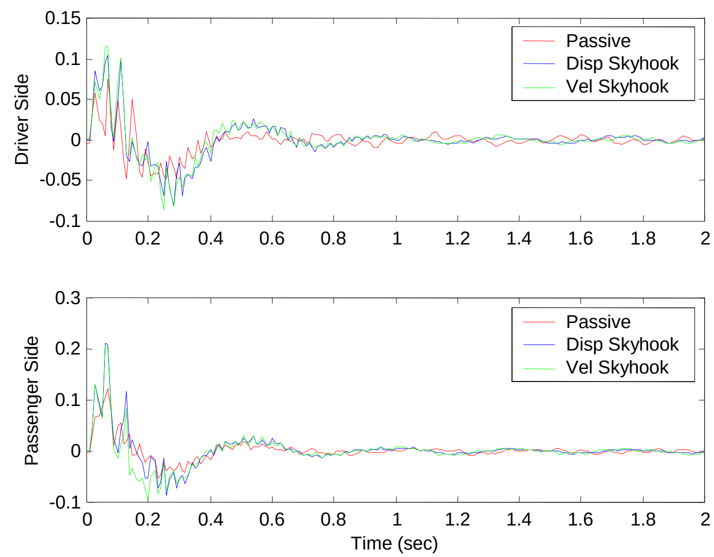

(d) Frame Acceleration

Figure 3.129. Heave Step Input System Performance Results

This figure shows that in many cases both the velocity and the displacement based skyhook policies are able to initially reduce the induced vibration faster than the passive system. However, after the initial attenuation, they both exhibit much greater overshoot than the passive stock system does.

3.3.2 *Roll Step Input*

The roll step input was applied to the passive system, the system with velocity based skyhook control, and the system with displacement based skyhook control. The resulting time traces are shown in Figure 3.130.

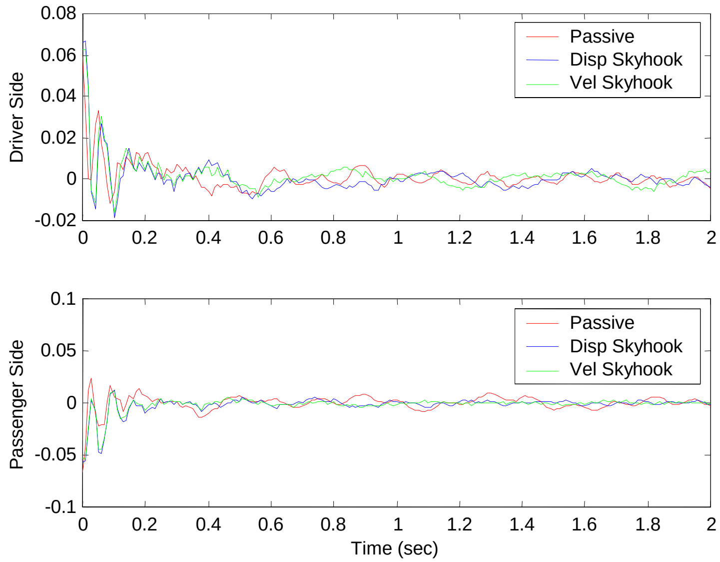

(a) Tire Deflection

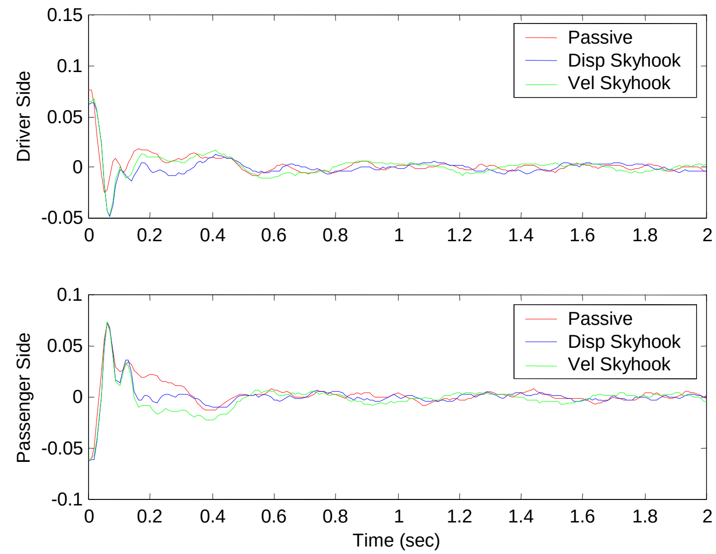

(b) Suspension Rattle

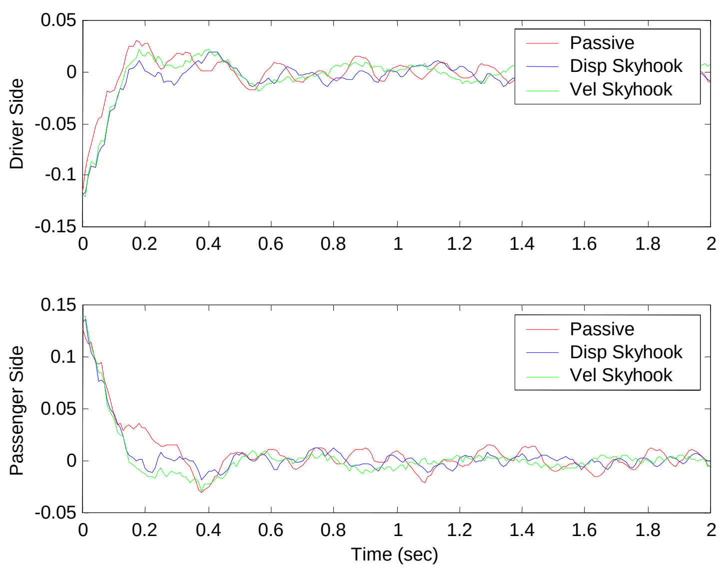

(c) Absolute Frame Position

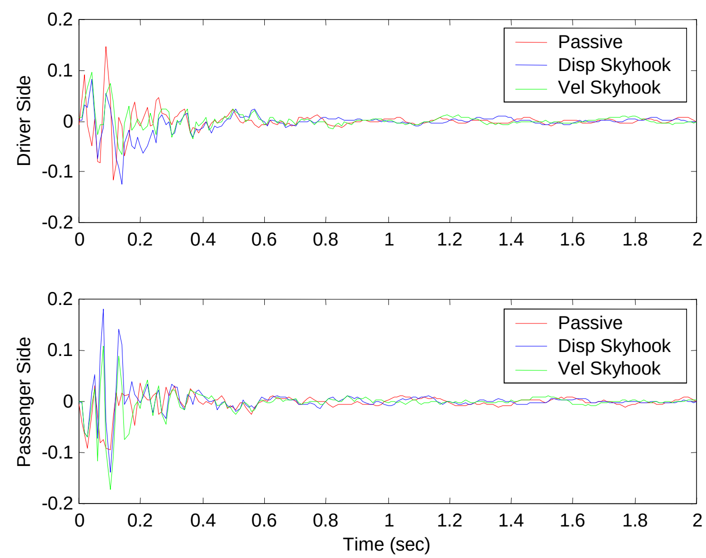

(d) Frame Acceleration

Figure 3.130. Roll Step Input System Performance Results

This figure shows that in many cases neither the velocity nor the displacement based skyhook policies are able to attenuate the induced vibration faster than the passive system.

3.3.3 Heave Chirp Input

The heave chirp input was applied to the passive system, the system with velocity based skyhook control, and the system with displacement based skyhook control. The resulting time traces are shown in Figures 3.131-134.

The response to the heave chirp input shows that in terms of frame acceleration, both the velocity and displacement based skyhook policies perform poorly at frequencies close to the suspension resonance frequency. However, at frequencies higher than the resonance frequency, both control policies exhibit performance that is superior to the stock passive configuration. Considering supension rattle, tire deflection, and absolute frame position, neither the velocity nor the displacement based skyhook policies improve performance at frequencies near the suspension resonance frequency.

3.3.4 Roll Chirp Input

The roll chirp input was applied to the passive system, the system with velocity based skyhook control, and the system with displacement based skyhook control. The resulting time traces are shown in Figures 3.135-138.

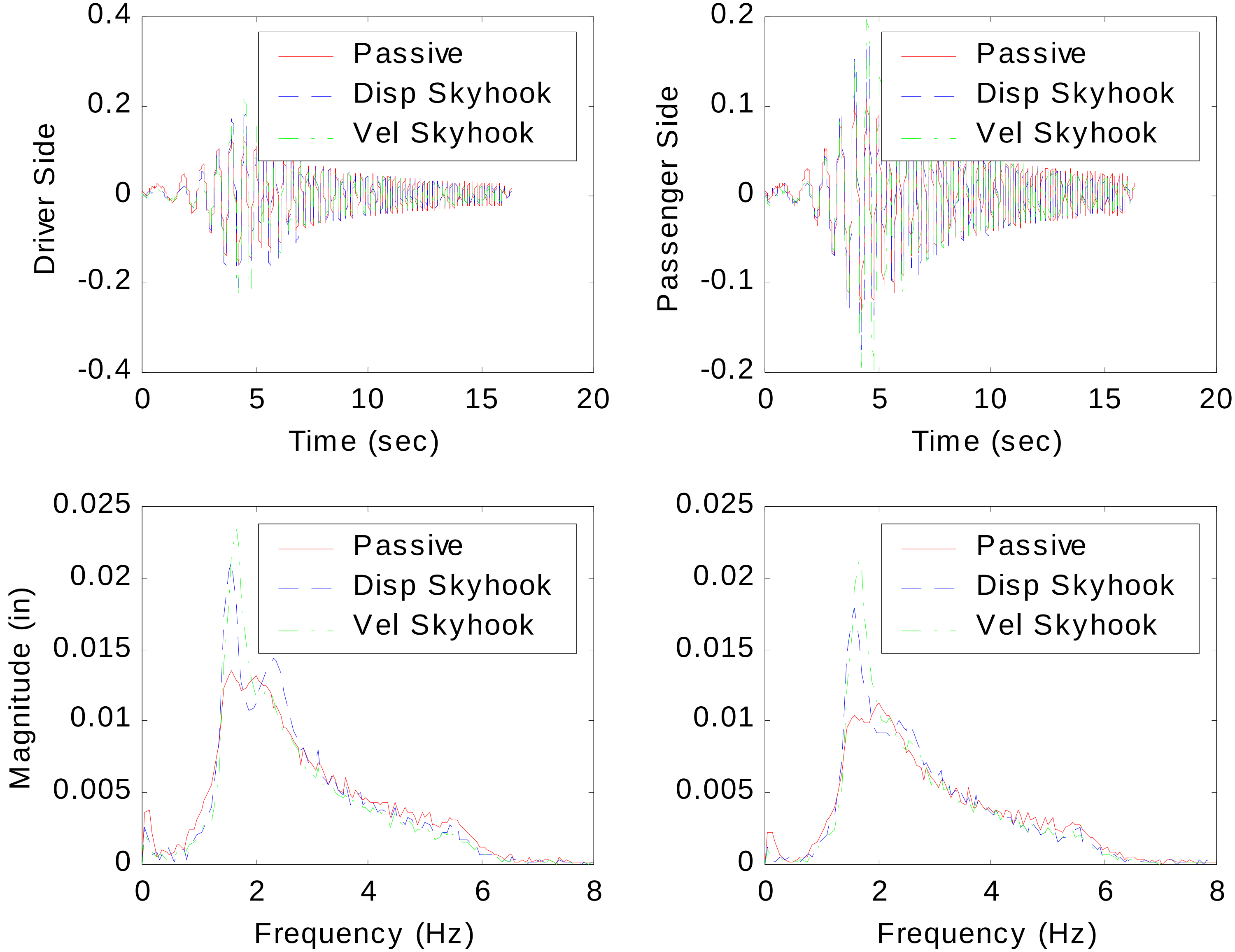

Passive
Disp Skyhook
Vel Skyhook
Driver Side
Passenger Side
Time (sec)
Magnitude (in)
Frequency (Hz)

Figure 3.131. Tire Deflection Time Trace and Frequency Response for Heave Chirp Road Displacement

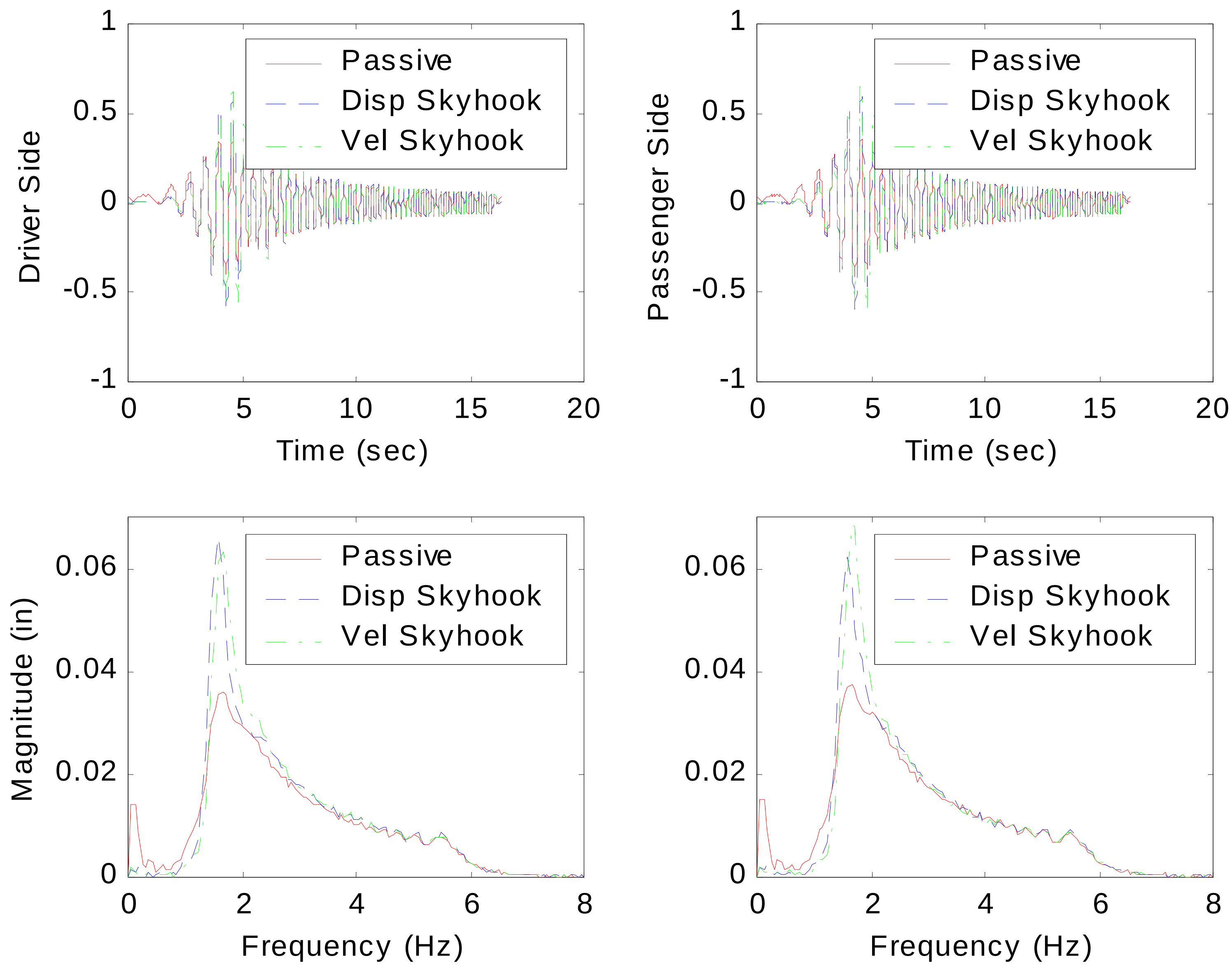

Figure 3.132. Suspension Rattle Time Trace and Frequency Response for Heave Chirp Road Displacement

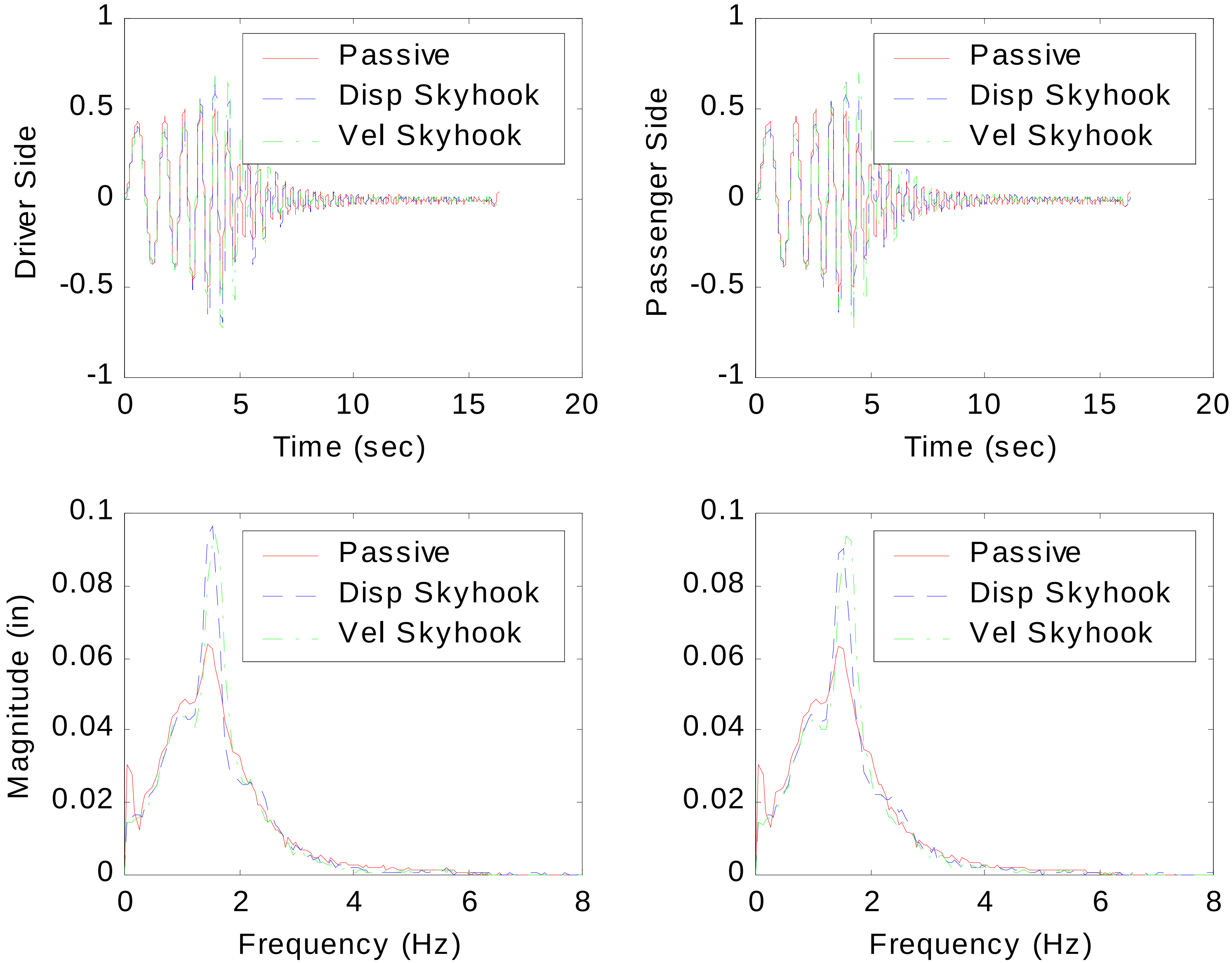
Passive
Disp Skyhook
Vel Skyhook
Driver Side
Time (sec)
Passenger Side
Time (sec)
Magnitude (in)
Frequency (Hz)
Frequency (Hz)

Figure 3.133. Absolute Frame Position Time Trace and Frequency Response for Heave Chirp Road Displacement

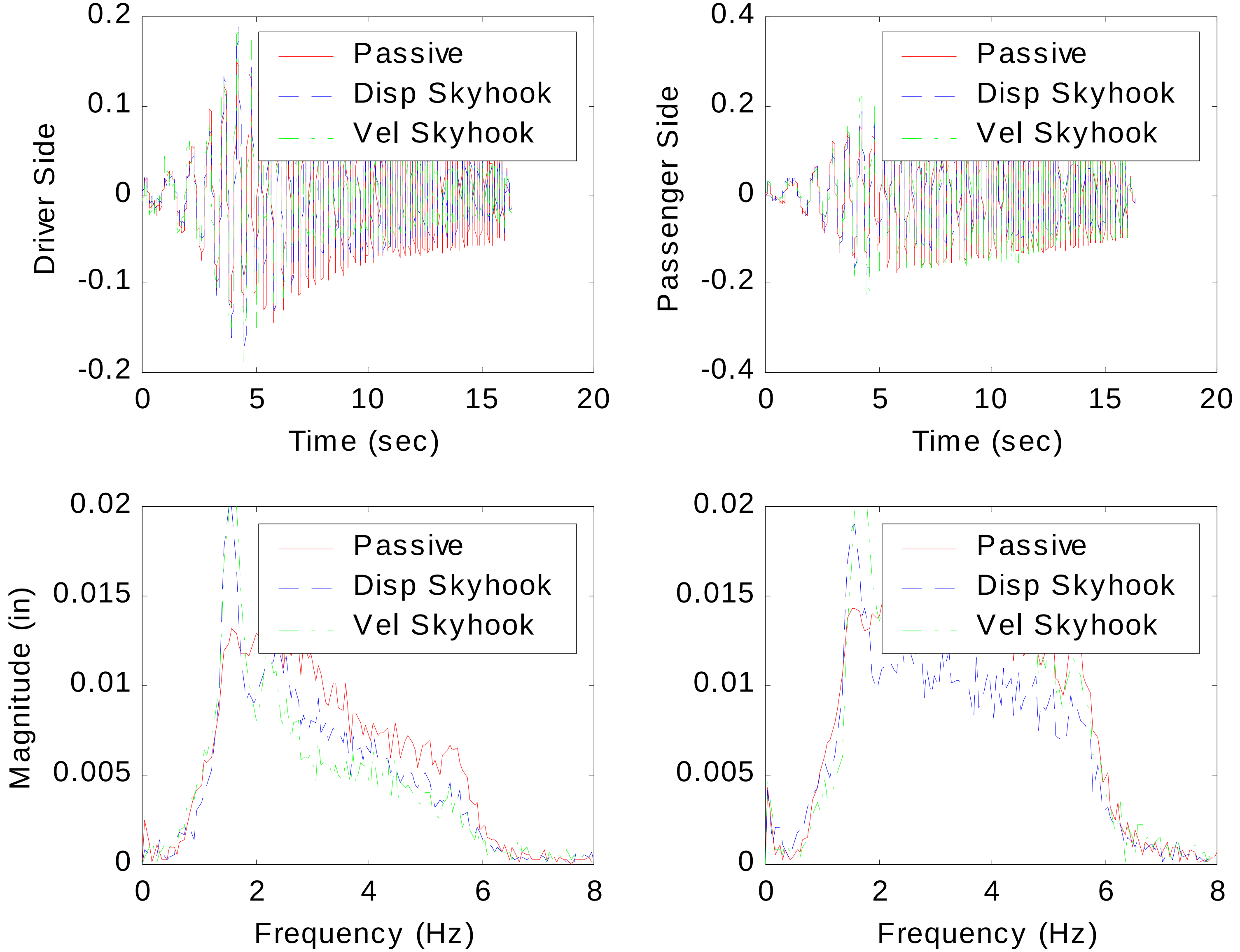

Figure 3.134. Frame Acceleration Time Trace and Frequency Response for Heave Chirp Road Displacement

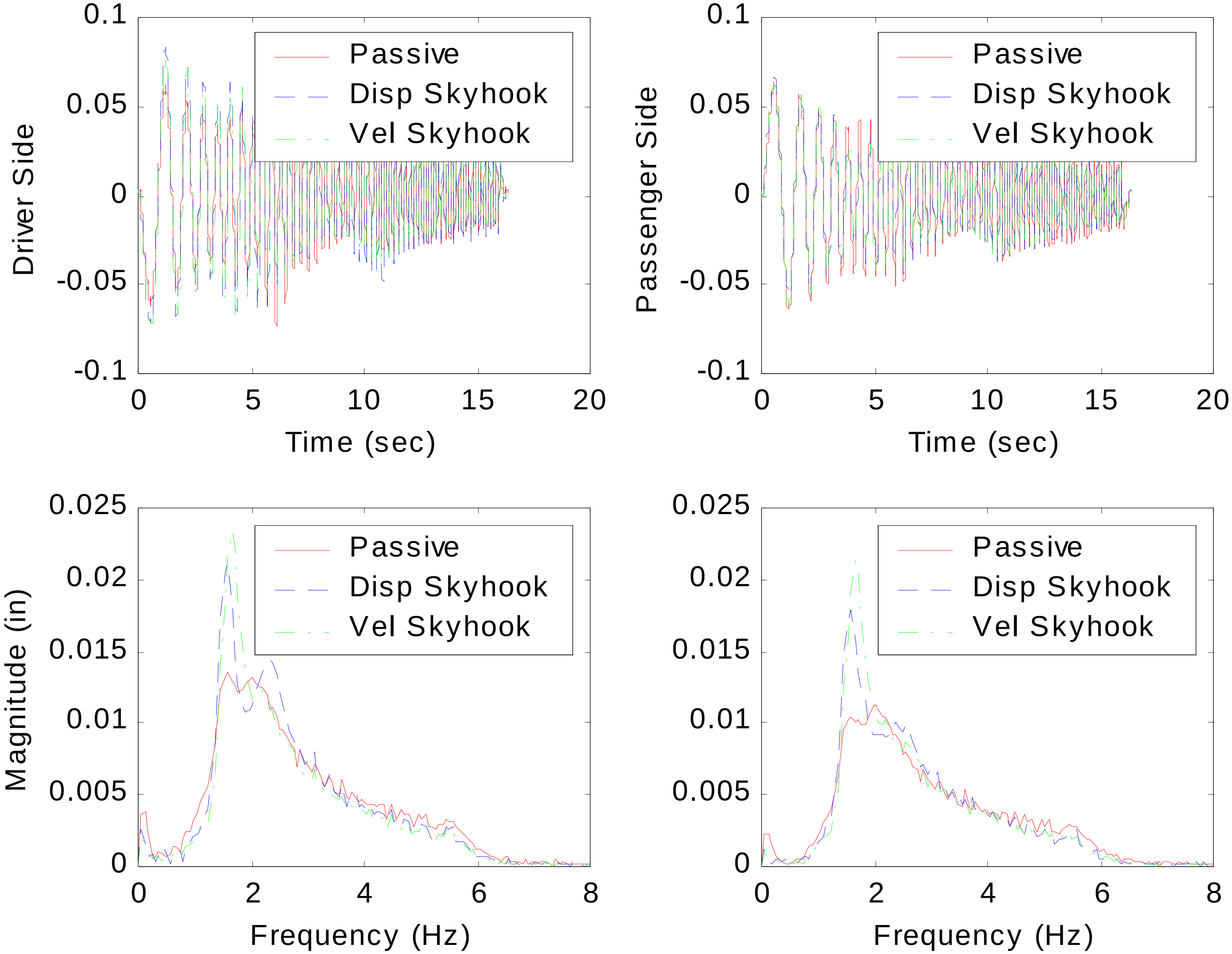
Driver Side
Passenger Side
Time (sec)
Time (sec)
Magnitude (in)
Frequency (Hz)
Frequency (Hz)
Passive
Disp Skyhook
Vel Skyhook

Figure 3.135. Tire Deflection Time Trace and Frequency Response for Roll Chirp Road Displacement

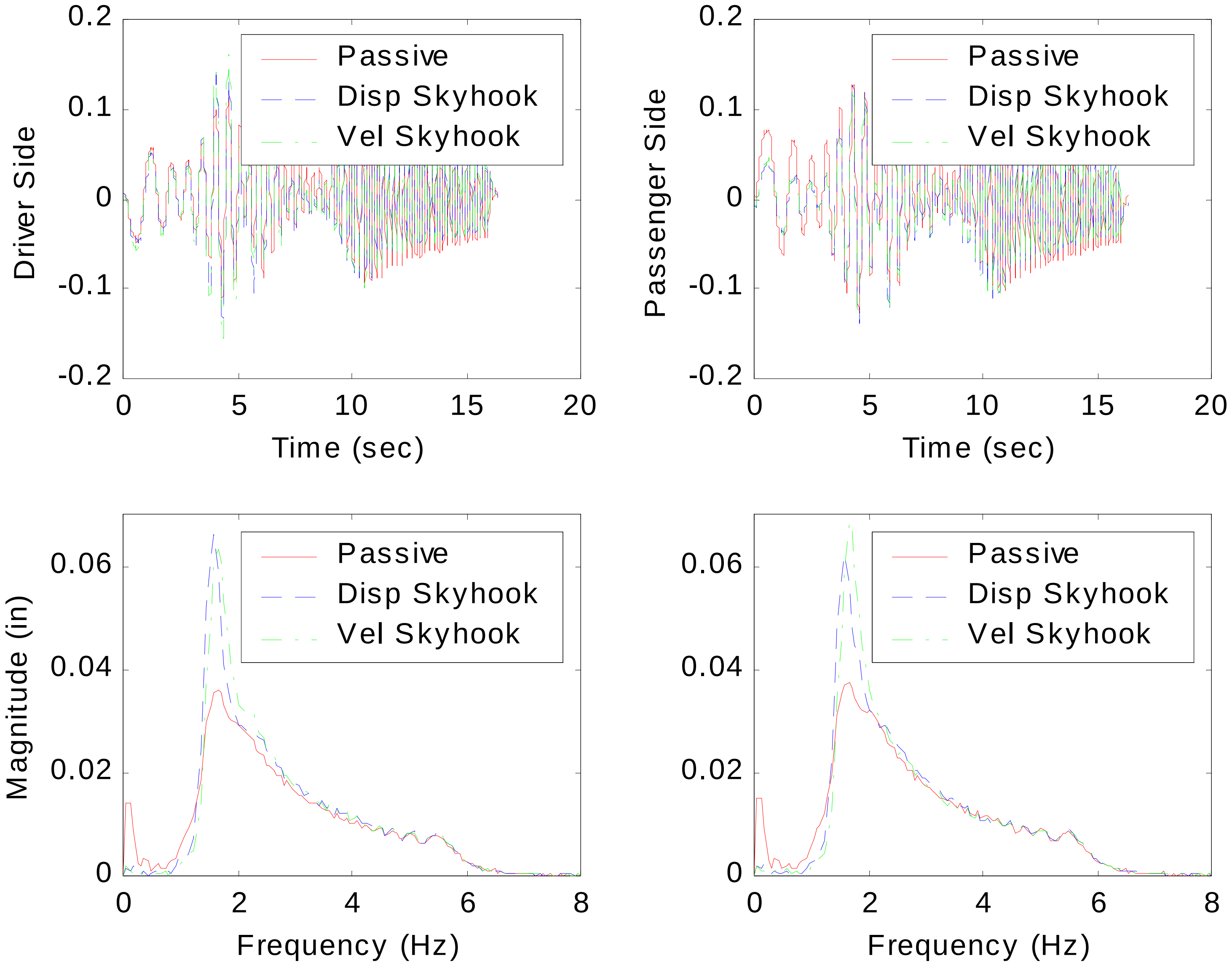

Figure 3.136. Suspension Rattle Time Trace and Frequency Response for Roll Chirp Road Displacement

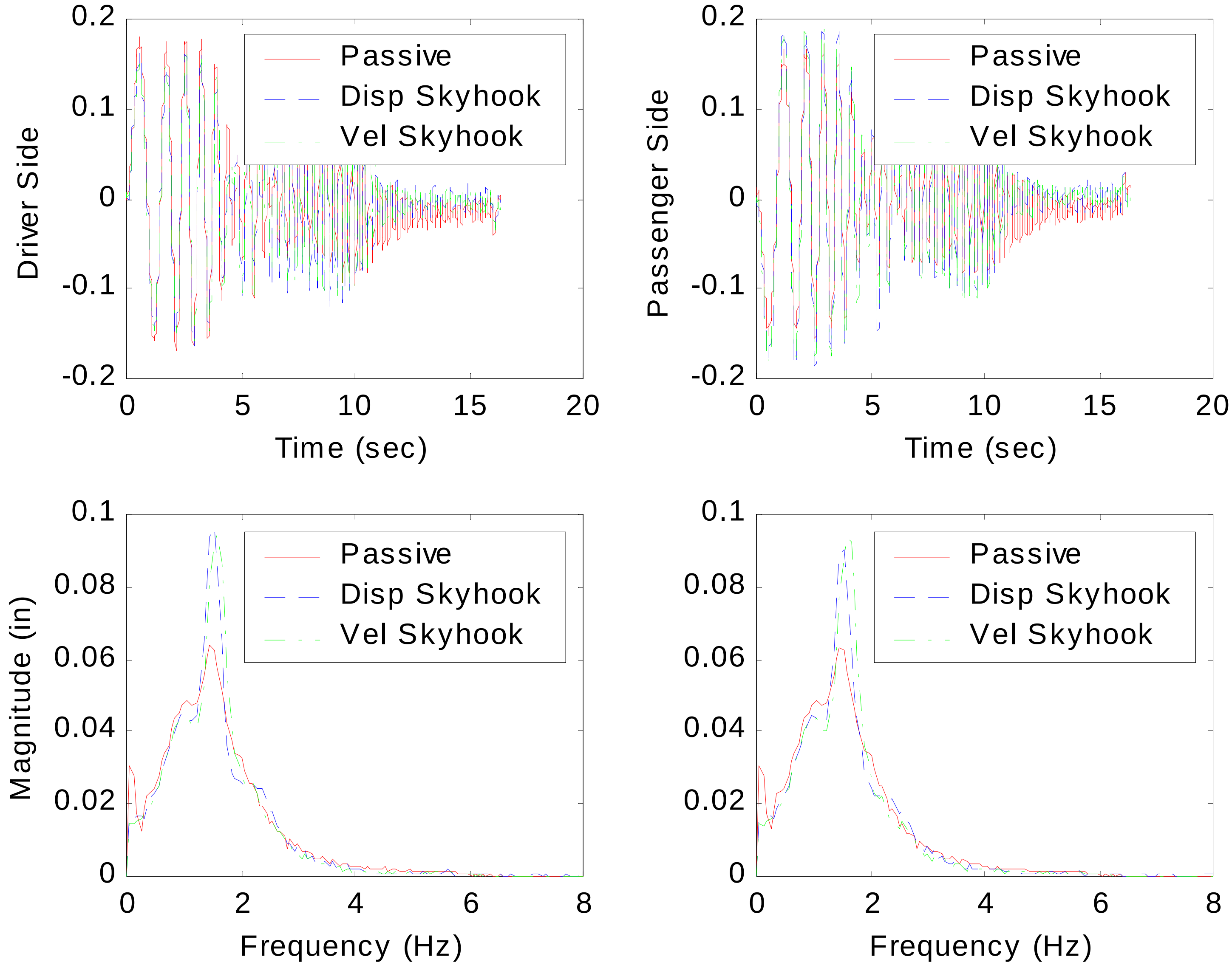

Figure 3.137. Absolute Frame Position Time Trace and Frequency Response for Roll Chirp Input

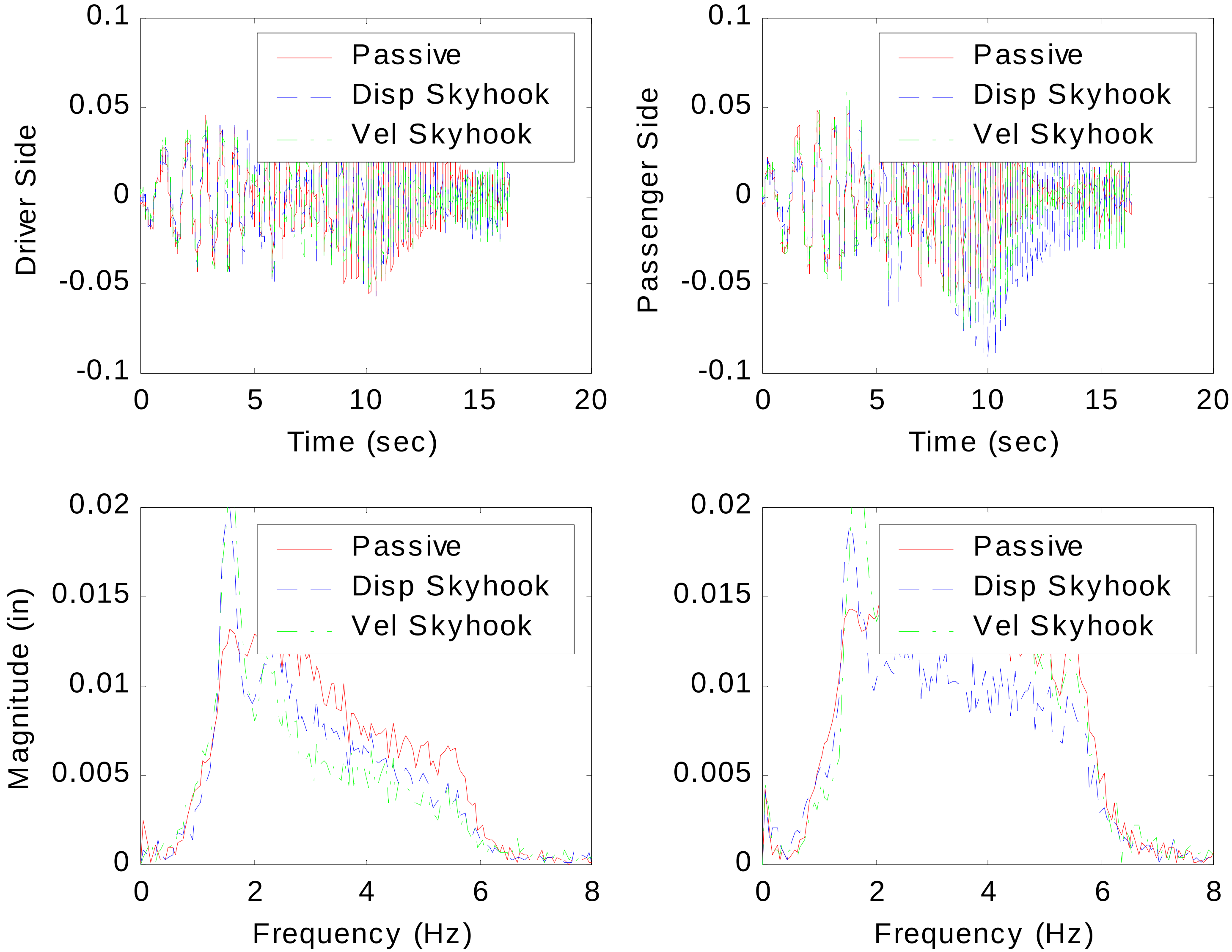

Figure 3.138. Frame Acceleration Time Trace and Frequency Response for Roll Chirp Road Displacement

The response to the roll chirp input shows that in terms of frame acceleration, both the velocity and displacement based skyhook policies perform poorly at frequencies close to the suspension resonance frequency. As was shown for the heave chirp input, at frequencies higher than the resonance frequency, both control policies exhibit performance that is superior to the stock passive configuration. Examining supension rattle, tire deflection, and absolute frame position reveals that neither the velocity nor displacement based skyhook policies can improve performance significantly at frequencies near the suspension resonance frequency. The results for the roll measures of testing with the roll chirp are shown Figure 3.139.

Figure 139 shows that neither velocity nor displacement based skyhook control offer any reduction in vehicle roll. This is not unexpected as prior results have shown that the dampers, either passive or conventionally controlled, are not effective at controlling vehicle roll. In terms of roll acceleration, this performance is slightly better, with displacement skyhook showing slight improvement over the stock passive case for many frequencies.

3.3.5 Multi-Sine Input

The multi-sine input was applied to the passive system, the system with velocity based skyhook control, and the system with displacement based skyhook control. The resulting time traces are shown in Figure 3.140.

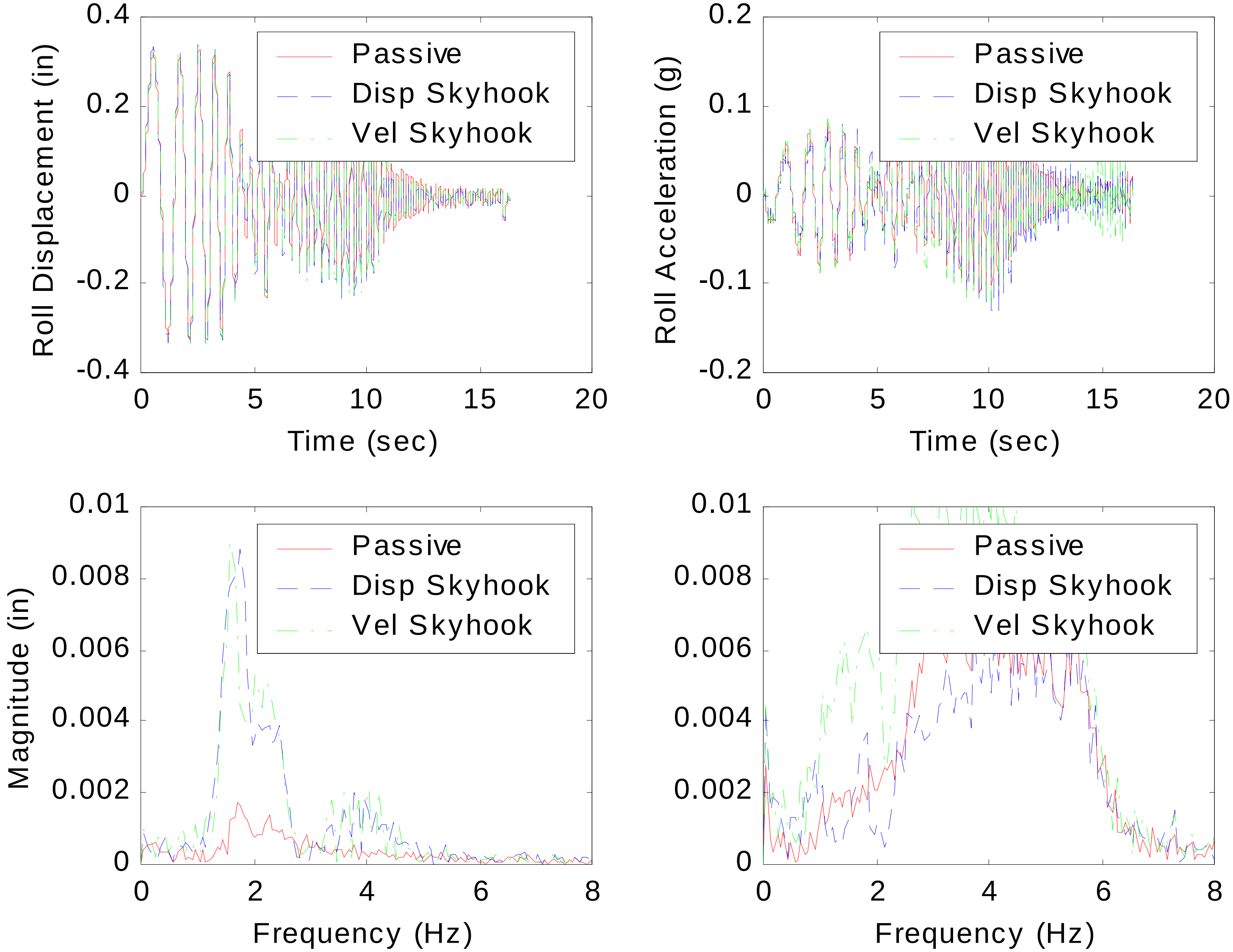

Figure 3.139. System Roll Time Trace and Frequency Response for Roll Chirp Road Displacement

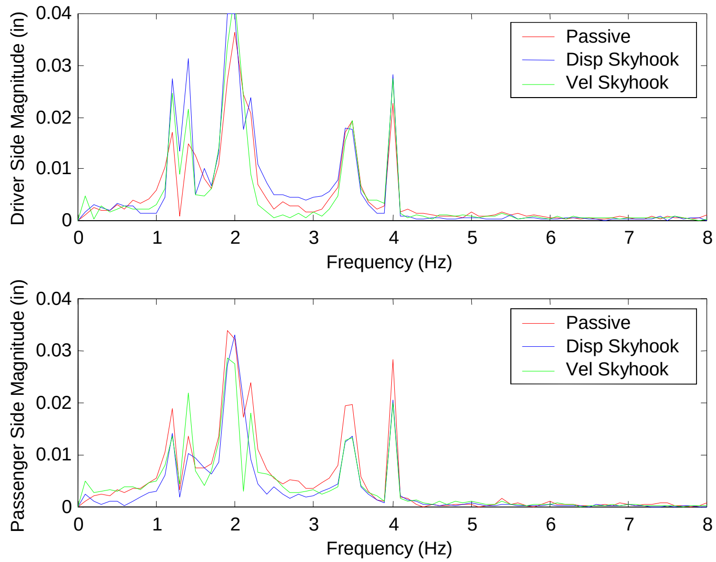

(a) Tire Deflection

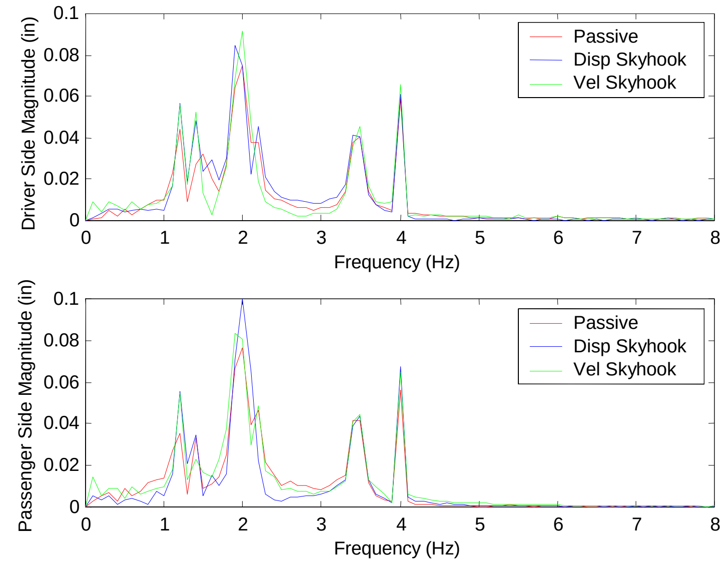

(b) Suspension Rattle

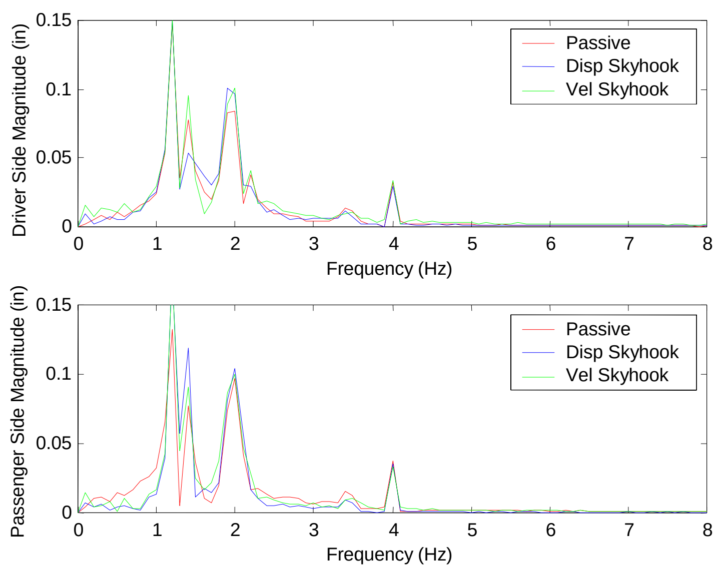

(c) Absolute Frame Position

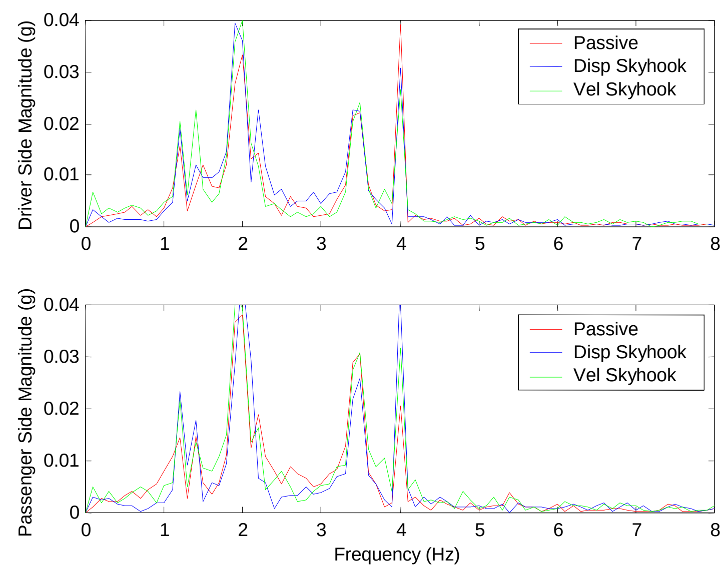

(d) Frame Acceleration

Figure 3.140. Various Vehicle Measurements due to Multi-Sine Road Displacement

The response to the multi-sine input shows that in terms of frame acceleration, suspension rattle and absolute frame position, both the velocity and displacement based skyhook policies do not offer any reductions at frequencies close to the input frequencies. Performance at frequencies other than the input frequencies is better. In terms of tire deflection, both of the skyhook policies improve performance at many frequencies. The roll measure results of the multi-sine input testing are shown in Figure 3.141.

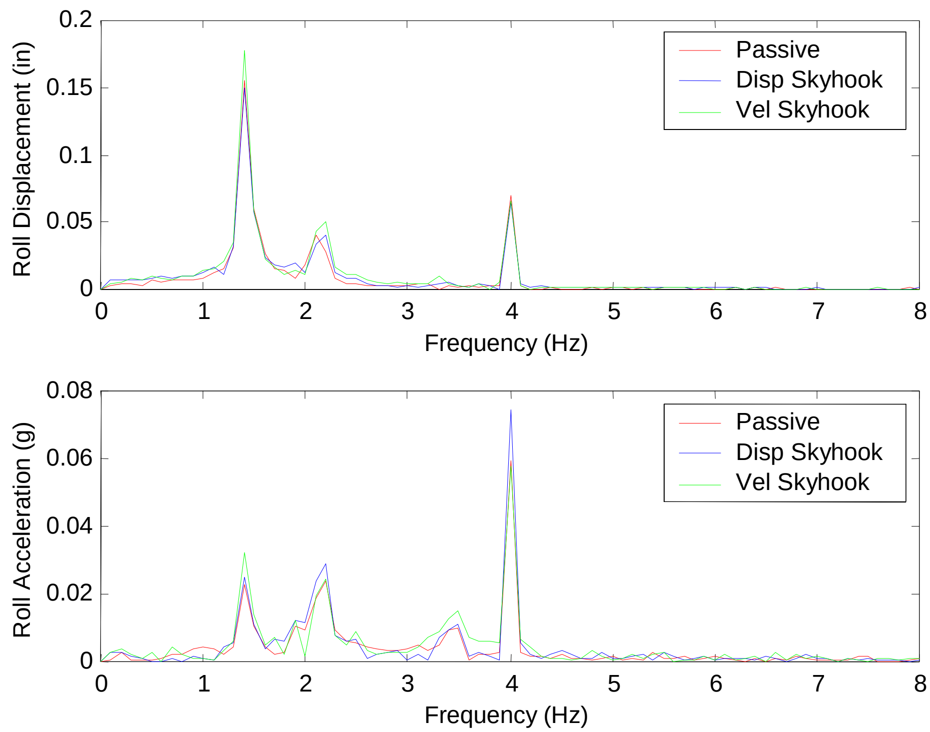

Figure 3.141. Multi-Sine Road Displacement Input System Roll Performance Results

In terms of roll displacement, this figure shows that neither velocity nor displacement based skyhook control exhibit performance significantly different from the passive stock configuration. This further validates the earlier premise that in a conventional arrangement, the dampers are not an effective mechanism for controlling vehicle roll.

3.3.6 Summary of Vehicle Test Results

The results from testing with the five inputs are difficult to assimilate individually, and need to be combined in order for their relevance to be apparent. For each input, the average of the absolute value as well as the maximum value of the response has been tabulated. The results for all the inputs have been concatenated and are presented in terms of their percent increase relative to the stock dampers in Tables 3.2-4.

Table 3.2. Controlled System Step Input Performance Summary

Step Input Summary

	Heave Input	Actuator Force	Frame Acceleration	Suspension rattle	Tire deflection	Absolute Frame Position	Frame Roll Disp	Frame Roll Acceleration
Avg	Displacement	38.35	45.01	58.05	30.71	34.05	-9.80	16.55
	Velocity	41.90	49.92	55.68	30.52	33.19	-13.59	14.36
Max	Displacement	-8.98	49.23	341.46	108.15	225.76	-45.90	84.00
	Velocity	-5.51	67.62	337.28	104.54	226.39	-35.18	128.59

Roll Input							
Displacement	12.21	11.37	-61.61	-38.21	-65.69	430.05	113.99
Velocity	38.11	6.19	-98.21	-54.85	-141.97	109.38	57.53
Displacement	-37.15	23.95	163.31	96.74	57.19	98.71	362.86
Velocity	-32.79	-12.28	59.31	17.40	7.74	88.76	83.57

Table 3.3. Controlled System Chirp Input Performance Summary

Chirp Input Summary

Heave Input							
Displacement	15.70	-18.70	7.29	1.38	3.05	242.00	-6.12
Velocity	3.15	-10.53	7.52	-1.28	4.85	224.00	68.30
Displacement	61.85	17.24	67.35	46.60	27.60	289.00	2.30
Velocity	55.20	25.90	81.45	71.15	31.70	371.00	77.90

Roll Input							
Displacement	-1.10	-69.15	-58.95	-31.20	-53.00	3110.00	34.80
Velocity	-1.40	-239.50	-137.00	-48.70	-117.00	103.00	29.70
Displacement	-11.32	-56.90	-61.15	-37.65	-66.05	1730.00	100.00
Velocity	-16.05	-149.00	-171.00	-74.20	-194.50	97.60	45.90

Table 3.4. Controlled System Multi-Sine Input Performance Summary

Multi-Sine Input Summary

Displacement	10.29	11.16	16.06	0.32	14.08	-2.25	19.17
Velocity	1.88	3.45	6.04	-2.48	13.42	11.67	7.00
Displacement	0.63	10.72	8.47	-1.68	1.16	-4.26	33.02
Velocity	5.71	19.81	2.96	-22.42	13.95	21.29	21.26

The frame acceleration results are presented graphically in Figure 3.142. This figure shows that neither the velocity based nor the displacement based control strategy is more effective than the stock passive system at controlling the maximum frame acceleration resulting from a heave step, a roll step, or the multi-sine input. However, the velocity based control is effective at controlling the maximum value of the response to the roll step input (while the displacement based control is not), and both are effective at controlling the maximum value of the response to the roll chirp input. In terms of the average of the absolute value of the response, again both strategies are effective at controlling the response to both the heave and roll chirp inputs, but are less effective at controlling the response to the other inputs.

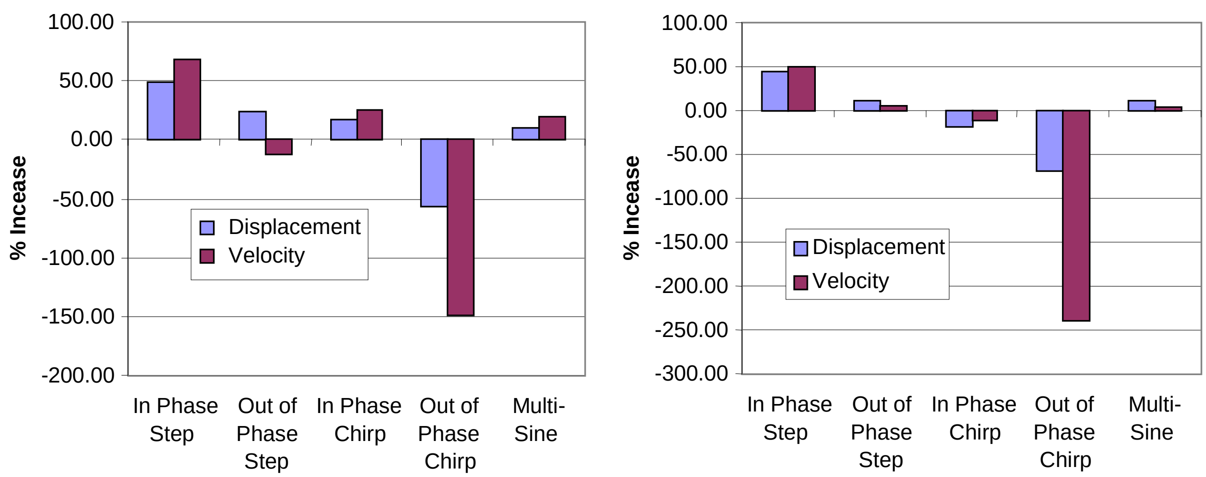

(a) Maximum Frame Acceleration (b) Average Frame Acceleration

Figure 3.142. Frame Acceleration Performance (Relative to Stock Dampers) Summary

The supension rattle results are presented graphically in Figure 3.143. This figure shows both policies are less effective than the stock passive system at controlling the maximum value of the supension rattle resulting from the heave and roll step inputs, as well as for the heave chirp and multi -sine input. The response to the roll chirp input was clearly improved over the stock passive case. In terms of the average of the absolute value of the response, both strategies are only effective at controlling the response to the roll step and roll chirp inputs.

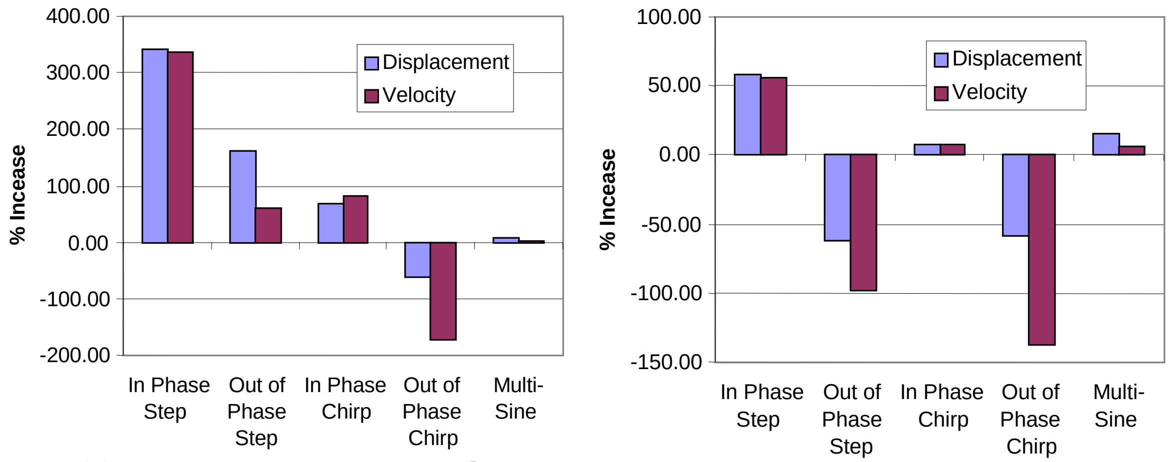

(a) Maximum Suspension Rattle (b) Average Suspension Rattle

Figure 3.143. Supension rattle Performance (Relative to Stock Dampers) Summary

The tire deflection results are presented graphically in Figure 3.144. This figure shows both policies are less effective than the stock dampers at controlling the maximum value of the tire deflection resulting from the heave step, the roll step, and the heave chirp. The responses to the roll chirp and multi-sine inputs were clearly improved over the stock passive case. In terms of the average of the absolute value of the response, both strategies are effective at controlling the response to the roll step and roll chirp inputs. Additionally, the velocity based skyhook strategy was effective at controlling the absolute value of the response to the heave chirp and multi-sine inputs as well.

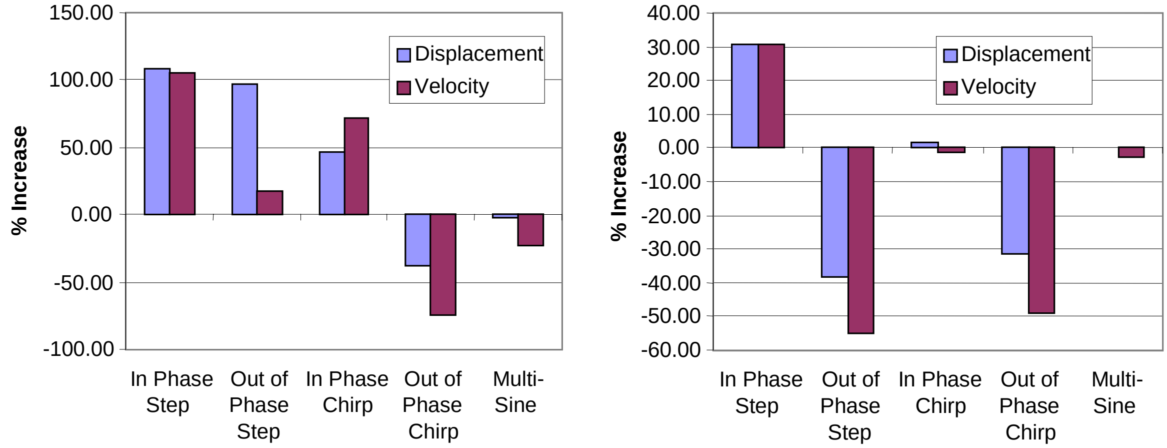

(a) Maximum Tire Deflection (b) Average Tire Deflection

Figure 3.144. Tire Deflection Performance (Relative to Stock Dampers) Summary

The absolute frame position results are presented graphically in Figure 3.145. This figure shows both policies are less effective than the stock passive system at controlling the maximum value of the absolute frame position resulting from the heave step, the roll step, the heave chirp, and the multi-sine input. The response to the roll chirp input was clearly improved over the stock passive case. In terms of the average of the absolute value of the response, both strategies are only effective at controlling the response to the roll step and roll chirp inputs.

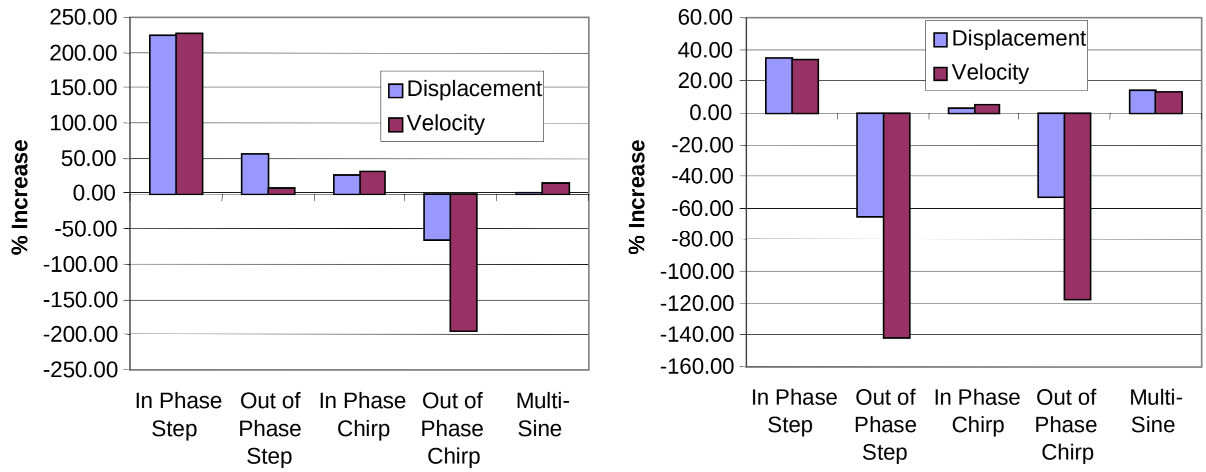

(a) Maximum Absolute Frame Position (b) Average Absolute Frame Position

Figure 3.145. Absolute Frame Position Performance (Relative to Stock Dampers) Summary

The frame roll displacement results are presented graphically in Figure 3.146. This figure shows both policies are less effective than the stock passive system at controlling the both the maximum value of the absolute frame position and the average of the absolute value of the response to the roll step, heave chirp, and roll chirp inputs. The response to the heave step input was improved by both strategies, in both measures. The response to the multi-sine input was also improved for both measures with the displacement based skyhook policy.

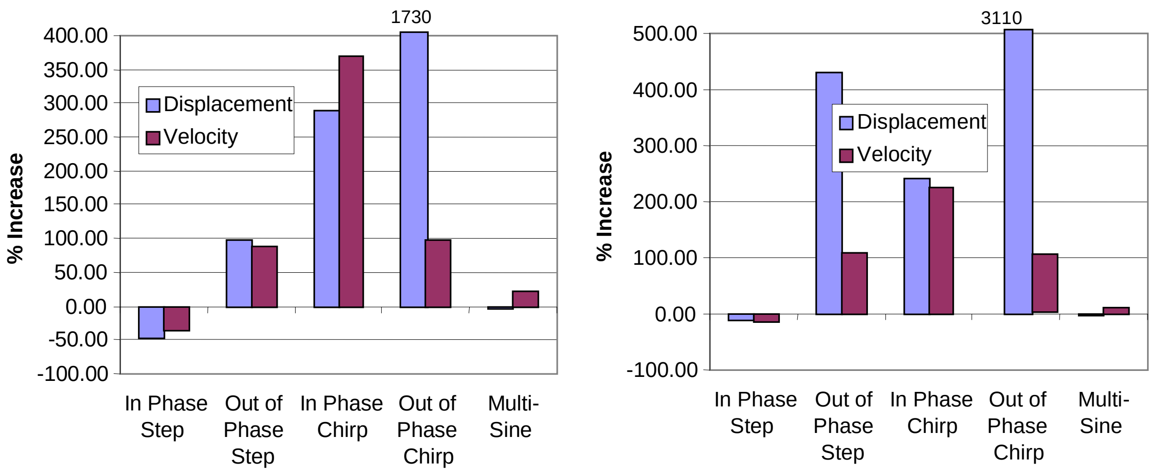

(a) Maximum Frame Roll Displacement (b) Average Frame Roll Displacement

Figure 3.146. Frame Roll Displacement Performance (Relative to Stock Dampers) Summary

The frame roll acceleration results are presented graphically in Figure 3.147. This figure shows both policies are less effective than the stock system at controlling either the maximum value of the absolute frame position or the average of the absolute value of the response each of the inputs. The single exception is that the displacement based skyhook strategy was able to reduce the average of the absolute value of the response to a roll chirp input.

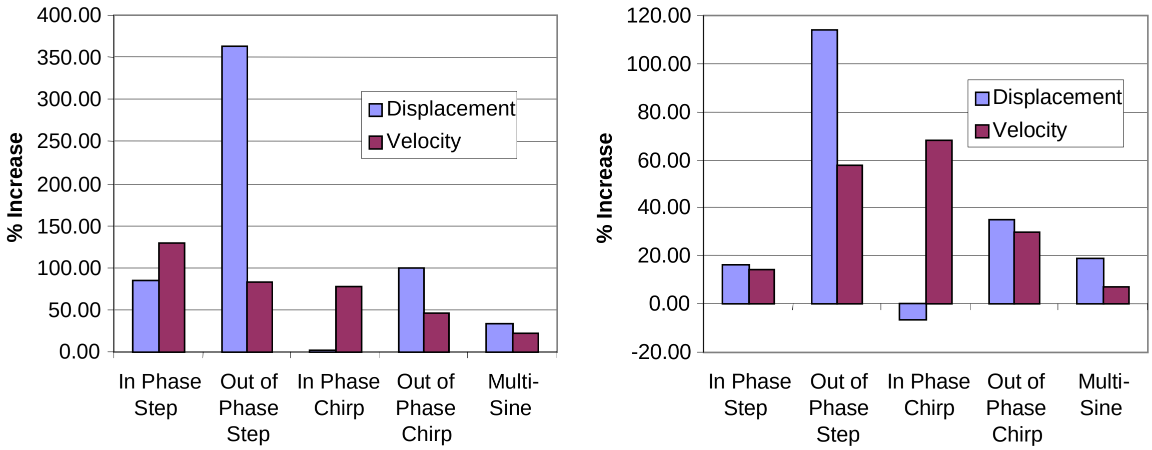

(a) Maximum Frame Roll Acceleration (b) Average Frame Roll Acceleration

Figure 3.147. Frame Roll Acceleration Performance (Relative to Stock Dampers) Summary

3.4 Lab Testing Summary

This phase of the study focused on determining the effectiveness of various semiactive suspension control policies through testing performed in a lab setting. A two-post test rig was used to apply various inputs to a Ford Expedition. The response of the test vehicle was examined with and without the roll bar, as well as with and without the stock dampers in order to determine the effect of each. Then the response of the test vehicle to varied inputs was compared for the case of the vehicle having the stock suspension as well as for the vehicle equipped with a number of different semiactive control policies. In contrast with the first phase of this research, control policies augmented by steering wheel position feedback are not investigated. This is due to an inability to model the combined effect of vehicle velocity and a steering wheel input within the confines of the lab.

The performance comparison of the velocity and displacement based skyhook control policies was performed using various inputs including puretone excitation (heave and roll), step inputs (heave and roll), chirp inputs (heave and roll) as well as a multi-sine input. Many of the results stemming from the use of these different inputs appear contradictory, while others are in complete agreement.

The results of testing with and without the roll bar indicate that the presence of the roll bar does have an effect on both the vehicle heave and roll modes. In terms of heave, the presence of the roll bar results in a slight frequency shift in the maximum transmissibility between road displacement and frame acceleration. In terms of roll, the presence of the roll bar increases the transmissibility ration at low frequencies as well as decreasing the transmissibility ration at high frequencies. In neither case (heave or roll inputs) was it found that the basic nature of the dynamics of the vehicle was determined by the presence of the roll bar. Testing has also shown that the damper is generally effective at controlling the acceleration resulting from steady state inputs transmitted to the frame of the test vehicle, though it is not effective at attenuating the response to a roll input. It has also been shown that the damper is most effective at controlling the response to inputs in the 1 to 2 Hz range.

After determining that the dynamics of the test vehicle are not dominated by the presence of a roll bar, an MR damper was developed to replace the stock passive damper. The MR damper was tested to determine both its damping characteristics (force-velocity curves) and its dynamic effect in a single suspension (quarter-car) rig. The latter tests were performed in an uncontrolled mode, in the sense that constant currents were supplied to the damper and its effect on the spring and unsprung body were studied. These showed that the damper can significantly effect the heave dynamics of the unsprung mass (vehicle body) as current to the damper was varied.

After installing the MR dampers onto the test vehicle, testing was performed with different levels of constant current supplied to the dampers. The results of this testing are a rough indicator of the performance envelope attainable with MR dampers. This testing showed that MR dampers can be effective at attenuating both supension rattle and the body displacement of the vehicle, although not affecting the vehicle roll dynamics at different currents.

Control strategies for the MR dampers were then developed. The first step of this development was to estimate a relationship between damper force, velocity across the damper, and current supplied to the damper. For both the velocity and displacement based skyhook control policies this relationship was developed and used to control the MR dampers. Both the velocity and displacement based control policies were tuned by finding optimal values of the nominal damping and stiffness used within each control policy respectively.

The performance of the velocity and displacement based skyhook control strategies were compared with each other as well as with the performance of the stock suspension. In terms of the response to an heave step input, both skyhook policies are less effective than the stock suspension at reducing the absolute displacement of the frame of the vehicle. Response data from chirp inputs show that the skyhook policies perform poorly at reducing acceleration at frequencies close to the first mode of the suspension, though at higher frequencies, both exhibit performance superior to the stock suspension. Testing has also indicated that the skyhook policies are less effective than the stock passive suspension at controlling the maximum frame acceleration, maximum supension rattle, maximum tire deflection, and maximum absolute frame displacement from either the step or multi-sine inputs.

These results are not unilateral; that is, they are not evident at every measurement position, for every measure, or for every input. Rather, they represent general conlusions drawn from examining the response to many inputs. What they do clearly show is that in order to realize real life performance improvements, it is necessary to augment these control policies with additional feedback. The type of additional feedback to be added is steering wheel position. In a real driving situation, the position of the steering wheel correlates (together with vehicle velocity) to the magnitude of the driver induced input to the vehicle suspension. This effect cannot be investigated in a static lab setting, but will be investigated in the following section in which results of testing the vehicle in real driving situations are presented.

CHAPTER 4

VEHICLE ROAD TESTING

The expected performance of a vehicle suspension can be inferred from numerical simulation and lab testing, but must ultimately be verified by road testing. Road testing allows performance investigations to be carried out in the expected service environment. The conditions of the road and the vehicle are the same as they will be in actual service. Though many of the advantages of lab testing (i.e., ability to replicate specific inputs, simplified instrumentation, etc…) are not evident in road testing, the added benefit of being more true-to-life makes it an important part of a complete study. It imparts a more compete understanding of the performance of the vehicle as a whole system than either one of the other two methods previously discussed. Additionally, real driving situations are an opportunity to investigate control methodologies that rely on driver feedback. In this part of the study we investigate the performance gains achievable using a semiactive suspension system controlled with a variety of control strategies. The actual road upon which testing of the Ford Expedition was performed is shown in Figure 4.1.

Figure 4.1. Road Used for Vehicle Testing

A variety of tests were performed, representing a range of driving conditions that the vehicle/driver may be exposed to.

4.1 Test Design

Three types of testing were performed in this part of the study. They are:

- Straight and level driving
- Bump testing
- Swerve based testing

Each of these tests will be described in more detail in the following sections.

4.1.1 Straight and level driving

The straight and level driving test is aimed at characterizing the performance of the semiactive suspension with various control strategies in driving situations where the input from the road is basically small in magnitude and constant in time, with respect to frequency content. The tests were performed with a vehicle speed of 20 mph. Scenarios investigated include:

- the original stock vehicle,
- the vehicle equipped with MR dampers without power, and
- the MR dampers controlled according to the displacement and velocity based skyhook policies previously discussed.

Control strategies that include feedback based on steering wheel angle which are investigated in other sections of this research were not tested as the steering wheel angle remained unchanged during this test. This test was performed on an isolated stretch of roadway so as to eliminate interaction between the test vehicle and other vehicles.

4.1.2 Bump testing

The bump test is designed to examine the effect of a variety of suspension inputs encountered in real world driving. These inputs include speed bumps, potholes, railroad crossings and driveway ramps. In this test, the vehicle was driven over a speed bump arranged at an angle of 68° relative to the path of the vehicle (22° relative to a line perpendicular to the path of the vehicle), as shown in Figure 4.2.

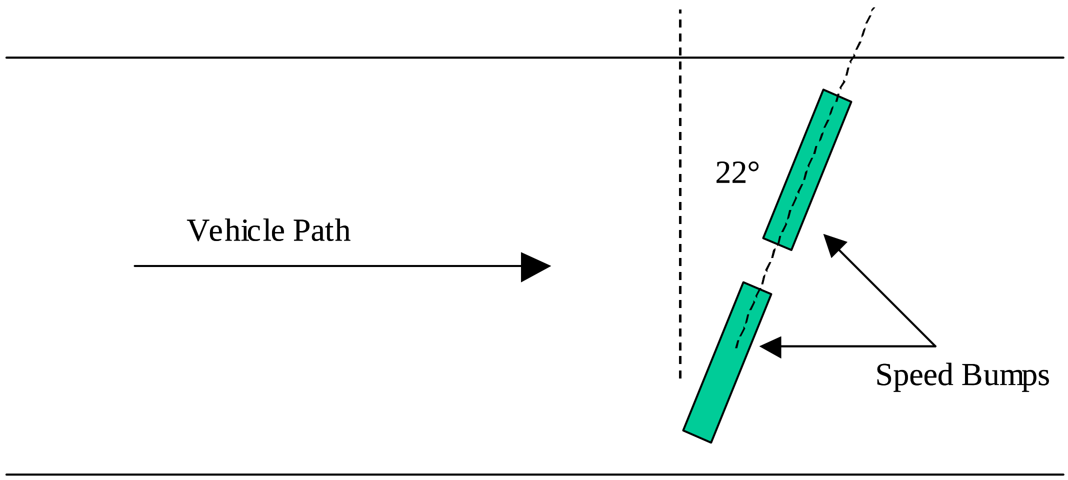

Figure 4.2. Speed Bump – Vehicle Path Orientation

This orientation of the speed bumps was chosen in order to excite both heave and roll modes of the vehicle. A vehicle speed of 5 mph was maintained as the speed bump was crossed. The profile of the speed bump used in this test is shown in Figure 4.3.

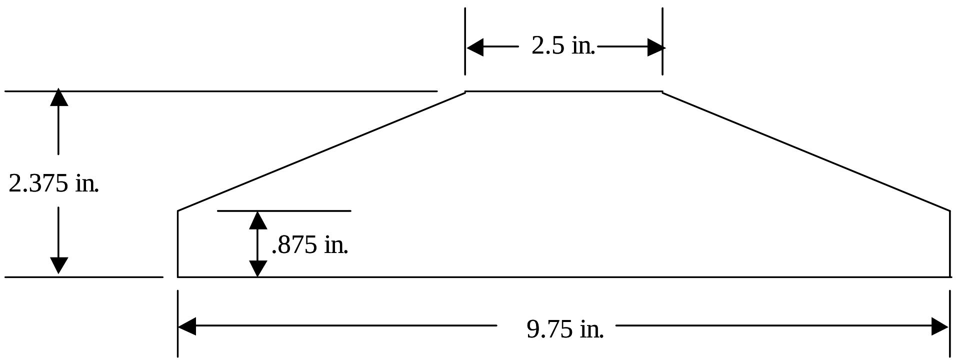

Figure 4.3. Speed Bump Profile

Testing included the original stock vehicle, the vehicle equipped with MR dampers but not powered, and the MR dampers controlled according to the displacement and velocity based skyhook policies previously discussed. The control strategies that include feedback based on steering wheel angle were not tested as the steering wheel angle remained unchanged as the driver traversed the speed bump. This test was performed on an isolated stretch of road. The actual bumps used in this test are shown in Figure 4.4.

Figure 4.4. Speed Bump Shown on Road

4.1.3 Swerve testing

The swerve test is designed to characterize the effect of a variety of driver induced vehicle maneuvers, including collision avoidance, highway on-off ramps, lane changes, and turns. In this test, the driver maintained a constant speed of 20 mph while negotiating the course shown in Figure 4.5.

(a) Without Test Vehicle

(a) With Test Vehicle

Figure 4.5. Swerve Test Course

The course consists of a straight section followed by an obstruction (a barrel) which the driver must avoid by swerving to the left. The driver must then immediately swerve back into the original lane and then continue on the original heading. A schematic representation of the test course in shown in Figure 4.6.

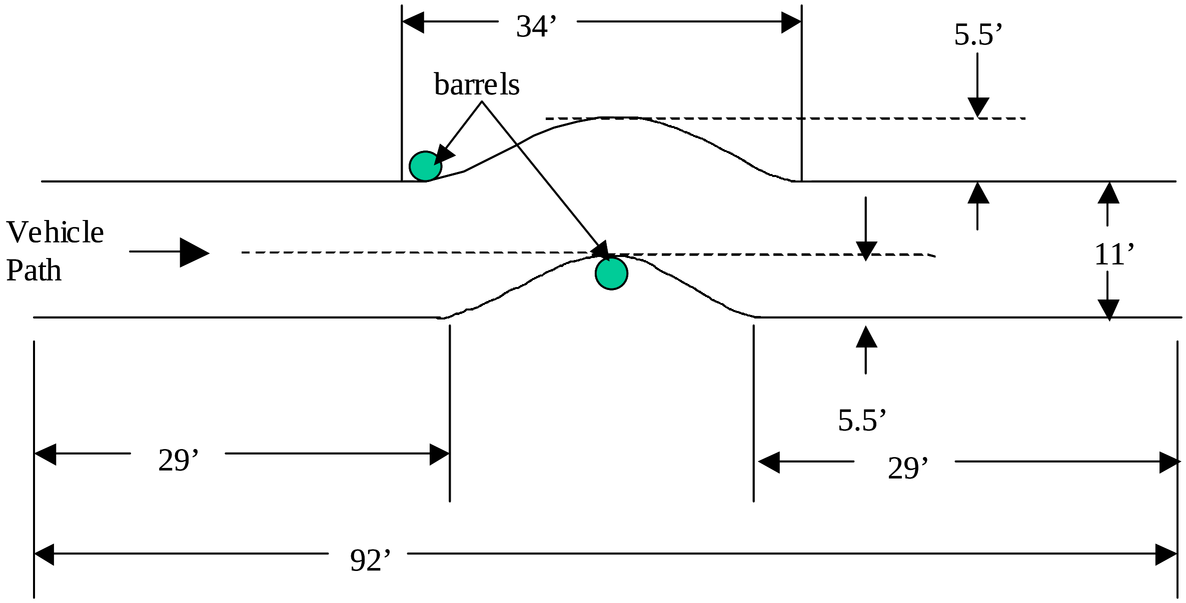

Figure 4.6. Swerve Test Course Schematic

As the driver traversed the course, the vehicle first rolls to the right (as the driver turns to the left to avoid the barrel). This roll to the right loads the vehicle springs. The driver then turns to the right, causing the vehicle to again roll to the outside, (i.e., to the left, away from the barrel). In this part of the swerve, the suspension unloading (from the previous turn) exacerbates the natural motion of the vehicle, which is to roll towards the outside of the turn. In this way, the nature of the maneuver induces levels of vehicle roll exceeding that present in a simple turn. The driver must again turn to the left in order to regain the original heading of the vehicle. This test was initially performed for the vehicle in stock configuration, providing a baseline measurement against which the performance of the other configurations can be judged. Following this the test was repeated with the vehicle equipped with MR dampers but not powered. The test was then repeated with the displacement and velocity based skyhook control policies. Finally, the test was again repeated, this time with each of the control policies augmented by the addition of feedback of the angle of the steering wheel. Two values of the gain associated with this feedback were tested for each of the displacement and velocity control policies. This tests the effectiveness of steering wheel position feedback, but only for the specific speed tested. It is apparent that the value of the gain associated with the steering feedback should be a function directly proportionate to vehicle speed. In other words, when the vehicle is not moving, or moving very slowly, this steering feedback gain should be zero. Likewise, when the vehicle is moving fast, small changes in steering wheel angle have a large effect on the dynamics of the vehicle; therefore the gain associated with steering feedback for higher vehicle speeds should be high. Since for this maneuver, the speed of the vehicle remained unchanged, the dependency of the steering gain on vehicle speed was not investigated. It should be understood that the results are for a relationship between the vehicle velocity and the value of the gain associated with the steering feedback that is unknown, but which results in the values henceforth referred to as ‘steering gain’ at a vehicle speed of 20 mph. The two values of the steering gain tested in this study are 2 and 4, and will be referred to as low and high steering gain as the actual numerical values are contingent on the voltage supplied to the steering position sensor. In this case, the lower of the two values was chosen such that in the absence of any other control signal, the damper would saturate when the steering wheel was turned halfway to the full steering lock in either the left or right side. A detail showing the part of the control code in which the steering gain enters is shown in Figure 4.7.

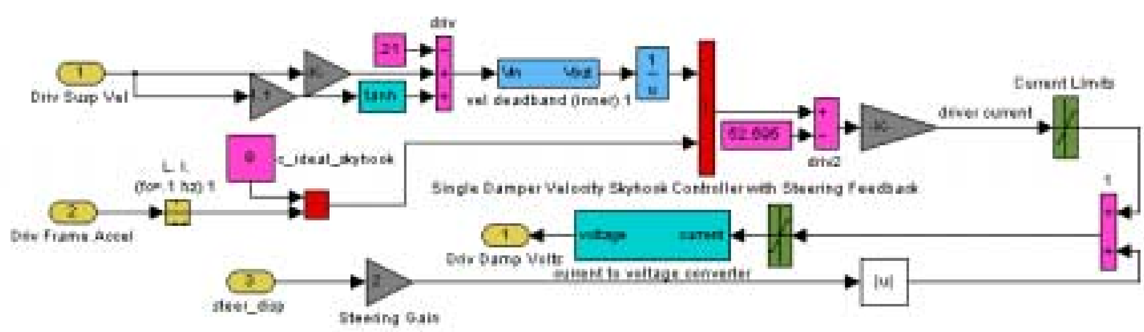

Figure 4.7. Steering Gain Shown in Control Code

4.2 *Vehicle Instrumentation*

The test vehicle has been instrumented in order to supply the signals necessary for the control of the suspension, as well has to provide data which can be used to characterize the performance of various systems. Instrumentation used for this phase of testing, includes:

- Four LVDTs measuring both position and velocity (Unimeasure model VP510-10 with sensitivity of 999.98 mV/in, 196.37 mV/inch/sec),
- six accelerometers (PCB model U352C65 ICP accelerometers with sensitivities ranging from 84.1 to 111.4 mV/g),
- and one position sensor (Unimeasure model LX-PA with sensitivity of 39.236mV/V/inch).

The four velocimeter/LVDTs were used to measure the displacement and velocity across of the four corners of the vehicle's suspension. Two of these sensors are shown on the front and rear of the test vehicle in Figure 4.8.

(a) Front of Vehicle (b) Rear of Vehicle

Figure 4.8. LVDTs Shown on the Front and Rear of the Test Vehicle

While the controller uses measurements of the velicity across the suspension, the displacement measurements are used solely to characterize the performance of the various systems tested. Four of the six accelerometers used measure the acceleration of the four corners of the frame of the vehicle. Two of these sensors are shown on the front and rear of the test vehicle in Figure 4.9.

(a) Front of Vehicle (b) Rear of Vehicle

Figure 4.9. Accelerometers Shown on Both the Front and Rear of the Test Vehicle

These measurements are used directly in order to characterize the performance of the various systems and to compute both velocity and displacement; which are signals used by the velocity and displacement based skyhook policies respectively. The remaining two accelerometers are arranged and mounted on the B-Post. These sensors provide measures of the roll and pitch of the vehicle body; signals used solely for the characterization of the various systems tested. The acceleration measurements are conditioned using a PCB signal conditioner and gained by a factor of one hundred to preserve a good signal to noise ratio. The position sensor is used to measure the displacement of the steering arm, which is a measure of the driver applied steering input. This sensor is shown in Figure 4.10.

Figure 4.10. Position Sensor Measuring Steering Wheel Input

The collection of the data supplied by the various sensors is accomplished by way of a dSpace Autobox and laptop computer.

4.3 Results

The results of the vehicle testing presented here include discussion of the data processing performed as well as characterization of the overall performance of the various systems tested. The results are presented in sections corresponding to the type of testing discussed.

4.3.1 Straight and level driving results

The straight and level driving tests were repeated multiple times for each case. The cases investigated, as well as the numbers of repeated data sets recorded are:

- Stock configuration; repeated six times
- MR dampers operated passively; repeated six times
- Displacement skyhook without steering gain; repeated three times
- Velocity skyhook without steering gain; repeated three times

The tests were repeated to increase the reliability of the results, which are presented in both time and frequency domains. In time domain, the average of the absolute value of each was recorded and then averaged across repeated data sets. The four values relating to the acceleration of the four corners of the vehicle frame were then also averaged together. These numbers were then normalized and presented as percent increase relative to stock, and are shown in Figure 4.11.

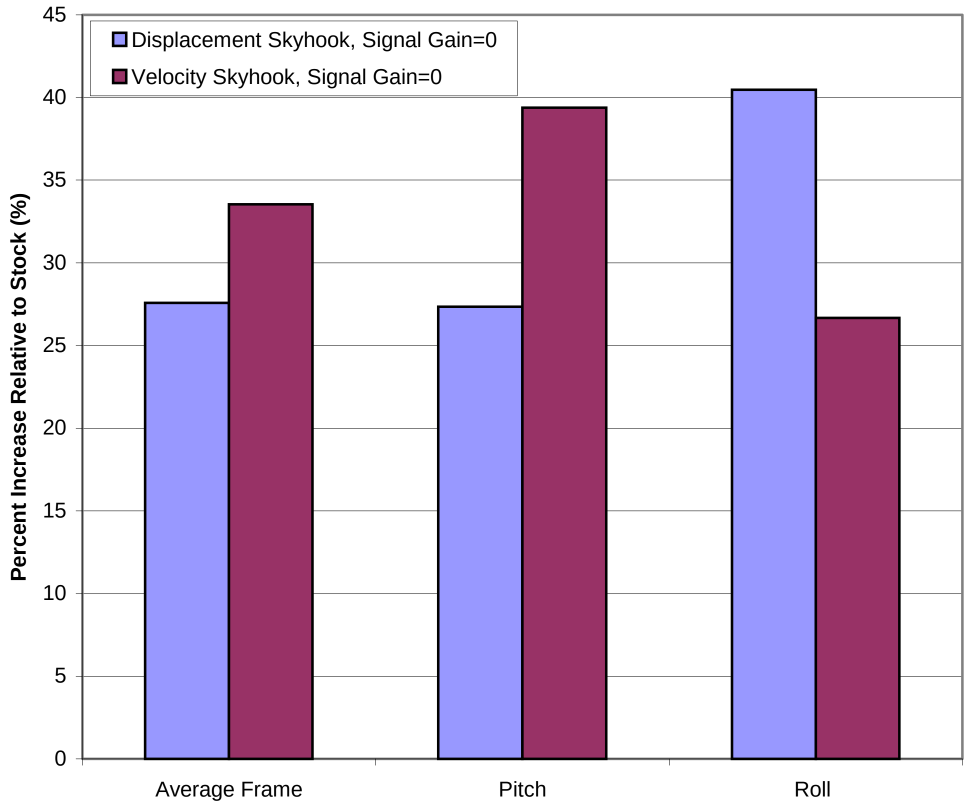

Figure 4.11. Straight and Level Driving Average Absolute Acceleration Results

This figure shows that the average absolute value of the acceleration transmitted from the road to the frame is higher with both the displacement and velocity based skyhook control policies (27.6% and 33.5% higher, respectively). This is an expected result based upon the off state jounce curve of the MR damper used being higher than the stock damper it replaces. This figure also shows that pitch and roll acceleration measured at the B-post are increased relative to the stock vehicle.

For the frequency domain analysis, FFTs were performed individually on each set of data. The resulting FFTs of each input were then averaged together across like data sets. The four averaged FFTs of the frame acceleration were then also averaged together. The averaged FFTs of the B-post accelerations as well as the averaged frame acceleration FFT are shown in Figure 4.12.

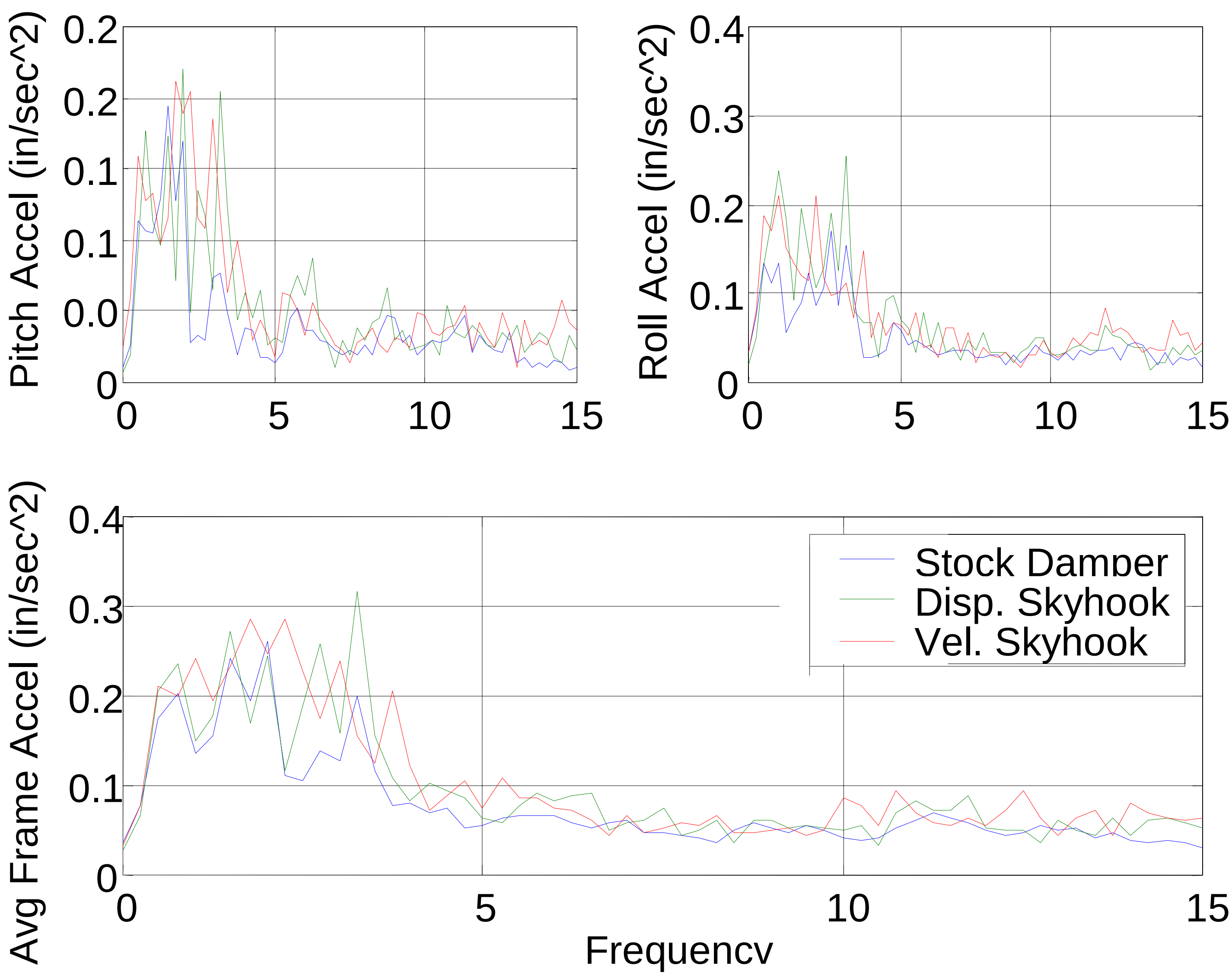

Figure 4.12. Straight and Level Driving Frequency Domain Results

In terms of the B-post accelerations, this figure shows essentially the same result as the time domain analysis. The stock suspension transmits lower levels of acceleration to the frame and body of the vehicle than either the displacement or velocity based skyhook control policies for most frequencies.

4.3.2 Bump Testing Results

The bump tests were repeated multiple times for each case. The cases investigated, as well as the numbers of repeated data sets recorded are:

- Stock configuration; repeated four times
- MR dampers operated passively; repeated two times
- Displacement skyhook without steering gain; repeated two times
- Velocity skyhook without steering gain; repeated two times

The tests were repeated to increase the reliability of the results. Time traces of the averaged supension rattle comparing the four test cases are shown in Figure 4.13.

These plots show that stock suspension both allows less and reduces the displacement across the suspension of the vehicle quicker than the MR based suspension with either of the control policies. This trend is repeated in terms of acceleration transmitted to the frame of the vehicle, as shown in Figures 4.14 and 4.15.

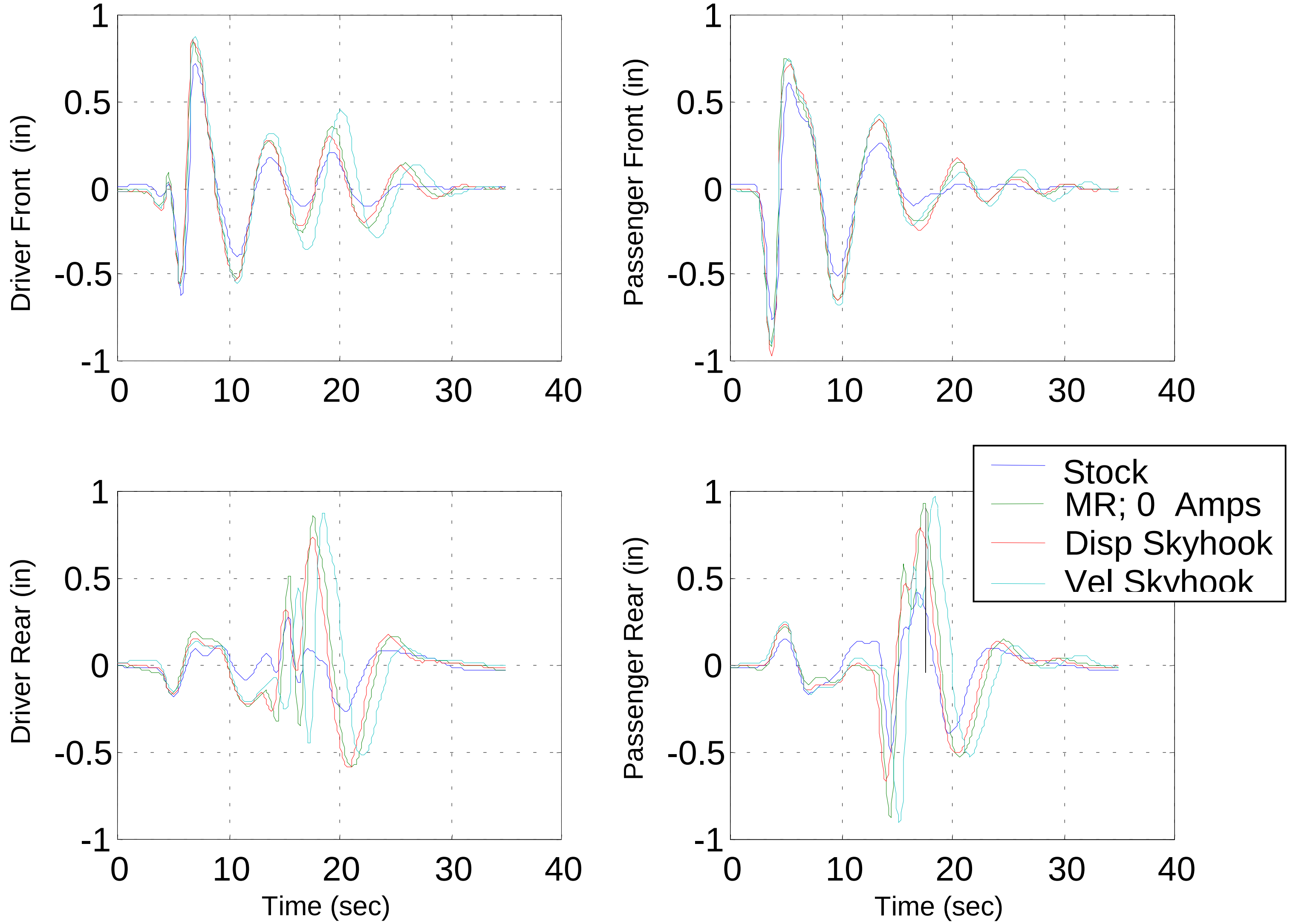

Figure 4.13. Bump Testing Suspension Rattle Time Traces

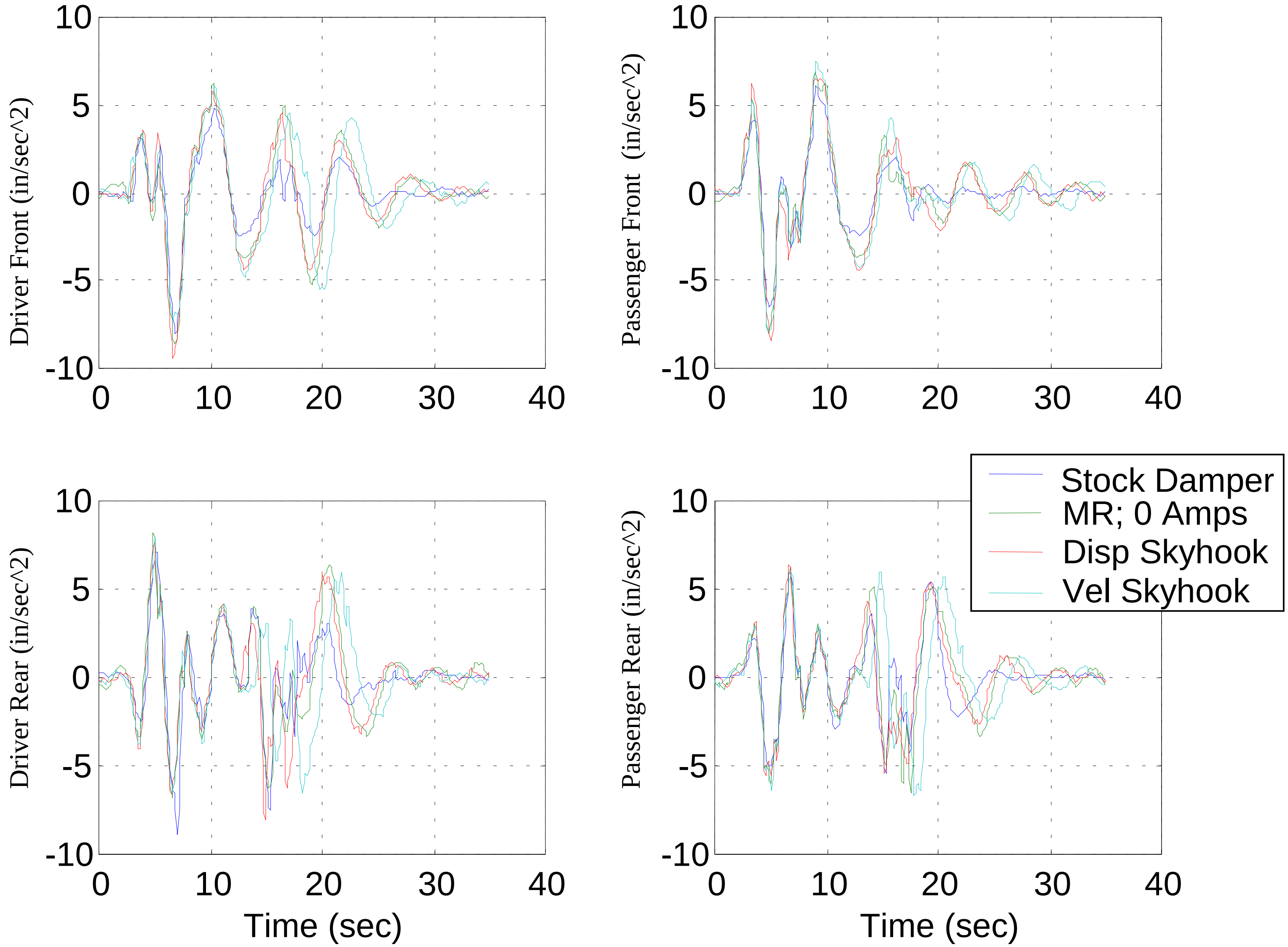
Driver Front (in/sec^2)
Passenger Front (in/sec^2)
Driver Rear (in/sec^2)
Passenger Rear (in/sec^2)
Time (sec)
Time (sec)
Stock Damper
MR; 0 Amps
Disp Skyhook
Vel Skyhook

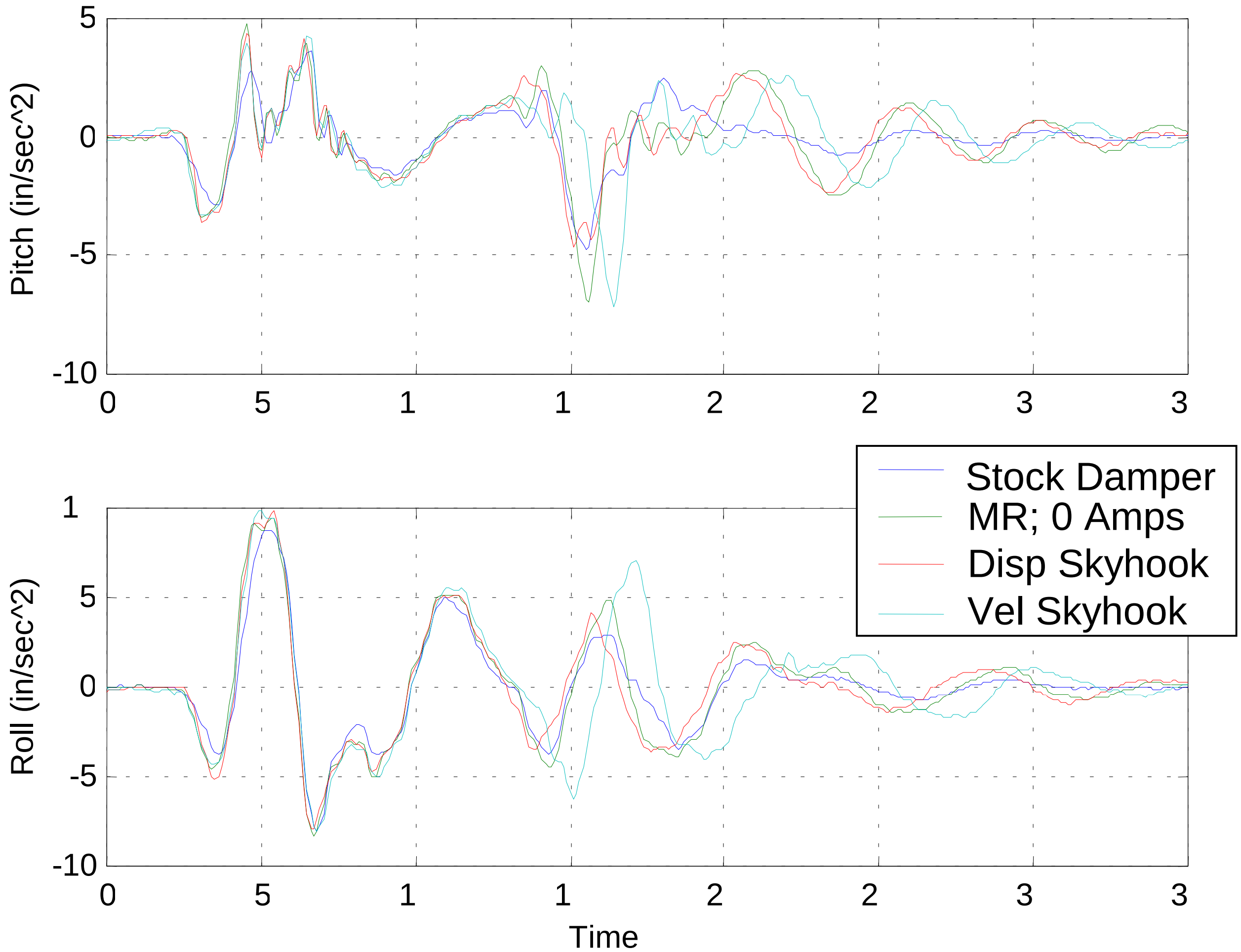

Figure 4.15. Bump Testing B-Post Acceleration Time Traces

These time traces can also be examined in terms of characteristic numbers. Plotting out the average of the absolute value of each of these traces results in Figures 4.16 and 4.17, which also show that the stock suspension allows less supension rattle and less acceleration of the frame and body of the vehicle.

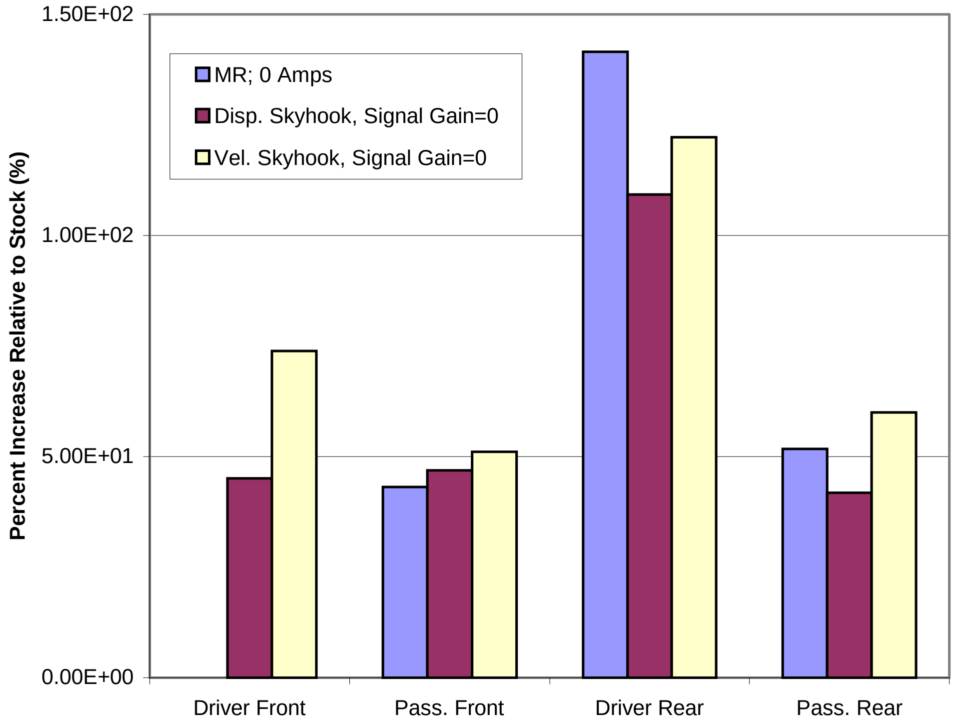

Figure 4.16. Bump Testing, Average Absolute Suspension Rattle

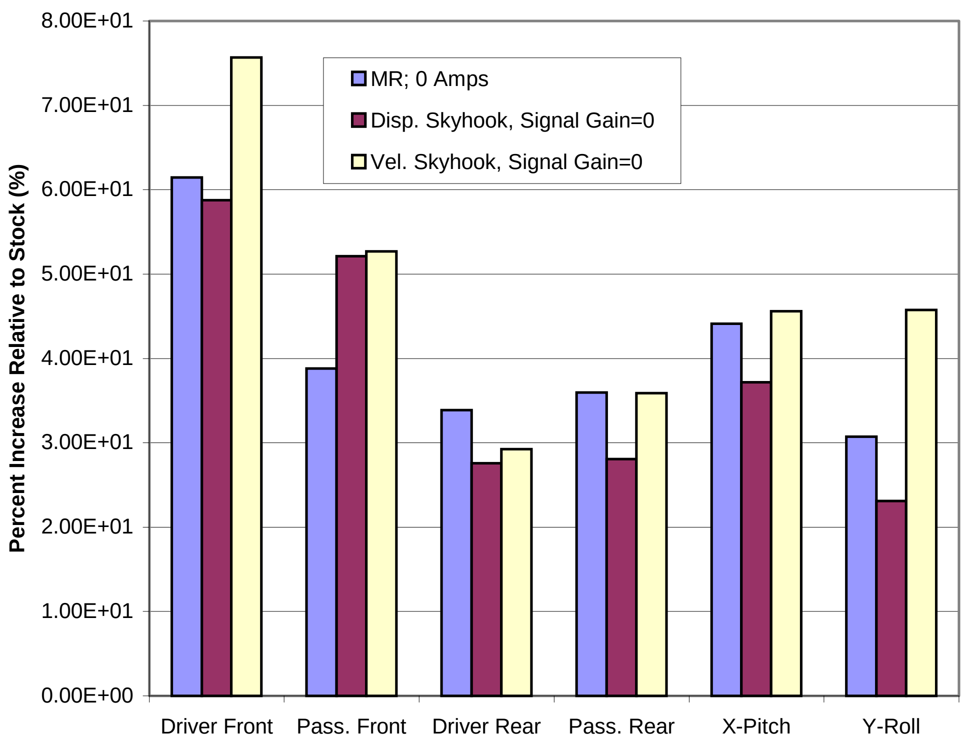

Figure 4.17. Bump Testing Average Absolute Frame Acceleration

4.3.3 Swerve Testing Results

The swerve tests were repeated multiple times for each case. The cases investigated, as well as the numbers of repeated data sets recorded are:

- Stock configuration; repeated six times
- MR dampers operated passively; repeated three times
- Displacement skyhook without steering gain; repeated three times
- Displacement skyhook with low steering gain; repeated three times
- Displacement skyhook with high steering gain; repeated three times
- Velocity skyhook without steering gain; repeated three times
- Velocity skyhook with low steering gain; repeated three times
- Velocity skyhook with high steering gain; repeated three times

For each case, the recorded data was averaged across repeated data sets, reducing the effects of noise and random variation. Figure 4.18 shows sample time traces of multiple test runs from both displacement and velocity based skyhook control, each with low steering gain, showing that the variation in results from run to run was small for each case.

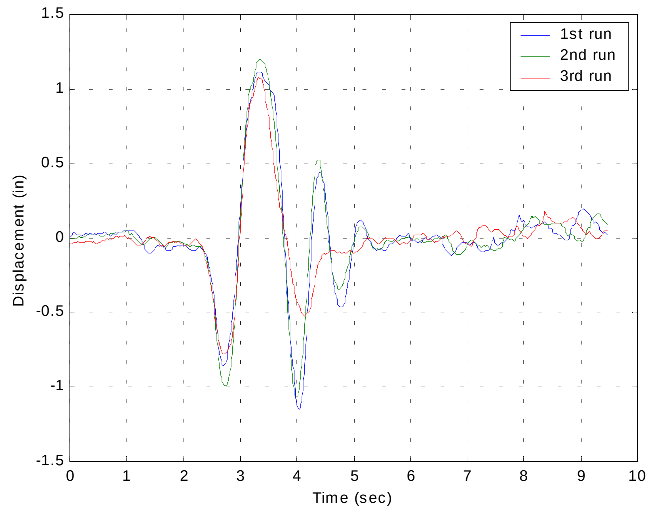

(a) Displacement Based Skyhook w/ Low Steering

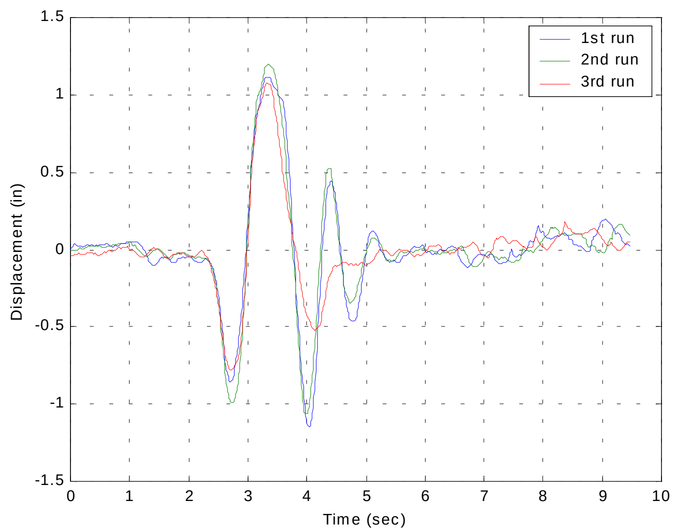

(b) Velocity Based Skyhook w/Low Steering Gain

Figure 4.18. Sample Time Traces from Repeated Test Runs

The results of the swerve testing will be presented in three sections. The first of the three sections will highlight the displacement based skyhook control strategies, while the second will highlight the velocity based skyhook control strategies. The third section will compare the performance of the displacement and velocity based skyhook policies; each with low steering gain.

4.3.3.1 Swerve Testing with Displacement Based Control Results

Time traces of the displacement across the vehicle suspension during the swerve maneuver with displacement based skyhook control, are shown in Figure 4.19.

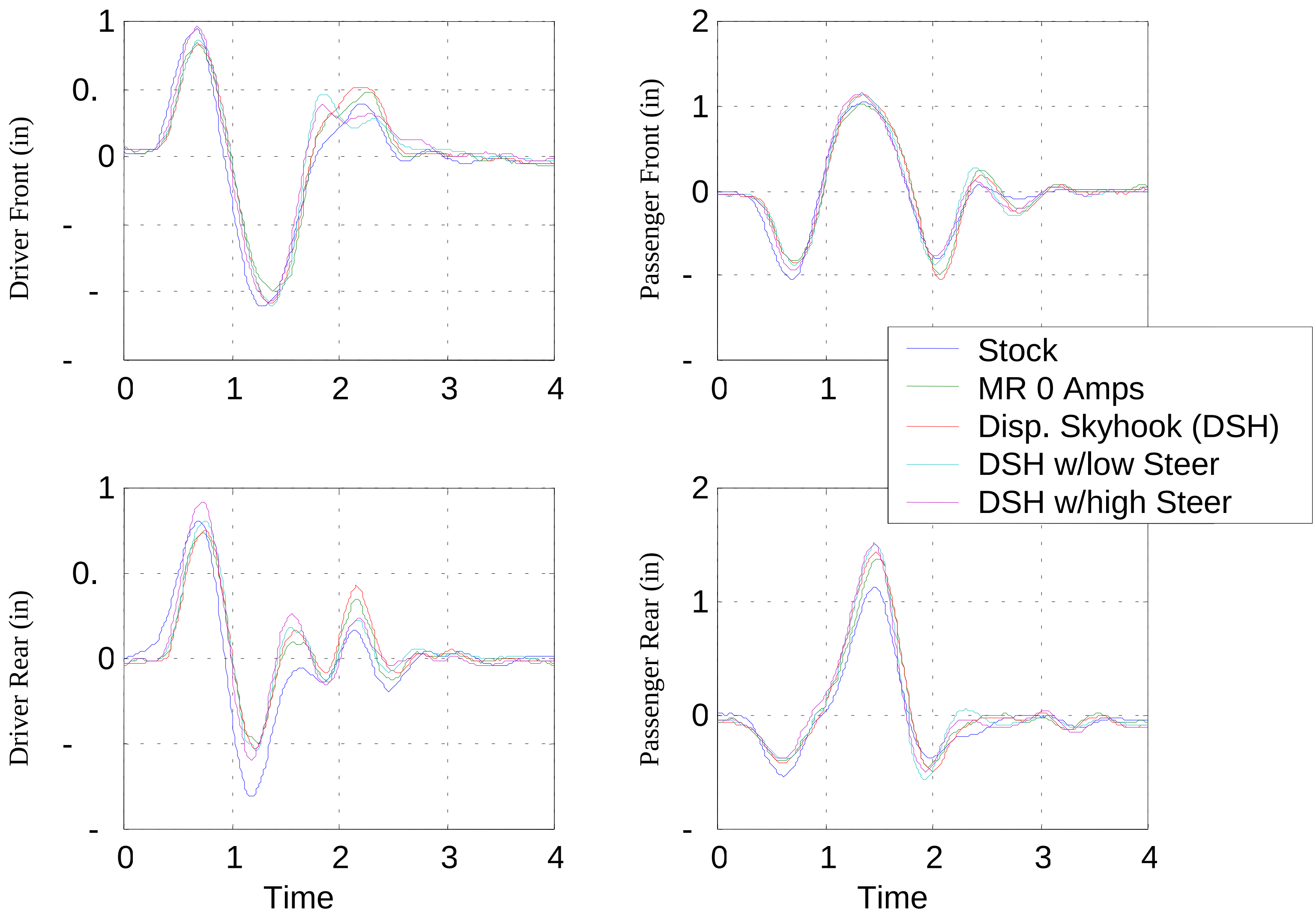

Figure 4.19. Swerve Testing with Displacement Based Skyhook Control Suspension Rattle Time Traces

These plots show that while the stock suspension is effective at damping out the motion resulting from a swerve type input, the amplitude of the first displacement peak is generally increased as compared to most of the displacement based skyhook control policies. The average of the absolute values of these time traces are shown in Figure 4.20.

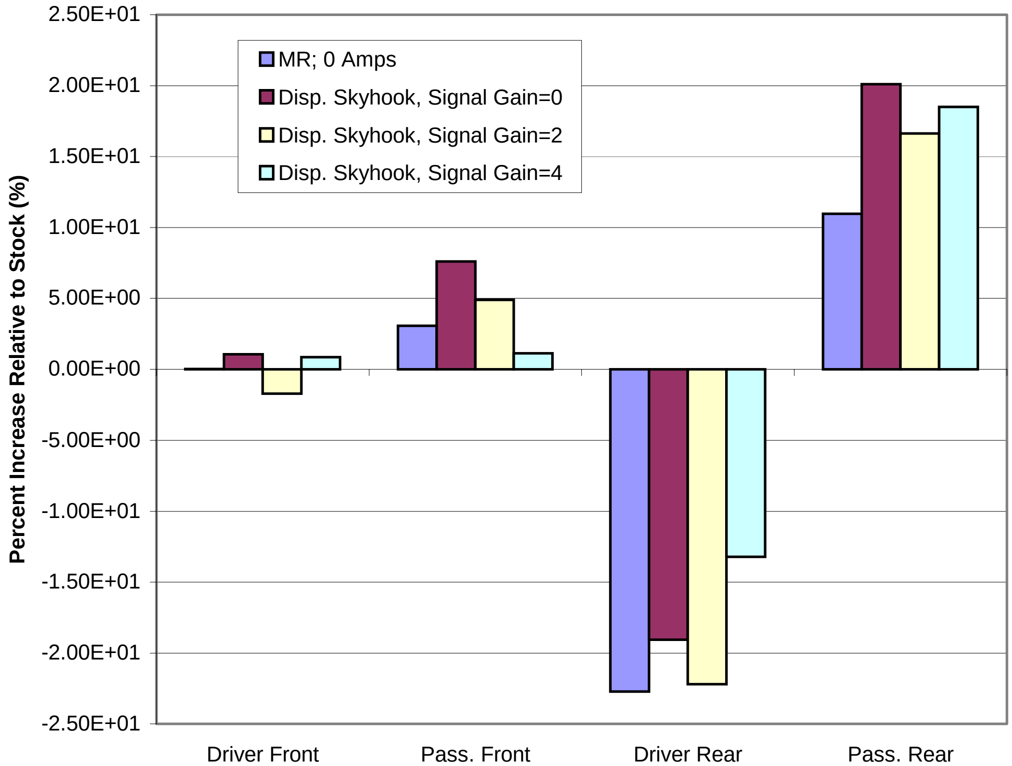

Figure 4.20. Swerve Testing with Displacement Based Skyhook Control, Average Absolute Value of Suspension Rattle Time Trace Summary

This figure indicates that over the whole data set, the stock suspension is close to equally effective as the displacement based skyhook policies. Additionally, it shows that the policies including steering feedback are more effective at reducing the average of the absolute value of the suspension rattle time traces than displacement based skyhook without this added feedback. Time traces of the acceleration of the frame of the vehicle during the swerve maneuver are shown in Figure 4.21.

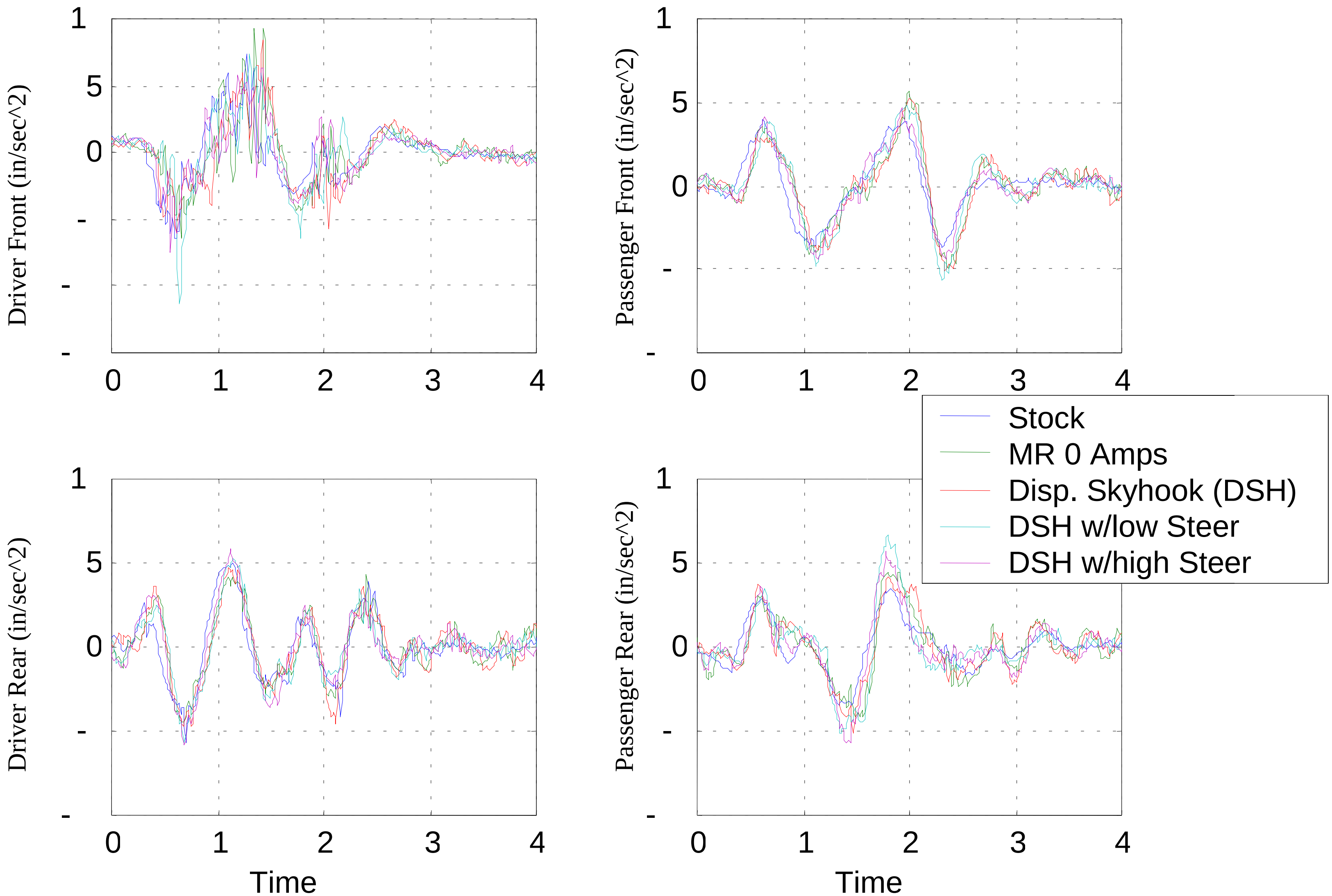

Figure 4.21. Swerve Testing with Displacement Based Skyhook Control Frame Acceleration Time Traces

It is more difficult to draw conclusions directly from these plots, though they do point to the same conclusions drawn from the suspension rattle plots. Time traces of the accelerations measured at the B-post are shown in Figure 4.22.

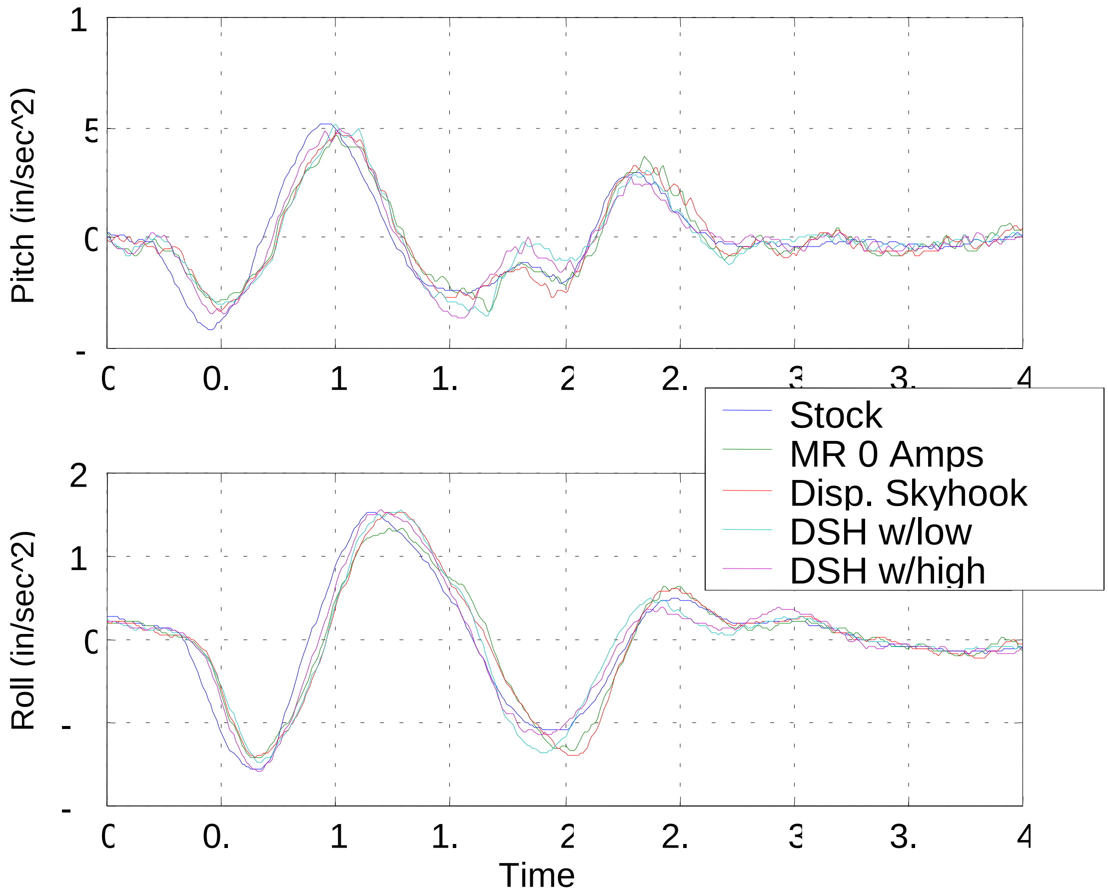

Figure 4.22. Swerve Testing with Displacement Based Skyhook Control Body Acceleration Time Traces

These plots show reductions in the magnitude (as compared to the stock case) of the initial acceleration peaks in both roll and pitch directions with the displacement based skyhook control strategy. They further show that the stock suspension is more effective at quickly reducing successive peaks. The average of the absolute values of the acceleration plots are summarized in Figure 4.23.

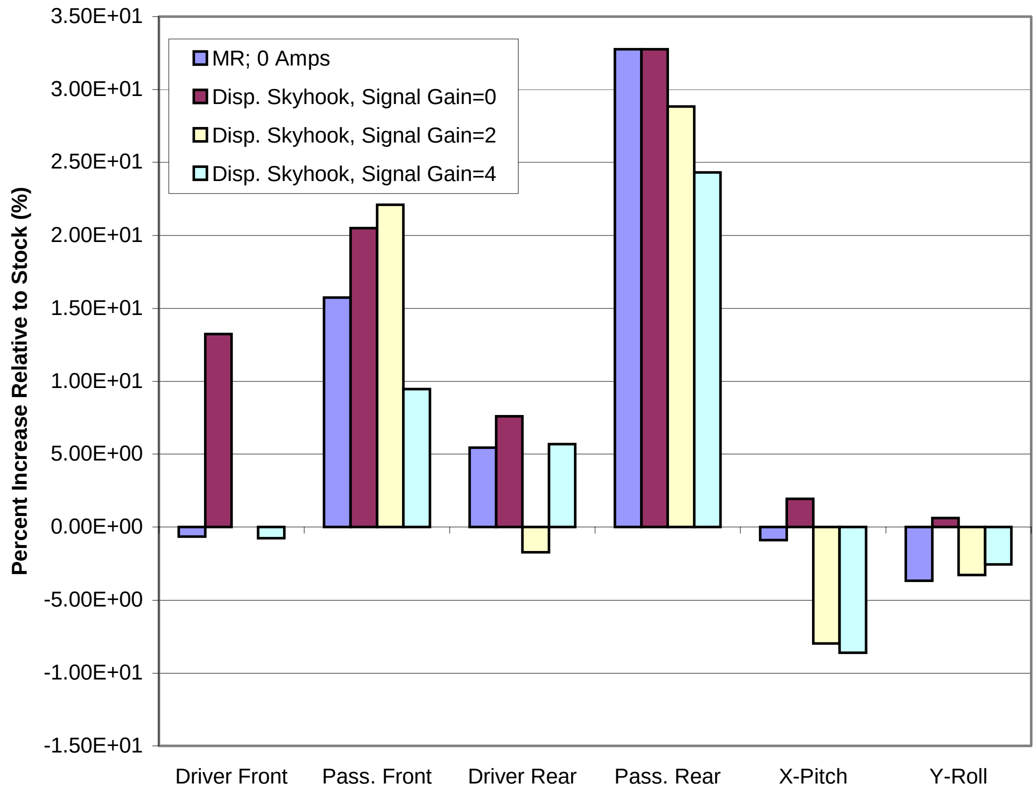

Figure 4.23. Swerve Testing with Displacement Based Skyhook Control Frame Acceleration, Average Absolute Value of Acceleration Time Trace Summary

This figure indicates that although the displacement based skyhook control policies generally increase the average of the absolute value of the acceleration of the frame of the vehicle, the strategies augmented with steering gain reduce value of the pitch and roll acceleration measured at the B-post.

4.3.3.2 Swerve Testing with Velocity Based Control Results

Averaged time traces of the displacement across the vehicle suspension during the swerve maneuver with velocity based skyhook control, are shown in Figure 4.24.

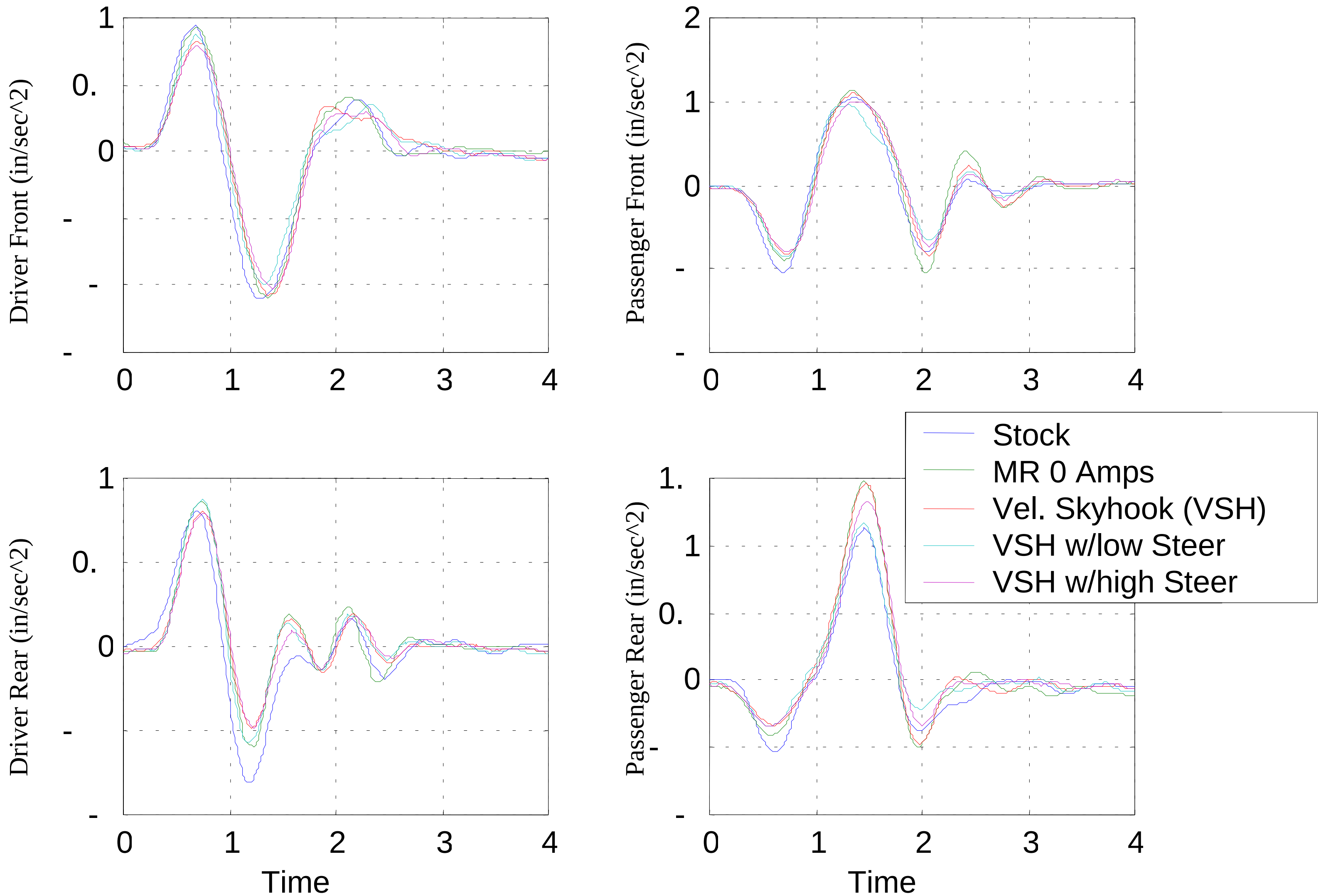

Figure 4.24. Swerve Testing with Velocity Based Skyhook Control Suspension Rattle Time Traces

These plots show that the velocity based skyhook control policies are more effective than the stock suspension at limiting the amplitude of the initial supension rattle peaks. However, the performance of the stock suspension as compared to the velocity based skyhook suspension improves on successive peaks. The average of the absolute values of these time traces are shown in Figure 4.25.

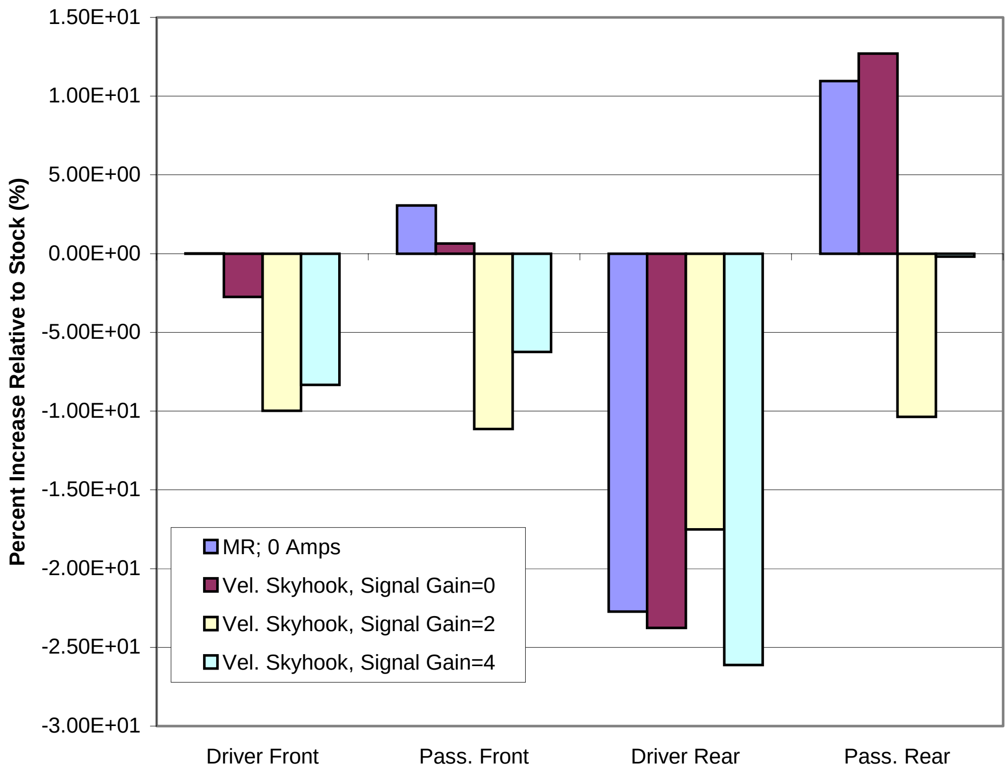

Figure 4.25. Swerve Testing with Velocity Based Skyhook Control, Average Absolute Value of Suspension rattle Time Trace Summary

This figure indicates that over the whole set of data, the velocity based skyhook control strategy by itself is close to equally as effective as the passive suspension at limiting the average of the absolute value of the supension rattle. Adding steering feedback to this policy, however, increases its effectiveness to more than the stock suspension. Additionally, the low steering gain version is generally more effective than the high steering gain version. Time traces of the acceleration of the frame of the vehicle during the swerve maneuver are shown in Figure 4.26.

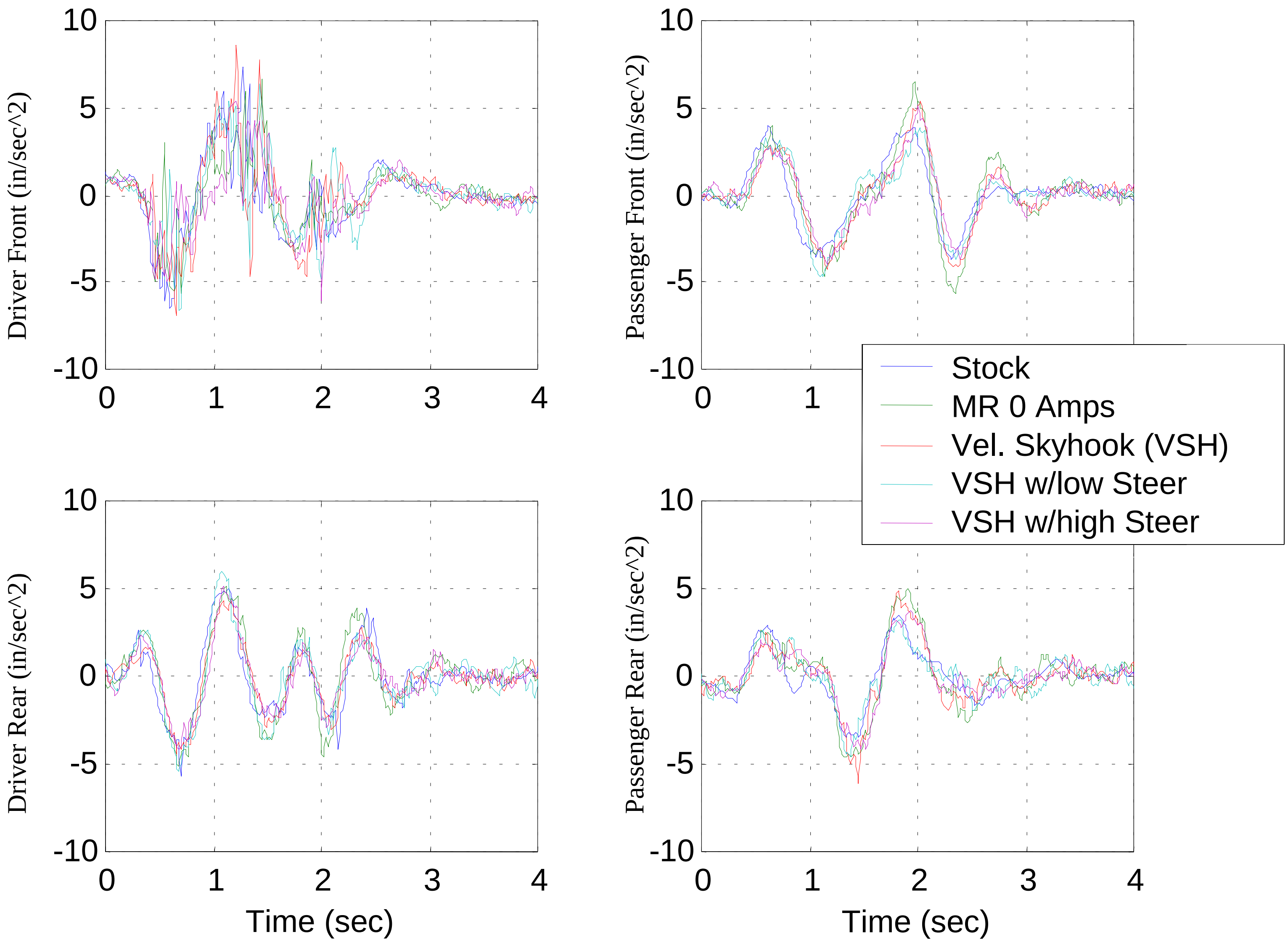

Figure 4.26. Swerve Testing with Velocity Based Skyhook Control Frame Acceleration Time Traces

It is more difficult to draw conclusions directly from these plots, though they do point to the same conclusions drawn from the suspension rattle plots. Time traces of the accelerations measured at the B-post are shown in Figure 4.27.

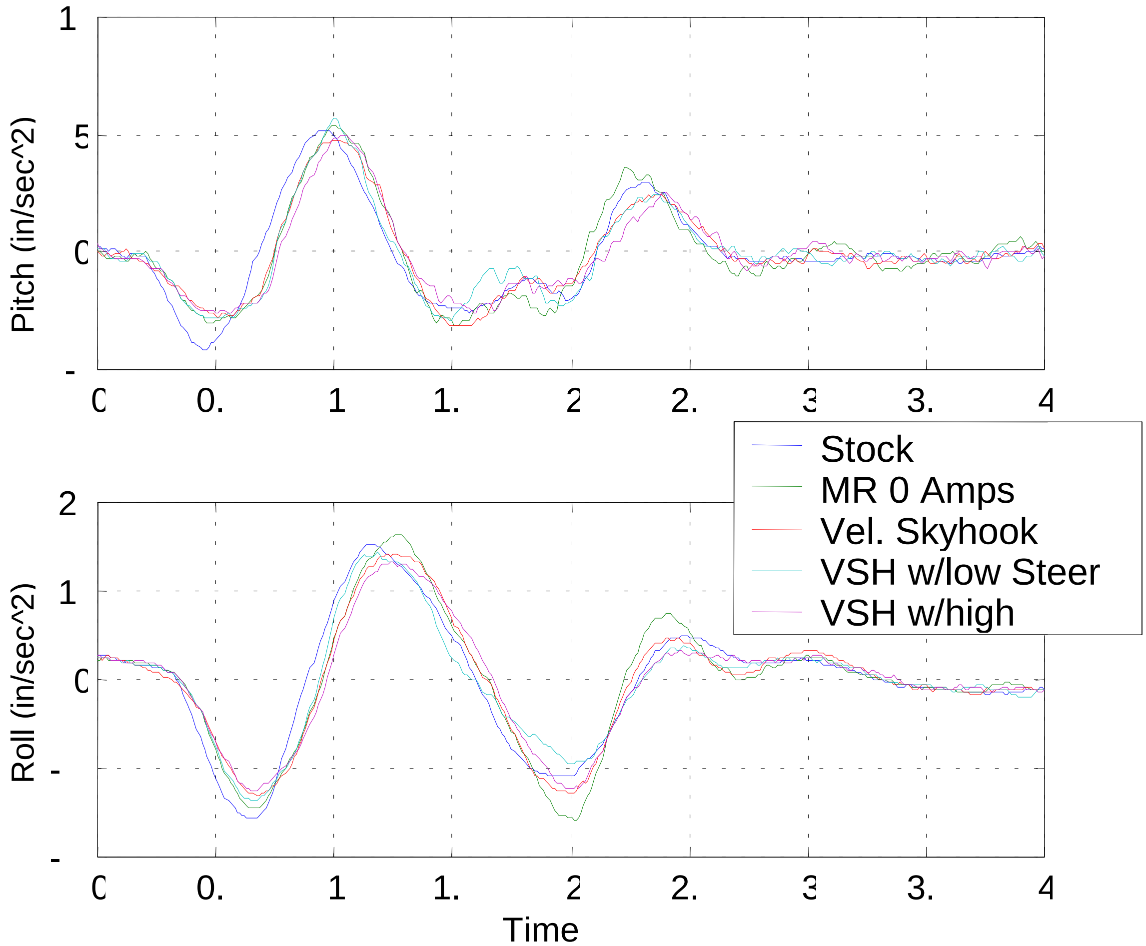

Figure 4.27. Swerve Testing with Velocity Based Skyhook Control BodyAcceleration Time Traces

These plots show reductions in the magnitude of the initial acceleration peaks in both the roll and pitch directions with the velocity based skyhook control strategy as compared to the stock suspension. The average of the absolute values of the acceleration plots are summarized in Figure 4.28.

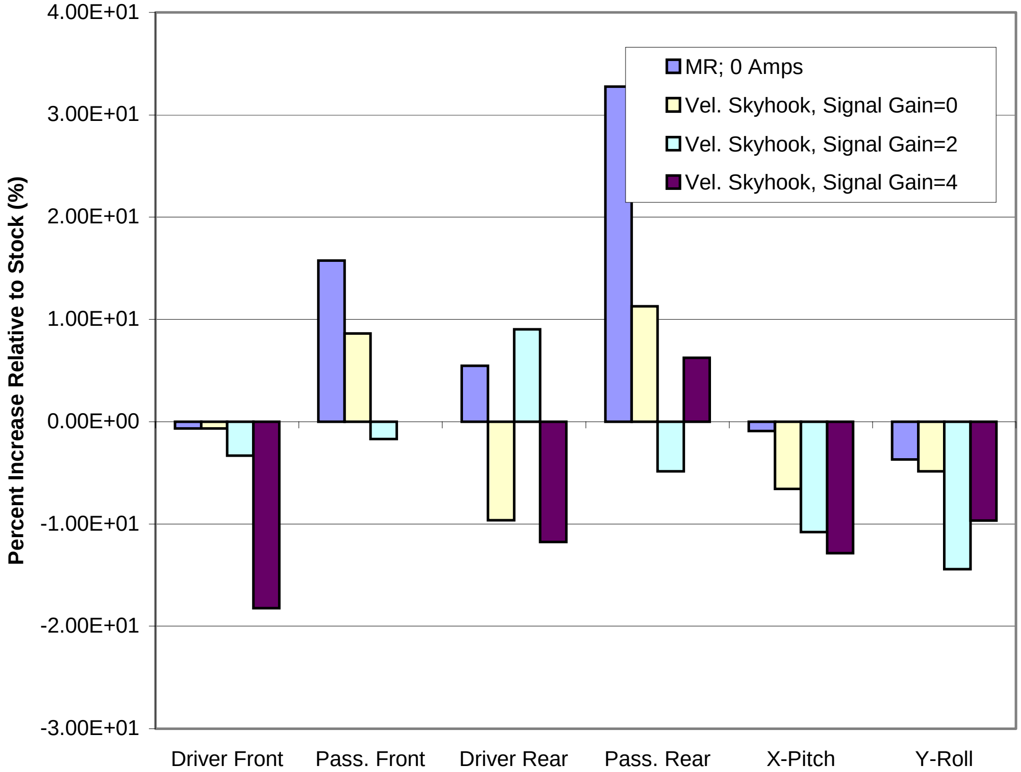

Figure 4.28. Swerve Testing with Velocity Based Skyhook Control, Average Absolute Value of Acceleration Time Trace Summary

This figure shows that the velocity based control strategies are both more and less effective than the stock suspension at controlling the average of the absolute value of the acceleration of the frame of the vehicle. It also shows that the velocity based policies are uniformly more effective than the stock suspension in terms of pitch and roll acceleration measured at the B-post.

4.3.3.3 Displacement and Velocity Based Control Swerve Testing Results Comparison

Averaged time traces of the displacement across the vehicle suspension during the swerve maneuver are shown in Figure 4.29 for the stock vehicle as well as for both displacement and velocity based skyhook control.

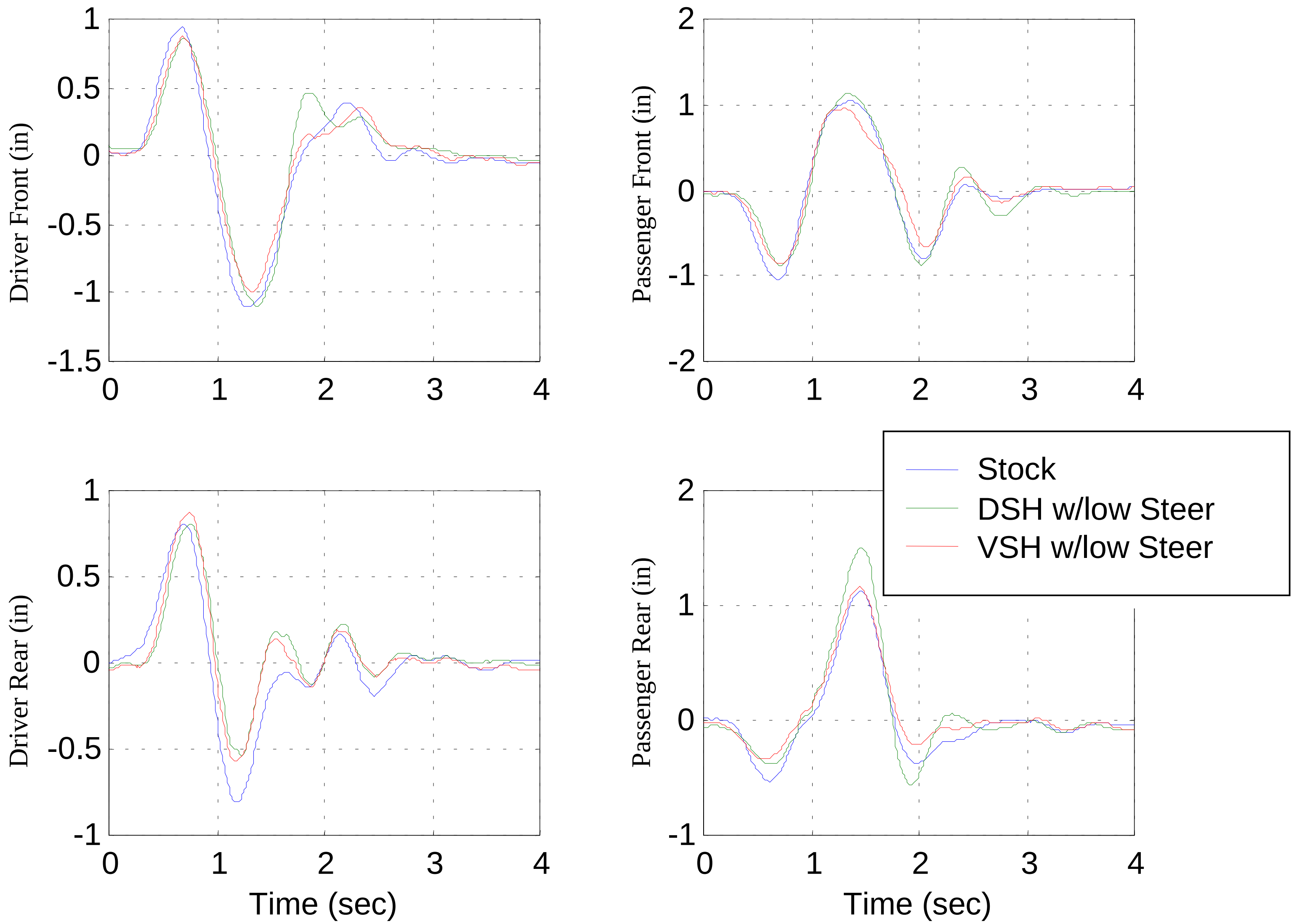

Figure 4.29. Swerve Testing with Both Displacement and Velocity Based Skyhook Control Suspension Rattle Time Traces

These plots show that the displacement and velocity based skyhook control policies with low steering gain are both more effective than the stock suspension at limiting the initial displacement across the vehicle suspension. Additionally, these plots indicate that the velocity based skyhook control policy with low steering gain is more effective than the displacement based skyhook control policy (also with low steering gain) at limiting successive peaks. The average of the absolute values of these time traces are shown in Figure 4.30.

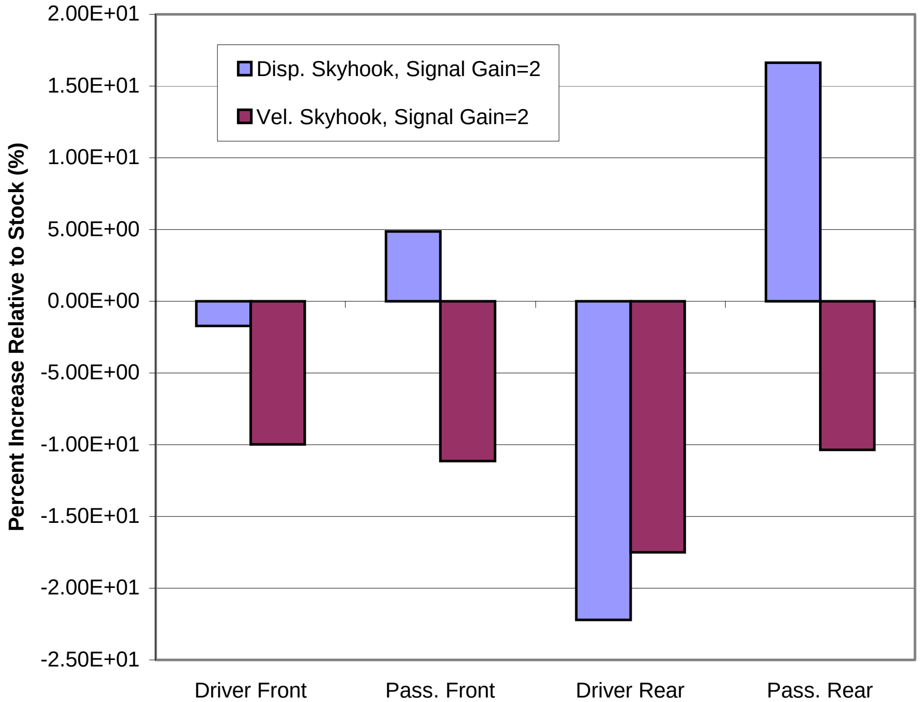

Figure 4.29. Swerve Testing with Displacement and Velocity Based Skyhook Control, Average Absolute Value of Supension rattle Time Trace Summery

This figure shows that while the displacement based skyhook control policy with low steering gain is more effective than the stock suspension at half of the measurement positions, the velocity based skyhook control policy with low steering gain is more effective at all measurement positions indicating that velocity based skyhook control with low steering gain may yield the best performance of the various strategies tested. Time traces of the acceleration of the frame of the vehicle during the swerve maneuver are shown in Figure 4.31.

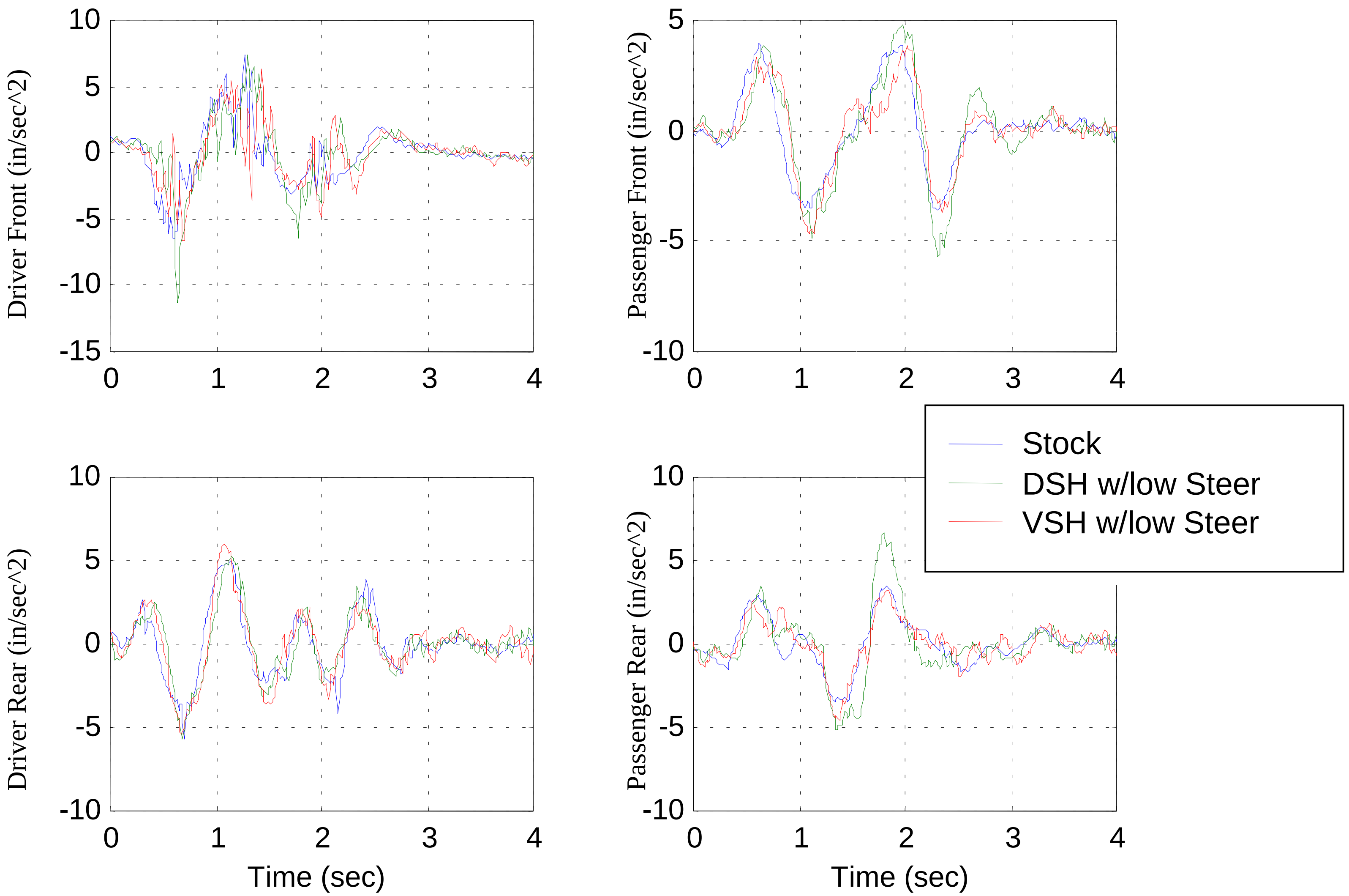

Figure 4.31. Swerve Testing with Both Displacement and Velocity Based Skyhook Control Frame Acceleration Time Traces

It is more difficult to draw conclusions directly from these plots, though they do indicate that the velocity based skyhook control with low steering gain strategy is more effective than the displacement based skyhook control with low steering gain strategy at limiting the acceleration of the frame. Time traces of the average acceleration measured at the B-post are shown in Figure 4.32.

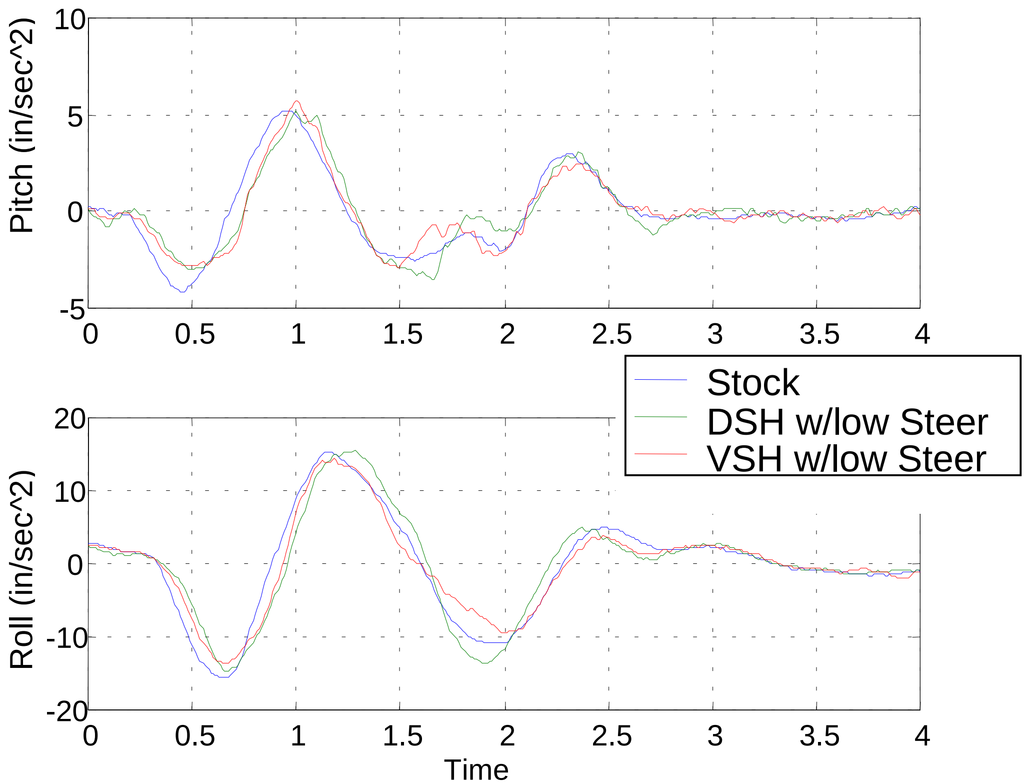

Figure 4.32. Swerve Testing with Both Displacement and Velocity Based Skyhook Control Body Acceleration Time Traces

These plots show reductions in the magnitude of the initial acceleration peaks in both the roll and pitch directions with both the velocity and displacement based skyhook control with low steering gain strategies, as compared to the stock suspension. Furthermore, this plot shows that the velocity based strategy is more effective than both the displacement based strategy and the stock suspension at limiting successive acceleration peaks. The average of the absolute values of the acceleration plots are summarized in Figure 4.33.

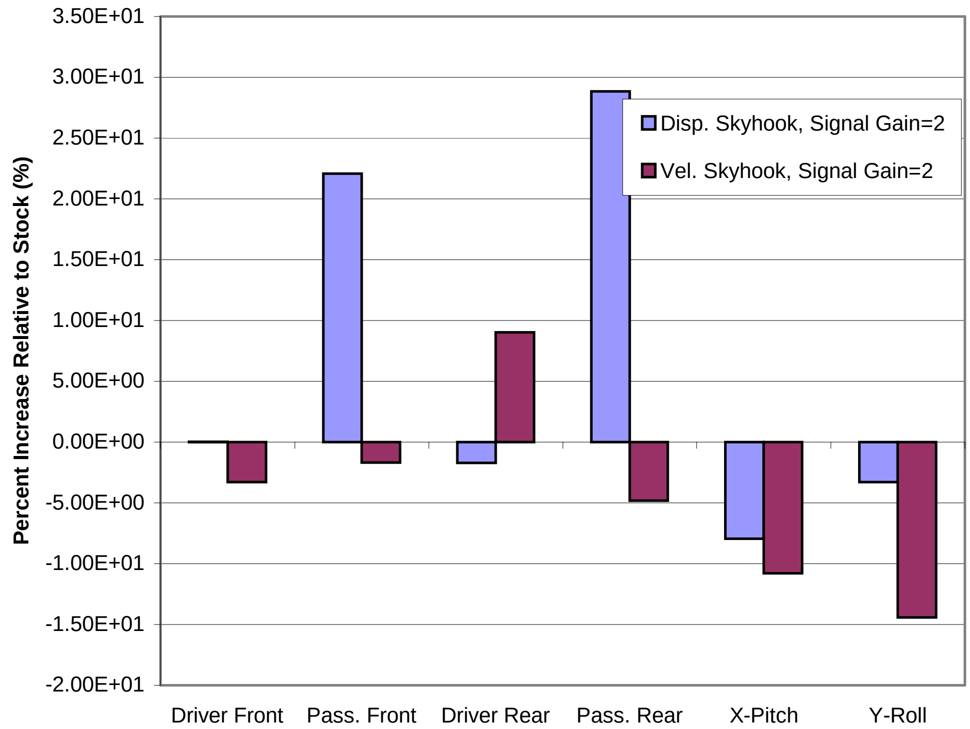

Figure 4.33. Swerve Testing with Displacement and Velocity Based Skyhook Control, Average Absolute Value of Acceleration Time Trace Summary

This figure shows that the velocity based control strategy is more effective than both the displacement based control strategy with low signal gain and the stock suspension at reducing the average absolute value of acceleration measured at the frame and B-post.

4.4 Road Testing Results Summary

This phase of the study focused on determining the effectiveness of various semiactive suspension control policies through road testing. The test vehicle was equipped with four MR dampers and driven on a level stretch of road. In order to judge the effectiveness of semiactive suspensions, three different driving scenarios were investigated, and the responses compared. The three driving scenarios investigated were straight and level driving (20 mph), driving across a speed bump (5 mph), and executing a swerve type maneuver through a predetermined course. Each of these scenarios represent multiple real world driving situations, and together can provide a good indicator of the performance benefits attainable by different semiactive suspension systems that were proposed here.

The straight and level driving test indicates that both the velocity and displacement based skyhook control strategies diminish performance (as measured by average absolute frame acceleration) compared to the stock vehicle. The average absolute value of pitch and roll acceleration measured at the B-post also increased with the skyhook policies. This may be caused by the level of off-state damping that was nearly as high as the stock dampers in jounce, as was discussed earlier.

The bump tests indicate that the stock suspension reduces both the suspension rattle and allows the accelerations of the vehicle body to die out quicker than any of the skyhook based control strategies.

The swerve test indicates that augmenting the displacement based skyhook policy with steering wheel position feedback improves the performance of the system. Furthermore, a relatively low value of the gain associated with this feedback results in improved performance relative to that resulting from the use of a higher gain. Testing also indicates that the performance of the velocity based skyhook policy can also be improved by the addition of steering wheel position feedback. As was the case with the displacement based skyhook control policy, the performance gains evident by augmenting the velocity based skyhook policy with steering wheel position feedback are greatest when the associated gain is relatively low.

Comparing the performance of the displacement and velocity based skyhook control strategies, each augmented with a low gain steering wheel position feedback, shows that both are more effective than the stock suspension at limiting the initial displacement across the vehicle suspension. Testing also shows that the velocity based control policy is more effective than the displacement based policy at limiting successive peaks. The velocity based skyhook control policy with low steering gain also resulted in superior (to both the stock suspension as well as the displacement based skyhook control policy) in terms of the average of the absolute value of the displacement across the vehicle suspension. Analysis of the average absolute value of the acceleration of the frame and B-post of the test vehicle also shows that the performance achieved through the use of velocity based skyhook control with low steering gain is superior to that attainable with both displacement based skyhook control (also with low steering gain) and the stock suspension.

CHAPTER 5
CONCLUSIONS

5.1 Summary

Sport utility vehicles have presented a unique design problem to suspension designers. As a class of vehicle, it is the same characteristics (size, adaptability, solid feel, and commanding view of the road) which attract buyers, that make it difficult for a suspension designer to create a vehicle that will both be comfortable to the operator, and be stable during vehicle maneuvers. Due predominately to the relatively high center of gravity common to this class of vehicle, a greater roll over propensity than automobiles is common. In order to maintain the high safety standards of automobiles, suspension designers have looked beyond conventional suspension systems. One of the most promising class of suspensions that has been examined in recent years, are semiactive suspensions. This study examined the effects of a semiactive suspension using magnetorheological dampers at controlling the response of a sport utility vehicle to various maneuvers that can occur in driving conditions. The control policies initially included in this study were displacement and velocity based skyhook schemes, and were later extended to include steering wheel position feedback. These different scenarios, in addition to being tested with a variety of system inputs, are examined in three distinct settings. The central techniques, in conjunction with the different inputs, were examined numerically (through computer simulation), in a lab setting (using a two-post test rig), and on the road.

The part of the investigation performed using computer simulations allows examination of a wide variety of inputs/cases; greater than can reasonably be examined with a physical system. Some of the important aspects of the development of the computer model used for this part of the investigation included the mathematical development and coding of the model itself, determination of accurate vehicle parameters, development and coding of the controllers being investigated, creation of viable system inputs, as well as determination of important aspects of system for laboratory and field testing.

The numerical simulation investigation initially examined the effectiveness of velocity and displacement based skyhook control. This investigation led to the development of additional semiactive control strategies; velocity and displacement based skyhook control with force control. Simulation results performed on a four-degree-of-freedom roll-plane model indicated that the performance of different control strategies heavily depended on the controllable damper's high and low state damping levels.

For each control policy, a tuned controllable damper was developed and the performances of the tuned policies were compared. It was found that the velocity based skyhook control policy with force control is most effective at controlling both road induced vibration and driver induced roll. The effects of varying the modeled weight of the vehicle was also investigated and found to be minor.

The laboratory tests that were conducted subsequent to the simulation studies allowed various driving situations to be accurately and repeatedly emulated, while also affording greater opportunities for data collection. The on-vehicle laboratory tests were performed using a tire-coupled two-post dynamic rig. The response of the test vehicle was examined with and without both dampers and roll bar. The test results showed that the roll bar influences, but does not determine the dynamics of the vehicle. The dampers were found to be most effective at controlling the response to inputs of 1 to 2 Hz; the vehicle suspension resonance frequency range.

Velocity and displacement based control strategies were developed and tuned. They were then compared with each other as well as with the stock passive suspension system. This comparison was performed for a variety of system inputs including pure tones, step inputs, chirp inputs, and multi-sine inputs. The dominant results of this testing is that neither velocity nor displacement based skyhook control can achieve performance superior to the stock passive suspension, for a wide variety of system inputs. They do indicate that in order to realize significant performance gains in a real world driving situations, it is necessary to augment the various control policies with additional feedback, such as the steering wheel position.

The road testing phase of this investigation focused on determining the effectiveness of various semiactive suspension control policies on controlling the response to specific driving scenarios which commonly occur in real world driving conditions. The three scenarios that were investigated in this part of the study were straight and level driving, driving over a speed bump, and executing a swerve maneuver. The swerve maneuver allowed for an opportunity to quantify the performance potential of both displacement and velocity skyhook policies augmented with steering wheel position feedback.

The straight and level driving test indicated that both skyhook control strategies exhibit performance slightly inferior to that of the stock passive suspension. This result is based on acceleration measurements made on the frame of the vehicle as well as at the B-post. It was hypothesized that an MR damper with a lower off-state damping than what was tested here could have offered some ride improvement. No tests were carried out to prove this hypothesis due to the unavailability of MR dampers with lower off-state damping. Likewise, the bump test indicated that the stock passive suspension is more effective at limiting both the displacement across the suspension and the acceleration of the vehicle frame than either of the skyhook policies. The swerve test indicated that both the displacement and velocity based skyhook control policies exhibit the greatest performance improvement with the addition of steering wheel feedback with a low, as opposed to high, associated gain. Comparing the performance of the two skyhook control strategies, each augmented with a low gain steering wheel position feedback, showed that both are more effective than the stock suspension at limiting both the initial displacement across the vehicle suspension as well as successive peaks. The best performance was attained with the velocity based skyhook control augmented with steering wheel position feedback with low gain. This strategy exhibited decreased displacement across the vehicle suspension as well as reducing the acceleration measured on the frame of the vehicle as well as at the B-post, indicating that both stability and comfort issues have been addressed. It should be noted that this strategy is the same one that the numerical simulation stage of the study predicted to have the best performance, though the magnitude of ride improvement found in road testing was not as great as the numerical simulation had predicted.

In conclusion, this study has shown that the performance potential of various skyhook control policies is heavily dependent on the tuning of both the controllable damper used on the vehicle, as well as the control strategy itself. Additionally, through computer simulation, lab testing, and road testing, it was shown that velocity based skyhook control exhibits improved performance relative to displacement based skyhook control. The numerical and road testing portions of this investigation show that both versions of skyhook control benefit from the addition of feedback of the position of the steering wheel, and that the velocity based skyhook control policy augmented with low gain steering wheel feedback exhibits the best performance of all strategies investigated.

Lastly, it is worth noting that the results presented in this study are greatly affected by the class of vehicle as well as the specific dampers that were used for our tests. One can expect different results for a different class of vehicle or with dampers that are significantly different in their dynamics than those used here.

5.2 Recommendations for Future Studies

Future work that can expand on the investigation presented here would include a investigation of the performance gains possible with controllable dampers with a lower level of damping in the jounce direction. Additionally, an investigation into the effectiveness of the type of semiactive suspensions discussed here applied to other classes of vehicles (particularly heavy trucks) would be especially informative. It would also be useful to investigate the effectiveness of the control policies augmented with steering wheel position feedback at other vehicle speeds, and for other common vehicle maneuvers. Additionally, the use of other vehicle information (inclination, brake pressure, throttle position) should be investigated in terms of how they also can improve the performance of semiactive suspensions.

References

1. Chalasani, R.M., “Ride Performance Potential of Active Suspension Systems-Part I: Simplified Analysis Based on a Quarter-Car Model,” Proceedings of 1986 ASME Winter Annual Meeting, Los Angeles, CA, December 1986.

2. Chalasani, R.M., “Ride Performance Potential of Active Suspension Systens-Part II: Comprehensive Analysis Based on a Full-Car Model,” ASME Symposium on Simulation and Control of Ground Vehicles and Transportation Systems, AMD-Vol. 80, DSC-VOL. 2, 1986, pp.187-204.

3. Barak, P., “Design and Evaluation of an Adjustable Automobile Suspension,” Autotechnologies Conference and Exposition, SAE paper #890089, Vol. 98, Section 6, January 1989.

4. Lord Corporation Web Page; www. Rheonetic.com.

5. Karnopp, D.C., Crosby, M.J., and Harwood. R.A., “Vibration Control Using Semi-Active Force Generators,” ASME Journal of Engineering for Industry, Vol. 96, No. 2, May 1975, pp 619-626.

6. Fodor, M. and Redfield, R. “Resistance Control, Semi-Active Damping Performance,” Advanced Automotive Technologies American Society of Mechanical Engineers, Dynamic Systems and Control Division, DSC. v 56 1995. ASME, New York, NY, USA. pp. 161-169.

7. Palkovics, L. and El-Gindy, M. “Examination of Different Control Strategies on Heavy-Vehicle Performance,” Advanced Automotive Technologies American Society of Mechanical Engineers, Dynamic Systems and Control Division, DSC. v 52 1993. ASME, New York, NY, USA. pp. 349-360.

8. Heo, S., Park, K., and Hwang, S. “Performance and Design Consideration for Continuously Controlled Semi-Active Suspension Systems,” International Journal of Vehicle Design. v 23 n 3 2000. pp. 376-389.

9. Ursu, I., Ursu, F., Sireteanu, T., and Stammers, C. W. “Artificial Intelligence Based Synthesis of Semiactive Suspension Systems,” Shock & Vibration Digest. v 32 n 1 Jan 2000. pp. 3-10.

10. Fang, X., Chen, W., Wu, L., Wang, Q., Fan, D., and Li, Z. “Fuzzy Control Technology and the Application to Vehicle Semi-Active Suspension,” Chi Hsieh Kung Ch'Eng Hsueh Pao/Chinese Journal of Mechanical Engineering. v 35 n 3 1999. pp. 98-100.

11. Lieh, J. and Li, W. “Adaptive Fuzzy Control of Vehicle Semi-Active Suspensions,” ASME Dynamic Systems and Control Division American Society of Mechanical Engineers, Dynamic Systems and Control Division DSC. v 61 1997. ASME, Fairfield, NJ, USA. pp. 293-297.

12. Nicolas, C. F., Landaluze, J., Castrillo, E., Gaston, M., and Reyero, R., " Application of Fuzzy Logic Control to the Design of Semi-Active Suspension Systems," IEEE International Conference on Fuzzy Systems. v 2 1997. IEEE, Piscataway, NJ, USA,97CB36032. pp. 987-993.

13. Hashiyama, T., Furuhashi, T., and Uchikawa, Y., "Study on Finding Fuzzy Rules for Semi-Active Suspension Controllers with Genetic Algorithm" Proceedings of the IEEE Conference on Evolutionary Computation. v 1 1995. IEEE, Piscataway, NJ, USA. pp. 279-282.

14. Al-Holou, N., Sung Joo, D., and Shaout, A. "Development of Fuzzy Logic Based Controller for Semi-Active Suspension System," Midwest Symposium on Circuits and Systems. v 2 1994. IEEE, Piscataway, NJ, USA,94CH35731. pp. 1373-1376.

15. Holdmann, P. and Holle, M. "Possibilities to Improve the Ride and Handling Performance of Delivery Trucks by Modern Mechatronic Systems," JSAE Review. v 20 n 4 1999. pp. 505-510.

16. Ahmadian, M. "Ride Evaluation of a Class 8 Truck with Semiactive Suspensions" Advanced Automotive Technologies American Society of Mechanical Engineers, Dynamic Systems and Control Division, DSC v 52 1993, ASME, New York, NY, USA. pp. 21-26.

17. Margolis, D. and Nobles, C. M. "Semi-Active Heave and Roll Control for Large Off-Road Vehicles," SAE Special Publications. n 892. pp. 25-34.

18. Giua, A., Savastano, A., Seatzu, C., and Usai, G. "Approximation of an Optimal Gain Switching Active Law with a Semiactive Suspension," IEEE Conference on Control Applications - Proceedings. v 1 1998. IEEE, Piscataway, NJ, USA,98CH36104. pp. 248-252.

19. Saxon, N. L., Meldrum, W. R. Jr., and Bonte, T. K. "Semiactive Suspension: a Field Testing Case Study," Developments in Tire, Wheel, Steering, and Suspension Technology SAE Special Publications. v 1338 Feb 1998. SAE, Warrendale, PA, USA. pp. 187-194 .

20. Nakai, H., Yoshida, K., Ohsaku, S., and Motozono, Y. "Design of Practical Observer for Semiactive Suspensions," Nippon Kikai Gakkai Ronbunshu, C Hen. v 63 n 615 Nov 1997. pp. 3898-3904.

21. Hwang, S., Heo, S., Kim, H., and Lee, K. "Vehicle Dynamic Analysis and Evaluation of Continuously Controlled Semi-Active Suspensions Using Hardware-in-the-Loop Simulation," Vehicle System Dynamics. v 27 n 5-6 June 1997. pp. 423-434.

22. Lieh, J. “Semiactive and Active Suspensions for Vehicle Ride Control Using Velocity Feedback,” JVC/Journal of Vibration & Control. v 3 n 2 May 1997. pp. 201-212.

23. Gordon, T. J., and Best, M. C. “Dynamic Optimization of Nonlinear Semi-Active Suspension Controllers,” IEE Conference Publication. Publ by IEE, Michael Faraday House, Stevenage, Engl. v 1 n 389 1994. pp. 332-337.

24. Venhovens, P. J. Th., Van Der Knaap, A. C. M., Savkoor, A. R., and Van Der Weiden, A. J. J., “Semi-Active Control of Vibration and Attitude of Vehicles,” Vehicle System Dynamics. v 23 n SUPPL 1994. pp. 522-540.

25. Venhovens, P. J. Th., Van Der Knaap, A. C. M., and Pacejka, H. B., “Semi-Active Attitude and Vibration Control,” Vehicle System Dynamics. v 22 n 5-6 Sep-Nov 1993. pp. 359-381.

26. Lieh, J. “Effect of Bandwidth of Semiactive Dampers on Vehicle Ride,” Journal of Dynamic Systems Measurement & Control-Transactions of the ASME. v 115 n 3 Sep 1993. pp. 571-575.

27. Redfield, R. C. “Performance of Low-Bandwidth, Semi-Active Damping Concepts for Suspension Control,” Vehicle System Dynamics. v 20 n 5 1991 pp. 245-267.

28. Yi, K., and Hedrick, K. “Dynamic Tire Force Control by Semiactive Suspensions,” Journal of Dynamic Systems Measurement & Control-Transactions of the ASME. v 115 n 3 Sep 1993. pp. 465-474.

29. Lieh, J. “Control of Vibrations in Elastic Vehicles Using Saturation Nonlinear Semiactive Dampers,” American Society of Mechanical Engineers, ASME, New York, NY, USA, 91-WA-DSC-4. pp. 1-6.

30. Miller, L. R. and Nobles, C. M. “Methods for Eliminating Jerk and Noise in Semi-Active Suspensions,” SAE (Society of Automotive Engineers) Transactions. v 99 n Sect 2 1990 pp. 943-951.

31. Crolla, D. A., and Abdel-Hady, M. B. A. “Semi-Active Suspension Control for a Full Vehicle Model,” SAE (Society of Automotive Engineers) Transactions. v 100 n Sect 6 1991, 911904 pp. 1660-1666.

32. Poynor, J. A., “Innovative Designs for Magneto-Rheological Dampers,” Master Thesis, Virginia Tech. August 2001.

33. Goncalves, F., “Dynamic Analysis of Semi-Active Control Techniques for Vehicle Applications,” Master Thesis, Virginia Tech. August 2001

Vita

David E. Simon was born on June 27, 1974 in Long Island, New York where his parents still live. He lived in Long Island through high school and then moved to attend Virginia Tech where he earned a Bachelor of Science in Mechanical Engineering in 1996. After graduating, he decided to remain at Virginia Tech and pursue a Master of Science, in Mechanical Engineering. His Masters studies emphasized the field of dynamic control through his research at the Advanced Vehicle Dynamics Lab (AVDL) of Virginia Tech. In August 1998, he earned his M.S. degree, and started his work toward a doctoral degree. In December 2001, he completed his work at AVDL and earned his Ph.D. in Mechanical Engineering.